Biodiversity, phylogeny, biogeography and ecophysiology of benthic diatoms from the West Antarctic Peninsula

Inaugural-Dissertation

to obtain the academic degree

Doctor rerum naturalium (Dr. rer. nat.)

submitted to the Department of Biology, Chemistry, Pharmacy

of Freie Universität Berlin

by

Katherina Schimani

2024

The work on this doctoral thesis was conducted from June 2021 to April 2024 at the Botanic Garden and Botanical Museum Berlin of Freie Universität Berlin under the supervision of Dr. Jonas Zimmermann.

1st reviewer: Dr. Jonas Zimmermann

2nd reviewer: Prof. Dr. Thomas Borsch

Date of defence: 02.09.2024

Acknowledgements

I express my deepest gratitude to Dr. Jonas Zimmermann for the initiation of the project, for his constant guidance, and for giving me the freedom to conduct my research but also helping me staying focused. I would also like to thank Prof. Dr. Thomas Borsch for his time to be the second reviewer of this thesis and the opportunity to conduct my research activities at the Botanic Garden and Botanical Museum Berlin-Dahlem.

I acknowledge the support though the funding from the Priority Program "Antarctic Research with Comparative Studies in Arctic Ice Regions" of the German Research Foundation which made this research project possible.

I am very grateful to the Diatom Research group at the Botanic Garden and Botanical Museum for the valuable scientific discussion and for creating an inspirational and productive work environment. I thank Dr. Nélida Abarca for her supervision concerning diatom morphology and taxonomy and all the fun office talks, Dr. Oliver Skibbe for introducing me to diatom cultivation and taking over culturing in times when it was not possible for me, Wolf-Henning Kusber for all his help untangling diatom nomenclature, Dr. Demetrio Mora for his guidance in molecular phylogeny and during the resulting publication as well as Dr. Regine Jahn for all her valuable insights and stimulating questions.

My special gratitude goes to Prof. Dr. Ulf Karsten for co-reviewing my research, for his valuable advice throughout this project as well as for all his support organising the field trip to Spitsbergen.

I would also like to thank Dr. Petra Werner for her introduction to the microscopy of diatoms and her valuable teaching during field work and in the O-lab.

Many thanks to Heba Mohamed, Doris Ilicic, Desirée Juchem, Dr. Lara Prelle and Kiara Franke for the motivation, shared experiences and making the research work both fun and educational.

I am deeply thankful to Kim Govers, Jana Bansemer and Juliane Bettig who assisted me during the laboratory work. Thank you for your patience and constant support concerning molecular work, processing of diatom samples and the work at the scanning electron microscope.

I thank Susan Mbedi and Sarah Sparmann from the BeGenDiv for their advice and support concerning metabarcoding and next generation sequencing.

I thank my family and friends who always support me and believed in me. Thank you, André, for all your patience and pep talks. Many thanks to my parents, to Alex and Laura as well as to Susann, Michael, Grace, Helena, Ilona and Günther. Thank you, Adrian, for being a special gift during this time.

Declaration of Independence

I hereby declare that I alone am responsible for the content of my doctoral dissertation and that I have only used the sources or references cited in the dissertation.

Contents

Summary

Polar regions play a critical role in the Earth's climate system and global nutrient circulation and comprise many different habitats with unique organisms. The seasonal change from the polar night to the midnight sun distinguishes the polar regions from all others of the world. The marine organisms living in these regions have to cope with extreme seasonality of light, temperature, salinity and sea ice. One ecologically particularly important group of eukaryotic microorganisms in polar shallow water coastal zones are benthic diatoms. Diatoms are among the largest and ecologically most successful groups of protists, as they are widespread in almost all aquatic habitats on Earth and contribute significantly to annual carbon fixation. Despite their influential ecological role, there is still little information on their biodiversity in the polar seas.

The Diatom Research group of the Botanic Garden and Botanical Museum Berlin in cooperation with the Applied Ecology and Phycology group of the University of Rostock initiated a first study to expand the knowledge about the biodiversity of benthic diatoms in Antarctica by using a combined approach of morphology, culturing and DNA metabarcoding. This project was funded by the Priority Program "Antarctic Research with Comparative Studies in Arctic Ice Regions" of the German Research Foundation. Benthic samples from marine, brackish and freshwater habitats were collected in Potter Cove, King George Island on the Antarctic Peninsula.

162 clonal cultures were successfully established at the Botanic Garden Berlin, resulting in the identification of 60 taxa. A taxonomically validated reference library for Antarctic benthic diatoms with comprehensive information on habitat, morphology and DNA barcodes (*rbc*L and 18SV4) was created. Three of the most abundant species were *Navicula* cf. *perminuta*, *Nitzschia annewillemsiana* and *Navicula gregaria* in marine, freshwater and brackish water habitats, respectively. Combining the total morphological richness of 174 taxa, including clones, with an additional 72 taxa assigned by metabarcoding only, resulted in 238 taxa in total. Taxa, which could be assigned on species level showed a high level of endemicity. Finally, all reference sequences were linked to diatom specimens deposited in the Herbarium Berolinense to ensure a complete chain of evidence and further subsequent investigations. The barcode reference library of Antarctic species made it possible to assign 47 taxa in the metabarcoding analyses that could not be assigned previously because no suitable reference sequences were available.

Two taxa, *Planothidium wetzelii* and *Chamaepinnularia australis*, were newly described within this thesis. The separation of both taxa was only possible by the combined investigation of

morphological and molecular traits, which highlights the importance of an integrative taxonomy for diatoms. *Chamaepinnularia australis* belongs to a genus that is frequently found in the Antarctic and Arctic. Since its first description almost 30 years ago, its position in the diatom tree of life remained uncertain. Molecular phylogeny in combination with the study of morphological features revealed the monophyly of this genus and its allocation to the Sellaphoraceae family. Molecular data are valuable for determining the phylogenetic position of diatom taxa and have proven particularly useful for genera that have been difficult to classify solely based on morphological characters.

The clonal diatom cultures have been integrated into the culture collection of the University of Rostock and have been successfully used for ecophysiological studies. The exposure of five strains to total darkness over a period of three months showed that the utilization of storage lipids is one of the key mechanisms in Antarctic benthic diatoms to survive the polar night. Despite an ultrastructural observable degradation of the chloroplast, photosynthetic performance did not change significantly. Further, photosynthesis, respiration, and growth response patterns were investigated as functions of varying light availability, temperature, and salinity in six benthic diatom strains. All of them showed a high ecophysiological plasticity with activity patterns exceeding the environmental range they usually experience in situ. This may represent an important trait to cope with climate change in the Antarctic Peninsula. A thorough taxonomic investigation combined with the evaluation of the biogeographical expansion of a species is required as a baseline for ecophysiological experiments to draw sound conclusions about their adaptation to environmental conditions.

To summarise, this project has revealed a remarkably high benthic diatom diversity in the coastal areas of Antarctica. Still, many species are not yet recorded in reference databases. Furthermore, the metabarcoding results indicate a high cryptic diversity with many unassigned taxa even on genus level, which emphasises the need for a further intensive taxonomic investigation of benthic diatom in this region. The genotypic data obtained by DNA barcoding combined with phenotypic information obtained by studying the morphology of marine benthic diatoms are urgently needed to improve our fundamental understanding of the biodiversity and biogeography of diatom communities in the Antarctic. Such data sets not only provide a basis for biodiversity studies, but also for future monitoring programmes, e.g. when investigating the effects of coastal erosion on the benthic diatom flora, for geological questions on the reconstruction of the palaeoenvironment and for the effects of climate change.

Zusammenfassung

Die Polarregionen spielen eine entscheidende Rolle für das Klimasystem der Erde und die globale Nährstoffzirkulation. Sie umfassen viele verschiedene Lebensräume mit einzigartigen Organismen. Der jahreszeitliche Wechsel von der Polarnacht zur Mitternachtssonne unterscheidet die Polargebiete von allen anderen Regionen der Welt. Infolgedessen müssen die hier lebenden Meeresorganismen mit extremen jahreszeitlichen Schwankungen von Licht, Temperatur, Salzgehalt und Meereis zurechtkommen. Eine ökologisch besonders wichtige Gruppe von eukaryotischen Mikroorganismen in den polaren Flachwasserküstenzonen sind benthische Diatomeen. Diatomeen gehören zu den ökologisch erfolgreichsten Gruppen von Protisten, da sie in fast allen aquatischen Lebensräumen der Erde weit verbreitet sind und wesentlich zur jährlichen Kohlenstofffixierung beitragen. Trotz ihrer wichtigen ökologischen Rolle gibt es immer noch wenig Informationen über ihre Artenvielfalt in den Polarmeeren.

Die Diatomeen-Forschungsgruppe des Botanischen Gartens und Botanischen Museums Berlin initiierte in Zusammenarbeit mit der Arbeitsgruppe Angewandte Ökologie und Phykologie der Universität Rostock 2019 eine erste Studie, um das Wissen über die Artenvielfalt benthischer Diatomeen in der Antarktis mit Hilfe eines kombinierten Ansatzes aus Morphologie, Kultivierung und DNA-Metabarcoding zu erweitern. Dieses Projekt wurde durch das Schwerpunktprogramm „Antarktisforschung mit vergleichenden Untersuchungen in arktischen Eisgebieten“ der Deutschen Forschungsgemeinschaft gefördert. Benthische Proben aus Meeres-, Brack- und Süßwasserhabitaten wurden in Potter Cove, King George Island auf der Antarktischen Halbinsel, gesammelt.

Insgesamt wurden 162 Klonkulturen im Botanischen Garten Berlin erfolgreich etabliert, was zur Identifizierung von 60 Taxa führte. Eine taxonomisch validierte Referenzbibliothek für antarktisch benthische Diatomeen mit umfassenden Informationen über Lebensraum, Morphologie und DNA-Barcodes (*rbc*L und 18SV4) wurde erstellt. Drei der am häufigsten vorkommenden Arten waren *Navicula* cf. *perminuta*, *Nitzschia annewillemsiana* und *Navicula gregaria* in Meeres-, Süß- bzw. Brackwasserhabitaten. Die Kombination des gesamten morphologischen Reichtums von 174 Taxa, einschließlich der Klonkulturen, mit zusätzlichen 72 Taxa, die nur durch das Metabarcoding zugeordnet wurden, ergab insgesamt 238 Taxa. Taxa, die auf Artniveau identifiziert werden konnten, wiesen einen hohen Anteil an Endemiten auf. Schließlich wurden alle Referenzsequenzen mit den im Herbarium Berolinense hinterlegten Belegmaterial verknüpft, um eine vollständige Datenlage für weitere Untersuchungen zu gewährleisten. Die Barcode-Referenzbibliothek antarktischer Arten

ermöglichte es, in den Metabarcoding-Analysen 47 Taxa zuzuordnen, die zuvor nicht identifiziert werden konnten, da keine Referenzsequenzen verfügbar waren.

Zwei Taxa, *Planothidium wetzelii* und *Chamaepinnularia australis*, wurden im Rahmen dieser Arbeit neu beschrieben. Die Neubeschreibung beider Taxa war nur durch die kombinierte Untersuchung von morphologischen und molekularen Merkmalen möglich, was die Bedeutung einer integrativen Taxonomie für Diatomeen unterstreicht. *Chamaepinnularia australis* gehört zu einer Gattung, welche häufig in der Antarktis sowie der Arktis vorkommt. Seit ihrer Erstbeschreibung vor fast 30 Jahren blieb ihre Position im Stammbaum der Diatomeen ungewiss. Die molekulare Phylogenie in Kombination mit der Untersuchung morphologischer Merkmale ergab die Monophylie dieser Gattung und ihre Zuordnung zur Familie der Sellaphoraceae. Molekulare Daten sind wertvoll für die Bestimmung der phylogenetischen Position von Diatomeen und haben sich als besonders nützlich bei Gattungen erwiesen, deren Klassifikation basierend auf morphologischen Merkmalen schwierig war.

Die klonalen Diatomeenkulturen wurden in die Kultursammlung der Universität Rostock integriert und erfolgreich bei ökophysiologischen Studien eingesetzt. Die Exposition von fünf Stämmen in totaler Dunkelheit über einen Zeitraum von drei Monaten zeigte, dass die Nutzung von Speicherlipiden einer der Schlüsselmechanismen in antarktisch benthischen Diatomeen ist, um die Polarnacht zu überleben. Trotz einer ultrastrukturellen Degradation der Chloroplasten änderte sich die photosynthetische Leistung nicht wesentlich. Darüber hinaus wurden Photosynthese, Respiration und Wachstum von sechs benthischen Diatomeenstämmen in Abhängigkeit von der Lichtverfügbarkeit, der Temperatur und dem Salzgehalt untersucht. Alle zeigten eine hohe ökophysiologische Plastizität mit Aktivitätsmustern, die über den Umweltbereich hinausgehen, welchen sie normalerweise in situ vorfinden. Dies könnte eine wichtige Eigenschaft zur Anpassung an den Klimawandel auf der Antarktischen Halbinsel sein. Eine gründliche taxonomische Untersuchung in Verbindung mit der Bewertung der biogeografischen Ausbreitung einer Art ist als Grundlage für ökophysiologische Experimente erforderlich, um fundierte Schlussfolgerungen über ihre Anpassung an die Umweltbedingungen zu ziehen.

Zusammenfassend lässt sich sagen, dass dieses Projekt eine bemerkenswert hohe Vielfalt an benthischen Diatomeen in den Küstengebieten der Antarktis zutage gefördert hat. Dennoch sind viele Arten noch nicht in Referenzdatenbanken erfasst. Darüber hinaus deuten die Metabarcoding-Ergebnisse auf eine hohe kryptische Vielfalt hin mit vielen sogar auf Gattungsebene nicht zuordenbaren Taxa, was die Notwendigkeit einer weiteren intensiven

taxonomischen Untersuchung der benthischen Diatomeen in dieser Region hervorhebt. Die durch DNA-Barcoding gewonnenen genotypischen Daten in Kombination mit phänotypischen Informationen, die durch die Untersuchung der Morphologie mariner benthischer Diatomeen gewonnen werden, werden dringend benötigt, um unser grundlegendes Verständnis der Biodiversität und Biogeographie der Diatomeengemeinschaften in der Antarktis zu verbessern. Solche Datensätze bieten nicht nur eine Grundlage für Biodiversitätsstudien, sondern auch für zukünftige Monitoringprogramme, z.B. bei der Untersuchung der Auswirkungen der Küstenerosion auf die benthische Diatomeenflora, für geologische Fragen zur Rekonstruktion der Paläoumwelt und für die Auswirkungen des Klimawandels.

1 General Introduction

The diversity of life on Earth is remarkable ranging from microbes to mammalians and from genes to ecosystems. Life is found in almost all environments and the number of species is many times greater than we could have imagined a century ago. Mora et al. (2011) suggests that some 86 % of the species on Earth, and 91 % in the ocean, still await description. Microorganisms represent the majority of the phylogenetic and functional diversity on Earth. However, we are just beginning to grasp the drivers of microbial diversity and biogeography, which presents a substantial barrier to recognizing community dynamics and ecosystem functioning (Barberán et al. 2014, Escalas et al. 2019). Recently, an explosion of research took place fueled by methodological improvements that make it feasible to characterize microbial communities to a new extent (Falciatore et al. 2019, Clark et al. 2023). Particularly, the rapid accumulation of molecular data is uncovering a vast diversity, abundant uncultivated microbial groups and novel microbial functions (Prosser et al. 2007, Barberán et al. 2014, Srivastava et al. 2019).

1.1 Introduction to diatoms

An ecologically particularly important group of eukaryotic microorganisms are diatoms (Bacillariophyta, Figures 1-7) belonging to the division Heterokontophyta, also known as stramenopiles (Round et al. 1990, Stiller et al. 2014, Falciatore et al. 2019). They are one of the largest and ecologically most successful protist groups as they are distributed in nearly all waters on Earth from tropical and subtropical regions to polar ecosystems (Round et al. 1990). They inhabit a broad spectrum of habitats, such as marine (Witkowski et al. 2000) to fresh waters (Lange-Bertalot et al. 2017), terrestrial (Van de Vijver et al. 2002, Foets et al. 2020) and even aerial environments (Wetzel et al. 2013, Furey et al. 2020). According to their life mode, they can be separated into planktonic forms, suspended in the water column, and benthic forms, living on top of or associated with sediments, rocks, sea ice or as epiphytes.

1.1.1 Evolution and phylogeny

Diatoms are characterised by a complex evolutionary history. The plastids of plants and algae, such as diatoms, are considered to be remnants of a photosynthetic cyanobacterium. Phylogenetic dating of duplicated ATPase proteins suggest that a cyanobacterium was engulfed by a heterotrophic host via primary endosymbiosis in the later Proterozoic approximately 900 mya (Shih and Matzke 2013) and gave rise to the red and green algal lineages as well as to the glaucophytes. This endosymbiosis event involved the transfer of many hundreds of genes, e.g. genes that encode proteins involved in photosynthesis, from the cyanobacterial endosymbiont

to the host nucleus. Those cyanobacterial genes persist in the red algal nucleus (Martin et al. 1998, Nisbet et al. 2004).

Suggested by the structure of the plastids, a second endosymbiotic event of a heterotrophic eukaryote and a red alga gave rise to the stramenopiles, including the diatoms, cryptophytes, and haptophytes (Cavalier-Smith 1999) which together comprise the chromealveolate group (Adl et al. 2005). The plastids in this group are still surrounded by the red algal plasma membrane and the plastids' stroma is separated from the cytoplasm by four topologically distinct membranes (Cavalier-Smith 1999). Furthermore, diatom genome sequence reveals a second gene transfer of genes with cyanobacterial origin from the primary host nucleus into the secondary host nucleus (Armbrust et al. 2004, Nisbet et al. 2004).

However, a clear understanding of how the chromealveolate group acquired photosynthetic organelles has been complicated by conflicting phylogenetic results. Investigating the evolution of photosynthesis by using complete genomes from three of the four major chromalveolate algal lineages provides robust support for acquisitions of photosynthesis through serial endosymbiosis within this group (Stiller et al. 2014). In addition, some plastid-targeted genes in chromalveolates are apparently coming from green algae. Moustafa et al. (2009) estimated by a genome-wide approach that 16 % of the diatom nuclear coding potential are of green algal derivation. A repeated analysis on an extended dataset found approximately equal evidence for red and green algal origins for diatoms genes (Morozov and Galachyants 2019). Horizontal gene transfer also contributed to the complex history of gene acquisitions in diatoms (Chan et al. 2012).

The diatom crown age is estimated at approximately 190 mya, placing the origin of diatoms near the Triassic-Jurassic boundary (Nakov et al. 2018a). However, the oldest diatom fossil is dated approximately 125 mya, thus creating a 75 my gap. The lack of a Jurassic diatom fossil records could have several explanations: diatoms were not present in the Jurassic, a patchy distribution that makes them difficult to find, they could have been lightly silicified or the oceanic crust from the Jurassic that might have contained sediments with marine diatom microfossils has been subducted (Bryłka et al. 2023).

Diatoms were divided into three classes: Coscinodiscophyceae Round & Crawford, emend. Medlin & Kaczmarska with centric cells usually radially ornamented from a central point, Mediophyceae (Jouse & Prosbkina-Lavrenko) Medlin & Kaczmarska with usually bi-or multipolar cells with radial ornamentation and Bacillariophyceae Haeckel, emend. Medlin & Kaczmarska with bipolar cells, usually with bilateral symmetry also called pennate diatoms

(Medlin and Kaczmarska 2004). However, monophyly of those classes is under debate (Theriot et al. 2009, Medlin 2016).

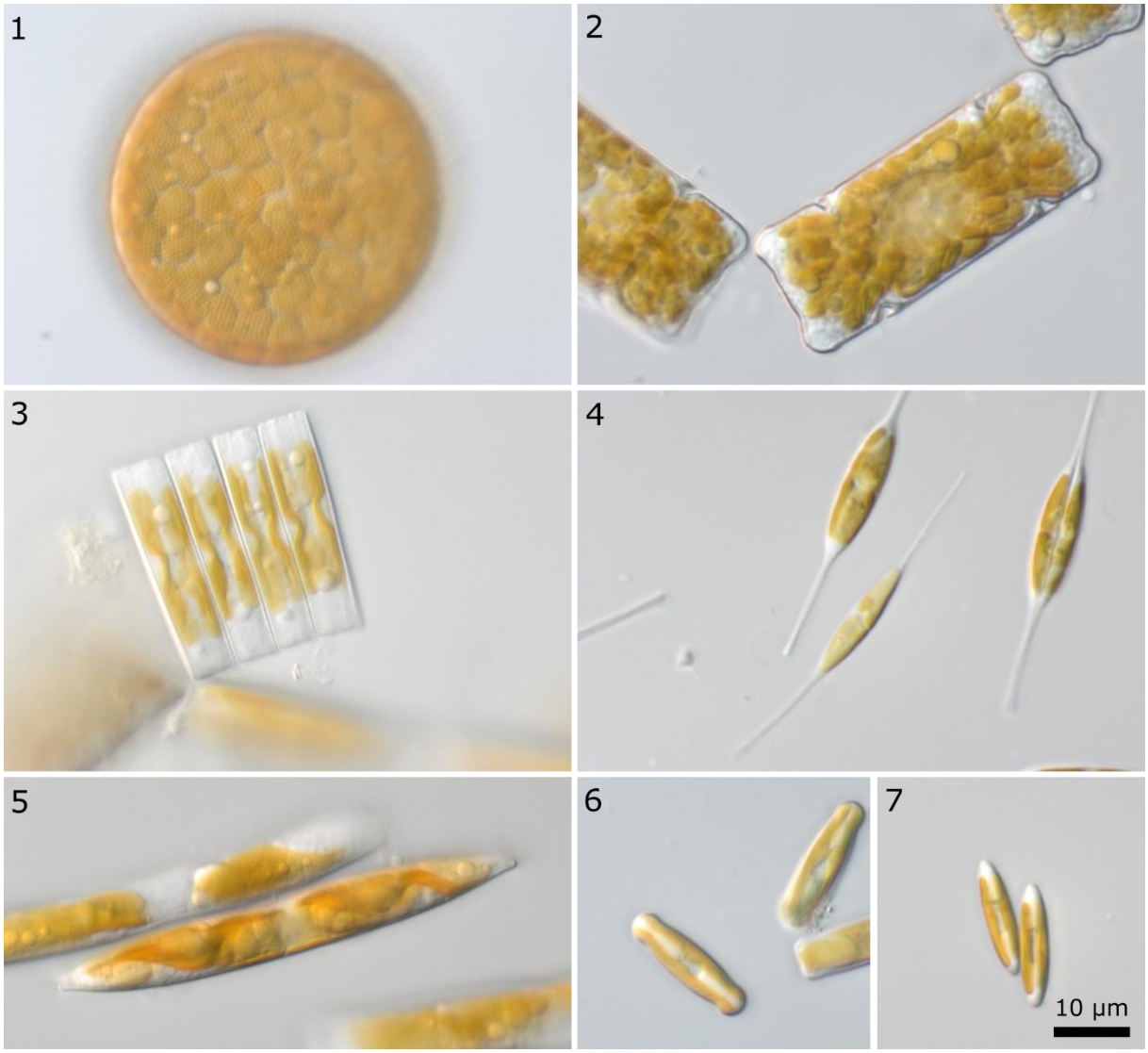

Figures 1-7 LM pictures of different forms of alive Antarctic diatoms. **1** planktonic centric *Porosira* cf. *glacialis* **2** chain forming bipolar frustules of *Odontella litigiosa* (Van Heurck) Hoban **3** chain forming *Synedropsis* cf. *recta* **4** needle like *Cylindrotheca* cf. *closterium* **5** benthic pennate *Nitzschia medioconstricta* Hustedt **6** benthic pennate *Chamaepinnularia australis* Schimani & N.Abarca **7** benthic pennate *Navicula* sp.

Pennate diatoms evolved from the centric forms (Nakov et al. 2018a). They can be subdivided into nonmotile araphid and raphid species. Species processing a raphe, a longitudinal slit in the cell wall, utilize gliding for cell movement through secretion of mucilage containing actin-myosin protein complexes (Preston et al. 1990, Poulsen et al. 1999). The raphid group outnumbers the species diversity estimated for both centric and araphid pennate diatoms (Guiry and Guiry 2024). The evolution of motility in vegetative cells, following an earlier transition from oogamy to anisogamy, may eased outcrossing and improved utilization of habitat

complexity finally leading to enhanced opportunity for adaptive divergence across a variety of novel habitats (Nakov et al. 2018a).

Genome sequencing of *Thalassiosira pseudonana* Hasle & Heimdal (Mediophyceae) by Armbrust et al. (2004) and *Phaeodactylum tricornutum* Bohlin (Bacillariophyceae) by Bowler et al. (2008) revealed that only about 57 % of genes are shared (Prihoda et al. 2012). The divergence can be compared with the difference between *Homo sapiens* and *Takifugu rubripes* (puffer fish), which separated around 550 million years ago. This points to a high rate of diatom gene modification, as well as gene exchanges with other organisms, all of which most likely contributed to high diatom diversification rates (Prihoda et al. 2012).

1.1.2 Cell biology

Due to their dynamic evolutionary history with different endosymbiotic events, diatoms seem to have red algal-derived chloroplasts empowered by green algal proteins, and mitochondria derived from the non-photosynthetic exosymbiont (Prihoda et al. 2012). Consequently, diatoms are characterized by a complex combination of genes and metabolic pathways that may have contributed to their profound ecological success (Armbrust 2009).

Most diatom species are photosynthetic containing chlorophyll (Chl) a/c (Round et al. 1990, Prihoda et al. 2012, Falciatore et al. 2019). The diversity of chloroplast forms, their number and location within the cell, as well as pyrenoid structure, differentiates diatoms from other groups of stramenopile algae. The chloroplast structure is even considered to be informative for taxonomic and phylogenetic studies (Bedoshvili et al. 2009, Skibbe et al. 2022).

Unlike plants, diatoms store energy in the form of the polysaccharide chrysolaminarin (β-1,3-glucan (Huang et al. 2018), which can constitute up to 80 % of the organic dry weight in certain growth phases (Myklestad 1974). Furthermore, diatoms can synthesize storage lipids, mostly triacylglycerol, which are sequestered in lipid bodies (Leyland et al. 2020). The genetic mixture of diatoms results in unique biochemical capabilities, such as the combination of an animal-like ability to generate chemical energy from lipid degradation with a plant-like ability to generate metabolic intermediates from this reaction that probably allows diatoms to survive long periods of darkness (Armbrust 2009). In conclusion, the metabolic strategies among diatom species range from photoautotrophy to heterotrophy. Even parasitism has been reported for diatoms (Bavestrello et al. 2000).

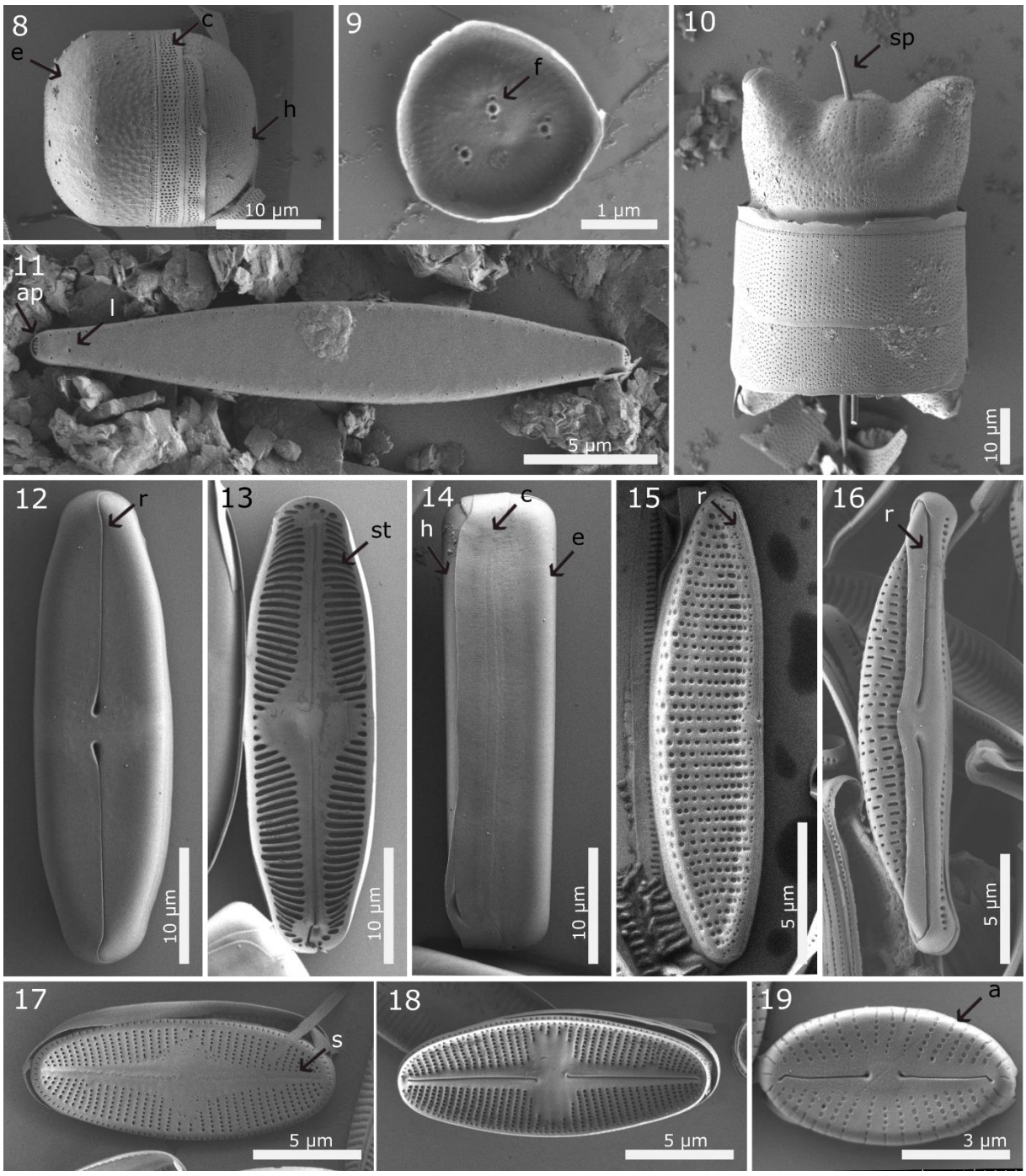

Figures 8-19 SEM pictures of valves from different Antarctic diatoms with their ultrastructural features. **8** *Melosira* sp. **9** *Minidiscus chilensis* P.Rivera **10** *Odontella litigiosa* **11** *Synedropsis* cf. *recta* **12-14** *Pinnularia australomicrostauron* Zidarova, Kopalová & Van de Vijver **15** *Nitzschia annewillemsiana* Hamsher, Kopalová, Kociolek, Zidarova & Van de Vijver **16** *Halamphora ausloosiana* Van de Vijver & Kopalová **17,18** *Psammothidium papilio* (D.E.Kellogg, Stuiver, T.B.Kellogg & G.H.Denton) Kopalová & Van de Vijver **19** *Mayamaea sweetloveana* Zidarova, Kopalová & Van de Vijver **a**: areola, one of the pores forming a stria **c**: cingulum series of thin band of silica associated with the valve **e**: epivalve, larger half of the frustule **f**: fultoportula, process passing through the valve **h**: hypovalve, smaller half of the frustule **r**: raphe, slit within the silica cell wall, can be positioned axial (*Pinnularia*), eccentric (*Halamphora*) or within a keel (*Nitzschia*). **s**: sternum, longitudinal hyaline silica element along the apical axis **sp**: spine, pointed silica extension **st**: stria, consisting of one or several rows of areolae, in *Pinnularia*: elongated chamber forms the stria, called the alveolus.

The hallmark of the diatom is its cell wall, called a frustule, which is highly differentiated and almost always heavily impregnated with silica (Figures 8-19). The wall consists of two large, intricately sculptured units called valves, together with several thinner, linking structures termed girdle elements or cineture (Round et al. 1990). Studies with the centric diatom *Thalassiosira pseudonana* showed that there are two major steps in valve formation: 1) formation of the base layer which defines the valve shape in the x/y plane and major features e.g. ribs and pores, and 2) expansion in the z-axis direction by additional polymerization of silica to form a rigid structure. The silica morphology of the valve varies depending on the structural feature being made (Hildebrand et al. 2018). Besides silica, the wall also contains organic material, which forms a thin layer around the valves and girdle elements (Round et al. 1990). Several classes of proteins known to be associated with the wall or embedded in the silica itself were identified. It is hypothesized that they catalyse polymerization of silica, constitutes an organized pattern for base layer formation and serve as intermediates that translate cytoskeletal assembly patterns into similar silica structures. Further, they may occlude the pores in the cell wall and thereby impart a level of control over what passes through the pores (Hildebrand et al. 2018).

1.1.3 Life cycle and reproduction

Diatoms are diploid organisms in their vegetative stage. Their life cycle consists of a prolonged vegetative phase lasting months to years, during which the cells divide mitotically and a comparatively short phase that includes sexual reproduction followed by a complex developmental process resulting in the formation of new vegetative cells (Chepurnov et al. 2004).

Like the cells of other organisms during the cell cycle, diatoms must double their organelles, replicate their chromosomes, and then segregate a full complement of components to each daughter cell. In addition, each daughter cell must synthesise a new set of wall elements to accompany the set inherited from its parent (Round et al. 1990). In general, the two valves of a cell are identically shaped but slightly different sized: the larger epitheca and the smaller hypotheca. When diatom cells divide, each daughter cell retains one valve from the original frustule and a new hypotheca is synthesized inside the cells of the previous generation resulting in a progressive reduction in cell size (Round et al. 1990, Montresor et al. 2016). Most diatoms species escape this progressive size reduction through sexual reproduction involving meiosis and syngamy. The zygote is not surrounded by a rigid siliceous frustule, and it can thus expand forming the auxospore - a specially constructed cell of diatoms that expands to re-establish

maximum size (Montresor et al. 2016, Poulíčková and Mann 2019). In many diatom species, sexual reproduction can only be induced below a specific cell size threshold (Falciatore et al. 2019).

Though the basic pattern of sexual behaviour in diatoms is generally conserved, there are important differences between centrics and pennates. Following meiosis, most centric diatoms produce large macro-gametes (egg cells) and small uni-flagellated microgametes (sperm cells). They are mostly homothallic, i.e. within a clonal strain, some cells produce egg-cells, and others sperm-cells (Montresor et al. 2016). However, the results of recent and older research suggest that the life cycles of centric diatoms may be more flexible and varied than previously thought since some species are able to enlarge by auxospores produced non-oogamously, or through vegetative enlargement (Poulíčková and Mann 2019).

Pennate diatoms produce non-flagellated gametes of equal (isogametes) or unequal (anisogametes) size (Montresor et al. 2016). Isogamy has been found in most pennate species, which is preceded by gametangial copulation. Formation of isogametes represents a major innovation and relates to their benthic way of life since this mode of reproduction works best when partner cells can remain in close contact with one another during gamete formation and do not disperse as in the plankton (Kooistra et al. 2007). Pennate diatoms include mostly heterothallic species, in which sex is induced only when strains of opposite mating type (MT^+ and MT^-) are in close contact (Poulíčková and Mann 2019). However, some species are not obligatorily heterothallic, as they exhibit intraclonal auxosporulation (Davidovich et al. 2010, Skibbe et al. 2022).

There is an enormous variation in sexual reproduction and auxosporulation in pennate diatoms which let Geitler (1973) to a detailed classification dividing them into categories on the basis of gamete behaviour, the presence/absence of copulation structures, pairing methods, and auxospore orientation. However, it is not easy to find characters that continue to give a convincing phylogenetic signal at higher taxonomic levels (Poulíčková and Mann 2019).

There has been a rapid progress during the last two decades in the understanding of sexual reproduction in pennate diatoms, mostly based on the model organism *Seminavis robusta* D.B.Danielidis & D.G.Mann. It has been shown that a sex-inducing pheromone triggers the switch from mitosis to meiosis in the opposing mating type, coupled with the transcriptional induction of proline biosynthesis genes, and the release of the proline-derived attraction pheromone (Moeys et al. 2016). Bondoc et al. (2016) reports that cells of the migrating mating type (MT^+) respond to pheromone gradients by simultaneous chemotaxis and chemokinesis.

Changes in movement behaviour enable MT^+ cells to locate the direction of the pheromone source and to maximize their encounter rate towards it. In addition, first insights into the influence of bacteria on diatom sexual reproduction suggest that different species of bacteria reduce or enhance the reproductive success, e.g. *Maribacter* sp. exudates cause a reduced production of the attraction pheromone (Cirri et al. 2019). However, there is still little or no information on sexual reproduction for most other pennate diatom genera.

1.1.4 Photosynthesis and ecosystem function of benthic diatoms

The general biochemical structures and functions of the complexes involved in oxygenic photosynthesis are conserved in most phototrophs (Falciatore et al. 2019). Though diatom photosynthesis is highly efficient under dynamic light regimes compared to green algae (Wagner et al. 2006). Viridiplantae (including plants and green algae) and diatoms have achieved a similar functional topology of the photosystems (PS) to optimize photosynthetic light utilization (Flori et al. 2017). However, this functional equivalence is achieved with different thylakoid architectures. In diatoms, the photosynthetic modules are embedded in the thylakoid membrane and thylakoids are organized in homogeneous stacks of three, which run along the whole diatom plastid (Berkaloff et al. 1990, Büchel et al. 2022). In contrast to plants, where the PSII is mainly located in grana stacks and the PSI is mostly found in stroma lamellae (Gu et al. 2022), the distance between the two photosystems in diatoms is short. Therefore, while PSs confinement constrains electron flow in plants, possibly limiting photosynthesis, no such limitation is observed in diatoms, where the less structured thylakoids allow very fast redox equilibration between the two PSs (Flori et al. 2017). Next to the above mentioned Chl c and a, diatoms use β-carotene as main carotenoids as well as the pigments fucoxanthin and diadinoxanthin/diatoxanthin (Falciatore et al. 2019).

Diatoms together with other aquatic protists are estimated to contribute less than 1 % to the Earth's total biomass (Bar-On et al. 2018). However, due to their high abundance especially in the plankton, diatoms alone contribute approximately 20 % to annual carbon fixation. Diatom photosynthesis in the sea generates thus about as much organic carbon as all the terrestrial rainforests combined (Field et al. 1998). Hence, diatoms are key contributors to marine food chains. In sequestering atmospheric carbon dioxide (CO_2) to the ocean through gravitational sinking of particles (biological carbon pump) they have high biogeochemical significance (Tréguer et al. 2018).

The assemblage of benthic diatoms together with other microalgae and photosynthetic bacteria is known as microphytobenthos (MPB). In coastal ecosystems MPB contributes significantly

to the primary production (MacIntyre et al. 1996) from estuaries (Colijn and de Jonge 1984, Underwood and Kromkamp 1999, Ask et al. 2016) to intertidal (Hargrave et al. 1983) and deeper subtidal sites (Cahoon and Cooke 1992, Woelfel et al. 2010) as well as exposed coastal sediments (Kuriyama et al. 2021). MPB biomass on temperate continental shelves greatly exceeds that of integrated phytoplankton biomass in the overlying water column (Pinckney 2018). Thus, the global production of benthic microalgae is estimated to range from 8.9 to 14.4 Gt C m^{-2} $year^{-1}$ and represents approximately 20 % of the global ocean production (Cahoon 1999).

In addition, MPB exerts multiple other important functions. As high primary producers it is providing a major food source for a diversity of organisms such as bacteria by excretion of soluble organic matter, benthic protozoans as well as metazoans (Cahoon 1999). Furthermore, the microphytobenthic assemblages influence elemental fluxes at the sediment-water interface (Risgaard-Petersen et al. 1994) and stabilize the sediment surface by excretion of sticky extracellular polymeric substances (de Brouwer et al. 2005).

1.1.5 Diversity and biogeography of diatoms

Currently, around 12,000 diatom species have been described. However, the number of extant species is estimated to be at least 30,000 but probably reaching up to 100,000 by extrapolation from an eclectic sample of genera and species complexes (Mann and Vanormelingen 2013). Already in the last decades the realization developed that the preexisting species classification was too coarse and hid significant diversity (Mann and Droop 1996). Evidence from morphology, genetic data, mating systems, physiology, ecology, and crossing behavior suggests that many species probably contain several reproductively isolated entities that are worth taxonomic recognition at species level (Mann 1999).

It is generally accepted that the distribution and community diversity of macroscopic organisms is shaped by a balance between processes operating on a regional scale, which both add species to communities, such as allopatric species formation and geographic dispersal, and processes capable of promoting local extinction, including predation, competitive exclusion and stochastic variation (Ricklefs 1987). For microorganisms, high dispersal rates and large population sizes have led to the ubiquity hypothesis (Finlay 2002) predicting a limited global species richness and cosmopolitan geographic distributions and making local extinction nearly impossible (Fenchel and Finlay 2004). As a result, microbial eukaryotes are less restricted by geographical barriers and allopatric speciation should be rare or non-existent (Finlay 2002). However, numerous recent studies indicate that microorganisms display patterns in abundance,

distribution, and diversity over space and time (Martiny et al. 2006, Hanson et al. 2012, Kivlin et al. 2020) and the majority of studies confirmed similar patterns of microbial and macro-organismal distributions (Dickey et al. 2021).

Diatom communities are regulated by the same processes that operate in macroorganisms, although possibly to a different degree, implying that dispersal limitation is significant (Vanormelingen et al. 2008). Although cosmopolitan species exist, a distinct biogeography is strongly supported by evidence from different freshwater, soil and marine diatoms (Malviya et al. 2016, Maltsev et al. 2021). Recent studies showed that cosmopolitan benthic as well as planktonic species complexes harbor distinct molecular variation and the presence of cryptic species - morphologically similar but genetically distinct species that, at some point, shared the same specific epithet. The truly cryptic pennate species complex *Pinnularia borealis* Ehrenberg (Pinseel et al. 2019) showed unprecedented high levels of species-diversity, reflecting a global radiation since the Eocene/Oligocene global cooling (Pinseel et al. 2020). The authors suggest that diversification was largely driven by colonization of novel geographic areas and subsequent evolution in isolation. The fine-scaled investigation of *Gomphonema parvulum* (Kützing) Kützing resulted in a separation of four taxa based on their biogeography in Mexico, Korea, central continental Europe and northern Atlantic Europe (Abarca et al. 2014). The planktonic species *Skeletonema costatum* (Greville) Cleve harbors at least eight cryptic species. Once considered to be a key species it may not be cosmopolitan. In fact, it may be absent throughout most of the global coastal ocean sites where it had been reported to dominate plankton dynamics (Kooistra et al. 2008, Smayda 2011). Further, the planktonic genus *Thalassiosira* Cleve encompasses at least ten marine and four freshwater diatom genera that range from 4–63 my in age (Nakov et al. 2018b).

Furthermore, large regions of the planet where diatoms are abundant remain unexplored. Several studies with sensitive taxonomies reveal endemism in isolated areas such as New Caledonia (Moser et al. 1998) and Antarctica (Verleyen et al. 2021) as well as lakes, e.g. Lake Tanganyika (Cocquyt 2000). Chonova et al. (2023) showed that the majority of diatom freshwater genotypes remained specific to a single geographic region and hypothesize that freshwater diatoms disperse over long distances and across oceans but at rates that allow the appearance of local genetic variants and the regionalization of assemblages. While comparing high-altitude alpine French and Georgian lakes Rimet et al. (2023) found that endemism was the rule at sub-species level. Most species were shared across both lakes, suggesting that geographic barriers strongly limited dispersal at the sub-species level but not species level.

In conclusion, the large number of species paired with the broad range of habitats in which diatoms survive suggest diatoms have a high capacity for adaptive evolution and radiation, large reservoirs of genetic variation that support contemporary evolution, and sufficient genetic subdivision to allow for speciation, even in planktonic environments where diatoms can experience high levels of dispersal across the surface ocean (Rynearson et al. 2022).

1.2 Methods to investigate taxonomy, biodiversity, and phylogeny of diatoms

1.2.1 Traditional morphological classification and identification

The valve structure has been studied more than any other aspect of the diatom cell since the frustule provides an array of ultrastructural traits. Traditionally, diatom classification depended largely upon morphological variation in shape and the arrangement of the wall organelles (e.g. striae, raphes, areolae, portulae, etc.; Figures 8-19) implying a morphological species concept (Round et al. 1990). Until the end of the last century, the classification was based on light microscopic (LM) observations and incorporated morphometric data like length width and striation density together with visible features like striation pattern.

The scanning electron microscope (SEM) revolutionized diatom systematics by revealing taxonomically important ultrastructural features. In many marine littoral and sublittoral benthic habitats, small diatoms with almost no features resolvable in LM can be frequently found and only SEM investigations revealed their true diversity, e.g species from the genera *Pteroncola* R.W.Holmes & D.A.Croll (Almandoz et al. 2014), *Ambo* Witkowski, Ashworth, Lange-Bertalot & G.Klein (Witkowski et al. 2020) or *Lunella* Snoeijs (Snoeijs 1996).

Taxonomy provides the fundamental units around which biodiversity is organized and assessed, and the binomial nomenclature emerged about as a standardized and common means to reference the identity of organisms (Sandall et al. 2023). Further, the detection of biogeographical patterns and the assessment of rarity are inextricably linked with taxonomy (Mann and Droop 1996). Unambiguous identification at the species level is crucial when assessing biodiversity and the distribution of diatoms. Species identification of diatoms is time-consuming and needs in-depth knowledge of organisms under investigation. Furthermore, identification of diatom frustules is greatly influenced by the magnification at which samples are examined. Many diagnostic features of diatoms cannot be recognized even at higher LM magnifications, which might lead to distortion of the biodiversity assessment or overestimation of geographical distribution (Morales et al. 2001). Reliable identifications are essential, with SEM observations largely improving resolution.

1.2.2 Integrated taxonomy and the application of molecular classification

Diatom taxonomy has developed using a limited range of characters mostly drawn from the valve as only one part of the phenotype. Morphological differences of the valve have been used to split taxa without any significant attempt to understand how these differences arose during ontogeny or how they developed in the course of evolution (Mann 1999). While the ultrastructure of the valve remains consistent, cell size and shape are subject to great variation over the life cycle of diatom species due to size reduction during mitosis or changing environmental conditions (Cox 2014, Mohamad et al. 2022).

Considering that diatoms are sexual, meiotic organisms and classification should thus recognise the entire life cycle of a species, the traditionally applied morphological species concept is under debate (Mann 1999, Kociolek and Spaulding 2002). The complexity of species biology requires that species boundaries be studied from multiple, complementary perspectives (Dayrat 2005) like morphological characters (valve, girdle, chloroplast), ecological data, reproductive traits as well as molecular data. An integrative approach to taxonomy is therefore needed. Several studies integrated evidence from mating experiments to investigate species boundaries pointing to a biological species (Mann et al. 2004, Kim et al. 2020, Postel et al. 2020). However, mating experiments in diatoms are not always possible and it remains unclear how the realization of breeding potential under controlled, laboratory conditions can be transferred to what occurs in vivo (Alverson 2008).

Especially the application of molecular techniques to diatom research has revealed to be an important key in the delimitation of diatom species, which led to the increasing discovery of cryptic and pseudo-cryptic species (e.g. Kaczmarska et al. 2014, Jahn et al. 2017, further see chapter 1.1.5) - the latter are species that can be distinguished morphologically once the appropriate characters are considered (Knowlton 1993). Non-repetitive DNA sequences are the primary source of data for molecular systematic studies of diatoms at all taxonomic levels (Alverson 2008) and several molecular markers including small subunit 18S ribosomal DNA (18S rDNA), large subunit 28S rDNA, the internal transcribed spacer (ITS) between the rDNA genes, ribulose-1,5-bisphosphate carboxylase/oxygenase (*rbc*L), and cytochrome c oxidase 1 (cox1) have been successfully applied. Tested for the genus *Sellaphora* Mereschowsky cox1 divergence was usually much greater than *rbc*L divergence and always much more variable than 18S rDNA (Evans et al. 2007). Wang et al. (2022) proven high resolution for mitochondrial DNA including cox 1. However, cox 1 shows very low amplification and sequencing success rates (Moniz and Kaczmarska 2009, Trobajo et al. 2010). The *rbc*L region has the power to

discriminate between species (Hamsher et al. 2011, Guo et al. 2015). The 18S rRNA gene is effective in clustering higher diatom taxa (Guo et al. 2015). However, long fragments are needed to achieve divergence sufficient for species separation and small genetic distances increase the potential for misidentifications (Moniz and Kaczmarska 2009). The ITS region is highly variable and often chosen to investigate within-population genetic variation (Evans et al. 2007).

In the end, whatever character underlies species delimitation, whether morphological or molecular, the fundamental question remains, how much intraspecific variation can exist before a new species should be separated. Although based on apparently objective data and formal measures for separating species, all decisions for the recognition of a new species will hold some degree of subjectivity (Silva 2008).

1.2.3 Phylogenetic systematics

Defining the names of taxa in terms of common ancestry quits with a tradition of character-based definitions by granting the concept of evolution a central role in taxonomy (Hennig 1966, de Queiroz and Gauthier 1990). The incorporation of phylogeny leads to a more natural classification, which aims to describe taxa that represent unambiguous, closed communities of descent: monophyletic groups. Phylogenetic analysis applies equally well to both molecular and morphological characters (Alverson 2008). In diatoms, qualitative and quantitative morphological characteristics of the silica cell wall and the chloroplast have been applied for phylogenetic inference (e.g. Edgar and Theriot 2004, Cox and Williams 2006).

Phylogenetic analysis of DNA sequences of marker genes has become commonplace in the delimitation of diatom taxa since the approach includes a large number of potential characters for inferring relationships and the utility of molecular data for modelling patterns of nucleotide substitution (Nadler 1995). The resulting gene phylogenies representing a proxy of the organismal phylogeny provided that the genes are ortholog. This special type of homology refers to genes in different species, which have diverged from each other due to speciation and as a result recapitulate the relationships among the species they derive from (Kapli et al. 2020).

During the last decades, phylogenetic analysis revealed non-monophyly of morphological characters long thought to be diagnostic to certain groups of diatoms. Ruck and Theriot (2011) disclosed the non-monophyly of the canal raphe system, a complex and presumably highly derived raphe that is physically separated from the cell interior, most often by a set of siliceous braces. The canal raphe appears to have evolved twice, once in the common ancestor of Rhopalodiales and Surirellales and once in the common ancestor of Bacillariales. A multigene

phylogeny of the Bacillariaceae displayed the non-monophyly of the most speciose diatom genus, *Nitzschia* Hassal as well as several major cryptic clades (Mann et al. 2021). Traditionally, the monoraphid diatoms have been considered as a group derived from biraphid forms and grouped together in the order Achnanthales (Round et al. 1990). Numerous studies indicate the polyphyly of the monoraphid diatoms suggesting the loss of the raphe occurred many times during the evolution of diatoms (Kulikovskiy et al. 2016, Thomas et al. 2016, Davidovich et al. 2017). A further example is the diatom genus *Diprora* S.P.Main. It was described from a cave on Hawai'i. Due to its lack of a raphe system and bilateral symmetry, the genus was first assigned to the araphid diatoms. Molecular phylogenetics show *Diprora* to nest deep within the raphid diatoms. Loss of the raphe system and reduction of other features may be related to its cave-dwelling habit (Kociolek et al. 2013).

Nonetheless, adequate and comprehensive taxon sampling, selection of appropriate target genes and outgroup, as well as the alignment strategy influence the phylogenetic accuracy and are crucial for a reliable phylogeny based on DNA sequences (Alverson and Theriot 2003, Alverson 2008, Lim et al. 2018).

1.2.4 Molecular identification and taxonomic reference library

To investigate the diatom diversity and biogeography of diatoms an accurate and reliable taxon identification is required. As mentioned above due to resolvability of valves in LM, phenotypic plasticity and the high species diversity, morphological identification of diatoms is time consuming and requires expertise. DNA marker genes that are used for taxonomical investigations can be used for molecular identification, too. DNA barcoding is an identification alternative based on the assumption that sequences of a certain marker locus exhibit sufficient variation between species to allow unambiguous identification (Hebert et al. 2003). Utilizing the DNA barcoding concept to diatoms promises an enormous potential to resolve the problem of inaccurate species identification and consequently facilitate analyses of the biodiversity of environmental samples.

A suitable barcode marker should consist of a short sequence that can be easily amplified and sequenced in one read following a standardized laboratory protocol, and still needs the power to resolve organisms at species level (Moritz and Cicero 2004, Zimmermann et al. 2011). Vasselon et al. (2017) proposed a 312 bp long segment of the *rbc*L gene locus as a barcode marker for the analysis of environmental samples with the slightly modified primer pair after Stoof-Leichsenring et al. (2012) and Bruder and Medlin (2007). Zimmermann et al. (2011)

presented in their study a 390–410 bp long fragment of the V4 region of the 18S rRNA gene locus as a barcode marker.

However, for a reliable identification an unambiguous link between geno- and phenotype is crucial. Therefore, a comprehensive taxonomic reference library is required where molecular and morphological data are tied together with a taxonomic name (Stachura-Suchoples et al. 2015). This means that the reference library should consist of taxon names belonging to specimens that have been identified by experts as well as provides descriptions together with barcode sequences, which were derived from well documented strains, e.g. voucher deposition in an herbarium, sampling localities and collectors, basic environmental data, high-resolution LM pictures, morphometrics, taxonomy and nomenclature, maps, literature and references to databases where this data is deposited (Zimmermann et al. 2014). For example, Diat.barcode is an open-access curated library dedicated to diatoms with data coming from the NCBI nucleotide database and from unpublished sequencing data of culture collections (Rimet et al. 2019).

For diatoms, clone cultures need to be established which offer sufficient material for sequencing as well as for identification by light and electron microscopy. Skibbe et al. (2022) presented a technique for culturing benthic diatoms by using enrichment cultures to promote diatom growth followed by single cell extraction including different culture media that had proven to be suitable for many different benthic diatom taxa. Additionally, the live images from cultured diatoms give many insights into chloroplast structures and their dynamic transformation during the diatom life cycle.

1.2.5 DNA Metabarcoding for diatom biodiversity research

DNA metabarcoding has emerged as an alternative to light microscope-based identifications to assess the composition of communities. It corresponds to the simultaneous DNA based identification of many taxa found in the same environmental sample e.g. from soil, water, sediment or even feces or from a bulk sample containing entire organisms (Taberlet et al. 2012). DNA of the targeted barcode is amplified aiming at detecting all taxa from a given taxonomic group, such as diatoms, followed by high throughput sequencing (HTS) to obtain a very large quantity of data per sequencing run (Taberlet et al. 2018). Subsequent sequence analysis includes bioinformatics steps for the preprocessing of the sequences (demultiplexing of samples, paired-end fragment assemblage), cleaning the HTS data (quality filtering, chimera removal) as well as link sequences to reference databases (Bailet et al. 2020).

Since this approach was first tested to assess diatoms communities (Kermarrec et al. 2013, Zimmermann et al. 2015) it has been widely used to investigate diatom biodiversity in

freshwater (e.g. Rimet et al. 2018, Mora et al. 2019) and marine environments (Malviya et al. 2016, Piredda et al. 2018, Pérez-Burillo et al. 2022). Furthermore, DNA metabarcoding based on benthic diatoms has been utilized to monitor community changes and assessing the biological status of a water body (Vasselon et al. 2017, Bailet et al. 2019, Mortágua et al. 2019, Kelly et al. 2020, Pérez-Burillo et al. 2020, Kulaš et al. 2022). A major drawback in all of those studies was the incompleteness of the reference database highlighting the need for cultures to enrich databases.

Despite the apparent simplicity of the method, each step can potentially introduce its own sources of artifacts and biases (see Taberlet et al. 2018, Zinger et al. 2019). PCR amplification is a well-known source of biases. An even more insidious source are “tag jumps”. Tags, unique short nucleotide sequences added on the 5’-end of the primers allow pooling all PCRs within a single sequencing run. However, false combinations of the used tags can occur (Schnell et al. 2015). Even the application of different bioinformatic pipelines can lead to discrepancies, despite the use of the same reference database (Bailet et al. 2020). Therefore, a robust experimental design is needed including several types of experimental controls to facilitate the exclusion of spurious signal and support the reliability of the biological conclusions, like biological and technical replicates, negative controls as well careful consideration of the bioinformatics workflow itself (Zinger et al. 2019). If those criteria are met, DNA metabarcoding can provide a faster and cheaper way of identifying diatom biodiversity as well as help exposing the concealed diversity (Zimmermann et al. 2015). Further, repeated investigations can help monitor community changes especially in changing environments.

1.3 The West Antarctic Peninsula – environment and biodiversity

1.3.1 Geographical background

The Scientific Committee on Antarctic Research (SCAR) considers the Antarctic region to include the continent, its offshore islands, and the surrounding Southern Ocean including the Antarctic Circumpolar Current (ACC, Summerhayes et al. 2009). Around 34 mya, the Drake Passage between South America and the Antarctic Peninsula, as well as the Tasmanian Gateway south of Australia opened. The ACC has begun to circulate around the continent of Antarctica. It is today the strongest and longest current system in the world’s oceans and serves as an important link between the basins of the Atlantic, Pacific and Indian Oceans. Simultaneously it limits meridional exchange and tend to isolate the ocean to the south from heat and substance sources (Borowski et al. 2004). The tectonic isolation coupled with decreasing global

temperatures and concentration of atmospheric CO_2 34 mya at the Eocene-Oligocene boundary induced the first ice formation on the continent's high elevations (Bell and Seroussi 2020).

Today, the continent Antarctica is dominated by the Antarctic Ice Sheet, a vast contiguous mass of glacial ice that covers over 99 % of the Antarctic continent and surrounding seas (Cooper et al. 1994). It is the only continent on Earth without a native human population and with the Antarctic treaty enter into force in 1961 "Antarctica shall continue forever to be used exclusively for peaceful purposes". The Antarctic Peninsula is the only part of the continent that extends a significant way northward from the main ice sheet towards the Drake Passage reaching latitude 63ºS (Figures 20). It is a mountainous region with a mean width of 70 km (Summerhayes et al. 2009).

The Antarctic Peninsula Ice Sheet is relatively small, around 500 m thick and situated on a mountain range. It has numerous steep and fast-flowing outlet glaciers and is perhaps the most vulnerable ice sheet in Antarctica to climate change (Davies et al. 2012). The marine ecosystem of the West Antarctic Peninsula extends for around 1,500 km from the Bellingshausen Sea to the northern tip of the peninsula. The glacially sculpted coastline along the peninsula is highly convoluted, with numerous islands, deeps, bays, fjords, often interconnected by channels, sometimes as deep as 900 m (Ducklow et al. 2012).

King George Island is the biggest of the South Shetland Islands, which lie north of the Antarctic Peninsula. Samples for this thesis were taken at Potter Cove, a shallow coastal bay at King George Island (62°14'S 58°31'W, Figures 22-26). The Argentinean Carlini-Station together with the Dallmann laboratory of the Alfred-Wegener-Institute is located there. The Potter Cove combines zones of glacier fronts, rocky shores as well as extensive soft bottom areas and thereby providing diverse habitats for benthic diatoms.

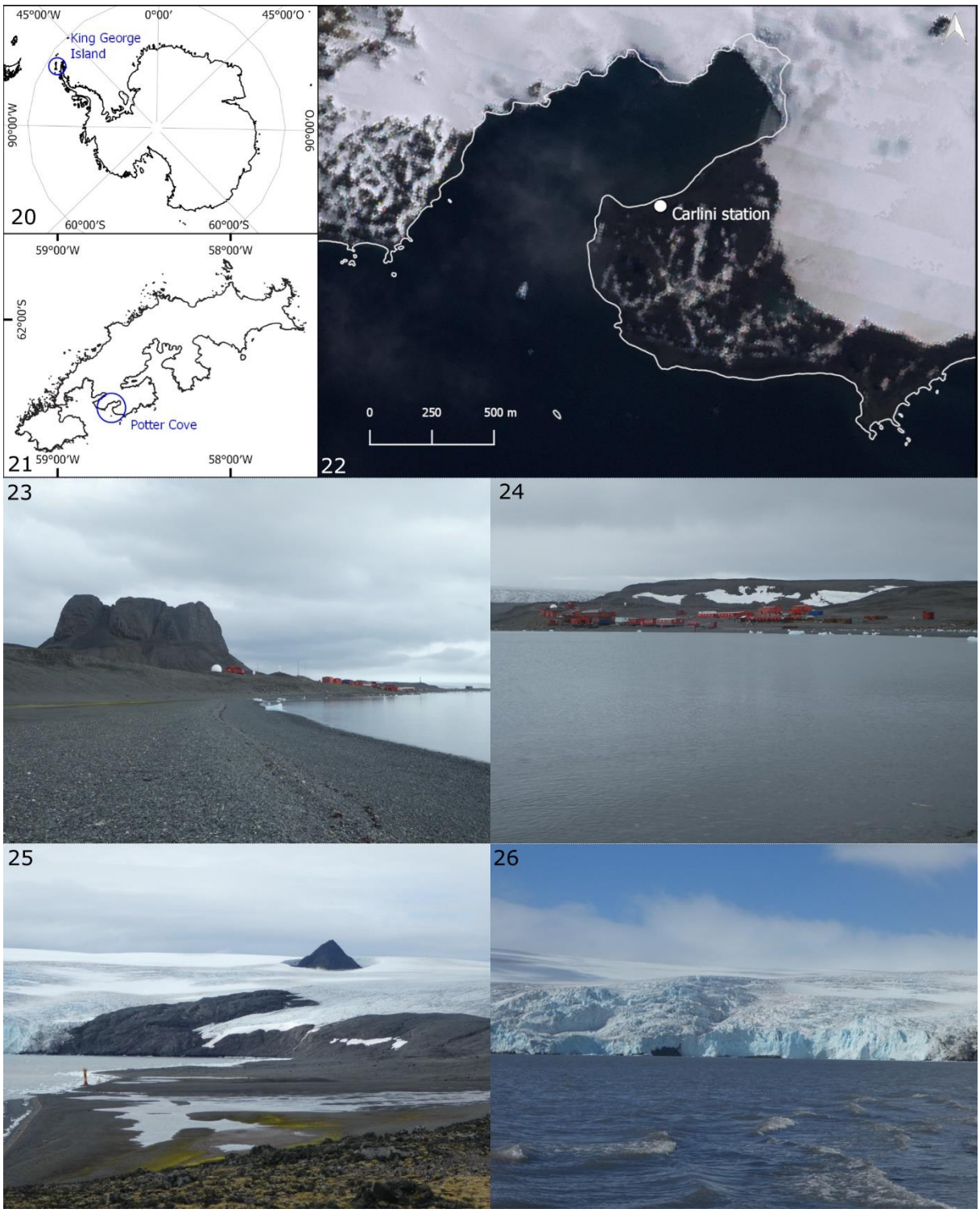

Figures 20-26 Map and pictures of the sampling location, Potter Cove, King George Island, Antarctic Peninsula. **20** Map of Antarctica **21** Map of King George Island **22** Map of the Potter Cove **23** View on the coastal area of Potter Cove with the Tree Brother Hill (Cerro Tres Hermanos) **24** the Argentinian Carlini Station **25** View on coastal area of Potter Cove partially not covered with ice and constituting a tundra like ecosystem **26** Fourcade Glacier at the head of Potter Cove. Basemap: Landsat Image Mosaic of Antarctica (LIMA), pictures by J. Zimmermann.

1.3.2 Environmental conditions and the impact of global warming

Antarctica is known as the driest and coldest continent with the lowest recorded temperature on Earth, -89.2ºC, at Russia's Vostok Station (Turner et al. 2009). Total darkness in winter is paired with low temperatures, strong winds and heavy snow cover. In contrast, permanent light and higher temperatures in summer produce ice and snow melt. The seasonal change from polar night to midnight sun is distinguishing the Arctic and the Antarctic from all other regions of the world and marine biota living in those regions must deal with extreme seasonality of light, temperature, salinity, and sea ice (Zacher et al. 2009, Pavlov et al. 2019).

The marine environment is physically heterogeneous and patchy, both spatially and temporally, with significant impact on biodiversity patterns. This heterogeneity is evident not only on the seabed but also in the water column due to variation in nutrient dynamics, length of the summer period of high light availability, salinity changes and run-off from glaciers and associated ice cover (Peck 2018). Shallow water (< 50 m depth) on the Western Antarctic Peninsula has an approximately consistent thermal gradient (-0.4° to 4°C) that extends from the Ross Sea (76°S) to sub-Antarctic South Georgia (54°S, Convey et al. 2014). In the terrestrial environment of the Antarctic Peninsula warming was greater than in any other location in the Southern Hemisphere in the latter half of the 20th century (Siegert et al. 2019). February 2020 registered one of the most intense heatwaves ever recorded in Western Antarctica with regional mean temperature anomalies (+4.5 °C) over the Antarctic Peninsula and the highest local temperature of the continental Antarctic region. The aggravated severity of the event can be largely attributed to long-term summer warming (González-Herrero et al. 2022). Under a global 1.5°C scenario, climate model projections suggest that Antarctic Peninsula temperatures will increase by more than the global average (Hoegh-Guldberg et al. 2018) and the number of days above 0°C might reach up to 130 (Siegert et al. 2019). Accelerating mass loss of Antarctic ice sheets has been observed, releasing large amounts of freshwater into the ocean along the Antarctic coast (Rignot et al. 2019, Pan et al. 2022). Driven by the ice melt, models suggest a weakening of 20 % of the ACC with major impact on global ocean circulation and the global climate system (Sohail et al. 2023).

Ocean acidification is another ecosystem stressor for the Southern Ocean arising from climate change. 21st century projections suggest pH declines of up to 0.36 (total scale) and severe ocean acidification throughout the water column in coastal waters of proposed and existing Antarctic Marine Protected Areas (Nissen et al. 2024).

The changing environmental conditions like increasing water temperatures, seabed scour from icebergs, ocean acidification, meltwater, sediment inflow as well as decreasing sea-ice habitats lead to different responses of marine biota such as changes in behavior, physiology, geographic- or depth distribution plus evolutionary adaptation (Henley et al. 2019, Siegert et al. 2019). Further, by weakening the temperature limitation of biological processes in warmer-water species coupled with increasing ship activities and declining duration of sea ice increasing the likelihood of the introduction of non-native species (Hughes and Ashton 2017, McCarthy et al. 2019, McCarthy et al. 2022).

1.3.3 Antarctic biodiversity

Antarctica contains some of the strongest environmental gradients on the planet. Therefore, the ecosystem varies on land from polar deserts including the continent's ice itself to lush grasslands (Convey et al. 2014). Parts of the Antarctic Peninsula including off-lying islands are not covered with ice and constitute a tundra like ecosystem containing only two vascular plants *Colobanthus quitensis* (Kunth) Bartling (Antarctic pearlwort) and *Deschampsia antarctica* Desvaux (Antarctic hairgrass, Day et al. 2008).

The biota in the Southern Ocean is unique. In contrast to the harsh environment, marine biodiversity is much more extensive, ecologically diverse, and biogeographically structured than previously thought (Chown et al. 2015). Spatial regionalization and temporal isolation are apparent in marine environments of Antarctica (Terauds et al. 2012, Convey et al. 2014). The major reason of isolation is the ACC (Griffiths et al. 2009). This current creates a steep temperature gradient of 3°–4°C over a distance of tens of kilometers and forms a strong biogeographic discontinuity (Convey et al. 2014). Further, Antarctica is the only continent that lacks a continental shelf connection with another continent. This isolation, along with the many millions of years of unique environmental conditions have led to significant radiations in marine species which resulted in high species-level endemism of around 50 % (Griffiths et al. 2009). This high Antarctic biodiversity is particularly evident in the benthos, where it is estimated that up to 20,000 species of invertebrate are likely living on the Antarctic continental shelves (Peck 2018).

The Register of Antarctic Marine Species is a marine species database that manages an authoritative taxonomic list of species occurring in the Southern Ocean and currently includes over 8,4330 species (De Broyer et al. 2024). However, our knowledge of the biodiversity of the Southern Ocean is still largely determined by the relative inaccessibility of the region and the

locations of scientific bases has a major influence on the distribution of sampling and observation data (Griffiths 2010)

1.3.4 Diatom diversity in the light of Antarctic exploration

The Antarctic has always been a source of fascination. For more than two millennia large southern land masses were theorized before the discovery of Antarctica. The Greek geographer Ptolemy called his version of the theoretical land 'Terra Incognita' which was still represented in medieval and Renaissance maps (Murray 2005). Since James Cook crossed the Antarctic circle as the first European explorer in 1773 many expeditions to the polar region followed. Together with the beginning of the early exploration of the Southern Ocean, the investigation of diatoms in this region started.

During the Ross expedition, a voyage of discovery and research from 1839 to 1843 led by James Clark Ross on the ships HMS Erebus and Terror (Ross 1847), samples from the Southern Ocean were collected and later investigated by Christian Gottfried Ehrenberg. From those samples he described the genus *Chaetoceros* (Ehrenberg 1844, Kooistra et al. 2022), which is today recognized as the most abundant and diverse diatom genus in the oceans (Malviya et al. 2016, De Luca et al. 2019, Xu et al. 2019).

The expedition on the HMS Challenger from 1872 to 1876 was the first global sea expedition designed purely for scientific research. Investigating the marine diatoms collected during the expedition, Conte Castracane concluded "it is by no means easy to understand how, during the long course of centuries, the different types have not been distributed far and wide and rendered common inhabitants of all seas." However, he observed that several distinct floras exist and described over 40 new species and the genus *Corethon* from the Antarctic Ocean (Castracane 1886, Crawford et al. 1998).

At the end of the 19th century, western European nations along with Japan and the United States began to set their sights on Antarctica for reasons of territorial expansion, natural resource extraction and increased global prestige. Over the next two decades, eight countries sent 16 expeditions south in what would come to be known as the Heroic age of Antarctic exploration (Barczewski 2023). Diatoms from pelagic as well as coastal habitats were examined following several expeditions and published with drawings of the valves (Karsten 1906, Van Heurck 1909, Peragallo 1921, Heiden and Kolbe 1928, Mann 1937). Later in the 20th century first biodiversity assessments based on LM of Antarctic diatoms were published (see Kellogg and Kellogg (2002) and references therein) e.g. by Hustedt (1958) from samples collected during

the German Antarctic Expedition 1938/1939 or by Simonsen (1992) who re-examined diatom types from Heiden and Kolbe (1928).

Recent floristic studies of marine diatoms exhibit a high but varying number of taxa where no assignment on species level was possible. No species affiliation was feasible in 27 % of the benthic taxa in the study of Al-Handal and Wulff (2008a) in Potter Cove, King Geoge Island and its re-examination by Al-Handal et al. (2022). Al-Handal and Wulff (2008b) evaluated epiphytic diatoms at the same location and found 16 % unidentified species. While examining marine benthic diatom diversity on Livingston Island, South Shetland Islands, Zidarova et al. (2022) discovered that 60 % of the taxa couldn't be identified on species level. An investigation of epiphytic diatoms in Terra Nova Bay in East Antarctica could not recognise 41 % of the taxa on species level (Majewska et al. 2013). A detailed taxonomic analysis of benthic diatoms in Potter Cove, King George Island was performed by Campana (2018) with a total of 40 diatom taxa identified, with eight diatom taxa as new records for the benthic habitats of Potter Cove. In the last decades various new species have been described from the region: e.g. *Cocconeis melchioroides* Al-Handal, Riaux-Gobin, Romero & Wulff, *C. dallmannii* Al-Handal, Riaux-Gobin, Romero & Wulff (Al-Handal et al. 2008), *C. pottercovei* Al-Handal, Riaux-Gobin & Wulff (Al-Handal et al. 2010), *Gomphonemopsis ligowskii* Al-Handal & E.W.Thomas (Al-Handal et al. 2018), *Pteroncola carlinii* Almandoz & Ferrario (Almandoz et al. 2014) or *Australoneis frenguelliae* (Riaux-Gobin & J.M.Guerrero) J.M.Guerrero & Riaux-Gobin (Guerrero et al. 2021). However, as the floristic studies reveal, little is still known about marine benthic diatoms in terms of biodiversity, biogeography and ecology in the Antarctic region, despite their crucial role. In addition, existing studies on diversity are solely based on valve morphology.

In contrast, marine planktonic species were more intensely examined in the Southern Ocean using molecular tools. Malviya et al. (2016) evaluated marine planktonic diatoms by 18S metabarcoding from a wide range of oceanic regions collected during the Tara Oceans circumnavigation. Only a few cosmopolitan 18S ribotypes were found and many of them could not be assigned with confidence to any known genus. A sudden drop in diversity was observed across the Drake Passage between the Atlantic and Southern Oceans, indicating the importance of the ocean circulation choke points in constraining diatom distribution and diversity. Genomic, morphometric, ecophysiological and mating compatibility data showed the ecotypic differentiation of the endemic pelagic diatom *Fragilariopsis kerguelensis* (O'Meara) Hustedt along the latitudinal expansion of the Southern Ocean (Postel et al. 2020). The authors

hypothesize that the observed pattern originated by an adaptive expansion accompanied by ecotypic divergence, followed by sympatric speciation.

Freshwater benthic diatoms in Antarctica were examined more profoundly than their marine counterparts, which resulted in the description of many new and endemic species, e.g. Van de Vijver et al. (2014), Kopalová et al. (2015), Van de Vijver et al. (2016), Zidarova et al. (2016). Already Vyverman et al. (2010) found evidence for a strong regionalization of diatom floras in the Antarctic and sub-Antarctic regions, mirroring the biogeographical regions that have been recognized for macroorganisms. A recent study of biogeographic patterns of Antarctic freshwater diatoms based on the analysis of species occurrences in a dataset of 439 lakes points to a highly distinct diatom flora, both in terms of composition and richness (Verleyen et al. 2021). A total of 44 % of all species is estimated to be endemic to the Antarctic, and most of them are confined to a single biogeographic region: Continental Antarctica, Maritime Antarctica and the sub-Antarctic islands. The level of endemism significantly increases with increasing latitude and geographic isolation. Comparing samples collected by Shackleton's Nimrod expedition (1907-1909) to samples collected during recent expeditions, Kohler et al. (2021) found limited evidence for species invasions and ecological change overall in the pond diatom communities of Ross Island, Continental Antarctica. This suggests that the species pool has remained essentially unchanged since the Heroic Age despite growing traffic in the area.

1.3.5 Ecophysiological response of diatoms in extreme environmental conditions

Benthic communities in Antarctica experience extreme seasonal variability concerning abiotic parameters e.g., temperature, irradiance and salinity (Zacher et al. 2009). At the southern distribution limits of benthic algae in the Antarctic at 77°S, the annual solar radiation is 30–50 % lower than in temperate to tropical regions with four months of complete darkness (Lüning 1990). At lower latitudes around the South Shetland Islands, daylengths vary between 5 h in winter and 20 h in summer (Zacher et al. 2009). Further, due to sea ice coverage light penetration decreases. It has been reported that diatoms can adapt their photosynthetic activity very efficiently to changing irradiance levels. Sea ice diatoms exhibit strong shade adaptation characteristics, which explain the relevant abundance of those algae within this habitat (Lazzara et al. 2007). A dense microphytobenthic community dominated by the diatom *Trachyneis aspera* (Ehrenberg) Cleve was found at 20-30 m water depth in McMurdo Sound, Antarctica. Those diatoms were light saturated at only 11 μmol photons m^{-2} s^{-1} and thereby ranked among the most shade adopted microalgae reported (Palmisano et al. 1985).

Diatom taxa from Antarctic habitats need to survive long periods of complete darkness. The recruitment of energy for a reduced basic metabolism through the decomposition of organelle components, stored lipid compound triacylglycerol and a pool of free fatty acids seems to be a key process for survival in benthic polar diatoms (Karsten et al. 2012, Schaub et al. 2017). Upon sea ice break-up, the autotrophs are suddenly exposed to high light intensities including ultraviolet radiation. Laboratory experiments with marine benthic diatoms from sediments from King George Island showed that they were able to resume photosynthetic activity after 64 days in darkness and can cope with relatively high intensities of UV radiation (Wulff et al. 2008). In general, Antarctic benthic diatoms from both the inter- and subtidal seem to be able to acclimatize to comparably high UV intensities (Zacher et al. 2007, Karsten et al. 2009).

Studies investigating primary production of benthic diatoms from this region are still scarce. Following the disappearance of the ice, Gilbert (1991) reported that benthic algae from Signy Island in the Sub-Antarctic displayed highly significant rates of primary productivity and increased in biomass rapidly to reach a peak in December, just prior to the phytoplankton bloom. McMinn et al. (2012) described that after the sea ice broke in Brown Bay, East Antarctica, the marine environment supported a small phytoplankton biomass and a large benthic microalgal biomass. The latter made a larger contribution to total primary production than the phytoplankton or sea ice algae at water depth less than approximately 5 m. Investigations from the Arctic show that benthic diatoms play an exceptionally important role in coastal food webs (Glud et al. 2009). Benthic diatoms from Young Sound, Greenland exhibit a primary production that is equivalent to that of benthic macroalgae. Benthic net photosynthesis was almost 7 times higher than the gross photosynthetic rates of the pelagic community for water depths <30 m (Glud et al. 2002). At the Arctic model ecosystem Kongsfjorden (Svalbard, Norway) microphytobenthic production was found to be as high as in temperate regions and comparable to the pelagic production in Kongsfjorden (Woelfel et al. 2010) which was further corroborated by follow-up studies (Sevilgen et al. 2014).

Although comprehensive data are still lacking, some studies indicate that Antarctic benthic diatoms are rather polar stenothermal and psychrophilic, while their Arctic counterparts are more eurythermal and psychrotolerant (Karsten et al. 2012, Schlie and Karsten 2017). Rising air temperatures in summer lead to melting of snow and glaciers and the coastal marine habitats are flushed by fresh meltwater. Consequently, the salinity within the upper few meters of the water column is reduced from 34.5 psu to 31 psu or even 27 psu in tide pools, as measured in Potter Cove, King George Island (Zacher et al. 2009). However, the effect of salinity on benthic diatoms from polar waters is generally little studied. Results from Torstensson et al. (2019)

suggests that changes in temperature and salinity may have more effects on the biochemical composition of the Antarctic sea-ice species *Nitzschia lecointei* Van Heurck than ocean acidification. In Enderby Bay, East Antarctica the decrease in sea-surface salinity was associated with an increase in pCO_2 and a reduction in total diatom abundance (Shetye et al. 2021).

The West Antarctic Peninsula is experiencing a rapid change, where ocean warming results in more sea ice melt. Simultaneously the oceanic CO_2 levels are increasing. Since benthic diatoms play a key role in coastal food webs there is an urgent need to develop a better understanding of how these organisms will be affected by these changes in the Southern Ocean.

1.4 Objectives and outline of the dissertation

This doctoral project was carried out in the framework of the project "Biodiversity and biogeography of marine benthic diatoms in Antarctic and Arctic coastal zones to evaluate the degree of endemism using fine-grained taxonomy and metabarcoding" launched by the Botanischer Garten and Botanisches Museum Berlin in cooperation with the University of Rostock and funded by the priority programme "Antarctic Research with Comparative Investigations in Arctic Ice Areas" of the German Research Foundation.

The objective of this thesis was to add knowledge to the biodiversity of marine benthic diatoms in Antarctic shallow water coastal zone environments. In addition, some brackish and maritime freshwater environments connected to the marine realm were explored. This goal was achieved via the identification of the almost unknown benthic diatom biodiversity in communities sampled in Potter Cove (Antarctica) by the means of morphological and molecular methods. In addition, for the first time, a taxonomically validated reference library for Antarctic benthic diatoms was established based on clone cultures with comprehensive information on habitat, morphology and DNA barcodes for unambiguous identification.

This taxonomic reference library was utilised for DNA metabarcoding to access the concealed biodiversity beyond the limits of morphological and cultivating methods to assess the status of the taxonomic coverage of benthic diatoms in the West Antarctic Peninsula. The generated genotypic data by DNA barcoding in combination with phenotypic information developed by investigating the morphology of marine benthic diatoms is urgently needed to improve our fundamental understanding on the biodiversity and biogeography of microphytobenthic communities in Antarctica. Generating the thus far most extensive biodiversity dataset on Antarctic benthic diatoms provides a baseline to monitor community changes including the incursion and excursion of taxa and to provide information on biodiversity patterns as well as

dispersal mechanisms. Even genetic diversity and phenotypic plasticity within species can be addressed. Further, it can serve as a baseline for future monitoring programmes, for example when addressing coastal erosion effects on the benthic diatom flora, for geological questions reconstructing paleo-environments as well as the effects of climate change.

In the framework of this thesis taxonomy and systematics of several taxa were elucidated. The species *Planothidium wetzelli* sp. nov. was newly described based on observations from living cells, valve morphology and sequence data. Further, the phylogenetic placement of the genus *Chamaepinnularia* Lange-Bertalot & Krammer was investigated in this thesis. This diatom genus was first published by Lange–Bertalot et Krammer in 1996 to accommodate several small species previously included within *Navicula* Bory and *Pinnularia* Ehrenberg. Despite its morphological similarity to those two genera, the family–level classification of *Chamaepinnularia* has been uncertain since its description almost three decades ago.

Clone cultures of Antarctic diatoms established within this project were integrated into the culture collection at the University of Rostock and examined using physiological, cell biological, and biochemical methods to better understand the underlying mechanisms for coping with the polar night as well as the ecophysiological response patterns under a temperature, light, and salinity gradient.

The thesis is divided into six chapters: **Chapter 1** gives a general introduction to this study. **Chapter 2** provides in-depth insights into benthic diatom biodiversity in West Antarctic coastal zones via identification by means of morphology, DNA metabarcoding and cultured isolates. The performance of morphology and metabarcoding in the identification and quantification of diatom abundances is compared. In addition, the taxonomically validated reference library for Antarctic benthic diatoms is introduced. In **Chapter 3** an integrated taxonomy and family–level classification of *Chamaepinnularia* is presented. The first molecular characterization (18S and *rbc*L) of the genus based on Arctic and Antarctic strains is provided and its phylogenetic placement investigated. Molecular data are complemented with observations on living cells, as well as detailed examination of oxidized material with light microscopy and scanning electron microscopy. The 12 investigated strains were identified as three taxa: two already described species (*C. gerlachei* Van de Vijver & Sterken, *C. krookii* (Grunow) Lange-Bertalot & Krammer) and one here newly described (*C. australis* sp. nov.). **Chapter 4 and 5** present the results of the cooperation with the University of Rostock. **Chapter 4** shows lipid degradation and photosynthetic traits after a dark period of three months from four Antarctic benthic diatoms, including the newly described species *Planothidium wetzelii* sp. nov. The importance

of taxonomy as baseline for ecophysiological investigations is here discussed. In **Chapter 5** photosynthesis, respiration, and growth response patterns are presented as functions of varying light availability, temperature, and salinity for six Antarctic benthic diatoms.

2 Exploring benthic diatom diversity in the West Antarctica Peninsula: insights from a morphological and molecular approach

Katherina Schimani[1], Nélida Abarca[1], Oliver Skibbe[1], Heba Mohamad[1], Regine Jahn[1], Wolf-Henning Kusber[1], Gabriela Laura Campana[2,3], Jonas Zimmermann[1]

[1] Botanischer Garten und Botanisches Museum Berlin, Freie Universität Berlin, Germany

[2] Department of Coastal Biology, Argentinean Antarctic Institute, Buenos Aires, Argentina

[3] Department of Basic Sciences, National University of Luján, Buenos Aires, Argentina

Metabarcoding and Metagenomics 7:339-384. https://doi.org/10.3897/mbmg.7.110194

2.1 Abstract

Polar regions are among the most extreme habitats on Earth. However, diatom biodiversity in those regions is much more extensive and ecologically diverse than previously thought. The objective of this study was to add knowledge to benthic diatom biodiversity in Western Antarctic coastal zones via identification by means of morphology, DNA metabarcoding and cultured isolates. In addition, a taxonomically validated reference library for Antarctic benthic diatoms was established with comprehensive information on habitat, morphology and DNA barcodes (*rbc*L and 18SV4). Benthic samples from marine, brackish and freshwater habitats were taken at the Antarctic Peninsula. A total of 162 clonal cultures were established, resulting in the identification of 60 taxa. The combination of total morphological richness of 174 taxa, including the clones, with an additional 73 taxa just assigned by metabarcoding resulted in 247 infrageneric taxa. Of those taxa, 33 were retrieved by all three methods and 111 only by morphology. The barcode reference library of Antarctic species with the new references obtained through culturing allowed the assignment of 47 taxa in the metabarcoding analyses, which would have been left unassigned because no matching reference sequences were available before. Non–metric multidimensional scaling analyses of morphological as well as molecular data showed a clear separation of diatom communities according to water and substratum types. Many species, especially marine taxa, still have no record in reference databases. This highlights the need for a more comprehensive reference library to further improve routine diatom metabarcoding. Overall, a combination of morphological and

molecular methods, along with culturing, provides complementary information on the biodiversity of benthic diatoms in the region.

Key words: Antarctic Peninsula, benthic diatoms, DNA metabarcoding, morphology, *rbc*L, taxonomic reference library, unialgal cultures, 18SV4

2.2 Introduction

The polar regions are among the most extreme environments on Earth. Total darkness in winter is paired with low temperatures, strong winds and heavy snow cover. In contrast, permanent light and higher temperatures in summer result in ice and snow melt (Pavlov et al. 2019). Marine biota living in those regions must deal with extreme seasonality of light, temperature, salinity and sea ice (Zacher et al. 2009). In contrast to this harsh environment, biodiversity in polar regions is much more extensive, ecologically diverse, and biogeographically structured than previously thought and the prevalence of such conditions for millions of years has led to the evolution of a truly unique flora and fauna (Griffiths 2010; Chown et al. 2015; Danis et al. 2020).

An ecologically particularly important group of eukaryotic microorganisms in Antarctic shallow water coastal zones are benthic diatoms living on top of or associated with sediments, rocks or sea ice. Their benthic assemblage exerts multiple important functions as primary producers, providing a major food source for a diverse range of organisms such as bacteria by excretion of soluble organic matter, benthic protozoans as well as metazoans (Cahoon 1999), including mesograzers such as amphipodes and gastropodes (Zacher et al. 2007; Campana et al. 2008; Aumack et al. 2017; Amsler et al. 2019). Furthermore, diatoms influence elemental fluxes at the sediment–water interface (Risgaard–Petersen et al. 1994) and stabilize the sediment surface by excretion of sticky extracellular polymeric substances (de Brouwer et al. 2005). Due to their abundance, marine planktonic diatoms account for up to one fifth of the global photosynthetic carbon fixation (Falkowski et al. 2000).

Numerous recent studies indicate that microorganisms display a distinct biogeography, which is also strongly supported by evidence from different freshwater and soil diatoms (Vanormelingen et al. 2008; Abarca et al. 2014; Pinseel et al. 2020). Freshwater benthic diatoms in Antarctica have been intensively studied e.g. Van de Vijver et al. (2002); Kopalová et al. (2015); Sterken et al. (2015); Zidarova et al. (2016a, b); Van de Vijver et al. (2018) and revisions of freshwater Antarctic and sub–Antarctic diatom floras point to a strong regionalization (Vyverman et al. 2010; Verleyen et al. 2021). Despite their crucial role, information about the biodiversity of Antarctic marine benthic diatoms is scarce and only a few

studies exploring their biodiversity exist (Klöser 1998; Al-Handal and Wulff 2008a, b; Campana 2018; Al-Handal et al. 2022; Zidarova et al. 2022).

DNA metabarcoding has emerged as an alternative to light microscope-based identifications (LM) as it provides a faster and cheaper way of identifying species in an environmental sample because the morphological identification and counting of diatoms species in LM is time–consuming and demands extensive expertise since diatom taxonomy is constantly evolving (Kermarrec et al. 2014; Zimmermann et al. 2015). This approach has been used to investigate freshwater diatom biodiversity (Rimet et al. 2018b; Mora et al. 2019) and has been applied to some extent to marine environments (Malviya et al. 2016; Piredda et al. 2018; Pérez-Burillo et al. 2022). Benthic diatoms are commonly used as bioindicators to monitor water quality because of their rapid response to environmental pressures and their omnipresence (Rimet and Bouchez 2012; Desrosiers et al. 2013). DNA metabarcoding based on benthic diatoms has been utilized to monitor community changes and assessing the biological status of a water body (Vasselon et al. 2017; Bailet et al. 2019; Mortágua et al. 2019; Kelly et al. 2020; Pérez-Burillo et al. 2020) and a taxonomy-free biomonitoring approach has emerged that allows the computing of a molecular index directly without any reference to morphotaxonomy to overcome the limitations of the reference databases and the lack of phylogenetic resolution (Apothéloz-Perret-Gentil et al. 2017; Tapolczai et al. 2019a, b, Gregersen et al. 2023).

For a reliable identification, an unambiguous link between geno– and phenotype is crucial. Therefore, a comprehensive taxonomic reference library is required where molecular and morphological data are tied together with a taxonomic name (Zimmermann et al. 2014; Stachura-Suchoples et al. 2015). For diatoms, clone cultures need to be established which offer sufficient material for sequencing as well as for identification by light and electron microscopy. Finally, all reference sequences should be linked to diatom voucher specimens deposited in a herbarium in order to offer a complete chain of evidence back to the formal taxonomic literature.

The objective of this study was to add knowledge to the biodiversity of marine benthic diatoms in Western Antarctic shallow water coastal zone environments. In addition, some brackish and freshwater environments connected to the marine realm were explored. Benthic diatom biodiversity in communities sampled in Potter Cove, King George Island/ Isla 25 de Mayo, West Antarctic Peninsula were identified by the means of morphological and molecular methods to assess the status of their taxonomic coverage in Antarctic regions. To compare the performance of morphology and metabarcoding in the identification and quantification of

diatom abundances, our objective was to compare the number of taxa retrieved by both analysis of environmental samples. A further goal was to create a regional vouchered barcode reference library with the help of clone cultures with comprehensive information on habitat, morphology and DNA barcodes (*rbc*L and 18SV4). This taxonomic reference library was utilized for DNA metabarcoding to access the concealed biodiversity beyond the limits of morphological and cultivating methods. Generating the thus far most extensive biodiversity dataset on Antarctic marine benthic diatoms provides a reference to monitor community changes to predict the potential impact of climate change on the coastal ecosystems of this region.

2.3 Methods

2.3.1 Study area and sampling collection

Epipsammic and epilithic samples from marine, brackish and freshwater habitats were taken in Austral summer 2020 at Potter Cove, a shallow coastal bay at King George Island/ Isla 25 de Mayo, West Antarctic Peninsula (Fig. 1). Potter Cove combines zones of glacier fronts and rocky shores as well as extensive soft bottom areas and thereby providing diverse habitats for benthic diatoms (Klöser 1998).

In total 39 samples were taken (Table 1, Fig. 1). At eight of the locations freshwater samples were taken from glacial run–off water or drinking water reservoirs. At 17 locations the littoral zone was sampled, and additional 14 marine locations were sampled by scuba diving reaching down to a water depth of 20 m (Table 1). A map of the sampling points was generated with the software QGIS 2.18 (QGIS Development Team 2021).

At each sample location a composite sample of 60 ml was taken along a transect of approximately 10 m. At sample locations with rocky substrate the biofilm of three to four stones along the transect was scratched with a knife. At locations with soft sediment a sediment corer was used to collect the material of three to four spots along the transect. The top layer of the cores was then sampled with a syringe. The composite samples were homogenized, and divided into 3 subsamples of 20 ml each, which were used for 3 different purposes: 1) fixed in 70 % alcohol for morphological identification of the mixed diatom community, 2) stored cooled for the establishment of clone cultures to build the barcode library and 3) fixed in 99 % ethanol and frozen for a community analysis via DNA metabarcoding.

Table 1 Sample sites with information on the location, georeference, altitude, collector, water type, substrate type and voucher at the BGBM.

Sample ID	Sampling date	Location	Latitude - South	Longitude - West	Altitude	Collector	Water type	Substrate type	Voucher at BGBM
D283	28.01.2020	Coastal zone at Peñón 1	62.245938	58.681731	0 m	J. Zimmermann	marine	biofilm from stones	B 50 0021363
D284	28.01.2020	Lighthouse Melting Pond	62.240866	58.677563	28 m	J. Zimmermann	freshwater	biofilm from stones	B 50 0021364
D285	29.01.2020	IT Resevoire	62.237876	58.662233	12 m	J. Zimmermann	freshwater	biofilm from stones	B 50 0021365
D286	29.01.2020	Drinking water pond at Carlini station	62.238091	58.657689	23 m	J. Zimmermann	freshwater	biofilm from stones	B 50 0021366
D288	29.01.2020	Coastal zone at Peñón 0	62.241809	58.681931	0 m	J. Zimmermann	marine	biofilm from stones	B 50 0021367
D289	30.01.2020	Coastal zone at island A7	62.234665	58.664624	10 m deep	J. Zimmermann, G. L. Campana, Divers Carlini Station	marine	epipsammic biofilm	B 50 0021368
D290	30.01.2020	Coastal zone at island A7	62.234665	58.664624	10 m deep	J. Zimmermann, G. L. Campana, Divers Carlini Station	marine	epipsammic biofilm	B 50 0021369
D292	30.01.2020	Coastal zone at island A7	62.234665	58.664624	10 m deep	J. Zimmermann, G. L. Campana, Divers Carlini Station	marine	epipsammic biofilm	B 50 0021370
D293	30.01.2020	Coastal zone at island A7	62.234665	58.664624	10 m deep	J. Zimmermann, G. L. Campana, Divers Carlini Station	marine	epipsammic biofilm	B 50 0021371
D294	30.01.2020	Coastal zone east of Carlini station	62.235314	58.656489	0 m	J. Zimmermann	brackish water	epipsammic biofilm	B 50 0021372
D295	30.01.2020	Coastal zone east of Carlini station	62.235771	58.658364	0 m	J. Zimmermann	brackish water	epipsammic biofilm	B 50 0021373
D296	31.01.2020	Coastal zone at island A4	62.229219	58.663369	15 m deep	J. Zimmermann, G. L. Campana, Divers Carlini Station	marine	epipsammic biofilm	B 50 0021374
D297	31.01.2020	Coastal zone at island A4	62.229219	58.663369	15 m deep	J. Zimmermann, G. L. Campana, Divers Carlini Station	marine	episammic biofilm	B 50 0021375
D299	01.02.2020	Glacier meltwater run-off in Tres Hermanos area	62.251939	58.652703	60 m	J. Zimmermann	freshwater	biofilm from stones	B 50 0021376
D300	01.02.2020	Drinking Water Reservoire	62.237861	58.662250	51 m	J. Zimmermann	freshwater	biofilm from stones	B 50 0021377
D301	04.02.2020	Coastal zone at island A4	62.229219	58.663369	5 m deep	J. Zimmermann, G. L. Campana, Divers Carlini Station	marine	biofilm from stones	B 50 0021378
D302	04.02.2020	Coastal zone at island A4	62.229219	58.663369	5 m deep	J. Zimmermann, G. L. Campana, Divers Carlini Station	marine	epipsammic biofilm	B 50 0021379
D303	04.02.2020	Glacier meltwater run-off Fourcade	62.236639	58.647028	10-15 m	J. Zimmermann	freshwater	biofilm from stones	B 50 0021380

D304	04.02.2020	Glacier meltwater run-off Fourcade	62.236639	58.647028	10-15 m	J. Zimmermann	freshwater	biofilm from stones	B 50 0021381
D305	05.02.2020	Coastal zone at island A4	62.229219	58.663369	20 m deep	J. Zimmermann, G. L. Campana, Divers Carlini Station	marine	epipsammic biofilm	B 50 0021382
D306	06.02.2020	Coastal zone at Punta Elefante	62.237353	58.679569	0 m	J. Zimmermann	marine	biofilm from stones	B 50 0021383
D307	07.02.2020	Coastal zone at Peñón 1	62.247261	58.680051	0 m	J. Zimmermann	marine	biofilm from stones	B 50 0021384
D308	07.02.2020	Coastal zone at Peñón 1	62.247261	58.680051	0 m	J. Zimmermann	marine	biofilm from stones	B 50 0021385
D309	07.02.2020	Diver's container at Carlini station	62.237459	58.667529	2 m deep	J. Zimmermann, G. L. Campana, Divers Carlini Station	marine	biofilm from stones	B 50 0021386
D310	07.02.2020	Coastal zone at Peñón de Pesca	62.237906	58.712278	5 m deep	J. Zimmermann, G. L. Campana, Divers Carlini Station	marine	biofilm from stones	B 50 0021387
D311	08.02.2020	Coastal zone at Punta Stranger	62.256388	58.625618	2 m	J. Zimmermann	marine	biofilm from stones	B 50 0021388
D312	08.02.2020	Coastal zone at Punta Stranger	62.256296	58.626069	2 m	J. Zimmermann	marine	biofilm from stones	B 50 0021389
D313	08.02.2020	Coastal zone at Punta Stranger	62.258227	58.642172	1 m	J. Zimmermann	marine	biofilm from stones	B 50 0021390
D314	09.02.2020	Glacier meltwater run-off Refugio Albatros	62.252046	58.659456	49 m	J. Zimmermann	freshwater	biofilm from stones	B 50 0021391
D315	09.02.2020	Coastal zone at Peñón 4	62.256107	58.659703	2 m	J. Zimmermann	marine	biofilm from stones	B 50 0021392
D316	09.02.2020	Coastal zone at Peñón 2	62.250540	58.675029	2 m	J. Zimmermann	marine	biofilm from stones	B 50 0021393
D317	09.02.2020	Coastal zone at Peñón 1	62.247073	58.683764	2 m	J. Zimmermann	marine	biofilm from stones	B 50 0021394
D318	10.02.2020	Coastal zone at Peñón 2	62.250704	58.675778	1 m	J. Zimmermann	marine	biofilm from stones	B 50 0021395
D319	12.02.2020	Coastal zone at Carlini station	62.236950	58.663583	1 m	J. Zimmermann	marine	biofilm from stones	B 50 0021396
D320	13.02.2020	Coastal zone at Punta Stranger	62.256109	58.630578	0 m	J. Zimmermann	marine	biofilm from stones	B 50 0021397
D321	13.02.2020	Coastal zone at Punta Stranger-Peñón 4	62.256615	58.641681	0 m	J. Zimmermann	marine	biofilm from stones	B 50 0021398
D322	14.02.2020	Coastal zone at island A2	62.227633	58.678734	10 m deep	J. Zimmermann, G. L. Campana, Divers Carlini Station	marine	epipsammic biofilm	B 50 0021399
D324	16.02.2020	Coastal zone at island A6	62.223800	58.642639	15 m deep	J. Zimmermann, G. L. Campana, Divers Carlini Station	marine	epipsammic biofilm	B 50 0021400
D325	17.02.2020	Coastal zone at island A6	62.223800	58.642639	20 m deep	J. Zimmermann, G. L. Campana, Divers Carlini Station	marine	epipsammic biofilm	B 50 0021401

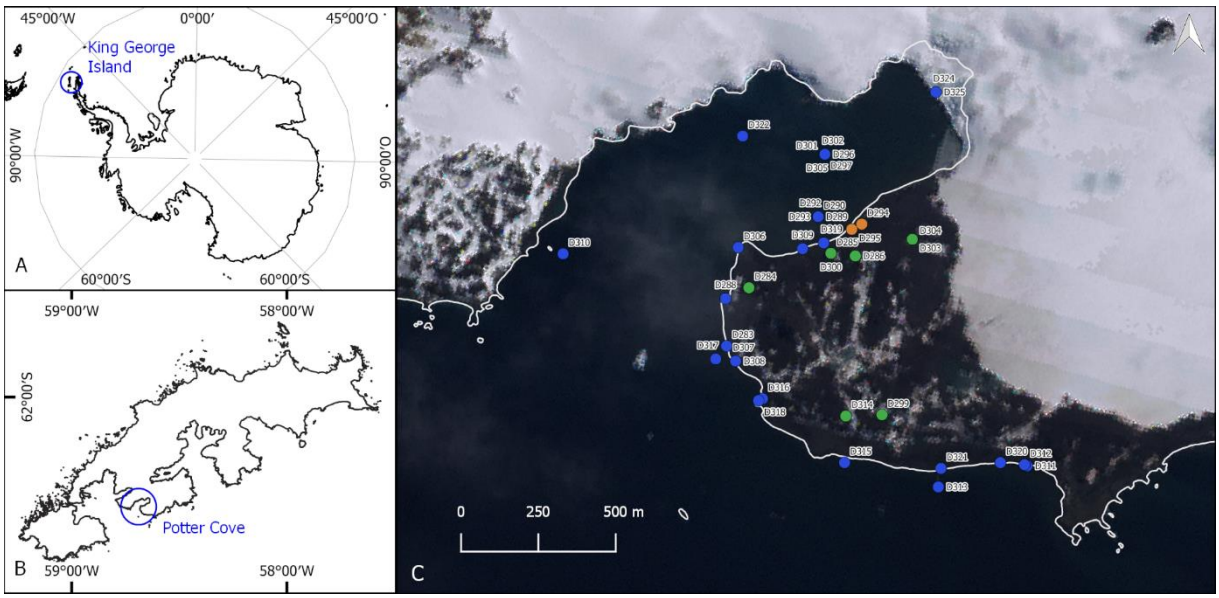

Figure 1 A Map of Antarctica. **B** Map of King George Island/Isla 25 de Mayo. **C** Map of the Potter Cove, with the 39 sample locations. Blue points represent marine sample locations, green points represent freshwater sample locations and orange points represent brackish water locations. Basemap: Landsat Image Mosaic of Antarctica (LIMA).

2.3.2 Establishment of clonal cultures

Following the procedures outlined in Skibbe et al. (2022), benthic diatoms were isolated from aliquots of environmental samples to establish clonal cultures afterwards. For this purpose, a small subsample of the biofilm was transferred from the collected environmental samples to 5 cm (diameter) Petri dishes filled with liquid culture media. Different media were used for each sample to obtain as many species with different requirements as possible. The cultivation media was prepared with sterile water enriched with one of the following media: f/2 seawater medium (Guillard and Ryther 1962), Alga–Gro medium (Carolina Biological Supply Company) or Walne's medium (Walne 1970) and salted up to a salinity of 34 psu in case of a marine sample and 12 psu for brackish samples. Using an inverted light microscope (100–400× magnification, Olympus) and microcapillary glass pipettes, single cells were transferred into microwell plates containing culture medium. After reaching sufficient densities, isolates were transferred to 5 cm petri dishes. All water samples, isolates and cultures were maintained at 5–7 °C. Illumination was accomplished by white light LEDs under a 16/8 day/night cycle with 15 min dark phases every hour during the day to prevent photo–oxidative stress.

2.3.3 Morphological analysis from environmental samples and clonal cultures

Environmental samples and material harvested from the unialgal cultures were treated with 35 % hydrogen peroxide at room temperature to oxidize the organic material and washed with distilled water as described in Mora et al. (2019). To prepare permanent slides for light microscopy analyses, the cleaned material (frustules and valves) was dispersed on cover

glasses, dried at room temperature and embedded with the high refraction index mounting medium Naphrax.

Each environmental sample was inspected for their benthic diatom composition using LM. Observations were conducted with a Zeiss Axioplan Microscope equipped with Differential Interference Contrast (DIC) using a Zeiss 100× PlanApochromat objective. Microphotographs were taken with an AXIOCAM MRc camera. To record the occurrence and abundance of each diatom taxon at all sampling sites, at least 400 frustules were counted per sample and the relative abundance of each taxon calculated. All samples were scanned for rare species.

Furthermore, morphological identification of the unialgal cultures were conducted also by LM and extended by scanning electron microscopy (SEM) if appropriate. Therefore, aliquots of cleaned culture material were dried on silicon wafers and mounted on stubs and observed under a Hitachi FE 8010 scanning electron microscope operated at 1.0 kV.

2.3.4 Molecular identification of diatom cultures

Cultured material was first centrifuged, and culture medium was discarded by carefully pipetting. DNA was isolated from the remaining pellet using NucleoSpin Plant II Mini Kit (Macherey–Nagel, Düren, Germany) following product instructions. DNA fragment size and concentrations were evaluated via gel electrophoresis (1.5 % agarose gel) and Nanodrop (PeqLab Biotechnology LLC; Erlangen, Germany) respectively. Amplification was conducted by polymerase chain reaction (PCR) after Zimmermann et al. (2011) for the V4 region of 18S. The protein–coding plastid gene *rbc*L was amplified after Abarca et al. (2014) with M13 tailed primers rcbL–iF/rbcL–R. PCR products were visualized in a 1.5 % agarose gel and cleaned with MSB Spin PCRapace (Invitek Molecular GmbH, Berlin, Germany) following manufacturer instructions. Concentrations of PCR products were measured using Nanodrop (PeqLab Biotechnology) and normalized to >100 ng μl^{-1} for sequencing. Sanger sequencing was conducted bidirectionally by Starseq (GENterprise LLC; Mainz, Germany), with the same primers used for the amplifications. The DNA material is stored in the Berlin DNA Bank Network (Gemeinholzer et al. 2011).

2.3.5 DNA metabarcoding

A volume of 2–4 ml of each sample was centrifuged at 4 °C and 11.000 rpm for 5 min. The supernatant was removed and from the remaining pellet the DNA was extracted with the NucleoSpin Soil Kit (Macherey and Nagel) following the manufacturer instructions. Short areas of the hypervariable region V4 of the 18S rRNA gene and the *rbc*L plastid gene were amplified in separated target PCRs. For the 18S V4 region the Nextera primers DIV4for: 5'–

GCGGTAATTCCAGCTCCAATAG–3' and DIV4rev3: 5'–CTCTGACAATGGAATACGA-ATA–3' were used after Zimmermann et al. (2011) with a modification for 300–bp paired–end sequencing for Illumina MiSeq following Visco et al. (2015). The *rbc*L marker was amplified using an equimolar mix of the modified versions of the Diat_rbcL_708F and R3 primers established by Vasselon et al. (2017). For each sample PCR was once repeated for technical replication. Purification of the samples was performed with 25 ml aliquots of the amplicons with HighPrep PCR Clean–up System (Magbio Genomics). Indexing PCR on the purified samples to ligate a unique combination of tags to the 5' end of the primer, DNA quantitation and Illumia MiSeq v3 sequencing (300 bp paired–end reads) with 600 cycles were conducted at the Berlin Center for Genomics in Biodiversity Research (BeGenDiv) of the Berlin Brandenburg Institute of Advanced Biodiversity Research (BBiB).

Raw demultiplexed reads were deposited at GenBanks Sequence Read Archive and are publicly available under project number PRJNA997374.

2.3.6 Bioinformatic analysis

The BeGenDiv performed demultiplexing of the samples providing two fastq files per sample containing forward reads (R1) and reverse reads (R2) respectively. Primers were removed from the reads with cutadapt (Martin 2011). To process the resulting reads the R package DADA2 was used (Callahan et al. 2016). The quality profile was checked, and reads were truncated consecutively for *rbc*L at R1 to 200 bp and at R2 to 160 bp and for 18SV4 at R1 to 230 bp and at R2 to 170 bp. Truncated reads were filtered using a maximum expected error rate of 2. Hereinafter, amplicon sequence variants (ASVs) were selected based on the error rates model determined by the DADA2 denoising algorithm and paired reads were merged into one sequence. Chimeras were identified and removed from the dataset.

Taxonomic assignment for each barcode was performed using an own established reference library comprising the Diat.barcode library (Rimet et al. 2019), the reference library of the Diatom research group of the Botanic Garden Berlin (5768 taxa for 18SV4 and 5604 taxa for *rbc*L) and the newly generated sequences from Antarctic cultures. In case of unclassified taxa on phylum level, the ASV was checked using the Basic Local Alignment Search Tool (BLAST, Camacho et al. 2009) against NCBI GenBank.

After bioinformatic analyses with DADA2 the R package metabaR was used to identify artefactual sequences like contaminants and tag–jumps (Zinger et al. 2021). The dataset was checked for dysfunctional PCRs based on PCR replicate similarities. Then, reads from replicates were aggregated.

2.3.7 Data analysis

Venn diagrams with eulerr (Larsson 2021) were used to visualize how well morphology (LM of environmental samples and cultures) and DNA metabarcoding were able to identify taxa. Barplot diagrams on genus level were generated for the metabarcoding and morphology data using the R package phyloseq (McMurdie and Holmes 2013). Alpha diversity indices (taxa richness and Shannon diversity index) were calculated with the vegan 2.6 R package (Oksanen et al. 2022). Differences in community structure regarding water types (marine, brackish water and freshwater) and substrate (epipsammic biofilm, biofilm on rocks) between samples based on metabarcoding and morphology at the ASV– and species level respectively were calculated by a Bray–Curtis dissimilarity measure using phyloseq and visualized through non–metric multidimensional scaling (NMDS) ordination. Permutational multivariate analysis of variance (PERMANOVA) was used to evaluate the statistically significant differences in diatom community composition regarding water and substate types for the DNA metabarcoding and the LM dataset. In case of significance, an analysis of similarity percentages (SIMPER) was conducted to identify the taxa contributing most to the differences in community composition. For both the PERMANOVA and the SIMPER analyses the R package vegan was used.

2.4 Results

2.4.1 Morphological inventory

In total, 142 diatom taxa were identified through counts of valves in LM, 50 to genus level and 88 to species level (Table 2, Figs 2–7, 8A). The number of taxa per sample ranged between 2 and 52 with an average of 20 per sample. The additional 23 taxa were found by scanning the whole slides under LM to look for rare taxa, whereby 11 could be unambiguously assigned to a species name (Table 2, Figs 2–7, 8A). In marine samples 116 taxa were found, in the freshwater samples 93 taxa and in brackish water samples 21 taxa.

Table 2 List of all taxa observed in light microscopy (LM) with author, references and morphometric information. (R) behind the taxa indicates that it was a rare species just observed in a thorough scan of the slide.

Taxa	Author	Reference	Length [µm]	Width [µm]	Diameter [µm]	Striae RV in 10 µm	Striae RLV in 10 µm	Areolae in 10 µm	Fibulae in 10 µm
Achnanthes bongrainii	(M. Peragallo) A. Mann	Peragallo 1921: p. 11, pl: I figs 4-6; as *A. brevipes* in Scott and Thomas 2005: p. 121, fig. 2.65; Zidarova et al. 2022: p. 91, fig. 3	27.2-50.3	7.6-11.1		6-8	6-7		
Achnanthes vicentii	Manguin	Manguin 1957: p. 124, pl. V, fig. 26a-e; Zidarova et al. 2022: p. 93, fig. 4D-G	4.6-16.2	4.0-7.1		12-16	11-16		
***Achnanthes* sp. 1**			21.8-32.4	8.4-10.3		8-10	8		
***Achnanthes* sp. 2**			16.2-47.8	6.2-10.5		6-8	6-8		
***Achnanthes* sp. 3**			31.8-34.3	4.0-5.5		11	9-10		
***Achnanthes* sp. 4 (R)**			13.9-23.4	4.3-4.5		10	8-10		
***Achnanthes* sp. 5 (R)**			48.5	9.8		6			
Achnanthidium australexiguum	Van de Vijver	Taylor et al. 2014, p. 47, figs 65-92	13.1-16.9	5.6-7.4		26-28	24-26		
Achnanthidium* cf. *maritimo-antarcticum	Van de Vijver & Kopalová	Van de Vijver and Kopalová 2014: p. 6, figs 29-53	14.0-16.9	2.3-2.6		28-32			
Actinocyclus actinochilus	(Ehrenberg) Simonsen	Villareal and Fryxell 1983: p: 461, figs 21-32; Scott and Thomas 2005, p. 52, fig. 2.22; Al-Handal et al. 2022: p. 85, figs 20,21			57.5			9-10	
Amphora gourdonii	M. Peragallo	Peragallo 1921: p. 60, pl. II, fig. 23; Al-Handal and Wulff 2008b: p. , fig. 85; Zidarova et al. 2022: fig. 10Y	23.2-64.4	6.6-10.8		9-13			
***Amphora* cf. *gourdonii* (R)**	M. Peragallo	Peragallo 1921: p. 60, pl. II, fig. 23; Al-Handal and Wulff 2008b: p. , fig. 85; Zidarova et al. 2022: fig. 10Y	25.7-37.3	4.8-7.2		11-16			
***Amphora* cf. *pusio* (R)**	Cleve	Levkov 2009: 112, pl. 76, figs 22-30	21.4-30.3	3.9-6.8		13-17			
***Amphora* sp. (R)**			37.7	7.5		11			
Australoneis frenguelliae	(Riaux-Gobin & J.M.Guerrero) J.M.Guerrero & Riaux-Gobin	Guerrero et al. 2021: fig. 1-75	22.4-34.3	12.5-20.5		4-5	5-6		
Berkeleya rutilans	(Trentep. ex Roth) Grunow	Witkowski et al. 2000: p. 157, pl. 62, figs 14-17; Scott and Thomas 2005: 148, fig. 283d	21.6-24.6	5.6-6.9		28-30			
***Berkeleya* cf. *sparsa* (R)**	Mizuno	Witkowski et al. 2000: p. 158, pl 62, figs 7-9	24.8-35.9	5.0-6.0		22-26			

Biremis ambigua	(Cleve) D.G. Mann	Simonsen 1992: p. 42, pl. 40, figs 4-10; Witkowski et al. 2000: p. 158, pl. 155, figs 2-6; Al-Handal et al. 2022: p. 93, figs 75, 76	33.7-48.8	5.0-5.8		6-8			
Brachysira minor	(Krasske) Lange Bertalot	Lange-Bertalot and Moser 1994: p. 47, pl. 47, figs 1-8; Zidarova et al. 2016a: p. 250, pl. 110, figs 1-25	10.4-18.1	3.4-4.3					
Brandinia charcotii	(Perag.) Zidarova & P.Ivanov	Peragallo 1921: p. 68, pl. III, fig. 5; Zidarova et al. 2022, p. 94, fig. 5	68.7	8.7		13			
Caloneis australis	Zidarova, Kopalova & Van de Vijver	Zidarova et al. 2016b: p. 40, figs 1-17	25.6	4.3		22			
Chamaepinnularia australis	Schimani & N. Abarca	Schimani et al. 2023: p. 8, figs 7-9	9.7-19.2	4.2-5.5		18-24			
Chamaepinnularia gerlachei	Van de Vijver & Sterken	Van de Vijver et al. 2010 : p. 432, figs 1-18	9.0-21.8	3.1-5.2		16-20			
cf. *Chamaepinnularia*			17.7-39.9	3.6-5.1		14-15			
cf. *Cocconeis* 1			10.6-22.2	6.5-15.2		14-19	14-18		
Cocconeis antiqua	Tempère & Brun	Romero 2011: p. 185, figs 13-35	49.3-79.0	31.1-51.5		11-15	13-19		
Cocconeis californica	Grunow	Witkowski et al. 2000: p. 102, pl. 36, figs 29,30, pl. 42, fig. 8-15; Riaux-Gobin and Romero 2003: p. 21, pl. 8-10	11.2-24.8	6.4-15.5		17-20	11-16		
Cocconeis costata	Gregory	Riaux-Gobin and Romero 2003: p. 22, pl. 1-2; Al-Handal and Wulff 2008b: p. 425, figs 43, 44; Zidarova et al. 2022: fig. 8D	14.9-30.4	8.3-15.0		10-12	8-10		
Cocconeis dallmannii	Al-Handal, Riaux-Gobin, Romero & Wulff	Al-Handal et al. 2008: p. 275, fig 33-48	11.9-20.7	8.2-14.9		13-19	10-12		
Cocconeis fasciolata	(Ehrenberg) Brown	Riaux-Gobin and Romero 2003: p. 26, pl. 19; Scott and Thomas 2005, p. 127, fig. 2.68a–d; Al-Handal and Wulff 2008b: p. 426, figs 45, 51, 52; Zidarova et al. 2022: fig. 8F-G	21.7-45.0	12.4-28.3		5-6	5-7		
Cocconeis imperatrix	A. Schmidt	Manguin 1960: p. 305, pl. 24, fig. 358, 359; Riaux-Gobin and Romero 2003: p. 28, pl. 21, figs 1-8; Al-Handal and Wulff 2008b, 426, figs 46-49, 55,56; Al-Handal et al. 2022: p. 91, fig. 52	47.2-68.8	31.8-44.4		4-5	4-5		
Cocconeis infirmata	Manguin	Manguin 1957: p. 123, pl. V, fig. 24a-c	10.7-24.9	6.0-17.4			8-16		
Cocconeis matsii	(Al-Handal, Riaux-Gobin & Wulff) Riaux-Gobin, Compère, Romero & D.M.Williams	Al-Handal et al. 2010: p. 6, figs 13-15, 25-30	9.2-19.4	5.7-11.9			5-8		

Cocconeis melchioroides	Al-Handal, Riaux-Gobin, Romero & Wulff	Al-Handal et al. 2008: p. 271, figs 2-15, 18-32	9.9-20.4	7.0-10.6		12-14	6-10		
Cocconeis pottercovei	Al-Handal, Riaux-Gobin et Wulff	Al-Handal et al. 2010: p. 3, figs 2-12, 19-24	11.2-14.8	7.1-8.9		11-13	10-12		
Corethron pennatum	(Grunow) Ostenfeld	Van Heurck 1909: p. 30, pl. VI, fig. 86; Crawford et al. 1998: p. 5, figs 1, 6-25			17.8				
Craspedostauros laevissimus	(West & G.S.West) Sabbe	Sabbe et al. 2003: p. 235, figs 35-37, 85; Van de Vijver et al. 2012: p. 154, figs 24-39	30.2-49.4	4.7-5.6		26-29			
***Diploneis* sp.**			17.8	6.6		16			
Ellerbeckia sol	(Ehrenberg) R.M.Crawford & P.A.Sims	as *Melosira sol* in Scott and Thomas 2005, p. 66, fig. 2.32; Al-Handal et al. 2022: p. 85, figs 9,10			94.4-102.6				
Encyonema ventricosum	(C.Agardh) Grunow	Lange-Bertalot et al. 2017: p. 209, pl. 89, figs 18-22	12.9-23.4	4.7-6.4		15-19			
***Entomoneis* sp.**			52.1-53.2	6.5-11.1		30			
Entopyla ocellata	(Arnott) Grunow	Al-Handal and Wulff 2008b: p. 427, figs 57-62; Al-Handal et al. 2022: p. 89, figs 37, 38, 109-111	60.8	16.6			3		
Fallacia marnieri	(Manguin) Witkowski, Lange-Bertalot & Metzeltin	as *Navicula marnieri* in Manguin 1957: p. 127, pl. 5, figs 35a, 35b; Witkowski 2000: p. 207, pl. 71, figs 1-3; Al-Handal and Wulf 2008b: p. 427, figs 105,106; Zidarova et al 2022, fig. 9A	10.1(6.1)-24.5	5.4(3.8)-11.0		9-14(15)			
Fragilaria* cf. *parva	Tuji & Williams	Zidarova et al. 2016a: p. 36-40, pl. 3-5	16.1-52.1	2.6-4.8		15-20			
Fragilaria* cf. *striatula	Lyngbye	Zidarova et al. 2022: p. 96, figs AP-R	43.0-51.7	7.5-8.1		13-14			
Fragilariopsis curta	(Van Heurck) Hustedt	Hustedt 1958: p. 160, pl. 11, figs 140-144, pl. 12, fig. 159; Scott and Thomas 2005: p. 171, fig. 2.99; Cefarelli et al. 2010: p. 1466, figs 2a-d, 7a, b	11.7-31.4	5.7-6.6		10-13			
Fragilariopsis cylindrus	(Grunow ex Cleve) Helmcke & Krieger	Scott and Thomas 2005: p. , fig. 2.100; Cefarelli et al. 2010: p. 1470, figs 2e-1, 7c-e	3.7-16.4	2.4-3.4		15-16			
Fragilariopsis kerguelensis	(O'Meara) Hustedt	Scott and Thomas 2005: p. 183, fig. 2.101; Cefarelli et al. 2010: p. 1470, figs 3a-h, 7f, g	25.8-27.5	7.8-8.7		5-6		11	
Fragilariopsis rhombica	(O'Meara) Hustedt	Scott and Thomas 2005: p. 179, fig. 2.104; Cefarelli et al. 2010: p. 1475, fig. 5a-e	12.6-33.2	8.4-11.6		11-16			
Fragilariopsis separanda	Hustedt	Hustedt 1958: p. 165, pl. 10, figs 108–112; Scott and Thomas 2005: p. 184, fig.	11.8-15.3	7.6-9.1		8-13			

		2.104; Cefarelli et al. 2010: p. 1476, fig. 6a-d							
cf. *Gedaniella*			9.3-18.9	2.4-4.4			14-18		
Gomphonema maritimo-antarcticum	Van de Vijver, Kopalová, Zidarova & Kociolek	Van de Vijver et al. 2016a: p. 212, figs 22-74	15.3-39.7	4.7-7.5		10-15			
Gomphonemopsis ligowskii	Al-Handal & E.W.Thomas	Al-Handal et al. 2018: p. 98, figs 2-25	11.4-16.3	2.1-2.9		14-16			
Gyrosigma* cf. *fasciola	J.W. Griffith & Henfrey	Jahn et al. 2005: p. 306, figs 1-7; Al-Handal and Wulff 2008a: fig. 101; Al-Handal et al. 2022: p. 94, fig. 80	101.2-172.8	12.4-15.9		20-22			
Gyrosigma tenuissimum* var. *angustissimum	Simonsen	Simonsen 1959: p. 83, pl 12, fig. 7; Cardinal 1986: p. 179, figs 37, 38	155.2-159.6	7.4		19			
***Gyrosigma* sp.**			158.0-256.9	15.5-20.4		22-24			
cf. *Halamphora* (R)			21.7	3.0					
Halamphora ausloosiana	Van de Vijver & Kopalová	Van de Vijver et al. 2014a: p. 379, figs 4S-AG, 6	16.4-36.5	4.5-6.9		22-24			
Halamphora lineata	(Gregory) Levkov	Levkov 2009: p. 202, pl 101, figs 12-19	37.0-44.0	5.8-7.1		15			
Halamphora* cf. *staurophora	(Juhlin-Dannfelt) Álvarez-Blanco & S.Blanco	Witkowski et al. 2000: p. 150, pl 163, figs 34-35; Álvarez and Blanco 2014: p. 65,pl. 36, figs 7-8	13.7-21.0	3.3-3.6		24			
***Halamphora* cf. *veneta* (R)**	(Kützing) Levkov	Levkov 2009: p. 242, pl. 94, fig. 9-19, p. 102, figs 17-30	39.1	5.8		23			
***Halamphora* sp. 1 (R)**			36.9	7.6		16			
***Halamphora* sp. 2**			34.9-38.3	4.4-6.2		11-14			
***Halamphora* sp. 3 (R)**			17.4-21.0	4.3-5.0		14			
***Hantzschia amphioxys* (R)**	(Ehrenberg) Grunow	Lange-Bertalot et al. 2017: p. 338, pl. 104, figs 1-5	31.5-49.8	6.1-6.3		21-22			4-6
Hantzschia hyperaustralis	Van de Vijver & Zidarova	Zidarova et al. 2010: p. 326, fig. 6A-I	79.7-109.2	12.4-14.8		20-21			4-7
Hantzschia* cf. *virgata	(Roper) Grunow	Witkowski et al. 2000: p. 364, pl. 175, fig. 10, pl. 176, figs 1-3; Sabbe et al. 2003: p. 238, fig. 59; Silva et al. 2019: p. 800, fig. 2(22)	72.3-81.6	7.7-9.0		11-13		24	6
Hippodonta hungarica	(Grunow) Lange-Bertalot, Metzeltin & Witkowski	Zidarova et al. 2016a: p. 124, pl. 47	12.4-18.2	4.8-5.4		9-10			
Humidophila sceppacuerciae	Kopalová	Kopalová et al. 2015: p. 121, figs 2-26	7.7-9.6	2.1-3.1					
Humidophila tabellariaeformis	(Krasske) R.L. Lowe et al.	Zidarova et al. 2016a: p. 234, pl. 102	13.9-15.0	4.9-5.1		25-26			
Licmophora antarctica	M. Peragallo	Fernandes et al. 2014: p. 469, figs 1-9	47.1-100.5	9.6-12.6		6-7			

***Licmophora belgicae* (R)**	M. Peragallo	Fernandes et al. 2014: p. 470, figs 10-20	134.6	15.6		11			
Licmophora* cf. *gracilis	(Ehrenberg) Grunow	Witkowski et al. 2000: p. 65, pl. 18, figs 12-15, pl. 19, figs 7-15; Al-Handal and Wulff 2008b: p. 429, figs 6-8; Fernandes et al. 2014, p. 471, figs 21-29; Al-Handal et al. 2022, p. 88, fig 33	22.2-56.9	5.0-12.2		17-25			
Luticola australomutica	Van de Vijver	Van de Vijver and Mataloni 2008: p. 458, figs 39-51	18.8	6.7		20			
***Luticola austroatlantica* (R)**	Van de Vijver, Kopalová, Spaulding & Esposito	Esposito et al. 2008: p. 1383, figs 9-27	21.4-23.6	7.4		16			
Luticola desmetii	Kopalová & Van de Vijver	Kopalová et al. 2011: p. 47, figs 2-13	21.9-29.3	10.6-12.6		15-16			
Luticola higleri	Van de Vijver, Van Dam & Beyens	Van de Vijver et al. 2006: p. 71, figs 3-42	10.7-28.5	7.2-10.3		12-18			
Luticola* cf. *muticopsis	(Van Heurck) D.G. Mann	Zidarova et al. 2016a: p. 188, pl. 79	13.7-20.0	6.6-8.2		16			
Luticola* cf. *truncata	Kopalová & Van de Vijver	Kopalová et al. 2009: p. 118, figs 34-50	13.7-20.0	6.6-8.2		16			
Mayamaea* cf. *permitis	(Hustedt) K.Bruder & Medlin	Lange-Bertalot et al. 2017: p. 366, pl. 50, figs 13-19; Zidarova et al. 2016a:p. 260, pl. 115, figs 1-19	6.4-7.3	3.3-3.5					
Mayamaea sweetloveana	Zidarova, Kopalová & Van de Vijver	Zidarova et al. 2016b: p. 43, figs 46-58	6.8-7.7	3.8-4.7		20-26			
Minidiscus chilensis	Rivera	Rivera and Kock 1984: p. 281, pl. 2, 3, figs 5-14; Kang et al. 2003: p. 95, fig. 2, 3; Kaczmarska et al. 2009 : p. 463, figs 1, 2			2.9-3.5				
Navicula australoshetlandica	Van de Vijver	Van de Vijver et al. 2011 : p. 287, figs 2-15	13.0-30.5	4.5-6.0		12-15			
Navicula concordia	Riaux-Gobin & Witkowski	Witkowski et al. 2010: p. 121, figs 8-24	19.5-30.5	4.7-6.9		13-15			
Navicula cremeri	Van de Vijver & Zidarova	Van de Vijver et al. 2011 : p. 289, figs 30-45	27.3	5.5		12			
Navicula criophiliforma	Witkowski, Riaux-Gobin & Daniszewska-Kowalczyk	Witkowski et al. 2010: p. 121, figs 25-38	23.3-55.9	5.8-8.5		11-13			
Navicula directa	(W.Smith) Ralfs	Witkowski et al. 2000: p. 275 , pl. 129, fig 1, pl. 133, fig. 10-12; Scott and Thomas 2005, p. 157, fig. 2.87a–d; Al-Handal and Wulff 2008a, p. 64-66, 95; Zidarova et al. 2022: fig. 9N	67.7-123.6	8.2-13.1		7-9			
Navicula glaciei	Van Heurck	Van Heurck 1909: p. 11, pl. I, fig. 13; Scott and Thomas 2005: p. 158, fig. 2.89; Zidarova et al. 2022: fig. 9H	16.3-25.6	5.2-6.7		13-18			
Navicula gregaria	Donkin	Van de Vijver et al. 2002: p. 64, pl. 35, figs 9-18, pl. 36, fig. 3	16.4-25.6	5.1-6.6		16-20			

***Navicula* cf. *pagophila* var. *manitounukensis* (R)**	Poulin & Cardinal	Poulin and Cardinal 1982: p. 2836, fig. 3; Witkowski et al. 2000: p. 293, p. 128, figs 4-6	27.0-32.1	10.8-12.8		21-26			
Navicula* cf. *perminuta	Grunow	Busse and Snoeijs 2002: p. 277, fig. 11-15, 34-40; Lange-Bertalot et al. 2017: p. 400, pl. 30, fig. 25-32; Al-Handal et al. 2022: p. 92, fig. 69, 70	5.5-19.9	1.9-5.0		12-20			
***Navicula* sp. 2**			20.9-48.6	3.6-6.6		12-16			
***Navicula* sp. 3**			18.0-31.5	3.9-5.4		10-15			
***Navicula* sp. 4**			14.2-24.0	2.8-3.7		11-14			
***Navicula* sp. 5**			16.9-48.9	4.4-7.4		10-14			
***Navicula* sp. 6**			21.8-24.4	3.8-4.3		12-14			
***Navicula* sp. 7**			14.4-28.1	4.3-5.2		12-15			
***Navicula* sp. 8**			17.8-29.6	3.0-4.7		9-11			
***Navicula* sp. 9**			14.0-17.3	2.9-3.3		19-21			
***Navicula* sp. 10**			40.3-57.7	5.8-7.4		8-9			
***Navicula* sp. 11**			27.3-31.4	4.9-5.3		8-9			
***Navicula* sp. 12**			31.9-42.2	6.4-7.6		8-9			
***Navicula* sp. 13**			16.5-31.9	4.5-6.3		11-14			
***Navicula* sp. 14**			6.0-13.5	3.2-5.5		14-20			
Nitzschia annewillemsiana	Hamsher, Kopalová, Kociolek, Zidarova & Van de Vijver	Hamsher et al. 2016: p. 81, figs 2-22; Zidarova et al. 2016: p. 422, pl 194	10.6-23.1	2.9-4.1		24-26			10-12
Nitzschia kleinteichiana	Hamsher, Kopalová, Kociolek, Zidarova & Van de Vijver	Hamsher et al. 2016: p. 88, figs 77-97; Zidarova et al. 2016: p. 430, pl 198	14.2-23.3	2.5-3.3		25-29			10-14
Nitzschia* cf. *gracilis	Hantzsch	Hamsher et al. 2016: p. 83, figs 37-59; Zidarova et al. 2016a: p. 426, pl. 196	29.0-54.7	2.5-4.3					14-18
Nitzschia homburgiensis	Lange-Bertalot	Hamsher et al. 2016: p. 86, figs 60-76; Zidarova et al. 2016: p. 428, pl 197	29.1-39.2	3.9-5.1					10-16
Nitzschia* cf. *hybrida	Grunow	Witkowski et al. 2000: p. 386, pl. 191, figs 12-14; Al-Handal and Wulff 2008b: p. 429, fig. 117; Al-Handal and Wulff 2008a: fig. 122	59.8-73.5	5.1-6.9		24-25			8-12
Nitzschia medioconstricta	Hustedt	Hustedt 1958: p. 174, pl. 13, fig. 165,166; Scott and Thomas 2005: p. 191, fig. 2.108d-f	52.3-72. 1	4.4-6.8		24-26			8-11

Nitzschia soratensis	Morales & Vis	Morales and Vis 2007: p. 128, figs 253-256, 277-280; Zidarova et al. 2016a: p. 434, pl. 200	6.4-17.1	2.6-3.5		28-30			8-12
***Nitzschia* sp. 1 (R)**			17.6	3.5					13
***Nitzschia* sp. 2**			23.9-31.6	2.9-4.4					10-12
***Nitzschia* sp. 4**			32.8-44.3	4.1-6.8		24-29			8-12
***Nitzschia* sp. 5**			41.4-48.1	3.6-3.7					9-11
***Nitzschia* sp. 6**			22.3-28.2	4.4-5.5					14-17
***Nitzschia* sp. 7**			12.2-24.3	3.1-5.0					12-17
Odontella litigiosa	(Van Heurck) Hoban	as *Biddulphia litigiosa* in Van Heurck 1909: p. 40, pl. 10, fig. 141; Scott and Thomas 2005, p. 48, fig. 2.20a–f ;Al-Handal and Wulff 2008b: p. 430, figs 80-82; Al-Handal et al. 2022: p. 87, figs 24-26	23.6-52.5	17.6-60.7					
***Orthoseira roeseana* (R)**	(Rabenhorst) Pfitzer	Zidarova et al. 2016a: p. 34, pl. 2			13.3				
***Parlibellus* cf. *schuetii* (R)**	(Van Heurck) E.J.Cox	Van Heurck 1909: p. 13, pl. I, fig. 10;	71.0	24.0		14			
Petroneis* cf. *plagiostoma	(Grunow) D.G.Mann	Witkowski et al. 2000: p. 329, pl. 102, figs 5,6	36.6-48.8	18.1-20.8		10-12		6-12	
***Petroneis* sp. 1**			19.0-22.0	7.7-8.1		19		12-20	
***Petroneis* sp. 2**			21.3-26.6	10.2-11.1		16-19		12-20	
Pinnularia australoglobiceps	Zidarova, Kopalová & Van de Vijver	Zidarova et al. 2016a: p. 362, pl. 166	30.1-35.8	10.4-12.9		12-14			
Pinnularia australomicrostauron	Zidarova, Kopalová & Van de Vijver	Zidarova et al. 2016a: p. 364-368, pl. 167-169	24.7-63.0	9.7-12.7		12-14			
***Pinnularia australorabenhorstii* (R)**	Van de Vijver	Van de Vijver 2008: p. 224, figs 7-15, 24-28	42.0	16.7		6-8			
***Pinnularia borealis* (R)**	Ehrenberg	Zidarova et al. 2016a: p. 376, 378, pl 173, 174	42.3	9.0		5-6			
Pinnularia parallelimarginata	Simonsen	Simonsen 1992: p. 41, pl. 42, figs 1-8	30.5	5.1		15			
Pinnularia* cf. *quadratarea	(A.Schmidt) Cleve	Witkowski et al. 2000: p. 335, pl. 155, fig. 17-21; Al-Handal and Wulff 2008a: fig. 76,77; Al-Handal and Wulff 2008b: p. 430, fig. 116	18.0-79.8	6.1-10.5		8-12			
***Pinnularia subantarctica* var. *elongata* (R)**	(Manguin) Van de Vijver & Le Cohu	Van de Vijver et al. 2002 : p. 96, pl. 114, figs 1-11	25.9-32.2	5.5-6.0		14			
Placoneis australis	Van de Vijver & Zidarova	Zidarova et al. 2009: p. 301, figs 44-58, 62-64	21.4-23.0	6.5-7.4		14-18			
Planothidium australe	(Manguin) Le Cohu	Zidarova et al. 2016a: p. 98, pl. 34	12.3-22.3	7.4-9.6		13-17	14-17		

Planothidium quadripunctatum	(Oppenheim) Sabbe	Van de Vijver et al. 2002: p. 101, pl. 23, figs 42-49	8.4-9.8	3.9-4.5		16-18	16-17		
Planothidium rostrolanceolatum	Van de Vijver, Kopalová & Zidarova	Van de Vijver et al. 2013: p. 109, figs 61-84	15.0-27.5	5.3-7.9		13-16	13-16		
Planothidium wetzelii	Schimani, N.Abarca & R.Jahn	Juchem et al. 2023	10.9-18.8	5.6-6.7		14-18	14-18		
***Planothidium* sp.**			13.6-19.9	5.6-8.6		10-13	10-12		
***Pleurosigma* sp. 1**			189.4-225.5	20.7-20.8		13-15			
***Pleurosigma* sp. 2**			153.2-187.2	20.7-24.4		21-22			
Porosira* cf. *glacialis	(Grunow) Jørgensen	Scott and Thomas 2005: p. 84, fig. 2.41; Al-Handal et al. 2022: p. 83, figs 2-4			19.5-81.0			18-22	
Psammothidium germainii	(Manguin) Sabbe	Van de Vijver et al. 2016b: p 146, figs 9-81	19.7	9.6		22			
***Psammothidium germainioides* (R)**	Van de Vijver, Kopalová & Zidarova	Van de Vijver et al. 2016b: p 150, figs 108-138	15.7	6.8			28		
Psammothidium incognitum	(Krasske) Van de Vijver	Van de Vijver et al. 2002: p. 105, pl 29, fig. 1-11, pl. 30, fig. 1,2; Zidarova et al. 2016a: p. 86, pl. 28	13.8-16.3	5.0-5.6					
***Psammothidium manguinii* (R)**	(Hustedt) Van de Vijver	Van de Vijver et al. 2002: p. 106, pl 29, figs 20-33, pl. 30, figs 5-8; Zidarova et al. 2016a: p. 88, pl. 29	14.3	6.6		23	22		
Psammothidium papilio	(D:E. Kellogg, M. Stuiver, T.B. Kellogg & G.H. Denton) Kopalová & Van de Vijver	Kopalova et al. 2012: p. 204, fig. 5Q-T; Zidarova et al. 2016a: p. 90, pl. 30	8.5-14.7	4.3-5.8		24-30	24-30		
Psammothidium rostrogermainii	Van de Vijver, Kopalová & Zidarova	Van de Vijver et al. 2016b: p 148, figs 82-107	16.0-19.3	8.1-8.8		16	18		
Pseudogomphonema kamtschaticum	(Grunow) Medlin	Medlin and Round 1986: p. 216, fig. 29; Scott and Thomas 2005: p. 163, figs 2.93, 2.94a, b; Al-Handal and Wulff 2008b: p. 439, fig 95-100; Zidarova et al. 2022: fig. 10A	9.9-51.6	3.2-7.5		10-16			
Pteroncola carlinii	Almandoz & Ferrario	Almandoz et al. 2014: p. 189, figs 1-15	5.0-23.4	2.5-3.3					
***Rhabdonema* sp.**			134.3-135.2	21.3-25.6			5-6		
Rhoicosphenia michalii	Ligowski	Ligowski et al. 2014: p. 143, figs 1-69	20.5-27.9	3.7-5.9		7-8			
Sabbea* cf. *adminii	(D.Roberts & McMinn) Van de Vijver, Bishop & Kopalová	Bishop et al. 2019: p. 45, figs 1-29	31.1-32.0	4.5-4.6					

Sellaphora jamesrossensis	(Kopalová, & Van de Vivjer) Van de Vivjer & C.E. Wetzel	as *Eolimna jamesrossensis* in Kopalová et al. 2009: p. 116, figs 15-33, Zidarova et al. 2016a: p. 246, pl. 108	11.8-14.2	5.5-6.0		20-22			
Shionodiscus gracilis* var. *expectus	(VanLandingham) Alverson, Kang et Theriot	as *Thalassiosira gracilis* var. *expecta* in Johansen and Fryxell 1985: p. 170, figs 8, 60-63; Alverson et al. 2006: p. 259			9.9-13.6			14-18	
***Stauroneis acidojarensis* (R)**	Zidarova, Kopalová & Van de Vijver	Zidarova et al. 2014: p. 197, figs 13-29	45.2	9		22			
Stauroneis latistauros	Van de Vijver & Lange Bertalot	Van de Vijver et al. 2004: p. 48, pl. 49; Zidarova et al. 2016: p. 318-322, pl. 144-146	26.4-35.1	7.4-8.4		20-24			
***Stauroneis pseudomuriella* (R)**	Van de Vijver & Lange Bertalot	Vijver et al. 2004: p. 56, pl. 61; Zidarova et al. 2016: p. 330, pl. 150	21.4-29.9	4.8-5.0		22			
Staurosira pottiezii	Van de Vijver	Van de Vijver et al. 2014b: p. 257, figs 1-25	25.8	4.2			13		
Synedropsis* cf. *recta	Hasle, Medlin & Syvertsen	Hasle et al. 1994: p. 252, figs 27-30, 51-55, 57-60, 68-75	6.4-54.7	3.0-6.9			9-15		
Thalassionema gelida	M.Peragallo	Peragallo 1921: p .69, pl. III, fig. 10; Zidarova et al. 2022: p. 102, fig. 7	63.1-153.5	3.5-6.3			10-11		
Thalassiosira antarctica	Comber	Johansen and Fryxell 1985: p. 158, figs 15-17, 37-39			29.0-44.6			13-15	
Thalassiosira scotia	Fryxell & Hoban	Johansen and Fryxell 1985: p. 176, figs 25, 26, 40-42			21.9-29.1			8-9	
Trachyneis aspera	(Ehrenberg) Cleve	Witkowski et al. 2000: p. 355, pl. 139, fig. 14, pl. 159, figs 1-6,9; Al-Handal and Wulff 2008b: p. 432, figs 89, 90, 101; Al-Handal et al. 2022: 93, fig. 74	94.0-188.7	17.5-31.7		7-8			
Trigonium arcticum	(Brightwell) Cleve	Scott and Thomas 2005: p. 18, fig. 2.6; Al-Handal et al. 2022: p. 87, fig. 22	123.0					3-4	
Tripterion* cf. *margaritae	(Frenguelli & Orlando ex Fernandes & Sar) Fernandes & Sar	Fernandes and Sar 2009: p. 67, figs 2-62	12.1-16.2	3.2-4.1		24-25			
Unidentified centric diatom					2.8-4.5				
Unidentified pennate diatom			12.4	3.0			12		

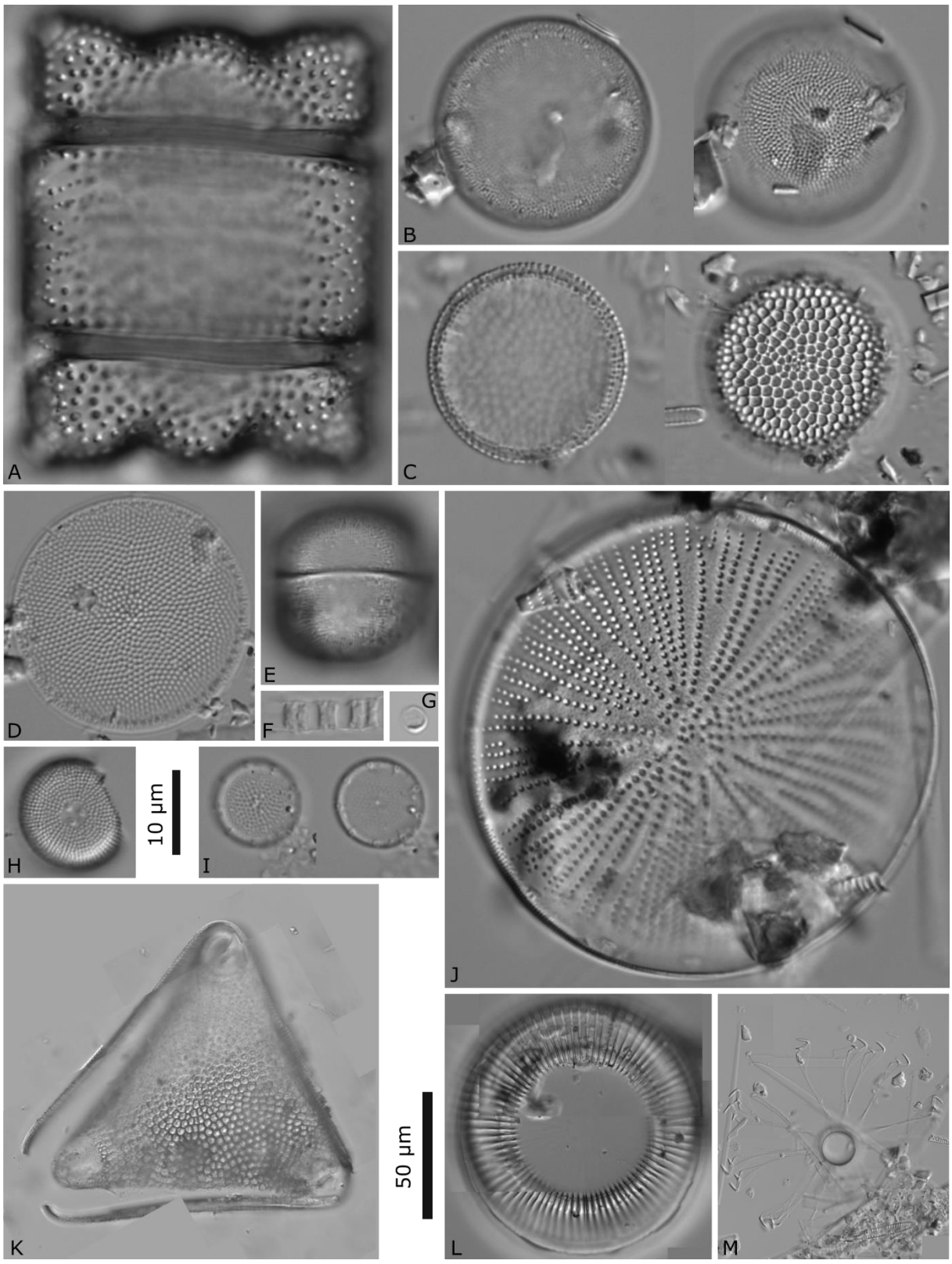

Figure 2 LM pictures of taxa found by morphological analyses. **A** *Odontella litigiosa* **B** *Porosira* cf. *glacialis* **C** *Thalassiosira scotia* **D** *Thalassiosira antarctica* **E** *Melosira* sp. **F** unidentified centric diatom **G** *Minidiscus chilensis* **H** *Orthoseira roeseana* **I** *Shionodiscus gracilis* var. *expectus* **J** *Actinocyclus actinochilus* **K** *Trigonium arcticum* **L** *Ellerbeckia sol* **M** *Corethron pennatum*. Scale bar: 10 µm (A-J); 50 µm (K-M).

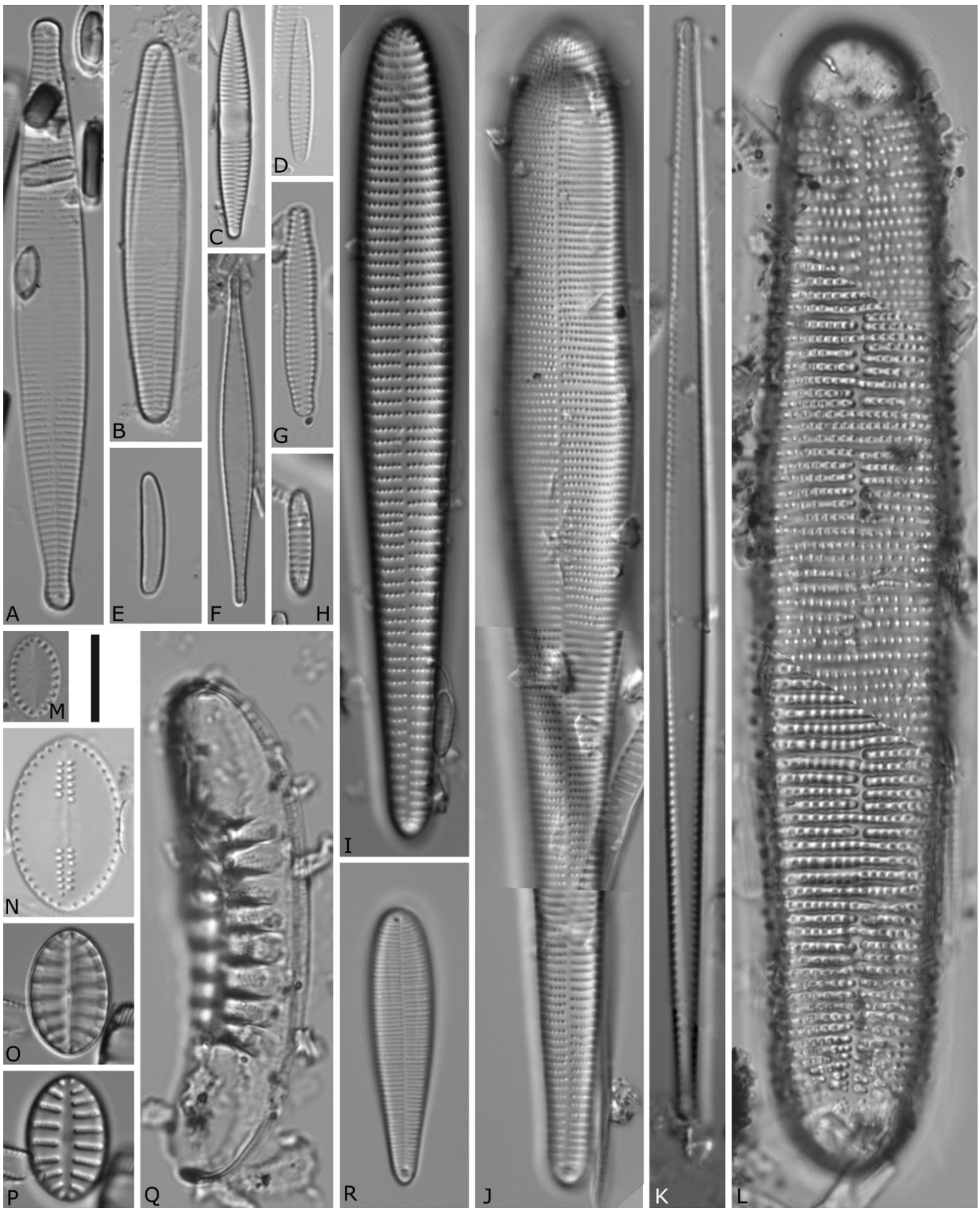

Figure 3 LM pictures of taxa found by morphological analyses. **A** *Brandinia charcotii* **B** *Fragilaria* cf. *striatula* **C** *Fragilaria* cf. *parva* **D** cf. *Gedaniella* **E** *Pteroncola carlinii* **F** *Synedropsis* cf. *recta* **G** *Staurosira pottiezii* **H** unidentified pennate diatom **I** *Licmophora antarctica* **J** *Licmophora belgicae* **K** *Thalassionema gelida* **L** *Rhabdonema* sp. **M** *Cocconeis pottercovei* **N** *Cocconeis infirmata* **O, P** *Cocconeis matsii* Q *Entopyla ocellata* R *Licmophora* cf. *gracilis*. Scale bar: 10 µm.

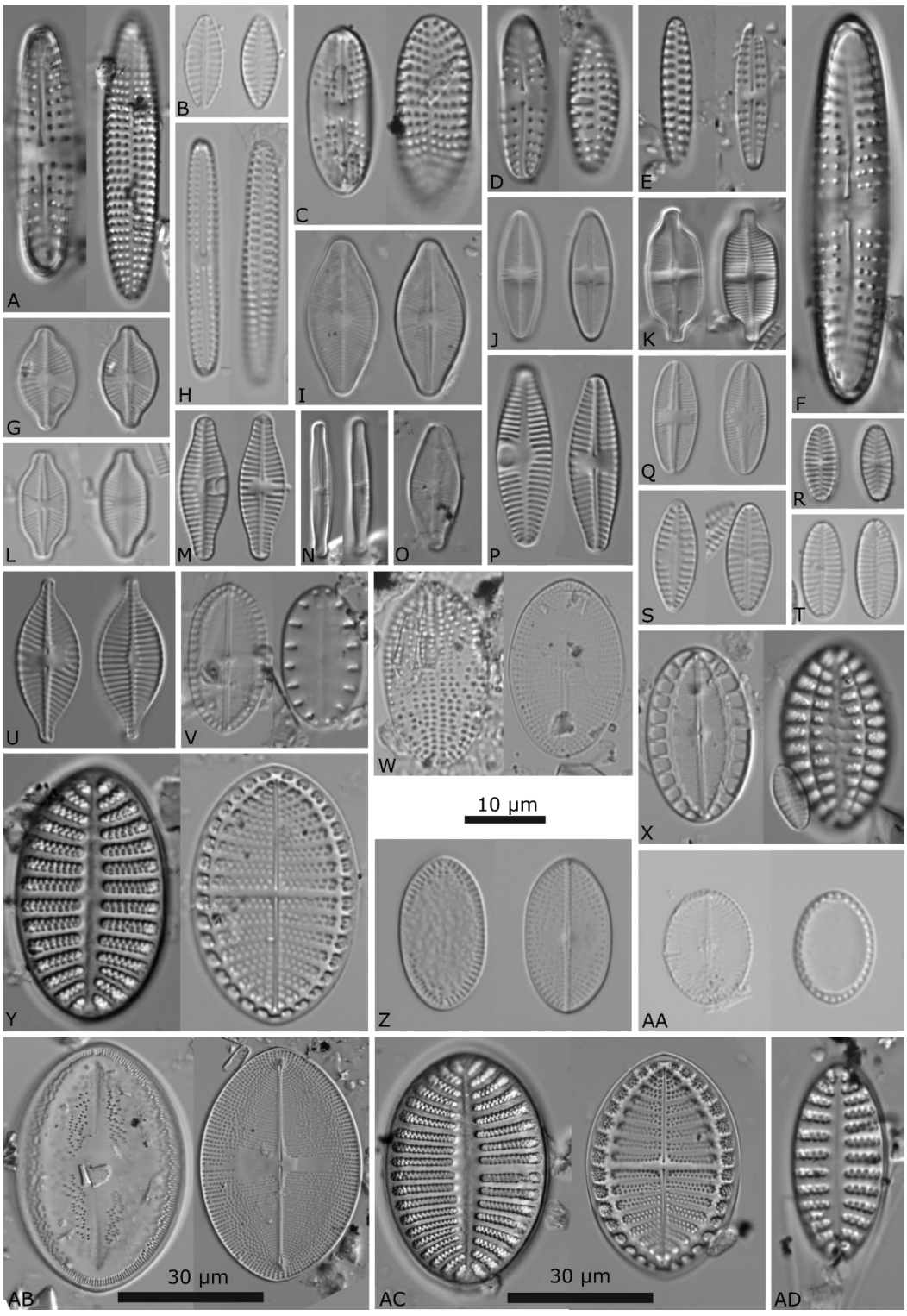

Figure 4 LM pictures of taxa found by morphological analyses. **A** *Achnanthes bongrainii* **B** *Achnanthes vicentii* **C** *Achnanthes* sp. 1 **D** *Achnanthes* sp. 2 **E** *Achnanthes* sp. 4 **F** *Achnanthes* sp. 5 **G** *Psammothidium rostrogermainii* **H** *Achnanthes* sp. 3 **I** *Psammothidium germainii* **J** *Psammothidium incognitum* **K** *Achnanthidium australexiguum* **L** *Psammothidium manguinii* **M** *Planothidium wetzelii* **N** *Achnanthidium* cf. *maritimo-antarcticum* **O** *Psammothidium germainioides* **P** *Planothidium rostrolanceolatum* **Q** *Psammothidium papilio* **R** *Planothidium quadripunctatum* **S** *Planothidium* sp. **T** cf. *Cocconeis* 2 **U** *Planothidium australe* **V** *Cocconeis melchioroides* **W** *Cocconeis californica* **X** *Australoneis frenguelliae* **Y** *Cocconeis fasciolata* **Z** cf. *Cocconeis* 1 **AA** *Cocconeis dallmannii* **AB** *Cocconeis antiqua* **AC** *Cocconeis imperatrix* **AD** *Cocconeis costata*. Scale bar: 10 µm (A-AA, AD); 30 µm (AB, AC).

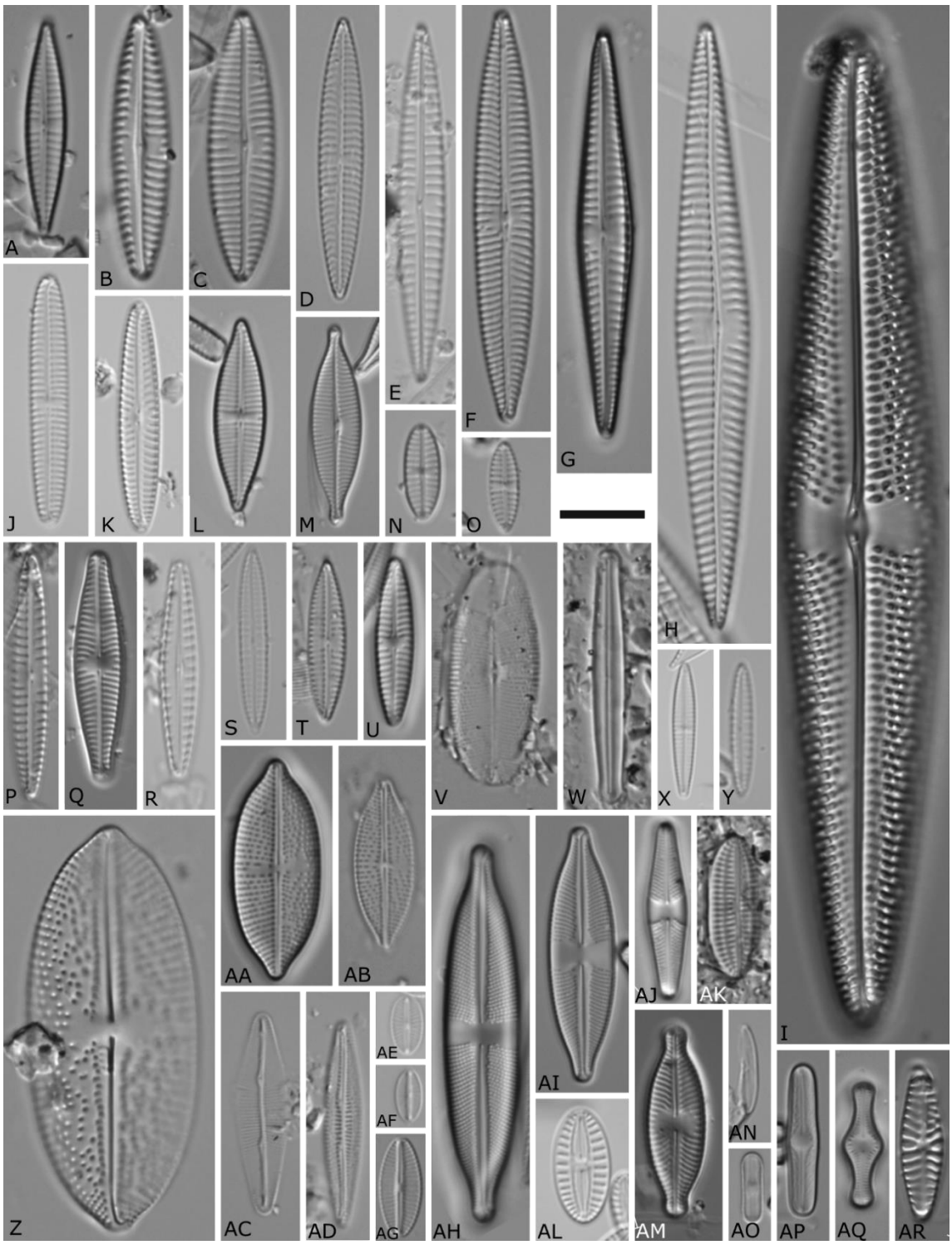

Figure 5 LM pictures of taxa found by morphological analyses. **A** *Navicula* sp. 3 **B** *Navicula* sp. 12 **C** *Navicula* sp. 1 **D** *Navicula* sp. 5 **E** *Navicula* sp. 10 **F** *Navicula criophiliforma* **G** *Navicula* sp. 2 **H** *Navicula directa* **I** *Trachyneis aspera* **J** *Navicula concordia* **K** *Navicula* sp. 13 **L** *Navicula glaciei* **M** *Navicula gregaria* **N** *Navicula* sp. 14 **O** *Navicula* cf. *perminuta* **P** *Navicula* sp. 8 **Q** *Navicula cremeri* **R** *Navicula* sp. 11 **S** *Navicula* sp. 6 **T** *Navicula* sp. 7 **U** *Navicula australoshetlandica* **V** *Navicula* cf. *pagophila* var. *manitounukensis* **W** *Sabbea* cf. *adminii* **X** *Navicula* sp. 9 **Y** *Navicula* sp. 4 **Z** *Petroneis* cf. *plagiostoma* **AA** *Petroneis* sp. 2 **AB** *Petroneis* sp. 1 **AC** *Berkeleya rutilans* **AD** *Berkeleya* cf. *sparsa* **AE** *Mayamaea sweetloveana* **AF** *Mayamaea* cf. *permitis* **AG** *Sellaphora jamesrossensis* **AH** *Stauroneis acidojarensis* **AI** *Stauroneis latistauros* **AJ** *Stauroneis pseudomuriella* **AK** *Diploneis* sp. **AL** *Fallacia marnieri* **AM** *Placoneis australis* **AN** *Lunella* sp. **AO** *Humidophila sceppacuerciae* **AP** *Brachysira minor* **AQ** *Humidophila tabellariaeformis* **AR** *Hippodonta hungarica*. Scale bar: 10 µm.

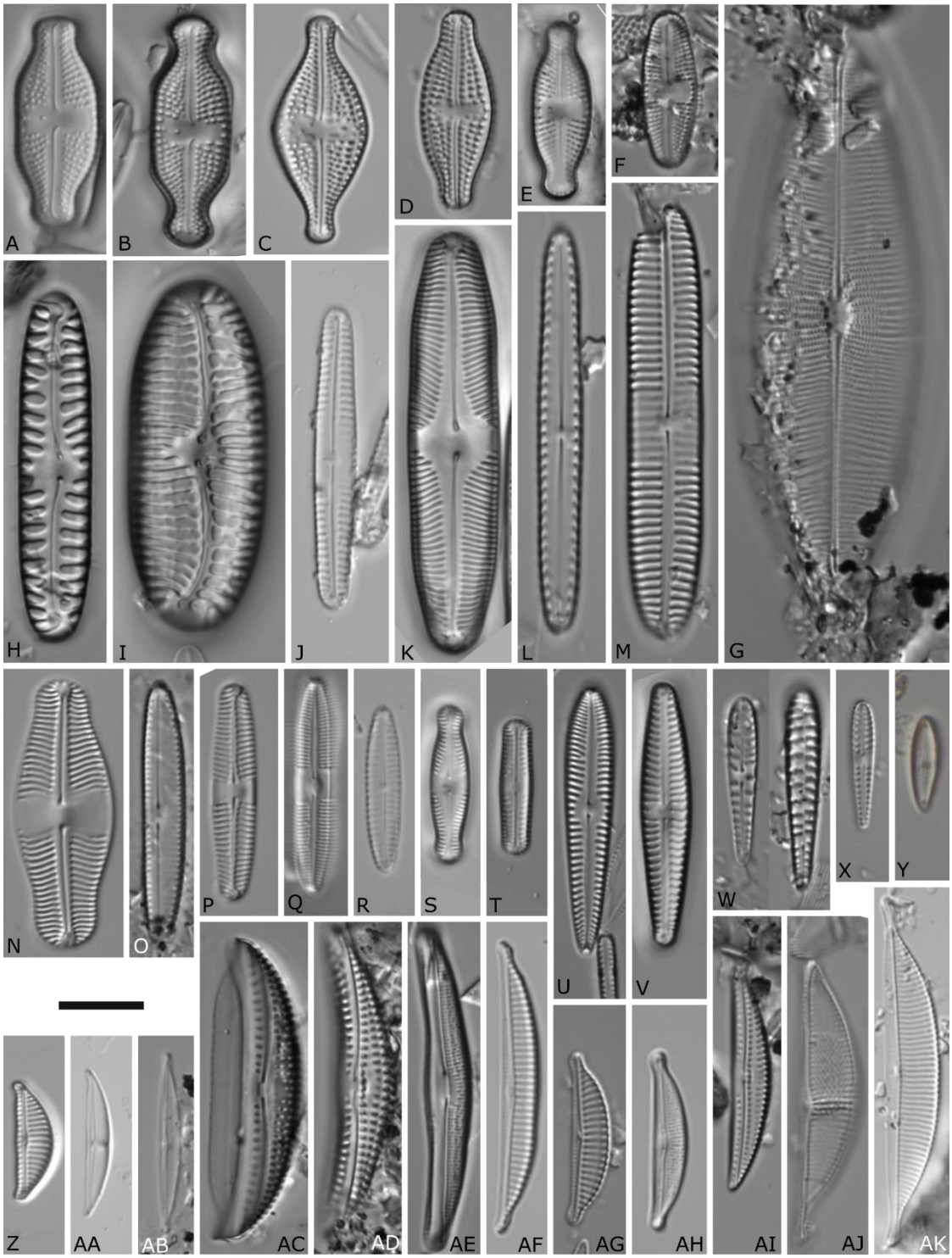

Figure 6 LM pictures of taxa found by morphological analyses. **A** *Luticola* cf. *truncata* **B** *Luticola* cf *muticopsis* **C** *Luticola desmetii* **D** *Luticola higleri* **E** *Luticola austroatlantica* **F** *Luticola australomutica* **G** *Parlibellus* cf. *schuetii* **H** *Pinnularia borealis* **I** *Pinnularia australorabenhorstii* **J** *Pinnularia* sp. **K** *Pinnularia australomicrostauron* **L** *Biremis ambigua* **M** *Pinnularia* cf. *quadratarea* **N** *Pinnularia australoglobiceps* **O** *Pinnularia parallelimarginata* **P** *Pinnularia subantarctica* var. *elongata* **Q** *Caloneis australis* **R** cf. *Chamaepinnularia* **S** *Chamaepinnularia australis* **T** *Chamaepinnularia gerlachei* **U** *Pseudogomphonema kamtschaticum* **V** *Gomphonema maritimo-antarcticum* **W** *Rhoicosphenia michalii* **X** *Gomphonemopsis ligowskii* **Y** *Tripterion* cf. *margaritae* **Z** *Encyonema ventricosum* **AA** *Halamphora* cf. *staurophora* **AB** cf. *Halamphora* **AC** *Amphora gourdonii* **AD** *Amphora* sp. **AE** *Halamphora* cf. *veneta* **AF** *Halamphora* sp. 2 **AG** *Halamphora* sp. 3 **AH** *Halamphora ausloosiana* **AI** *Amphora* cf. *pusio* **AJ** *Halamphora* sp. 1 **AK** *Halamphora lineata*. Scale bar: 10 µm.

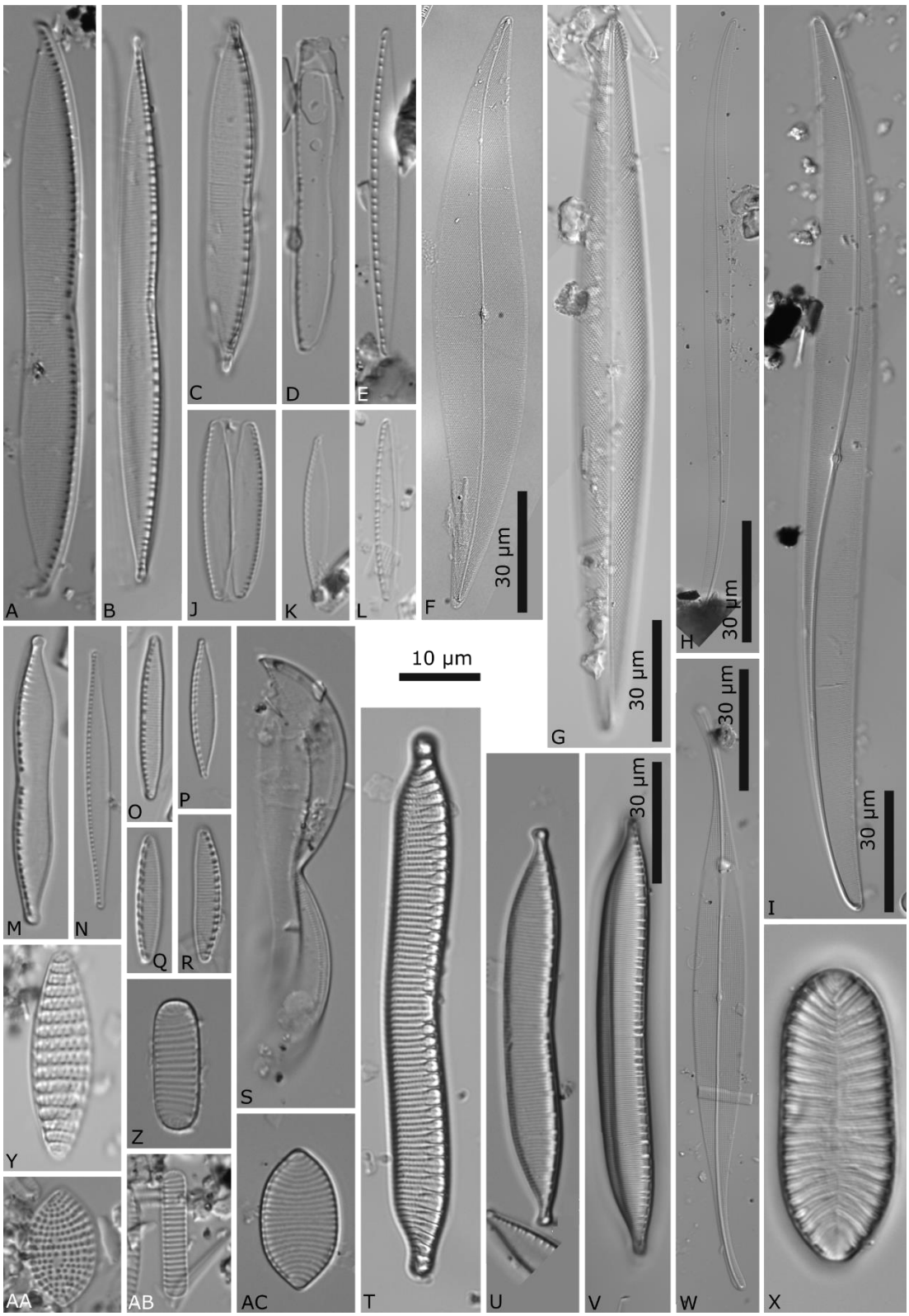

Figure 7 LM pictures of taxa found by morphological analyses. **A** *Nitzschia* cf. *hybrida* **B** *Nitzschia medioconstricta* **C** *Nitzschia* sp. 4 **D** *Nitzschia* sp. 3 **E** *Nitzschia* sp. 5 **F** *Pleurosigma* sp. 2 **G** *Pleurosigma* sp. 1 **H** *Gyrosigma tenuissimum* var. *angustissimum* **I** *Gyrosigma* sp. **J** *Nitzschia* sp. 6 **K** *Nitzschia* sp. 7 **L** *Nitzschia* sp. 2 **M** *Nitzschia homburgiensis* **N** *Nitzschia* cf. *gracilis* **O** *Nitzschia kleinteichiana* **P** *Nitzschia* sp. 1 **Q** *Nitzschia soratensis* **R** *Nitzschia annewillemsiana* **S** *Entomoneis* sp. **T** *Hantzschia* cf. *virgata* **U** *Hantzschia amphioxys* **V** *Hantzschia hyperaustralis* **W** *Gyrosigma* cf. *fasciola* **X** *Surirella australovisurgis* **Y** *Fragilariopsis kerguelensis* **Z** *Fragilariopsis curta* **AA** *Fragilariopsis separanda* **AB** *Fragilariopsis cylindrus* **AC** *Fragilariopsis rhombica*. Scale bar: 10 µm (A-E, J-U, X-AC); 30 µm (F-I, U, V).

The most abundant taxa (> 2 % of all counts per habitat, Table 3) across marine samples were in decreasing order *Navicula* cf. *perminuta*, *Minidiscus chilensis* P. Rivera, Navicula sp. 5, *Pseudogomphonema kamtschaticum* (Grunow) Medlin, *Achnanthes vicentii* Manguin, *Gyrosigma* sp., *Synedropsis* cf. *recta* and *Cocconeis fasciolata* (Ehrenberg) N.E.Brown. Across brackish water samples *Navicula gregaria* Donkin, *Navicula australoshetlandica* Van de Vijver, *Chamaepinnularia australis* Schimani & N.Abarca, *Nitzschia* cf. *gracilis*, *Nitzschia* sp. 6, *Halamphora ausloosiana* Van de Vijver & Kopalová and *Planothidium australe* (Manguin) Le Cohu were the most abundant taxa. Across the freshwater samples *Nitzschia annewillemsiana* Hamsher, Kopalová, Kociolek, Zidarova & Van de Vijver, *Nitzschia kleinteichiana* Hamsher, Kopalová, Kociolek, Zidarova & Van de Vijver, *Mayamaea sweetloveana* Zidarova, Kopalová & Van de Vijver, an unidentified centric diatom, *Nitzschia soratensis* E.A.Morales & M.L.Vis, Psammothidium papilio (D.E.Kellogg, Stuiver, T.B.Kellogg & G.H.Denton) K. Kopalová & Van de Vijver, *Achnanthidium* cf. *maritimo–antarcticum*, *Fragilaria* cf. *parva*, *Planothidium quadripunctatum* (D.R.Oppenheim) Sabbe, *Planothidium rostrolanceolatum* Van de Vijver, Kopalová & Zidarova and *Nitzschia* cf. *gracilis* were the most abundant taxa.

2.4.2 Antarctic taxonomic reference library

A total of 162 clonal cultures were established, resulting in the identification of 60 taxa: 33 of those taxa could be identified to species level, 23 to genus level and 4 where the genus affiliation is inconclusive (Table 4).

From the 60 taxa, only six had a sequence record in the International Nucleotide Sequence Database Collaboration (INSDC) databases (DDBJ, EMBL–EBI and NCBI) and 54 are new sequenced taxa. Some sequences from our Antarctic cultures were already published with a thorough morphological examination and in two cases with the description of a new species (Prelle et al. 2022; Juchem et al. 2023; Schimani et al. 2023).

Sequences of taxa, where identification was possible, were submitted to GenBank. The other sequences will be published when a thorough morphological description of the species has been performed. Those sequences can be retrieved from the DNA Databank of the Botanic Garden Berlin after personal communication.

Table 3 Most abundant taxa (> 2 % of average abundance) across marine, brackish water and freshwater samples for morphology count (LM) and metabarcoding *rbc*L and 18SV4, AA: average abundance across the habitat, NA: not taxonomically assigned. Several ASVs were assigned to the same taxon through the metabarcoding pipeline.

LM	AA [%]	*rbc*L	AA [%]	18SV4	AA [%]
Marine samples					
Navicula cf. *perminuta*	51.8	*Navicula* cf. *perminuta*	13.3	NA	24.8
Minidiscus chilensis	6.2	*Navicula* cf. *perminuta*	11.3	*Navicula* cf. *perminuta*	20.3
Navicula sp. 5	5.5	NA	11.0	NA	4.7
Pseudogomphonema kamtschatikum	4.5	NA	6.3	*Paralia sol (*syn. *Ellerbeckia sol)*	4.6
Achnanthes vicentii	3.1	NA	4.5	NA	4.4
Gyrosigma sp.	2.8	NA	3.7	*Thalassiosira minima*	2.5
Synedropsis cf. *recta*	2.2	*Navicula* cf. *perminuta*	3.2	*Navicula directa*	2.4
Cocconeis fasciolata	2.2	*Minidiscus chilensis*	2.9		
		Navicula sp.	2.9		
		Licmophora cf. *gracilis*	2.8		
		NA	2.5		
		Ellerbeckia sp.	2.2		
		NA	2.2		
Brackish water samples					
Navicula gregaria	52.3	*Navicula gregaria*	33.9	*Pinnularia australomicrostauron*	47.4
Navicula australoshetlandica	13.3	*Navicula australoshetlandica*	11.7	*Navicula gregaria*	20.6
Chamaepinnularia australis	7.1	*Nitzschia* sp.	8.8	*Navicula* cf. *veneta*	7.0
Nitzschia cf. *gracilis*	6.2	*Pinnularia australomicrostauron*	6.7	*Nitzschia* sp.	4.1
Nitzschia sp. 6	6.0	*Navicula gregaria*	6.4	*Pinnularia australomicrostauron*	2.8
Halamphora ausloosiana	5.3	*Chamaepinnularia australis*	5.2	*Pinnularia australomicrostauron*	2.6
Planothidium australe	2.2	NA	5.1		
		Nitzschia cf. *gracilis*	5.0		
		Halamphora ausloosiana	3.2		
		Pinnularia australoglobiceps	3.0		
		Nitzschia sp.	2.3		
Freshwater samples					
Nitzschia annewillemsiana	19.4	*Mayamaea sweetloveana*	13.6	*Pinnularia australomicrostauron*	28.1
Nitzschia kleinteichiana	16.0	*Fragilaria* sp.	9.9	*Nitzschia* cf. *frustulum*	10.9
Mayamaea sweetloveana	11.4	*Nitzschia* cf. *frustulum*	8.5	*Gomphonema maritimo antarcticum*	7.7
Unidentified centric diatom	10.8	*Nitzschia kleinteichiana*	8.3	NA	6.5
Nitzschia soratensis	10.5	*Nitzschia* sp.	7.6	*Fragilaria* sp.	5.8
Psammothidium papilio	7.0	NA	6.6	*Encyonema* sp.	3.4
Achnanthidium cf. *maritimo-antarcticum*	6.1	*Nitzschia* cf. *gracilis*	6.1	*Planothidium rostrolanceolatum*	3.4
Fragilaria cf. *parva*	4.6	*Encyonema* sp.	4.9	*Nitzschia* cf. *gracilis*	2.9
Planothidium quadripunctatum	2.4	*Achnanthidium* sp.	4.2	*Achnanthidium* sp.	2.4
Planothidium rostrolanceolatum	2.1	*Mayamaea* cf. *permitis*	3.6	NA	2.3
Nitzschia cf. *gracilis*	2.0	*Gomphonema maritimo antarcticum*	4.2	*Nitzschia* sp.	2.2
		Planothidium rostrolanceolatum	3.4	*Planothidium rostrolanceolatum*	2.2
		Planothidium cf. *pumilum*	2.6		
		Nitzschia sp.	2.0		

Table 4 Taxa which were established as clonal cultures, strain numbers, in case of publication: reference and accession number.

Taxon	Strain	Voucher at BGBM	DNA Bank	Publication of strain	Accession number *rbc*L	Accession number 18SV4
Achnanthes vicentii	D305_008	B 40 0045332	DB43189			
Achnanthes vicentii	D322_002	B 40 0045222	DB43092			
Achnanthes vicentii	D326_020	B 40 0045334	DB43015			
Brachysira minor	D300_027	B 40 0045258	DB42968			
Brachysira minor	D300_029	B 40 0045305	DB43129			
Chaetocerus* cf. *neogracilis	D305_007	B 40 0046208	DB43188			
Chamaepinnularia australis	D294_001	B 40 0045203	DB43033	(Schimani et al. 2023)	OX386460	OX386235
Chamaepinnularia australis	D294_002	B 40 0045204	DB43034	(Schimani et al. 2023)	OX386461	OX386236
Chamaepinnularia australis	D294_013	B 40 0045208	DB43043	(Schimani et al. 2023)	OX386464	OX386239
Chamaepinnularia australis	D294_014	B 40 0045209	DB43074	(Schimani et al. 2023)	OX386465	OX386240
Chamaepinnularia gerlachei	D294_005	B 40 0045272	DB43037	(Schimani et al. 2023)	OX386462	OX386237
Chamaepinnularia gerlachei	D294_006	B 40 0045207	DB43038	(Schimani et al. 2023)	OX386463	OX386238
Chamaepinnularia gerlachei	D296_001	B 40 0045355	DB43045	(Prelle et al. 2022; Schimani et al. 2023)	OX258987	OX258985
Chamaepinnularia gerlachei	D296_002	B 40 0045356	DB43046	(Schimani et al. 2023)	OX386466	OX386241
Chamaepinnularia gerlachei	D297_003	B 40 0045277	DB43047	(Schimani et al. 2023)	OX386467	OX386242
cf. *Chamaepinnularia*	D301_002	B 40 0045342	DB42990			
Cocconeis fasciolata	D326_023	B 40 0045353	DB43018			
cf. *Cocconeis* 1	D301_001	B 40 0045179	DB42989			
cf. *Cocconeis* 1	D301_009	B 40 0045315	DB42997			
cf. *Cocconeis* 2	D326_035	B 40 0045271	DB43025			
cf. *Cocconeis* 2	D326_037	B 40 0045328	DB43027			
cf. *Cocconeis* 2	D326_038	B 40 0045350	DB43028			

cf. *Cocconeis* 2	D326_039	B 40 0045329	DB43029			
Cylindrotheca* cf. *closterium	D322_018	B 40 0046211	DB43648			Not available
Fallacia marnieri	D301_003	B 40 0045314	DB42991	This study	OR355374	Not available
Fallacia marnieri	D301_004	B 40 0045217	DB42992	This study	OR355375	OR352010
Fallacia marnieri	D323_016	B 40 0045268	DB43144	This study	Not available	OR352011
Fallacia marnieri	D326_002	B 40 0045167	DB43001	This study	OR355376	OR352012
Fallacia marnieri	D326_005	B 40 0045169	DB43003	This study	OR355377	OR352013
Fallacia marnieri	D326_007	B 40 0045199	DB43005	This study	OR355378	OR352014
Fallacia marnieri	D326_014	B 40 0045235	DB43010	This study	OR355379	OR352015
Fallacia marnieri	D326_016	B 40 0045236	DB43012	This study	OR355380	OR352016
Fallacia marnieri	D326_017	B 40 0045346	DB43013	This study	OR355381	OR352017
Fallacia marnieri	D326_041	B 40 0045367	DB43209	This study	OR355382	OR352018
Fragilaria* cf. *parva	D299_016	B 40 0045214	DB43076			
Fragilaria* cf. *parva	D299_020	B 40 0045279	DB43080			
Fragilaria* cf. *parva	D299_026	B 40 0045255	DB43087			
Fragilaria* cf. *parva	D300_016	B 40 0045284	DB42962			
cf. *Gedaniella*	D291_001	B 40 0045201	DB43030			
cf. *Gedaniella*	D293_001	B 40 0045170	DB43183			
cf. *Gedaniella*	D324_004	B 40 0045231	DB43205			
Gomphonema maritimo-antarcticum	D299_018	B 40 0045245	DB43078	This study	OR355383	OR352019
Gomphonema maritimo-antarcticum	D299_021	B 40 0045290	DB43081	This study	OR355384	OR352020
Gomphonema maritimo-antarcticum	D299_028	B 40 0045294	DB43089	This study	Not available	OR352021
Gomphonema maritimo-antarcticum	D300_013	B 40 0045282	DB42959	This study	OR355385	OR352022
Gomphonema maritimo-antarcticum	D300_014	B 40 0045283	DB42960	This study	OR355386	OR352023

Gomphonema maritimo-antarcticum	D314_002	B 40 0045188	DB42971	This study	OR355387	OR352024
Gomphonema maritimo-antarcticum	D314_004	B 40 0045190	DB42973	This study	OR355388	OR352025
Gomphonema maritimo-antarcticum	D314_014	B 40 0045264	DB42983	This study	OR355389	OR352026
Gomphonema maritimo-antarcticum	D314_019	B 40 0045307	DB42988	This study	OR355390	OR352027
Halamphora ausloosiana	D294_007	B 40 0045273	DB43039	This study	OR355391	OR352028
Halamphora ausloosiana	D294_008	B 40 0045274	DB43040	This study	OR355392	OR352029
Hantzschia hyperaustralis	D314_011	B 40 0045306	DB42980	This study	OR355393	OR352030
Humidophila sceppacuerciae	D300_002	B 40 0045280	DB42950	This study	OR355394	OR352031
Humidophila sceppacuerciae	D300_022	B 40 0045302	DB42965	This study	OR355395	OR352032
Licmophora* cf. *gracilis	D308_002	B 40 0045343	DB43191			
Licmophora* cf. *gracilis	D308_003	B 40 0045220	DB43192			
Licmophora* cf. *gracilis	D308_004	B 40 0045316	DB43193			
***Lunella* sp.**	D292_010	B 40 0045571	DB43435			
***Lunella* sp.**	D309_004	B 40 0045580	DB43438			
***Lunella* sp.**	D323_012	B 40 0045228	DB43140			
***Lunella* sp.**	D326_015	B 40 0045200	DB43011			
Luticula higleri	D299_001	B 40 0045311	DB43062	This study	OR355396	OR352033
Luticola higleri	D299_010	B 40 0045312	DB43071	This study	OR355397	OR352034
Luticola desmetii	D300_028	B 40 0045313	DB43128	This study	OR355398	OR352035
Mayamaea sweetloveana	D299_006	B 40 0045175	DB43067	This study	OR355399	OR352036
Mayamaea sweetloveana	D299_007	B 40 0045176	DB43068	This study	OR355400	OR352037
Mayamaea sweetloveana	D299_009	B 40 0045178	DB43070	This study	OR355401	OR352038
Mayamaea sweetloveana	D304_001	B 40 0045246	DB42998	This study	OR355402	OR352039
Mayamaea sweetloveana	D304_002	B 40 0045259	DB42999	This study	OR355403	Not available

Mayamaea* cf. *permitis	D300_006	B 40 0045241	DB42969			
Mayamaea* cf. *permitis	D300_011	B 40 0045256	DB42958			
***Melosira* sp**	D323_018	B 40 0045309	DB43146	(Juchem et al. 2023)	OR036645	OR042180
***Melosira* sp**	D323_019	B 40 0045310	DB43147			
Minidiscus chilensis	D323_014	B 40 0045229	DB43142	This study	OR355404	OR352040
Minidiscus chilensis	D326_021	B 40 0045325	DB43017	This study	OR355405	OR352041
Navicula australoshetlandica	D295_001	B 40 0045460	DB43327	This study	OR355406	Not available
Navicula australoshetlandica	D300_018	B 40 0045330	DB43123	This study	OR355407	OR352042
Navicula concordia	D310_004	B 40 0045317	DB43201	(Prelle et al. 2022)	OX258991	OX259170
Navicula concordia	D310_002	B 40 0045186	DB43199	This study	OR355408	OR352043
Navicula concordia	D310_003	B 40 0045187	DB43200	This study	OR355409	OR352044
Navicula concordia	D310_006	B 40 0045576	DB43439	This study	OR355410	OR352045
Navicula criophiliforma	D288_003	B 40 0045335	DB43182	(Prelle et al. 2022)	OX258986	OX259166
Navicula criophiliforma	D288_002	B 40 0045247	DB43181	This study	OR355411	OR352046
Navicula criophiliforma	D326_027	B 40 0045237	DB43021	This study	OR355412	OR352047
Navicula criophiliforma	D322_014	B 40 0045380	DB43102	This study	OR355413	OR352048
Navicula directa	D326_001	B 40 0045166	DB43000	This study	OR355414	OR352049
Navicula gregaria	D294_003	B 40 0045205	DB43035	This study	OR355415	OR352050
Navicula gregaria	D300_003	B 40 0045281	DB42951	This study	OR355416	OR352051
Navicula gregaria	D300_004	B 40 0045296	DB42952	This study	OR355417	OR352052
Navicula gregaria	D300_007	B 40 0045216	DB42954	This study	OR355418	OR352053
Navicula* cf. *perminuta	D323_004	B 40 0045159	DB43133			
Navicula* cf. *perminuta	D323_011	B 40 0045322	DB43139			
Navicula* cf. *perminuta	D326_010	B 40 0045233	DB43008			

Navicula* cf. *perminuta	D326_012	B 40 0045234	DB43009			
***Navicula* sp. 1**	D326_009	B 40 0045232	DB43007			
***Navicula* sp. 4**	D307_001	B 40 0045475	DB43346			Not available
***Navicula* sp. 4**	D310_007	B 40 0045583	DB43440			Not available
***Navicula* sp. 5**	D301_007	B 40 0045242	DB42969			
***Navicula* sp. 5**	D301_008	B 40 0045331	DB42996			
***Navicula* sp. 6**	D291_006	B 40 0045474	DB43320			
***Navicula* sp. 13**	D310_001	B 40 0045185	DB43198			
***Navicula* sp. 13**	D326_006	B 40 0045198	DB43004			
***Navicula* sp. 13**	D326_019	B 40 0045347	DB43014			
Nitzschia annewillemsiana	D300_012	B 40 0045357	DB43122	(Prelle et al. 2022)	OX258988	OX259167
Nitzschia* cf. *gracilis	D299_014	B 40 0045212	DB43074			
Nitzschia homburgiensis	D299_002	B 40 0045172	DB43063	This study	OR355419	OR352054
Nitzschia kleinteichiana	D314_005	B 40 0045191	DB42974	This study	OR355420	OR352055
Nitzschia kleinteichiana	D314_008	B 40 0045194	DB42977	This study	OR355421	OR352056
Nitzschia medioconstricta	D309_001	B 40 0045569	DB43526	This study	OR355422	Not available
Nitzschia medioconstricta	D309_002	B 40 0045577	DB43527	This study	OR355423	Not available
Nitzschia soratensis	D300_026	B 40 0045257	DB42967	This study	OR355424	OR352057
***Nitzschia* sp. 3**	D322_015	B 40 0045364	DB43103			
***Nitzschia* sp. 3**	D322_016	B 40 0045365	DB43104			
***Nitzschia* sp. 4**	D310_008	B 40 0045584	DB43441			Not available
***Nitzschia* sp. 7**	D324_002	B 40 0045165	DB43203			
Odontella litigiosa	D305_005	B 40 0045181	DB43186			
Odontella litigiosa	D323_008	B 40 0045163	DB43137			

Pinnularia australoglobiceps	D294_004	B 40 0045206	DB43036			
Pinnularia australomicrostauron	D299_005	B 40 0045211	DB43066			
Pinnularia australomicrostauron	D314_001	B 40 0045261	DB42970			
Pinnularia australomicrostauron	D314_003	B 40 0045189	DB42972			
Pinnularia australomicrostauron	D314_010	B 40 0045195	DB42979			
Pinnularia australomicrostauron	D314_013	B 40 0045263	DB42982			
Pinnularia australomicrostauron	D314_017	B 40 0045287	DB42986			
Pinnularia* cf. *quadratarea	D324_001	B 40 0045164	DB43202			
***Pinnularia* sp.**	D322_010	B 40 0045321	DB43098			Not available
Planothidium australe	D294_010	B 40 0045275	DB43041	This study	OR355425	OR352058
Planothidium australe	D294_011	B 40 0045276	DB43042	This study	OR355426	OR352059
Planothidium australe	D300_005	B 40 0045297	DB42953	This study	OR355427	OR352060
Planothidium rostrolanceolatum	D299_003	B 40 0045173	DB43064	This study	OR355428	OR352061
Planothidium rostrolanceolatum	D299_008	B 40 0045177	DB43069	This study	OR355429	OR352062
Planothidium rostrolanceolatum	D299_022	B 40 0045252	DB43082	This study	OR355430	OR352063
Planothidium rostrolanceolatum	D300_021	B 40 0045286	DB42964	This study	OR355431	OR352064
Planothidium rostrolanceolatum	D314_007	B 40 0045193	DB42976	This study	OR355432	OR352065
Planothidium wetzelii	D300_015	B 40 0045340	DB42961	(Prelle et al. 2022)	OX258989	OX259168
Planothidium wetzelii	D300_019	B 40 0045358	DB43124	(Juchem et al. 2023)	OR036648	OR042183
Planothidium wetzelii	D300_020	B 40 0045301	DB43125	(Juchem et al. 2023)	OR036647	OR042182
Planothidium wetzelii	D300_025	B 40 0045341	DB42966	(Juchem et al. 2023)	OR036646	OR042181
***Planothidium* sp.**	D326_029	B 40 0045349	DB43022			Not available
***Pleurosigma* sp. 2**	D293_002	B 40 0045202	DB43184			
***Pleurosigma* sp. 2**	D322_007	B 40 0045320	DB43097			

***Pleurosigma* sp. 2**	D323_001	B 40 0045226	DB43130			
***Pleurosigma* sp. 2**	D323_002	B 40 0045267	DB43131			
***Pleurosigma* sp. 2**	D323_003	B 40 0045227	DB43132			
***Pleurosigma* sp. 2**	D324_003	B 40 0045230	DB43204			
***Pleurosigma* sp. 2**	D326_003	B 40 0045197	DB43002			
Porosira* cf. *glacialis	D308_005	B 40 0045182	DB43194			
Porosira* cf. *glacialis	D323_005	B 40 0045160	DB43134			
Psammothidium papilio	D300_023	B 40 0045303	DB43126	(Prelle et al. 2022)	OX258990	OX259169
Psammothidium papilio	D299_012	B 40 0045238	DB43072	This study	OR355433	OR352066
Psammothidium papilio	D299_013	B 40 0045239	DB43073	This study	OR355434	OR352067
Psammothidium papilio	D299_023	B 40 0045291	DB43083	This study	OR355435	OR352068
Psammothidium papilio	D299_024	B 40 0045253	DB43084	This study	OR355436	OR352069
Psammothidium papilio	D299_025	B 40 0045254	DB43086	This study	OR355437	OR352070
Psammothidium papilio	D300_001	B 40 0045295	DB43121	This study	OR355438	OR352071
Psammothidium papilio	D300_010	B 40 0045300	DB42957	This study	OR355439	OR352072
Psammothidium papilio	D314_015	B 40 0045319	DB42984	This study	OR355440	OR352073
Stauroneis latistauros	D314_009	B 40 0045318	DB42978	This study	OR355441	OR352074
Stauroneis latistauros	D314_016	B 40 0045344	DB42985	This study	OR355442	OR352075
Surirella australovisurgis	D300_017	B 40 0045285	DB42963			
Synedropsis* cf. *recta	D305_003	B 40 0045180	DB43185			

2.4.3 Metabarcoding Inventory

The Illumina MiSeq sequencing run generated 7,460,203 reads for the *rbc*L marker and 5,623,490 reads for the 18S V4 marker. After processing the reads through the DADA2 pipeline and improvement of the dataset by metbaR for *rbc*L 7,381,429 reads remained belonging to 1,041 ASVs and for 18S V4 5,570,517 reads remained belonging to 2,251 ASVs.

For the *rbc*L marker 6,002,917 of reads and 810 of ASVs belong to diatoms corresponding to 81.3 % and 77.8 % respectively. The majority of the non–diatom reads were assigned to green and brown algae. The average number of diatom–ASVs per sample ranged between 24 and 135. Of all ASVs, 283 could be assigned to a species in the reference library, whereby several ASVs were assigned to the same species and additional 156 ASVs could be assigned to genus level. In the marine samples, 611 ASVs were found; 292 ASVs could be assigned to genus level (47.8 %) and 190 to species level (31.1 %). In the freshwater samples, 216 ASVs were recovered; 152 could be assigned to genus level (70.4 %) and 96 to species level (44.4 %). Finally in the brackish water samples 52 ASVs were found; 38 could be assigned to genus level (73.0 %) and 25 to species level (48.1 %).

The most abundant taxa (sequence relative abundance ≥ 2 %, Table 3) in decreasing order across all marine samples belong to *Navicula* cf. *perminuta*, *Minidiscus chilensis*, *Navicula* sp., *Licmophora* cf. *gracilis*, *Ellerbeckia* sp. and six taxa where no genus could be assigned. Across the brackish samples *N. gregaria*, *N. australoshetlandica*, *Nitzschia* sp., *Pinnularia australomicrostauron* Zidarova, Kopalová & Van de Vijver, *C. australis*, *Nitzschia* cf. *gracilis*, *H. ausloosiana*, *Pinnularia australoglobiceps* Zidarova, Kopalová & Van de Vijver, *Nitzschia* sp. and one unassigned taxon were the most abundant taxa. Across the freshwater samples *Mayamaea sweetloveana*, *Fragilaria* sp., *Nitzschia* cf. *frustulum*, *N. kleinteichiana*, *Nitzschia* sp., *Nitzschia* cf. *gracilis*, *Encyonema* sp., *Achnanthidium* sp., *Mayamaea* cf. *permitis*, *Gomphonema maritimo–antarcticum* Van de Vijver, Kopalová, Zidarova & Kociolek, *P. rostrolanceolatum*, *Planothidium* cf. *pumilum*, *Nitzschia* sp. and one unassigned taxon were the most abundant taxa.

For the 18S V4 marker 2,835,064 of reads and 1,439 of ASVs belong to diatoms corresponding to 50.8 % and 63.9 % respectively. Here as well, the majority of the non–diatom reads were assigned to green and brown algae. The average number of diatom–ASVs per sample ranged between 5 and 248. Of all ASVs 344 could be assigned to a species in the reference library, whereby several ASVs were assigned to the same species and additional 348 could be assigned

to genus level. In the marine samples, 1090 ASVs were found; 462 ASVs could be assigned to genus level (42.4 %) and 207 to species level (19.0 %). In the freshwater samples, 300 ASVs were recovered; 211 could be assigned to genus level (70.3 %) and 131 to species level (43.3 %). Finally, in the brackish water samples 107 ASVs were found; 60 could be assigned to genus level (56.1 %) and 36 to species level (33.6 %).

The most abundant taxa (sequence relative abundance ≥ 2 %, Table 3) in decreasing order across all marine samples belong to *Navicula* cf. *perminuta*, *Paralia sol* (Ehrenberg) R.M.Crawford (regarded as a synonym of *Ellerbeckia sol* (Ehrenberg) R.M.Crawford & P.A.Sims), *Thalassiosira minima* Gaarder, *Navicula directa* (W.Smith) Brébisson and 3 taxa where no genus could be assigned. Across the brackish samples *Pinnularia australomicrostauron*, *N. gregaria*, *Navicula* cf. *veneta* and *Nitzschia* sp. were the most abundant taxa. Across the freshwater samples *P. australomicrostauron*, *Nitzschia* cf. *frustulum*, *G. maritimo–antarcticum*, *Fragilaria* sp., *Encyonema* sp., *Planothidium rostrolanceolatum*, *Nitzschia* cf. *gracilis*, *Achnanthidium* sp. and *Nitzschia* sp. were the most abundant taxa.

2.4.4 Comparison of diatom composition of taxa from cultures, morphological and metabarcoding inventories

In the clonal cultures 60 taxa could be identified, but 51 of them were also found in the microscopy examinations of environmental samples, which means that 9 taxa were only retrieved through culturing (*Lunella* sp., cf. *Cocconeis* 2, *Chaetocerus* cf. *neogracilis*, *Cylindrotheca* cf. *closterium*, *Melosira* sp., *Navicula* sp.1, *Nitzschia* sp.3, *Pinnularia* sp., *Surirella australovisurgis* Van de Vijver, Cocquyt, Kopalová & Zidarova, Fig. 8A). The morphological analysis found 174 taxa, in contrast to the 810 and 1439 ASVs, which were recovered with *rbc*L and 18SV4 metabarcoding respectively. However, several ASVs were assigned to the same taxon from the taxonomic reference library. Therefore, 58 and 57 genera were found based on *rbc*L and 18SV4 metabarcoding respectively and 58 genera were detected by morphological identification. In total, 34 genera were retrieved in all datasets, 11 genera only by morphological identification and as well 23 only by metabarcoding (Fig. 8B). On species level 92 and 82 taxa could be assigned based on *rbc*L and 18SV4 metabarcoding respectively. The combination of the total morphological richness of 165 taxa with 73 taxa solely assigned by metabarcoding resulted in a total of 238 infrageneric taxa (Fig. 8C). Of those taxa 33 were retrieved by all three methods and 111 only by morphology. The barcode reference library of Antarctic species presented here allowed the assignment of 47 infrageneric taxa in the metabarcoding analysis, which would have been left unassigned because no matching

reference sequences were available in the INSDC databases or Diat.barcode library before our study.

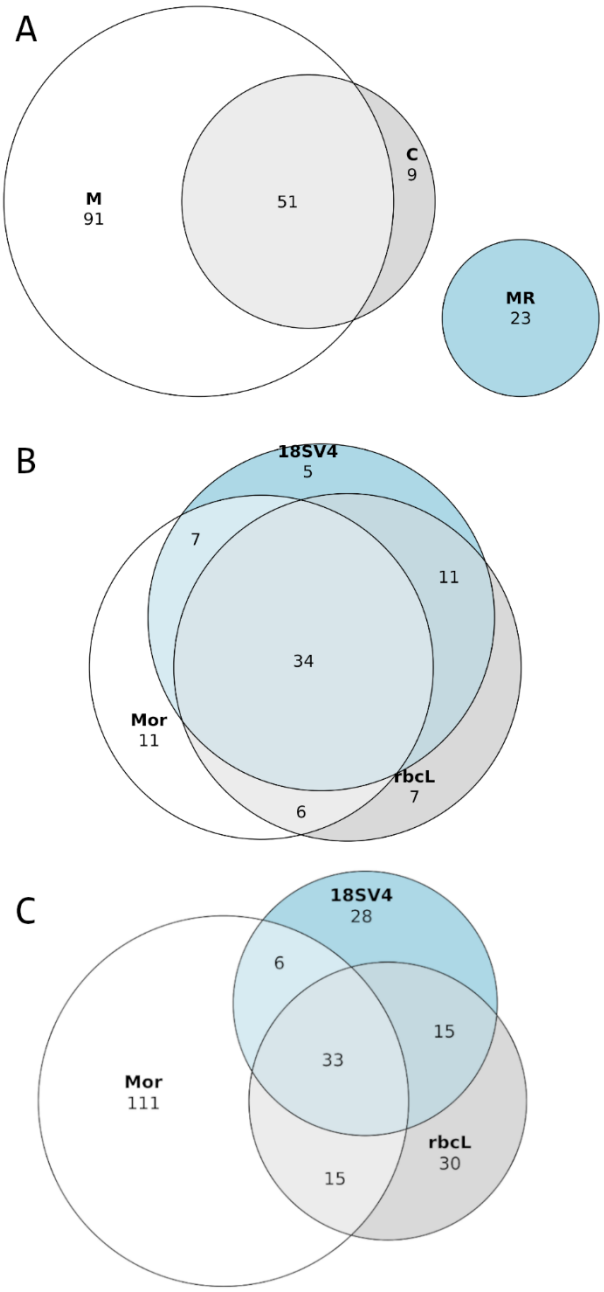

Figure 8 Venn diagrams comparing the performance of morphology and DNA metabarcoding in diatom identifications. **A** Morphological richness across all environmental samples and clonal cultures, M: infrageneric taxa identified by counting 400 valves per sample under light microscopy (LM), C: infrageneric taxa identified from clonal cultures, MR: infrageneric taxa identified by scanning LM slide for rare species **B** Genera identified by morphology (Mor) and metabarcoding with the *rbc*L and 18SV4 marker gene **C** Infrageneric taxa identified by morphology including rare taxa (Mor) and metabarcoding with the *rbc*L and 18SV4 marker gene (only assigned taxa to species level from metabarcoding shown).

The relative abundances on genus level shows that in general the same genera per samples are retrieved between the three datasets (Fig. 9). However, in both the 18SV4 and the *rbc*L dataset

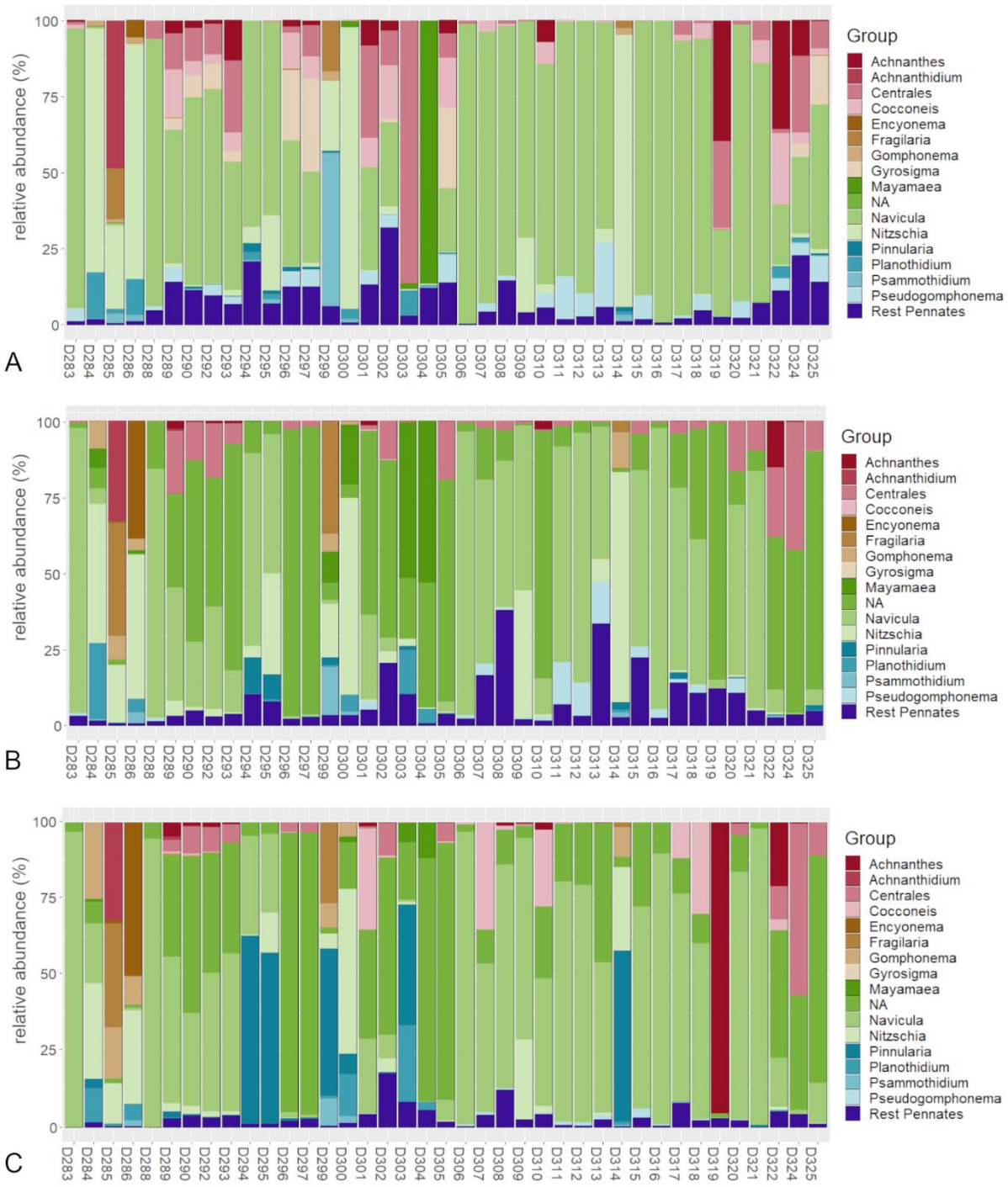

Figure 9 Relative abundance (%) of diatom genera across all sample locations. **A** morphology **B** *rbc*L marker gene **C** 18SV4 marker gene.

many sequences could not be assigned to genus level. This was especially true for the marine samples. A comparison to the morphological inventory indicates that *Gyrosigma* was underrepresented by both markers (D296, D297 and D305). In *rbc*L no reads and in 18SV4 13 reads were assigned to this genus. In some samples with a high abundance of not assigned genera, the morphology inventory shows a high abundance of *Navicula* (D289–D293, D296, D297, D310). A comparison between metabarcoding and the morphology inventory shows that

some genera were disproportionately higher in relative abundance like *Encyonema* in sample D286. This tendency of overrepresentation was more evident in the 18SV4 inventory, e.g. in the case of *Pinnularia* in most of the freshwater and brackish water samples and Achnanthes in sample D319. Interestingly, the genus *Cocconeis* was almost absent in the *rbc*L dataset.

2.4.5 Community analysis

Average taxa richness across water and substratum type was always higher in the metabarcoding inventories than in LM (Table 5, Suppl. material 1: table S1: results for the single sample locations). The Shannon diversity index based on the relative abundance of taxa was higher in the metabarcoding inventories as well (Table 5). The average diversity obtained for LM, *rbc*L and 18SV4 were 1.46, 1.94 and 1.85 respectively. The three approaches agree that a low diversity was found in marine habitats in biofilm from rocks and the highest diversity in marine or brackish waters in epipsammic biofilms.

The NMDS plots for morphology, *rbc*L and 18SV4 inventories show a clear separation in the community composition of samples taken from marine and freshwater habitats (Figure 10, stress =0.1). Brackish water habitats are more similar to freshwater habitats. Among marine habitats, community composition is more similar among samples taken from the same substrate. An exception is found in the LM dataset (Fig. 10C). Here D301 and D310 although taken from biofilm of stones are more similar to samples taken from epipsammic locations. The distinct separation was confirmed by PERMANOVA. Statistically significant differences in the community composition were found for the LM and DNA inventories among different water types (LM: $F_{2,36} = 8.588$, $p = 0.001$; *rbc*L: $F_{2,36} = 4.454$, $p = 0.001$; 18SV4: $F_{2,36} = 6.316$, $p = 0.001$) and substratum types (LM: $F_{1,37} = 8.899$, $p = 0.001$; *rbc*L: $F_{1,37} = 6.853$, $p = 0.001$; 18SV4: $F_{1,37} = 7.309$, $p = 0.001$).

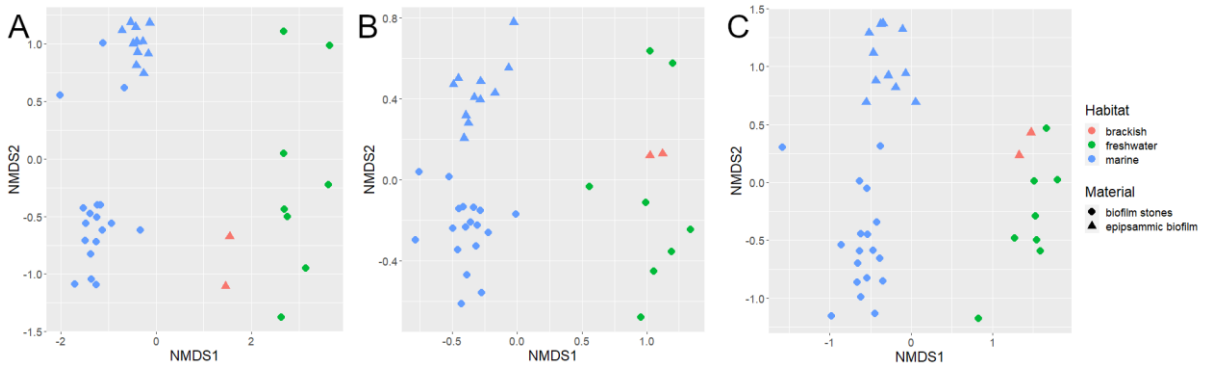

Figure 10 NMDS multivariate clustering of benthic diatom communities regarding water type and substratum type. **A** morphology **B** *rbc*L marker gene **C** 18SV4 marker gene. Stress: 0.1 (A-C).

According to the SIMPER results (Suppl. material 1: table S2), the species or ASVs contributing the most to the dissimilarity regarding the water types were *Navicula* cf. *perminuta* (marine–freshwater: LM 26.0 %, 18SV4: 13.2 %), *Mayamaea sweetloveana* (marine–freshwater: *rbc*L: 7.8 %), *Navicula gregaria* (marine–brackish water: LM: 26.2%, *rbc*L: 16.0%; freshwater–brackish water: LM: 26.8 %, *rbc*L: 14.5 %) and *Pinnularia australomicrostauron* (marine–brackish water: 18SV4: 29.3 %; freshwater–brackish water: 28.7 %). The dissimilarities regarding the substrate type were influenced by *Navicula* cf. *perminuta* (LM: 27.9 %) and two ASVs, that could not be taxonomically assigned (*rbc*L: 12.0 %, 18SV4: 22.7 %).

2.5 Discussion

2.5.1 Benthic diatom diversity in Potter Cove, Antarctic Peninsula

study demonstrated that the shallow coastal zone of Potter Cove harbours a rich diatom community with a total of 116 marine taxa identified by morphological investigation. Two floristic studies on benthic diatoms were already performed in Potter Cove by Al–Handal et al. (2022) and Al–Handal and Wulff (2008a), which retrieved 80 and 84 taxa respectively. However, here only surface sediments at four locations were sampled by SCUBA diving in different depths. A comparable study on neighbouring Livingston Island (Zidarova et al. 2022) with a larger variety of sampling locations also found a higher number of 133 taxa.

Even though fewer freshwater samples in our study were evaluated, 93 taxa were still found in these habitats. In general, many more studies investigating freshwater rather than marine habitats in Antarctica have been performed to date. Floristic studies found 122 taxa on King George Island/Isla 25 de Mayo (Kochman–Kędziora et al. 2018), 102 taxa on Livingston Island (Sterken et al. 2015) and 69 taxa on James Ross Island (Kopalová et al. 2012). Numerous new species endemic to maritime Antarctica have been described in recent decades e.g. Van de Vijver et al. (2006); Zidarova et al. (2009); Kopalová et al. (2011); Van de Vijver et al. (2012); Van de Vijver et al. (2013a); Kopalová et al. (2015); Zidarova et al. (2016b) and it is estimated that 44 % of all species might be endemic to the Antarctic, and most of them are confined to a single biogeographic region (Verleyen et al. 2021).

This study demonstrated that DNA metabarcoding presents an efficient method for surveying diatom biodiversity in coastal and freshwater ecosystems as it recorded a similar number of genera as the LM method with a high proportion of the genera identified by both methods. However, there are some discrepancies between the inventories. Some genera and species (23

and 73, respectively) were exclusively identified by DNA metabarcoding. DNA metabarcoding based on both marker genes retrieved a higher number of ASVs than taxa identified by LM. Several ASVs, however, were then assigned to the same taxon by the metabarcoding pipeline. Due to the incompleteness of the reference library the number of assigned species was lower for both marker genes in the metabarcoding approach compared to the LM approach which showed a greater efficiency for identifying taxa at species level.

Despite those restraints, similarity analyses of morphological as well as molecular data led to the same results. There was a clear statistically significant separation of diatom community according to water and substratum type. Based on all three approaches marine communities differ from freshwater communities and the brackish water communities are more similar to the freshwater ones. In addition, substratum type (sand or stones) seems to be a factor leading to dissimilarities in the diatom community as well. However, species contributing most to the dissimilarities between habitats differed, due to discrepancies in the inventories, which are discussed later.

2.5.2 Importance of the taxonomic reference library

60 diatom species were cultured and helped assign 47 taxa in our metabarcoding dataset because their sequence data were new to science. In the case of 27 taxa, sequence data was uploaded to ENA or GenBank in this or previous studies analysing the data from the same sampling campaign. Taxa, where a taxonomic investigation is still needed, will be published in combination with their sequence data, when a thorough taxonomic treatment is completed. Many of them will probably be described as new. In advance, their data is available at the Herbarium Berolinense. The large fraction of unidentified taxa especially in the marine habitat (~68 %) is not surprising since benthic diatoms were not broadly studied in this habitat.

Interestingly, some taxa established in culture were not observed in the morphological inventory. This was already shown in Mexican and Canadian streams in Mora et al. (2019) and Skibbe et al. (2022) where culture media and culturing conditions (i.e., light, day/night cycle and temperature) were listed as possibilities for the concealed diversity revealed by clonal culturing. Those may have allowed taxa to grow that were otherwise too rare to be detected through microscopy examinations. Valves of *Lunell*a sp., which were available due to culturing in this study, are very small, only lightly silicified with no visible ornamentation in LM. Valves might have been mistaken with non–diatom material or destroyed in processing of the samples as treatment with Naphrax tend to destroy delicate valves (Vermeulen et al. 2012). The living

cells of this species in enrichment medium might have been easier to spot due to their chloroplasts.

The multitude of successfully grown taxa indicates that our approach using several culture media with different salinities was suitable for culturing benthic diatoms from Potter Cove. Even though an extensive culturing effort was undertaken, many taxa could not be established as a unialgal culture. They were not observed as living cells in our enrichment culture as they might not be sampled alive, culture conditions were not suitable, or long–distance shipment might have destroyed more delicate species. Furthermore, some taxa were not able to grow after single cell isolation or the unialgal culture died before enough material was available for analysis. Therefore, an increased diversity of culture media and variation of culture conditions (e.g., temperature, agitation, light intensity or day/night cycle) could potentially stimulate the growth of additional less competitive species and thus improve culture success.

In our metabarcoding dataset many of the taxa could not be assigned by the reference library, even on genus level. This is especially true for marine habitats. The reference library established from the sequence database from the Herbarium Berolinense comprises mostly freshwater diatoms and already Pérez–Burillo et al. (2022) showed that the data availability in the Diat.barcode reference library has a strong tendency towards freshwater species. However, recent metabarcoding studies conducted in freshwater habitats highlight the need for a comprehensive reference database as well e.g. Rivera et al. (2018); Mortágua et al. (2019); Kulaš et al. (2022) to improve metabarcoding in routine monitoring.

Rimet et al. (2018a) suggested to complete reference libraries by using metabarcoding data. This could be a promising tool, however, the sequence needs to be abundant in the sample, with no insertions or deletions or stop codon and phylogenetic neighbour taxa have to correspond to neighbour taxonomic taxa expected from morphological observations. For taxa not matching those criteria, unialgal cultures as a reference for DNA metabarcoding studies are still needed. Furthermore, established data through culturing supports an integrative taxonomy as cultures show morphological variability within a species (Mohamad et al. 2022). In addition, sequence data supports phylogenetic analyses of diatoms (Kociolek et al. 2013; Downey et al. 2021) and especially longer sequences than short metabarcodes are needed for defining deep nodes of classification trees (Rimet et al. 2018b).

2.5.3 Discrepancies between morphological and molecular results

Several discrepancies between the morphological and the molecular inventory were evident. Most obvious was the above discussed fact, that many species and some genera were not encountered in the molecular inventory since the reference database was lacking a representative sequence. This was the case for e.g. *Gyrosigma* sp., *Pteroncola carlinii* Almandoz & Ferrario or *Achnanthidium* cf. *maritimo–antarcticum* listed with a relative high abundance in the LM inventory but without an entry for both metabarcoding inventories since both barcode sequences are unknown. Furthermore, some samples, where a high abundance of taxa in LM identified to the genera like *Navicula* and *Gyrosigma*, had no corresponding match in the metabarcoding inventories. This is indeed surprising, since those genera have a rather intensive representation in the reference databases. Studies in the last decades have shown that taxa morphologically assigned to an existing genus in Antarctica had been actually force fitted. Several new genera in the Antarctic or southern hemisphere have been established and existing taxa underwent a new combination (Williams 1988; Bishop et al. 2019; Guerrero et al. 2021). Our dataset suggests that there is a high cryptic diversity, which highlights the need for intensive taxonomic investigation of benthic diatoms in this region. An additional reason for discrepancies between the inventories might be found in morphological destruction or overlooked valves might lead to underrepresentation of taxa in LM like in the above described case of *Lunella* sp.

One of the key issues concerning sediment DNA metabarcoding is the distinction of living organisms that are part of the active benthic community from those organisms that are represented either by inactive resting stages or solely by DNA traces (Pawlowski et al. 2022). Sediments act as a repository of both intra– and extracellular DNA and the presence of extracellular DNA may have also influenced our molecular inventory, since taxa might have been detected in a sample even if their cells are not physically present. Those factors make it difficult to differentiate between living and dead organisms, or between species that live in the sediments or that have been settled from the water column.

Varying gene copy numbers per organism due to cell size and number of chloroplasts per cell is probably another reason for discrepancies between the LM and metabarcoding inventory. This correlation was noted in the case of *rbc*L by Vasselon et al. (2018) and Pérez–Burillo et al. (2022) and in the case of 18SV4 by Mora et al. (2019). This likely explains the higher abundances obtained by the DNA metabarcoding for the big cell species *P.*

australomicrostauron and *Paralia sol* (≡*Ellerbeckia sol*) in our study, which was especially apparent in the 18SV4 dataset.

The poor representation of *Cocconeis* in the *rbc*L inventory (1025 reads, 2 ASVs) despite the very high diversity of *Cocconeis* species revealed by LM was also an issue in the study of Burillo et al. 2022. Sequences of the Antarctic species *C. fasciolata* were available in our reference database as a culture of this species was established. No ASVs were assigned to this taxon in the *rbc*L inventory in contrast to the 18SV4 inventory. A worrying possibility is that primers of the *rbc*L barcode might not be suitable for marine *Cocconeis*. In fact, in comparable freshwater studies *C. placentula* was the most abundant taxon (Vasselon et al. 2017; Kulaš et al. 2022). A comparison with the forward *rbc*L primer region with the sequence of *C. fasciolata* showed a transition from the base G to an A. We suggest here to include a modified Diat_rbcL_708F forward primer at the third position from the back in the primer mix for marine samples:

TCGTCGGCAGCGTCAGATGTGTATAAGAGACAGAGGTGAAACTAAAGGTTCWTA CTTRAA.

In general, the list of taxa with the highest relative abundance of the LM data set correlates better with the *rbc*L than with the 18SV4 inventory. Similar results were found by Bailet et al. (2019), where the use of the 18SV4 marker generated more species inventories discrepancies. Bailet et al. (2020) investigated the performance of the *rbc*L and the 18SV4 marker using different bioinformatic pipelines. Here in addition, the use of the *rbc*L marker resulted in outcomes closer to these generated using traditional microscopy. Furthermore, it was shown that the choice of the pipeline had an influence on the taxonomic assemblage, but the results generated by *rbc*L correlated better among pipelines.

2.5.4 Prospects of DNA Metabarcoding for Antarctic benthic diatoms

It has been shown that the metabarcoding approach can complement and improve traditional identification via LM. It enables to detect tiny and delicate species. *Lunella* sp. and *Cylindrotheca* cf. *closterium* were detected in metabarcoding but not via the count of valves in LM. Rare species may be detected as well. In traditional identification, generally a few hundred valves are counted per sample probably not reaching saturation of species richness, while in metabarcoding several 10,000 to 100,000 reads are usually evaluated. Furthermore, it may detect cryptic diversity. Species that are morphologically similar may be better separated in the metabarcoding dataset.

In addition to the extension of information about Antarctic diatom diversity, our study also provided a new tool to survey water quality changes in Antarctica. In recent decades, climate change has had a crucial impact in the polar regions with increasing air and water temperature leading to glacial melting and the accompanying freshwater increase in coastal areas (IPCC 2019). DNA metabarcoding evaluation with a continuous sampling routine can give a valuable insight on community changes of benthic diatoms. Using those microorganisms as bioindicators may help assess the biological status and quality changes of water bodies in Antarctica, where environmental conditions are quickly evolving.

2.6 Conclusion

Antarctica is among the most extreme environments on Earth. An increased research effort is required in the light of desynchrony between the pace of change in polar regions and information demands to face engendered challenges (Danis et al. 2020). This study showed that a high benthic diatom diversity is apparent in this region, which was shown by traditional morphological identification and by the DNA metabarcoding approach. Overall, a combination of morphological, metabarcoding approaches accompanied by culturing increases the detection and identification of diatoms as the methods provide complementary information on biodiversity of benthic diatoms in this region. Furthermore, culturing is needed to enrich the reference barcode database. Ultimately, diatom diversity based on three approaches allowed a reliable dataset that can be used in routine monitoring assessment, which provides a deeper understanding of ecological status. Many taxa in both approaches could still not be identified on species level which emphasises the need for further taxonomic investigations in this region. In addition, the need for more efforts to complement the taxonomically curated reference database is evident.

The slides of the environmental samples, morphological and molecular data gained by LM and SEM investigation as well as sequencing of cultures together with the metabarcoding dataset represents the currently most extensive biodiversity dataset of marine benthic diatoms of Western Antarctica. All voucher material as well as the data are deposited at the Herbarium Berolinense and could be used as a baseline for further investigations, as a reference for monitoring routines and as training records in modelling tasks.

2.7 Acknowledgments

We would like to express our deep gratitude to Professor Andrzej Witkowski who has provided constructive comments improving this research. He was a prominent scientist and specialist of

marine diatoms. He was always a great supporter for early career scientists as well as a great cooperation partner. His invaluable contribution and commitment to diatom science will be remembered. We would like to thank the team of the Argentinian Antarctic Research Station "Carlini" of the Instituto Antártico Argentino (IAA) for their support and logistics, especially Dr. María Liliana Quartino. The authors are grateful to Jana Bansemer for work in the molecular lab and to Juliane Bettig for support at the SEM at the BGBM Berlin.

2.8 Funding

This project was funded within the framework of the SPP 1158 Antarktisforschung by the DFG under the grant number ZI 1628/2–1. OS acknowledges funding from the Verein der Freunde des Botanischen Gartens und des Botanischen Museums Berlin-Dahlem e.V.. GC acknowledges support from PADI Foundation (47918/2020), ANPCyT–DNA (PICT 2017–2691), UNLu (DCDD–CB 343/19 and 69/21) and the EU's H2020 research and innovation programme under the Marie Skłodowska–Curie grant agreement No 87269 CoastCarb. We acknowledge support by the Open Access Publication Fund of the Freie Universität Berlin.

2.9 References

Abarca N, Jahn R, Zimmermann J, Enke N (2014) Does the cosmopolitan diatom *Gomphonema parvulum* (Kützing) Kützing have a biogeography? PLoS ONE 9(1): e86885. https://doi.org/10.1371/journal.pone.0086885

Al-Handal AY, Wulff A (2008a) Marine benthic diatoms from Potter Cove, King George Island, Antarctica. Botanica Marina 51(1): 51–68. https://doi.org/10.1515/BOT.2008.007

Al-Handal AY, Wulff A (2008b) Marine epiphytic diatoms from the shallow sublittoral zone in Potter Cove, King George Island, Antarctica. Botanica Marina 51(5): 411–435. https://doi.org/10.1515/BOT.2008.053

Al-Handal AY, Riaux-Gobin C, Wulff A (2010) *Cocconeis pottercovei* sp. nov. and *Cocconeis pinnata* var. *matsii* var. nov., two new marine diatom taxa from King George Island, Antarctica. Diatom Research 25(1): 1–11. https://doi.org/10.1080/0269249X.2010.9705825

Al-Handal AY, Thomas EW, Torstensson A, Jahn R, Wulff A (2018) *Gomphonemopsis ligowskii*, a new diatom (Bacillariophyceae) from the marine Antarctic and a comparison to other *Gomphonemopsis*. Diatom Research 33(1): 97–103. https://doi.org/10.1080/0269249X.2018.1428916

Al-Handal AY, Torstensson A, Wulff A (2022) Revisiting Potter Cove, King George Island, Antarctica, 12 years later: New observations of marine benthic diatoms. Botanica Marina 65(2): 81–103. https://doi.org/10.1515/bot-2021-0066

Almandoz GO, Ferrario ME, Sullivan MJ, Ector L, Schloss IR (2014) A new *Pteroncola* species (Bacillariophyceae) from the South Shetland Islands, Antarctica. Phycologia 53(2): 188–194. https://doi.org/10.2216/13-210.1

Álvarez-Blanco I, Blanco S (2014) Benthic Diatoms from Mediterranean Coasts. Bibliotheca Diatomologica 60. J Cramer, 409 pp.

Alverson AJ, Kang S-H, Theriot EC (2006) Cell wall morphology and systematic importance of *Thalassiosira ritscheri* (Hustedt) Hasle, with a description of *Shionodiscus* gen. nov. Diatom Research 21(2): 251–262. https://doi.org/10.1080/0269249X.2006.9705667

Amsler C, Amsler M, Curtis M, McClintock J, Baker B (2019) Impacts of gastropods on epiphytic microalgae on the brown macroalga Himantothallus grandifolius. Antarctic Science 31(2): 89–97. https://doi.org/10.1017/S0954102019000014

Apothéloz-Perret-Gentil L, Cordonier A, Straub F, Iseli J, Esling P, Pawlowski J (2017) Taxonomy-free molecular diatom index for high-throughput eDNA biomonitoring. Molecular Ecology Resources 17(6): 1231–1242. https://doi.org/10.1111/1755-0998.12668

Aumack CF, Lowe AT, Amsler CD, Amsler MO, McClintock JB, Baker BJ (2017) Gut content, fatty acid, and stable isotope analyses reveal dietary sources of macroalgal–associated amphipods along the western Antarctic Peninsula. Polar Biology 40(7): 1371–1384. https://doi.org/10.1007/s00300-016-2061-4

Bailet B, Bouchez A, Franc A, Frigerio J-M, Keck F, Karjalainen S-M, Rimet F, Schneider S, Kahlert M (2019) Molecular versus morphological data for benthic diatoms biomonitoring in Northern Europe freshwater and consequences for ecological status. Metabarcoding and Metagenomics 3: e34002. https://doi.org/10.3897/mbmg.3.34002

Bailet B, Apothéloz-Perret-Gentil L, Baričević A, Chonova T, Franc A, Frigerio J-M, Kelly M, Mora D, Pfannkuchen M, Proft S, Ramon M, Vasselon V, Zimmermann J, Kahlert M (2020) Diatom DNA metabarcoding for ecological assessment: Comparison among bioinformatics pipelines used in six European countries reveals the need for standardization. The Science of the Total Environment 745: e140948. https://doi.org/10.1016/j.scitotenv.2020.140948

Bishop J, Kopalová K, Darling JP, Schulte NO, Kohler TJ, McMinn A, Spaulding SA, Mcknight DM, Van De Vijver B (2019) *Sabbea* gen. nov., a new diatom genus (Bacillariophyta) from continental Antarctica. Phytotaxa 418(1): 42–56. https://doi.org/10.11646/phytotaxa.418.1.2

Busse S, Snoeijs P (2002) *Navicula sjoersii* sp. nov., *N. bossvikensis* sp. nov. and N. perminuta Grunow from the Baltic Sea. Diatom Research 17(2): 271–282. https://doi.org/10.1080/0269249X.2002.9705547

Cahoon L (1999) The role of benthic microalgae in neritic ecosystems. Oceanography and Marine Biology 37: 47–86.

Callahan BJ, McMurdie PJ, Rosen MJ, Han AW, Johnson AJA, Holmes SP (2016) DADA2: High-resolution sample inference from Illumina amplicon data. Nature Methods 13(7): 581–583. https://doi.org/10.1038/nmeth.3869

Camacho C, Coulouris G, Avagyan V, Ma N, Papadopoulos J, Bealer K, Madden TL (2009) BLAST+: Architecture and applications. BMC Bioinformatics 10(1): e421. https://doi.org/10.1186/1471-2105-10-421

Campana GL (2018) Benthic micro- and macroalgae in a coastal Antarctic system (Potter Cove, South Shetland Islands): Effects of ultraviolet radiation and grazing on their colonization

and succession. PhD Thesis. National University of La Plata, Buenos Aires, Argentina, 239 pp. https://doi.org/10.35537/10915/71171

Campana GL, Quartino ML, Yousif A, Wulff A (2008) Effects of UV radiation and grazing on the structure of a subtidal benthic diatom assemblage in Antarctica. In: Wiencke C, Ferreyra GA, Abele D, Marenssi S (Eds) The Antarctic ecosystem of Potter Cove, King George Island (Isla 25 de Mayo). Reports on Polar and Marine Research (Ber. Polarforsch. Meeresforsch.) 571: 302–310.

Cardinal A (1986) Les Diatomées benthiques de substrats durs des eaux marines et saumâtres du Québec. 5. Naviculales, Naviculaceae; les genres Donkinia, Gyrosigma et Pleurosigma. Naturaliste Canadien 113: 167–190.

Cefarelli AO, Ferrario ME, Almandoz GO, Atencio AG, Akselman R, Vernet M (2010) Diversity of the diatom genus Fragilariopsis in the Argentine Sea and Antarctic waters: Morphology, distribution and abundance. Polar Biology 33(11): 1463–1484. https://doi.org/10.1007/s00300-010-0794-z

Chown SL, Clarke A, Fraser CI, Cary SC, Moon KL, McGeoch MA (2015) The changing form of Antarctic biodiversity. Nature 522(7557): 431–438. https://doi.org/10.1038/nature14505

Crawford RM, Hinz F, Honeywill C (1998) Three species of the diatom genus *Corethron* Castracane: Structure, distribution and taxonomy. Diatom Research 13(1): 1–28. https://doi.org/10.1080/0269249X.1998.9705432

Danis B, Van de Putte A, Convey P, Griffiths H, Linse K, Murray AE (2020) Editorial: Antarctic biology: Scale matters. Frontiers in Ecology and Evolution 8: e91. https://doi.org/10.3389/fevo.2020.00091

de Brouwer J, Wolfstein K, Ruddy G, Jones T, Stal L (2005) Biogenic stabilization of intertidal sediments: The importance of extracellular polymeric substances produced by benthic diatoms. Microbial Ecology 49(4): 501–512. https://doi.org/10.1007/s00248-004-0020-z

Desrosiers C, Leflaive J, Eulin A, Ten-Hage L (2013) Bioindicators in marine waters: Benthic diatoms as a tool to assess water quality from eutrophic to oligotrophic coastal ecosystems. Ecological Indicators 32: 25–34. https://doi.org/10.1016/j.ecolind.2013.02.021

Downey KM, Julius ML, Theriot EC, Alverson AJ (2021) Phylogenetic analysis places Spicaticribra within Cyclotella. Diatom Research 36(2): 93–99. https://doi.org/10.1080/0269249X.2021.1926332

Esposito RMM, Spaulding SA, McKnight DM, Van de Vijver B, Kopalová K, Lubinski D, Hall B, Whittaker T (2008) Inland diatoms from the McMurdo dry valleys and James Ross Island, Antarctica. Botany 86(12): 1378–1392. https://doi.org/10.1139/B08-100

Falkowski P, Scholes R, Boyle E, Canadell J, Canfield D, Elser J, Gruber N, Hibbard K, Högberg P, Linder S, Mackenzie FT, Moore III B, Pedersen T, Rosenthal Y, Seitzinger S, Smetacek V, Steffen W (2000) The global carbon cycle: A test of our knowledge of earth as a system. Science 290(5490): 291–296. https://doi.org/10.1126/science.290.5490.291

Fernandes LF, Sar EA (2009) Fine morphology of *Gomphonema margaritae* Frenguelli & Orlando and its validation and transfer to *Tripterion* Holmes, Nagasawa & Takano. Diatom Research 24(1): 63–78. https://doi.org/10.1080/0269249X.2009.9705783

Fernandes LF, Calixto-Feres M, Tenenbaum DR, Procopiak LK, Portinho D, Hinz F (2014) Fine morphology of four *Licmophora* (Bacillariophyta, Licmophorales) species from Admiralty Bay and Elephant Island, Antarctic Peninsula. Iheringia. Série Botânica 69: 465–477.

Gemeinholzer B, Droege G, Zetzsche H, Haszprunar G, Klenk HP, Güntsch A, Berendsohn W, Wägele JW (2011) The DNA Bank Network: The start from a German initiative. Biopreservation and Biobanking 9(1): 51–55. https://doi.org/10.1089/bio.2010.0029

Gregersen R, Pearman JK, Atalah J, Waters S, Vandergoes MJ, Howarth JD, Thomson-Laing G, Thompson L, Wood SA (2023) A taxonomy-free diatom eDNA-based technique for assessing lake trophic level using lake sediments. Journal of Environmental Management 345: e118885. https://doi.org/10.1016/j.jenvman.2023.118885

Griffiths HJ (2010) Antarctic Marine Biodiversity – What do we know about the distribution of life in the Southern Ocean? PLoS ONE 5(8): e11683. https://doi.org/10.1371/journal.pone.0011683

Guerrero JM, Riaux-Gobin C, Debandi JI, Zacher K, Quartino ML, Campana GL (2021) Morphology of *Australoneis* gen. nov. and *A. frenguelliae* comb. nov. (Achnanthales, Bacillariophyta) from the Antarctic Peninsula. Phytotaxa 513(2): 81–98. https://doi.org/10.11646/phytotaxa.513.2.1

Guillard RR, Ryther JH (1962) Studies of marine planktonic diatoms: I. *Cyclotella nana* Hustedt, and *Detonula confervacea* (Cleve) Gran. Canadian Journal of Microbiology 8(2): 229–239. https://doi.org/10.1139/m62-029

Hamsher S, Kopalová K, Kociolek P, Zidarova R, Van de Vijver B (2016) The genus *Nitzschia* on the South Shetland Islands and James Ross Island. Fottea 16(1): 79–102. https://doi.org/10.5507/fot.2015.023

Hasle G, Medlin L, Syvertsen E (1994) *Synedropsis* gen. nov., a genus of araphid diatoms associated with sea ice. Phycologia 33(4): 248–270. https://doi.org/10.2216/i0031-8884-33-4-248.1

Hustedt F (1958) Diatomeen aus der Antarktis und dem Südatlantik. Geographisch-kartographische Anstalt Mundus, Hamburg II: 103–191.

IPCC (2019) The ocean and cryosphere in a changing climate. Weyer NM, 1155 pp.

Jahn R, Sterrenburg FAS, Kusber W-H (2005) Typification and taxonomy of *Gyrosigma fasciola* (Ehrenberg) JW Griffith et Henfrey. Diatom Research 20(2): 305–311. https://doi.org/10.1080/0269249X.2005.9705639

Johansen JR, Fryxell GA (1985) The genus *Thalassiosira* (Bacillariophyceae): Studies on species occurring south of the Antarctic Convergence Zone. Phycologia 24(2): 155–179. https://doi.org/10.2216/i0031-8884-24-2-155.1

Juchem DP, Schimani K, Holzinger A, Permann C, Abarca N, Skibbe O, Zimmermann J, Graeve M, Karsten U (2023) Lipid degradation and photosynthetic traits after prolonged darkness in four Antarctic benthic diatoms including the newly described species

Planothidium wetzelii sp. nov. Frontiers in Microbiology 14: e1241826. https://doi.org/10.3389/fmicb.2023.1241826

Kaczmarska I, Lovejoy C, Potvin M, Macgillivary M (2009) Morphological and molecular characteristics of selected species of *Minidiscus* (Bacillariophyta, Thalassiosiraceae). European Journal of Phycology 44(4): 461–475. https://doi.org/10.1080/09670260902855873

Kang J-S, Kang S-H, Kim D, Kim D-Y (2003) Planktonic centric diatom *Minidiscus chilensis* dominated sediment trap material in eastern Bransfield Strait, Antarctica. Marine Ecology Progress Series 255: 93–99. https://doi.org/10.3354/meps255093

Kelly M, Juggins S, Mann DG, Sato S, Glover R, Boonham N, Sapp M, Lewis E, Hany U, Kille P, Jones T, Walsh K (2020) Development of a novel metric for evaluating diatom assemblages in rivers using DNA metabarcoding. Ecological Indicators 118: e106725. https://doi.org/10.1016/j.ecolind.2020.106725

Kermarrec L, Franc A, Rimet F, Chaumeil P, Frigerio JM, Humbert JF, Bouchez A (2014) A next-generation sequencing approach to river biomonitoring using benthic diatoms. Freshwater Science 33(1): 349–363. https://doi.org/10.1086/675079

Klöser H (1998) Habitats and distribution patterns of benthic diatoms in Potter Cove (King George Island) and its vecinity. In: Wiencke C, Ferreyra GA, Arntz W, Rinaldi C (Eds) The Potter Cove Coastal Ecosystem, Antarctica. Reports on Polar Research (Ber. Polarforsch.) 299: 95–105.

Kochman-Kędziora N, Noga T, Olech M, Van de Vijver B (2018) Freshwater diatoms of the Ecology Glacier foreland, King George Island, South Shetland Islands. Polish Polar Research 39: 393–412. https://doi.org/10.24425/118753

Kociolek JP, Stepanek JG, Lowe RL, Johansen JR, Sherwood AR (2013) Molecular data show the enigmatic cave–dwelling diatom *Diprora* (Bacillariophyceae) to be a raphid diatom. European Journal of Phycology 48(4): 474–484. https://doi.org/10.1080/09670262.2013.860239

Kopalová K, Nedbalová L, De Haan M, Van De Vijver B (2011) Description of five new species of the diatom genus Luticola (Bacillariophyta, Diadesmidaceae) found in lakes of James Ross Island (Maritime Antarctic Region). Phytotaxa 27(1): 44–60. https://doi.org/10.11646/phytotaxa.27.1.5

Kopalová K, Veselá J, Elster J, Nedbalová L, Komárek J, Van de Vijver B (2012) Benthic diatoms (Bacillariophyta) from seepages and streams on James Ross Island (NW Weddell Sea, Antarctica). Plant Ecology and Evolution 145(2): 190–208. https://doi.org/10.5091/plecevo.2012.639

Kopalová K, Kociolek JP, Lowe RL, Zidarova R, Van de Vijver B (2015) Five new species of the genus *Humidophila* (Bacillariophyta) from the Maritime Antarctic Region. Diatom Research 30(2): 117–131. https://doi.org/10.1080/0269249X.2014.998714

Kulaš A, Udovič MG, Tapolczai K, Žutinić P, Orlić S, Levkov Z (2022) Diatom eDNA metabarcoding and morphological methods for bioassessment of karstic river. The Science of the Total Environment 829: e154536. https://doi.org/10.1016/j.scitotenv.2022.154536

Lange-Bertalot H, Moser G (1994) *Brachysira*, Monographie der Gattung. Bibliotheca Diatomologica 29. J Cramer, 212 pp.

Lange-Bertalot H, Hofmann G, Werum M, Cantonati M, Kelly M (2017) Freshwater benthic diatoms of Central Europe: over 800 common species used in ecological assessment. Koeltz Botanical Books, Schmitten-Oberreifenberg, 942 pp.

Larsson J (2021) eulerr: Area-Proportional Euler and Venn Diagrams with Ellipses. R package version 6.1.1. https://CRAN.R-project.org/package=eulerr

Levkov Z (2009) Diatoms of Europe: diatoms of the European inland waters and comparable habitats. 5. Amphora sensu lato. Gantner.

Ligowski R, Al-Handal AY, Wulff A, Jordan RW (2014) *Rhoicosphenia michali*: A new species of marine diatom (Bacillariophyta) from King George Island, Antarctica. Phytotaxa 191(1): 141–153. https://doi.org/10.11646/phytotaxa.191.1.9

Malviya S, Scalco E, Audic S, Vincent F, Veluchamy A, Poulain J, Wincker P, Iudicone D, de Vargas C, Bittner L, Zingone A, Bowler C (2016) Insights into global diatom distribution and diversity in the world's ocean. Proceedings of the National Academy of Sciences of the United States of America 113(11): E1516. https://doi.org/10.1073/pnas.1509523113

Manguin E (1957) Premier inventaire des Diatomées de la Terre Adélie Antarctique éspèces nouvelles. Revue Algologique. Nouvelle Série 3 (3): 111–134.

Manguin E (1960) Les diatomées de la Terre Adélie campagne du" Commandant Charcot" 1949–1950, 141 pp.

Martin M (2011) Cutadapt removes adapter sequences from high–throughput sequencing reads. EMBnet.Journal 17(1): 10–12. https://doi.org/10.14806/ej.17.1.200

McMurdie PJ, Holmes S (2013) phyloseq: An R package for reproducible interactive analysis and graphics of microbiome census data. PLoS ONE 8(4): e61217. https://doi.org/10.1371/journal.pone.0061217

Medlin LK, Round FE (1986) Taxonomic studies of marine gomphonemoid diatoms. Diatom Research 1(2): 205–225. https://doi.org/10.1080/0269249X.1986.9704970

Mohamad H, Mora D, Skibbe O, Abarca N, Deutschmeyer V, Enke N, Kusber W-H, Zimmermann J, Jahn R (2022) Morphological variability and genetic marker stability of 16 monoclonal pennate diatom strains under medium–term culture. Diatom Research 37(4): 307–328. https://doi.org/10.1080/0269249X.2022.2141346

Mora D, Abarca N, Proft S, Grau JH, Enke N, Carmona J, Skibbe O, Jahn R, Zimmermann J (2019) Morphology and metabarcoding: A test with stream diatoms from Mexico highlights the complementarity of identification methods. Freshwater Science 38(3): 448–464. https://doi.org/10.1086/704827

Morales EA, Vis ML (2007) Epilithic diatoms (Bacillariophyceae) from cloud forest and alpine streams in Bolivia, South America. Proceedings. Academy of Natural Sciences of Philadelphia 156(1): 123–155. https://doi.org/10.1635/0097-3157(2007)156[123:EDBFCF]2.0.CO;2

Mortágua A, Vasselon V, Oliveira R, Elias C, Chardon C, Bouchez A, Rimet F, João Feio M, Almeida SFP (2019) Applicability of DNA metabarcoding approach in the bioassessment of Portuguese rivers using diatoms. Ecological Indicators 106: e105470. https://doi.org/10.1016/j.ecolind.2019.105470

Oksanen J, Blanchet FG, Friendly M, Kindt R, Legendre P, McGlinn D, Minchin P, O'Hara R, Simpson G, Solymos P (2022) vegan: Community Ecology Package. R package version 2.5–7. 2020.

Pavlov A, Leu E, Dieter H, Bartsch I, Karsten U, Hudson S, Gallet JC, Cottier F, Cohen J, Berge J, Johnsen G, Maturilli M, Kowalczuk P, Sagan S, Meler J, Granskog M (2019) The Underwater Light Climate in Kongsfjorden and Its Ecological Implications. In: Hop H, Wiencke C (Eds) The Ecosystem of Kongsfjorden, Svalbard. Springer, Cham. https://doi.org/10.1007/978-3-319-46425-1_5

Pawlowski J, Bruce K, Panksep K, Aguirre FI, Amalfitano S, Apothéloz-Perret-Gentil L, Baussant T, Bouchez A, Carugati L, Cermakova K, Cordier T, Corinaldesi C, Costa FO, Danovaro R, Dell'Anno A, Duarte S, Eisendle U, Ferrari BJD, Frontalini F, Frühe L, Haegerbaeumer A, Kisand V, Krolicka A, Lanzén A, Leese F, Lejzerowicz F, Lyautey E, Maček I, Sagova-Marečková M, Pearman JK, Pochon X, Stoeck T, Vivien R, Weigand A, Fazi S (2022) Environmental DNA metabarcoding for benthic monitoring: A review of sediment sampling and DNA extraction methods. The Science of the Total Environment 818: e151783. https://doi.org/10.1016/j.scitotenv.2021.151783

Peragallo M (1921) Botanique: Diatomées d'eau douce et Diatomées d'eau salée. in Expédition antarctique française 2nd: 1908–1910. [Masson.] https://doi.org/10.5962/bhl.title.64272

Pérez-Burillo J, Trobajo R, Vasselon V, Rimet F, Bouchez A, Mann DG (2020) Evaluation and sensitivity analysis of diatom DNA metabarcoding for WFD bioassessment of Mediterranean rivers. The Science of the Total Environment 727: e138445. https://doi.org/10.1016/j.scitotenv.2020.138445

Pérez-Burillo J, Valoti G, Witkowski A, Prado P, Mann DG, Trobajo R (2022) Assessment of marine benthic diatom communities: Insights from a combined morphological–metabarcoding approach in Mediterranean shallow coastal waters. Marine Pollution Bulletin 174: e113183. https://doi.org/10.1016/j.marpolbul.2021.113183

Pinseel E, Janssens SB, Verleyen E, Vanormelingen P, Kohler TJ, Biersma EM, Sabbe K, Van de Vijver B, Vyverman W (2020) Global radiation in a rare biosphere soil diatom. Nature Communications 11(1): e2382. https://doi.org/10.1038/s41467-020-16181-0

Piredda R, Claverie JM, Decelle J, de Vargas C, Dunthorn M, Edvardsen B, Eikrem W, Forster D, Kooistra WHCF, Logares R, Massana R, Montresor M, Not F, Ogata H, Pawlowski J, Romac S, Sarno D, Stoeck T, Zingone A (2018) Diatom diversity through HTS–metabarcoding in coastal European seas. Scientific Reports 8(1): e18059. https://doi.org/10.1038/s41598-018-36345-9

Poulin M, Cardinal A (1982) Sea ice diatoms from Manitounuk Sound, southeastern Hudson Bay (Quebec, Canada).: II. Naviculaceae, genus Navicula. Canadian Journal of Botany 60(12): 2825–2845. https://doi.org/10.1139/b82-343

Prelle LR, Schmidt I, Schimani K, Zimmermann J, Abarca N, Skibbe O, Juchem D, Karsten U (2022) Photosynthetic, Respirational, and Growth Responses of Six Benthic Diatoms from the Antarctic Peninsula as functions of salinity and temperature variations. Genes 13(7): e1264. https://doi.org/10.3390/genes13071264

QGIS Development Team (2021) QGIS Geographic Information System. Open Source Geospatial Foundation Project. http://qgis.osgeo.org

Riaux-Gobin C, Romero O (2003) Marine *Cocconeis* Ehrenberg (Bacillariophyceae) –species and related taxa from Kerguelen's Land (Austral-Ocean, Indian Sector). Bibliotheca Diatomologica 47. J Cramer, 188 pp.

Rimet F, Bouchez A (2012) Life-forms, cell-sizes and ecological guilds of diatoms in European rivers. Knowledge and Management of Aquatic Ecosystems 406(406): 1–1. https://doi.org/10.1051/kmae/2012018

Rimet F, Abarca N, Bouchez A, Kusber W-H, Jahn R, Kahlert M, Keck F, Kelly MG, Mann DG, Piuz A, Trobajo R, Tapolczai K, Vasselon V, Zimmermann J (2018a) The potential of high throughput sequencing (HTS) of natural samples as a source of primary taxonomic information for reference libraries of diatom barcodes. Fottea 18(1): 37–54. https://doi.org/10.5507/fot.2017.013

Rimet F, Vasselon V, Keszte BA, Bouchez A (2018b) Do we similarly assess diversity with microscopy and high–throughput sequencing? Case of microalgae in lakes. Organisms, Diversity & Evolution 18(1): 51–62. https://doi.org/10.1007/s13127-018-0359-5

Rimet F, Gusev E, Kahlert M, Kelly MG, Kulikovskiy M, Maltsev Y, Mann DG, Pfannkuchen M, Trobajo R, Vasselon V, Zimmermann J, Bouchez A (2019) Diat.barcode, an open–access curated barcode library for diatoms. Scientific Reports 9(1): e15116. https://doi.org/10.1038/s41598-019-51500-6

Risgaard-Petersen N, Rysgaard S, Nielsen LP, Revsbech NP (1994) Diurnal variation of denitrification and nitrification in sediments colonized by benthic microphytes. Limnology and Oceanography 39(3): 573–579. https://doi.org/10.4319/lo.1994.39.3.0573

Rivera P, Kock P (1984) Contributions to the diatom flora of Chile. II. Proceedings of the Seventh International Diatom Symposium, Philadelphia.

Rivera SF, Vasselon V, Jacquet S, Bouchez A, Ariztegui D, Rimet F (2018) Metabarcoding of lake benthic diatoms: From structure assemblages to ecological assessment. Hydrobiologia 807(1): 37–51. https://doi.org/10.1007/s10750-017-3381-2

Romero OE (2011) Morphological study of the genus *Cocconeis* Ehrenberg (Bacillariophyceae) collected during the 1897–1899 Belgian Antarctic Expedition. Botanica Marina 54(2): 179–188. https://doi.org/10.1515/bot.2011.020

Sabbe K, Verleyen E, Hodgson D, Vanhoutte K, Vyverman W (2003) Benthic diatom flora of freshwater and saline lakes in the Larsemann Hills and Rauer Islands, East Antarctica. Antarctic Science 15(2): 227–248. https://doi.org/10.1017/S095410200300124X

Schimani K, Abarca N, Zimmermann J, Skibbe O, Jahn R, Kusber W-H, Leya T, Mora D (2023) Molecular phylogenetics coupled with morphological analyses of Arctic and Antarctic strains place *Chamaepinnularia* (Bacillariophyta) within the Sellaphoraceae. Fottea 24(1): 1–22. https://doi.org/10.5507/fot.2023.002

Scott FJ, Thomas DP (2005) Diatoms. In: Scott FJ, Marchant HJ (Eds) Antarctic Marine Protists. Australian Biological Resources Study Canberra, 13–201.

Silva JF, Oliveira MA, Alves RP, Cassol APV, Anunciação RR, Silva EP, Schünemann AL, Pereira AB (2019) Geographic distribution of epilithic diatoms (Bacillariophyceae) in Antarctic lakes, South Shetland Islands, Maritime Antarctica Region. Check List 15(5): 797–809. https://doi.org/10.15560/15.5.797

Simonsen R (1959) Neue Diatomeen aus der Ostsee. I. Kieler Meeresf. 15, 74–83 (1960) Neue Diatomeen aus der Ostsee II. Kieler Meeresf. 16, 126–130 (1962) –Untersuchungen zur Systematik und Ökologie der Bodendiatomeen der westlichen Ostsee. Int. Internationale Revue der gesamten Hydrobiol Systematische Beihefte I, Berlin.

Simonsen R (1992) The diatom types of Heinrich Heiden in Heiden & Kolbe 1928. Bibliotheca Diatomologica 24. J Cramer, 229 pp.

Skibbe O, Abarca N, Forrest F, Werner P (2022) Exploring diatom diversity through cultures–a case study from the Bow River, Canada. Journal of Limnology 81(1). https://doi.org/10.4081/jlimnol.2022.2095

Stachura-Suchoples K, Enke N, Schlie C, Schaub I, Karsten U, Jahn R (2015) Contribution towards a morphological and molecular taxonomic reference library of benthic marine diatoms from two Arctic fjords on Svalbard (Norway). Polar Biology 39(11): 1933–1956. https://doi.org/10.1007/s00300-015-1683-2

Sterken M, Verleyen E, Jones V, Hodgson D, Vyverman W, Sabbe K, Van de Vijver B (2015) An illustrated and annotated checklist of freshwater diatoms (Bacillariophyta) from Livingston, Signy and Beak Island (Maritime Antarctic Region). Plant Ecology and Evolution 148(3): 431–455. https://doi.org/10.5091/plecevo.2015.1103

Tapolczai K, Keck F, Bouchez A, Rimet F, Kahlert M, Vasselon V (2019a) Diatom DNA metabarcoding for biomonitoring: Strategies to avoid major taxonomical and bioinformatical biases limiting molecular indices capacities. Frontiers in Ecology and Evolution 7: e409. https://doi.org/10.3389/fevo.2019.00409

Tapolczai K, Vasselon V, Bouchez A, Stenger-Kovács C, Padisák J, Rimet F (2019b) The impact of OTU sequence similarity threshold on diatom-based bioassessment: A case study of the rivers of Mayotte (France, Indian Ocean). Ecology and Evolution 9(1): 166–179. https://doi.org/10.1002/ece3.4701

Taylor CJ, Cocquyt C, Karthick B, Van de Vijver B (2014) Analysis of the type of *Achnanthes exigua* Grunow (Bacillariophyta) with the description of a new Antarctic diatom species. Fottea 14(1): 43–51. https://doi.org/10.5507/fot.2014.003

Van de Vijver B (2008) *Pinnularia obaesa* sp. nov. and *P. australorabenhorstii* sp. nov., two new large Pinnularia (sect. Distantes) from the Antarctic King George Island (South Shetland Islands). Diatom Research 23(1): 221–232. https://doi.org/10.1080/0269249X.2008.9705748

Van de Vijver B, Kopalová K (2014) Four *Achnanthidium* species (Bacillariophyta) formerly identified as *Achnanthidium minutissimum* from the Antarctic Region. European Journal of Taxonomy 79(79): 1–19. https://doi.org/10.5852/ejt.2014.79

Van de Vijver B, Mataloni G (2008) New and interesting species in the genus *Luticola* D.G. Mann (Bacillariophyta) from Deception Island (South Shetland Islands). Phycologia 47(5): 451–467. https://doi.org/10.2216/07-67.1

Van de Vijver B, Frenot Y, Beyens L (2002) Freshwater Diatoms from Ile de la Possession (Crozet Archipelago, Subantarctica). Bibliotheca Diatomologica 46. J Cramer, 412 pp.

Van de Vijver B, Beyens L, Lange-Bertalot H (2004) The genus *Stauroneis* in the Arctic and (sub–) Antarctic-regions. Bibliotheca Diatomologica 51. J Cramer, 317 pp.

Van de Vijver B, Van Dam H, Beyens L (2006) *Luticola higleri* sp. nov., a new diatom species from King George Island (South Shetland Islands, Antarctica). Nova Hedwigia 82(1–2): 69–79. https://doi.org/10.1127/0029-5035/2006/0082-0069

Van de Vijver B, Sterken M, Vyverman W, Mataloni G, Nedbalová L, Kopalová K, Elster J, Verleyen E, Sabbe K (2010) Four new non-marine diatom taxa from the Subantarctic and Antarctic regions. Diatom Research 25(2): 431–443. https://doi.org/10.1080/0269249X.2010.9705861

Van de Vijver B, Zidarova R, Sterken M, Verleyen E, de Haan M, Vyverman W, Hinz F, Sabbe K (2011) Revision of the genus *Navicula* ss (Bacillariophyceae) in inland waters of the Sub-Antarctic and Antarctic with the description of five new species. Phycologia 50(3): 281–297. https://doi.org/10.2216/10-49.1

Van de Vijver B, Tavernier I, Kellogg TB, Gibson J, Verleyen E, Vyverman W, Sabbe K (2012) Revision of type materials of Antarctic diatom species (Bacillariophyta) described by West & West (1911), with the description of two new species. Fottea 12(2): 149–169. https://doi.org/10.5507/fot.2012.012

Van de Vijver B, Kopalová K, Zidarova R, Cox E (2013a) New and interesting small-celled naviculoid diatoms (Bacillariophyta) from the Maritime Antarctic Region. Nova Hedwigia 97(1–2): 189–208. https://doi.org/10.1127/0029-5035/2013/0101

Van de Vijver B, Wetzel C, Kopalová K, Zidarova R, Ector L (2013b) Analysis of the type material of *Achnanthidium lanceolatum* Brébisson ex Kützing (Bacillariophyta) with the description of two new *Planothidiu*m species from the Antarctic Region. Fottea 13(2): 105–117. https://doi.org/10.5507/fot.2013.010

Van de Vijver B, Kopalová K, Zidarova R, Levkov Z (2014a) Revision of the genus *Halamphora* (Bacillariophyta) in the Antarctic Region. Plant Ecology and Evolution 147(3): 374–391. https://doi.org/10.5091/plecevo.2014.979

Van de Vijver B, Morales EA, Kopalová K (2014b) Three new araphid diatoms (Bacillariophyta) from the Maritime Antarctic Region. Phytotaxa 167(3): 256–266. https://doi.org/10.11646/phytotaxa.167.3.4

Van de Vijver B, Kopalová K, Zidarova R, Kociolek JP (2016a) Two new *Gomphonema* species (Bacillariophyta) from the Maritime Antarctic Region. Phytotaxa 269(3): 209–220. https://doi.org/10.11646/phytotaxa.269.3.4

Van de Vijver B, Kopalová K, Zidarova R (2016b) Revision of the *Psammothidium germainii* complex (Bacillariophyta) in the Maritime Antarctic Region. Fottea 16(2): 145–156. https://doi.org/10.5507/fot.2016.008

Van de Vijver B, Wetzel EC, Ector L (2018) Analysis of the type material of *Planothidium delicatulum* (Bacillariophyta) with the description of two new *Planothidium* species from the sub-Antarctic Region. Fottea 18(2): 200–211. https://doi.org/10.5507/fot.2018.006

Van Heurck H (1909) Expédition Antarctique Belge, Résultats du Voyage du SY Belgica en 1897–1898–1899. Raorts Scientifiques. Botanique, Diatomées. Imprim. J. E Buschmann, 129 pp.

Vanormelingen P, Verleyen E, Vyverman W (2008) The diversity and distribution of diatoms: From cosmopolitanism to narrow endemism. Biodiversity and Conservation 17(2): 393–405. https://doi.org/10.1007/s10531-007-9257-4

Vasselon V, Rimet F, Tapolczai K, Bouchez A (2017) Assessing ecological status with diatoms DNA metabarcoding: Scaling–up on a WFD monitoring network (Mayotte island, France). Ecological Indicators 82: 1–12. https://doi.org/10.1016/j.ecolind.2017.06.024

Vasselon V, Bouchez A, Rimet F, Jacquet S, Trobajo R, Corniquel M, Tapolczai K, Domaizon I (2018) Avoiding quantification bias in metabarcoding: Application of a cell biovolume correction factor in diatom molecular biomonitoring. Methods in Ecology and Evolution 9(4): 1060–1069. https://doi.org/10.1111/2041-210X.12960

Verleyen E, Van de Vijver B, Tytgat B, Pinseel E, Hodgson DA, Kopalová K, Chown SL, Van Ranst E, Imura S, Kudoh S, Van Nieuwenhuyze W, Sabbe K, Vyverman W (2021) Diatoms define a novel freshwater biogeography of the Antarctic. Ecography 44(4): 548–560. https://doi.org/10.1111/ecog.05374

Vermeulen S, Lepoint G, Gobert S (2012) Processing samples of benthic marine diatoms from Mediterranean oligotrophic areas. Journal of Applied Phycology 24(5): 1253–1260. https://doi.org/10.1007/s10811-011-9770-4

Villareal TA, Fryxell GA (1983) The genus *Actinocyclus* (Bacillariophyceae): Frustule morphology of a Sagittulus sp. nov. and two related species 1. Journal of Phycology 19(4): 452–466. https://doi.org/10.1111/j.0022-3646.1983.00452.x

Visco JA, Apothéloz-Perret-Gentil L, Cordonier A, Esling P, Pillet L, Pawlowski J (2015) Environmental Monitoring: Inferring the diatom index from Next-Generation Sequencing Data. Environmental Science & Technology 49(13): 7597–7605. https://doi.org/10.1021/es506158m

Vyverman W, Verleyen E, Wilmotte A, Hodgson DA, Willems A, Peeters K, Van de Vijver B, De Wever A, Leliaert F, Sabbe K (2010) Evidence for widespread endemism among Antarctic microorganisms. Polar Science 4(2): 103–113. https://doi.org/10.1016/j.polar.2010.03.006

Walne PR (1970) Studies on the food value of nineteen genera of algae to juvenile bivalves of the genera *Ostrea, Crassostrea, Mercenaria* and *Mytilus*. Fishery Investigations Series 2 26(5): 1–62.

Williams DM (1988) Tabulariopsis, a new genus of marine araphid diatom, with notes on the taxonomy of Tabularia (Kütz.) Williams et Round. Nova Hedwigia 47(1–2): 247–254.

Witkowski A, Lange-Bertalot H, Metzeltin D (2000) Diatom Flora of Marine Coasts I. Iconographia Diatomologica 7. Koeltz Scientific Books, 925 pp.

Witkowski A, Riaux-Gobin C, Daniszewska-Kowalczyk G (2010) New marine diatom (Bacillariophyta) species described from Kerguelen Islands coastal area and pertaining to *Navicula* s.s. with some remarks on morphological variation of the genus. Vie et Milieu 60: 117–133.

Zacher K, Hanelt D, Wiencke C, Wulff A (2007) Grazing and UV radiation effects on an Antarctic intertidal microalgal assemblage: A long-term field study. Polar Biology 30(9): 1203–1212. https://doi.org/10.1007/s00300-007-0278-y

Zacher K, Rautenberger R, Dieter H, Wulff A, Wiencke C (2009) The abiotic environment of polar marine benthic algae. Botanica Marina 52(6): 483–490. https://doi.org/10.1515/BOT.2009.082

Zidarova R, Van de Vijver B, Mataloni G, Kopalova K, Nedbalová L (2009) Four new freshwater diatom species (Bacillariophyceae) from Antarctica. Cryptogamie. Algologie 30(4): 295–310.

Zidarova R, Van de Vijver B, Quesada A, de Haan M (2010) Revision of the genus *Hantzschia* (Bacillariophyceae) on Livingston Island (South Shetland Islands, Southern Atlantic Ocean). Plant Ecology and Evolution 143(3): 318–333. https://doi.org/10.5091/plecevo.2010.402

Zidarova R, Kopalová K, Van de Vijver B (2014) The genus *Stauroneis* (Bacillariophyta) from the South Shetland Islands and James Ross Island (Antarctica). Fottea 14(2): 201–207. https://doi.org/10.5507/fot.2014.015

Zidarova R, Kopalová K, Van de Vijver B (2016a) Diatoms from the Antarctic Region. I: Maritime Antarctica. Iconographia Diatomologica 24. Koeltz Botanical Booksk, 509 pp.

Zidarova R, Kopalová K, Van de Vijver B (2016b) Ten new Bacillariophyta species from James Ross Island and the South Shetland Islands (Maritime Antarctic Region). Phytotaxa 272(1): 1–37. https://doi.org/10.11646/phytotaxa.272.1.2

Zidarova R, Ivanov P, Hineva E, Dzhembekova N (2022) Diversity and habitat preferences of benthic diatoms from South Bay (Livingston Island, Antarctica). Plant Ecology and Evolution 155(1): 70–106. https://doi.org/10.5091/plecevo.84534

Zimmermann J, Jahn R, Gemeinholzer B (2011) Barcoding diatoms: Evaluation of the V4 subregion on the 18S rRNA gene, including new primers and protocols. Organisms, Diversity & Evolution 11(3): 173–192. https://doi.org/10.1007/s13127-011-0050-6

Zimmermann J, Abarca N, Enke N, Skibbe O, Kusber W-H, Jahn R (2014) Taxonomic reference libraries for environmental barcoding: A best practice example from diatom research. PLoS ONE 9(9): e108793. https://doi.org/10.1371/journal.pone.0108793

Zimmermann J, Glöckner G, Jahn R, Enke N, Gemeinholzer B (2015) Metabarcoding vs. morphological identification to assess diatom diversity in environmental studies. Molecular Ecology Resources 15(3): 526–542. https://doi.org/10.1111/1755-0998.12336

Zinger L, Lionnet C, Benoiston A-S, Donald J, Mercier C, Boyer F (2021) metabaR: An r package for the evaluation and improvement of DNA metabarcoding data quality. Methods in Ecology and Evolution 12(4): 586–592. https://doi.org/10.1111/2041-210X.13552

3 Molecular phylogenetics coupled with morphological analyses of Arctic and Antarctic strains place *Chamaepinnularia* (Bacillariophyta) within the Sellaphoraceae

Katherina Schimani[1], Nélida Abarca[1], Jonas Zimmermann[1], Oliver Skibbe[1], Regine Jahn[1], Wolf–Henning Kusber[1], Thomas Leya[2] & Demetrio Mora[1,3]

[1] Botanischer Garten und Botanisches Museum Berlin, Freie Universität Berlin, Germany

[2] Fraunhofer Institute for Cell Therapy and Immunology, Branch Bioanalytics and Bioprocesses (IZI–BB), Extremophile Research & Biobank CCCryo, Potsdam, Germany

[3] Referat U2 – Mikrobielle Ökologie, Bundesanstalt für Gewässerkunde, Koblenz, Germany

Fottea 24(1): 1-22, https://doi.org/10.5507/fot.2023.002

4 Lipid degradation and photosynthetic traits after prolonged darkness in four Antarctic benthic diatoms, including the newly described species *Planothidium wetzelii* sp. nov.

Desirée P. Juchem[1]†, Katherina Schimani[2]†, Andreas Holzinger[3], Charlotte Permann[3], Nélida Abarca[2], Oliver Skibbe[2], Jonas Zimmermann[2], Martin Graeve[4] and Ulf Karsten[1]

†These authors have contributed equally to this work and share first authorship

[1]Applied Ecology and Phycology, Institute of Biological Sciences, University of Rostock, Rostock, Germany,

[2]Botanischer Garten und Botanisches Museum Berlin, Freie Universität Berlin, Berlin, Germany

[3]Department of Botany, Functional Plant Biology, University of Innsbruck, Innsbruck, Austria

[4]Alfred-Wegener-Institute Helmholtz-Center for Polar and Marine Research, Ecological Chemistry, Bremerhaven, Germany

Frontiers in Microbiology 14:1241826, https://doi.org/10.3389/fmicb.2023.1241826

4.1 Abstract

In polar regions, the microphytobenthos has important ecological functions in shallow-water habitats, such as on top of coastal sediments. This community is dominated by benthic diatoms, which contribute significantly to primary production and biogeochemical cycling while also being an important component of polar food webs. Polar diatoms are able to cope with markedly changing light conditions and prolonged periods of darkness during the polar night in Antarctica. However, the underlying mechanisms are poorly understood. In this study, five strains of Antarctic benthic diatoms were isolated in the field, and the resulting unialgal cultures were identified as four distinct species, of which one is described as a new species, *Planothidium wetzelii* sp. nov. All four species were thoroughly examined using physiological, cell biological, and biochemical methods over a fully controlled dark period of 3 months. The results showed that the utilization of storage lipids is one of the key mechanisms in Antarctic benthic diatoms to survive the polar night, although different fatty acids were involved in the investigated taxa. In all tested species, the storage lipid content declined significantly, along with an ultrastructurally observable degradation of the chloroplasts. Surprisingly, photosynthetic performance did not change significantly despite chloroplasts decreasing in

thylakoid membranes and an increased number of plastoglobules. Thus, a combination of biochemical and cell biological mechanisms allows Antarctic benthic diatoms to survive the polar night.

Keywords: Antarctica, benthic diatoms, photosynthesis, polar night, lipid consumption, plastid degradation

4.2 Introduction

The polar regions represent unique ecosystems characterized by low temperatures, ice and snow cover, and pronounced seasonal fluctuations in light availability with long periods of complete darkness during the polar night. The abiotic factor of light is especially challenging for autotrophic primary producers living in polar regions. Regional ice and snow cover can further extend the dark period for organisms (Cottier and Potter 2020). If sea ice is covered with snow, photon fluence rates can be reduced to 2 % of the solar surface radiation, leaving the organisms underneath exposed to extremely low light conditions or even darkness for up to 10 months in certain regions (Karsten et al. 2019a). Polar algae must, therefore, tolerate both very high light conditions after ice break-up and extremely low irradiances (Gómez et al. 2009; Zacher et al. 2009) and must have high adaptability to such fluctuating conditions in combination with always enhanced photosynthetic efficiency and plasticity (Longhi et al. 2003).

Diatoms are the most species-rich group of microalgae and dominate well-mixed water columns across all oceans as well as benthic algal communities of shallow-water soft bottoms, and rocky substrates (Lacour et al. 2019). They are responsible for ~20-2 5% of the global and 40-45 % of the marine primary production (Nelson et al. 1995; Field et al. 1998), which reflects their important role in marine food webs and in the global carbon cycle as well as other biochemical cycles (Field et al. 1998; Armbrust 2009). In depths down to 30 m, the primary production of microphytobenthic communities forms the main food source for benthic suspension or deposit feeders and thus plays a major role in the ecology of polar coastal habitats (Glud et al. 2009). Carbon budget measurements in Young Sound, Greenland, showed almost 50 % of primary production originating from microphytobenthos (Glud et al. 2002), which could also be confirmed for the Arctic Kongsfjorden (Svalbard, Norway; Woelfel et al. 2010). In Antarctica, McMinn et al. (2012) described that in <5m of water depth, benthic primary production exceeds that of phytoplankton or sea ice algae. Consequently, benthic diatoms play a crucial role in polar ecosystems and coastal food chains (Glud et al. 2009) but are still less studied compared to their planktonic or ice-associated counterparts. Marine Antarctic benthic diatoms are still

poorly studied in terms of biodiversity, biogeography, and ecology, while for freshwater habitats, comprehensive datasets exist (Verleyen et al. 2021; Al-Handal et al. 2022).

Diatom taxa from different Arctic and Antarctic habitats, such as sea ice, water column, and soft bottom, are reported to survive long periods of complete darkness (Schaub et al. 2017, and literature therein). The species-specific maximum survival periods are highly variable, ranging from 3 months to 1 year, and benthic diatoms have been reported with the longest survival times (Antia 1976). Experiments on the dark survival potential of different Arctic benthic diatom species indicated a high tolerance, i.e., survival for up to 5 months without light. Although chloroplast volume was strongly reduced with increasing dark treatment, *Cylindrotheca closterium* (Ehrenberg) Reimann & J. C. Lewin and *Surirella* cf. *minuta* showed high growth rates after a few days of lag phase after re-irradiation (Karsten et al. 2012; Schlie and Karsten 2017). During the polar night, the reallocation of energy toward maintenance metabolism through the decomposition of organelle components or lipid droplets seems to be a key process for survival in benthic polar diatoms. The lag phase after transfer to light can be interpreted as a recovery period, in which diatom cells rebuild cellular structures and metabolic activity (Karsten et al. 2012). In order to maintain viability, not only organelles but also membranes and DNA must remain intact (McMinn and Martin 2013). Benthic diatoms with intact plasmalemma can be distinguished from those with permeabilized membranes using the nucleic acid stain SYTOX Green, which only passes through compromised or damaged membranes, and stains the nucleus, leading to enhanced fluorescence under blue light excitation (Karsten et al. 2019a,b, and references therein). Application of the SYTOX Green stain to dark-incubated Arctic *Navicula directa* (W. Smith) Brébisson indicated that >95 % of all cells exhibited intact membranes, even after 5 months of darkness, and hence, the high degree of membrane integrity contributed to long-term dark tolerance (Karsten et al. 2019a,b). Lower temperatures generally reduce the metabolic activity of all organisms, thereby enhancing the dark survival potential of polar benthic diatoms. Reeves et al. (2011) reported for Antarctic sea ice diatoms a reduced dark survival time at 10°C compared to −2°C but no negative effect at 4°C. *Fragilariopsis cylindrus* (Grunow ex Cleve) Helmcke & Krieger survived 60 days of darkness at both -2 and 4°C but only 7 days at 10°C (Reeves et al. 2011).

The physiological state in which polar diatoms survive the darkness and the underlying metabolic processes is still almost unstudied. In the few diatoms studied, different mechanisms have been described for coping with the polar night (McMinn and Martin 2013). Those include the reduction of metabolic activity (Palmisano and Sullivan 1982), the utilization of stored energy products (Palmisano and Sullivan 1982; Schaub et al. 2017), formation of resting stages

(Durbin 1978; McQuoid and Hobson 1996), and a mixotrophic lifestyle (Hellebust and Lewin 1977; Tuchman et al. 2006). These adaptive mechanisms are not considered to be mutually exclusive, as they probably vary in relative importance among polar algae (Palmisano and Sullivan 1983). The utilization of energy storage products, such as the typical reserve carbohydrate chrysolaminarin or lipids (triacylglycerol), the latter being stored in cell vacuoles and/or in cytoplasmic lipid droplets, could sustain the cellular maintenance metabolism during long periods of darkness. Schaub et al. (2017) confirmed in the Arctic benthic diatom *Navicula* cf. *perminuta* the preferential utilization of the stored lipid compound triacylglycerol during prolonged dark periods, but also the pool of free fatty acids.

Diatoms are well-known for their metabolic strategy to store energy as lipids, often as neutral triacylglycerol, which consist of a glycerin backbone esterified with three fatty acids and which are deposited in densely packed lipid droplets intracellularly located in the cytoplasm (Hu et al. 2008; Leyland et al. 2020). Lipids can store more energy per molecule compared to carbohydrates or proteins (Morales et al. 2021), and hence, high proportions of such lipid bodies have been described in polar diatoms from the water column and sea ice, particularly in late autumn prior to the onset of the polar night (Fryxell 1989; Fahl and Kattner 1993; Zhang et al. 1998), while Antarctic benthic diatoms are almost unstudied.

For the present study, five benthic diatom strains from King George Island, Antarctic Peninsula, were morphologically and molecularly identified and examined using physiological, cell biological, and biochemical methods to better understand the underlying mechanisms for coping with the polar night. Over a period of 3 months of experimental dark treatment, we evaluated photosynthesis, respiration, and chlorophyll a content, as well as ultrastructure, lipid body size, and volume in combination with fatty acid concentrations prior to and after the dark treatment. Based on previous studies in Arctic benthic diatoms (Schaub et al. 2017, and references therein), we expected a strong involvement of storage lipids in the survival of the polar night in Antarctic benthic diatoms. In addition, our study provides transmission electron microscopic images of these ecologically important primary producers to our knowledge for the first time.

4.3 Material and methods

4.3.1 Description of the study site with ecological characterization

Sediment surface samples were taken from 28 January to 15 February 2020 from four study sites near the Argentinian research station Carlini Base (S 62°14′17.45”, W 58°40′2.19”) at Potter Cove on King George Island, Antarctic Peninsula, and used for benthic diatom isolation

(Figure 1, Table 1). The marine culture D288_003 originated from sample location D288 (S 62° 14′30.55”, W 58°40′54.96”) and was isolated from a biofilm of an intertidal rock pool. D296_001 was isolated from a marine sample at the inner part of Potter Cove (S 62°13′43.61“, W 58°39′49.36”), at 15m depth, from an epipsammic community. The marine culture D323_018 originated from a sample location closer to the glacier front in the inner part of the bay at 10m water depth from an epipsammic community (S 62°13′25.68”, W 58°38′33.50”). Both limnic isolates (D300_015 and D300_025) were established from biofilms on top of stones in a freshwater drinking reservoir (S 62° 14′16.30”, W 58° 39′44.10”).

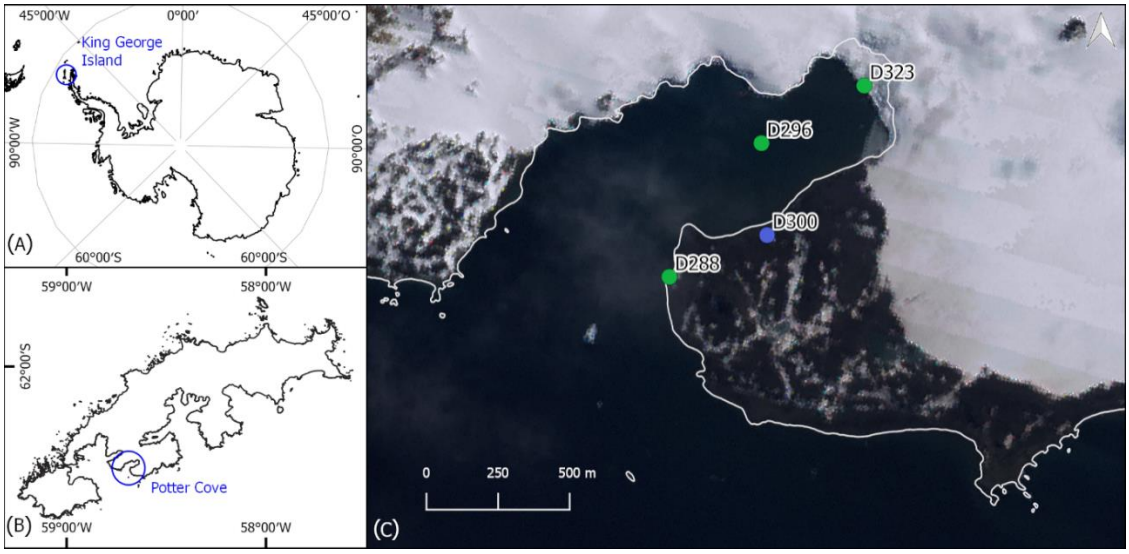

Figure 1 A Map of Antarctica **B** Map of King George Island **C** Map of Potter Cove, with the four sampling locations. The blue point represents the freshwater sampling site and green points represent marine sampling locations. Base map: Landsat Image Mosaic of Antarctica (LIMA).

At Carlini Base, various abiotic parameters were recorded. The minimum water temperature was -1.69°C in the inner part of Potter Cove and -1.4°C in the outer part, while the maximum temperature at both sites was 2.89 and 1.98°C, respectively. Furthermore, the salinity of the outer cove was stable at ~33.5 S_A, while the salinity in the inner cove can decline to 29.6 S_A because of meltwater run-off (Hernández et al. 2019). Light conditions are diurnally and seasonally highly variable, and more recent data were published by Hoffmann et al. (2019).

Table 1 List of benthic diatom strains established from Antarctic marine and freshwater samples with scientific name, information on dimensions of the valves, striae density, sequenced marker genes and accession numbers, RV: raphe valve, SV: sternum valve, * strains were only used for the description of the new species.

Strain	Scientific name	Water type	Length/Diameter [µm]	Width/per-valvar axis [µm]	Striae in 10 µm	Marker genes	Accession *rbc*L	Accession 18SV4/18S
D288_003	*Navicula criophiliforma*	marine	24.2-52.4	5.8-8.5	11-12	18S V4, *rbc*L	OX258986	OX259166
D296_001	*Chamaepinnularia gerlachei*	marine	17.1-20.6	4.1-5.4	18-20	18S, *rbc*L	OX258987	OX258985
D323_018	*Melosira* sp.	marine	18.6-20.9	19.4-22.0	-	18S V4, *rbc*L	OR036645	OR042180
D300_015	*Planothidium wetzelii* sp. nov.	freshwater	10.9-11.3	5.6-6.1	16-18 (RV) 17-18 (SV)	18S V4, *rbc*L	OX258989	OX259168
D300_025	*Planothidium wetzelii* sp. nov.	freshwater	17.8-18.8	6.0-6.3	14-15 (RV) 15-16 (SV)	18S V4, *rbc*L	OR036646	OR042181
D300_019*	*Planothidium wetzelii* sp. nov.	freshwater	11.1-11.8	5.8-6.7	16-18 (RV) 16-17 (SV)	18S V4, *rbc*L	OR036648	OR042183
D300_020*	*Planothidium wetzelii* sp. nov.	freshwater	17.5-18.5	5.8-6.5	14-15 (RV) 14-15 (SV)	18S V4, *rbc*L	OR036647	OR042182

4.3.2 Culture establishment

The diatom cells were isolated from aliquots of environmental samples to establish clonal cultures. Under an inverse light microscope (Olympus, Hamburg, Germany), single cells were transferred using microcapillary glass pipettes onto microwell plates containing culture medium [Guillard's f/2 medium (Guillard and Ryther 1962) or Walne's medium (Walne 1970), 34 S_A for marine samples and 1 S_A for freshwater samples]. All samples and isolated diatom cells from Antarctica were maintained at 5-7°C at the Botanische Museum Berlin. Irradiation was accomplished by white LEDs with 5,000K under a 16/8 day/night cycle with several dark phases during the day to prevent photo-oxidative stress. After the successful establishment of clonal cultures, they were separated into subsamples for DNA extraction, morphological analysis, and ecophysiological, biochemical, and cell biological experiments. For all experimental approaches, diatom cultures were transferred to the University of Rostock and cultured in sterile-filtered Baltic Sea water, enriched with Guillard's f/2 medium (Guillard and Ryther, 1962) and metasilicate (Na2SiO3 • 5 H2O; 10 g 100 mL^{-1}) to a final concentration of 0.6mM (further referred to as culture media). The salinity of 33 S_A for the marine cultures was adjusted by adding artificial sea salt (hw-Marinemix® professional, Wiegandt GmbH, Germany), while 1 S_A for the limnic cultures was achieved by dilution with deionized water. The media were regularly changed to replenish nutrients.

All stock cultures at the University of Rostock were kept at 8-9°C and 15–20 µmol photons $m^{-2}s^{-1}$ under a 16/8-h light/dark cycle [Osram Daylight Lumilux Cool White lamps L36W/840 (Osram, Munich, Germany)].

4.3.3 Taxonomic identification

In order to obtain clean diatom frustules for species identification, material harvested from the clonal cultures was treated with 35 % (v/v) hydrogen peroxide at room temperature to oxidize the organic material, followed by several washing steps with distilled water. To prepare permanent slides for light microscopy (LM) analyses, the cleaned material (frustules and valves) was dispersed on cover glasses, dried at room temperature, and embedded with the high refraction index mounting medium Naphrax®.

For each culture, 15–20 cells were measured for morphometry. Observations were conducted with a Zeiss Axioplan Microscope equipped with differential interference contrast (DIC) using a Zeiss 100x/1.30 Plan Apochromat objective, while microphotographs were taken with an AXIOAM MRc camera. Aliquots of cleaned sample material for scanning electron microscopy

(SEM) observations were mounted on stubs and observed under a Hitachi FE 8010 scanning electron microscope operated at 1.0 kV.

4.3.4 DNA extraction, amplification, sequencing, and processing

Clonal diatom material from log phase cultures was transferred to 1.5mL tubes. DNA was isolated using the NucleoSpin® Plant II Mini Kit (Macherey and Nagel, Düren, Germany), following the manufacturer's instructions. DNA fragment size and concentrations were evaluated via gel electrophoresis (1.5 % agarose gel) and NanoDrop® (Peqlab Biotechnology LLC; Erlangen, Germany), respectively. DNA samples were stored at -20°C until further use and finally deposited in the Berlin collection of the DNA Bank Network (Gemeinholzer et al. 2011). DNA amplification was conducted by polymerase chain reaction (PCR) after Zimmermann et al. (2011) for the V4 region of 18S. For strain D296_001, the whole 18S gene was amplified after Jahn et al. (2017). The protein-coding plastid gene *rbc*L was amplified by Abarca et al. (2014). PCR products were visualized on a 1.5 % agarose gel and cleaned with MSB Spin PCRapace® (Invitek Molecular GmbH; Berlin, Germany) following the manufacturer's instructions. DNA content was measured using NanoDrop® (Peqlab Biotechnology). The samples were normalized to a total DNA content >100 ng μL^{-1} for sequencing. Sanger sequencing of the PCR products was conducted bidirectionally by StarSEQ® (GENterprise LLC; Mainz, Germany).

Electropherograms obtained by Sanger sequencing were checked manually. The resulting reads from both sequencing directions overlapped, and the fragments were assembled in PhyDE® (Müller et al. 2010) to obtain the final sequences of the amplified markers.

The genetic differences of the newly described *Planothidium* to other species of this genus were investigated based on the 18S V4 and *rbc*L sequence matrices using MEGA 11 (Tamura et al. 2021) and the implemented p-distance option. Therefore, our dataset was complemented with 21 sequences of *Planothidium* from NCBI (Supplementary Tables 1, 2) and that of *P. tujii* C. E. Wetzel and Ector (molecular data supplied by A. Tuji). The alignments were trimmed to 437 bp for 18S V4 and 988 bp for *rbc*L.

4.3.5 Data curation

Vouchers and DNA of all strains were deposited in the collections at Botanischer Garten und Botanisches Museum Berlin, Freie Universität Berlin (B). DNA samples were stored in the Berlin DNA bank and were available via the Genome Biodiversity Network (GGBN; Droege et al. 2016). All sequences were submitted to GenBank. All cultures were available from the

authors at the culture collection of the Department of Applied Ecology and Phycology, University of Rostock.

4.3.6 Experimental part

After cultivation for 4–6 weeks to achieve sufficient biomass for the experiments, each strain was divided into different Erlenmeyer flasks. From the control condition (T0, control), three replicate samples were harvested for evaluation, and an additional three replicates were transferred to 3 months of darkness (T3) at 5°C. Cells from both T0 and T3 treatments were investigated concerning physiological, biochemical, and cell biological traits.

4.3.7 Photosynthetic efficiency

The efficiency of energy transfer in the diatom chloroplasts from the antenna to photosystem II (PS II) allows conclusions about the cell viability and the physiological state of the cells. It was measured using a pulse amplitude modulation (PAM) fluorimeter (PAM-2500, Heinz Walz GmbH, Effeltrich, Germany). The maximum quantum yield [$Y(II)_{max}$] of PS II was calculated by detecting the ground fluorescence (F_0) of the dark-adapted samples and the maximal fluorescence (F_m) after an oversaturating light pulse:

$$Y(II)_{max} = {}^{F_v}/_{F_m} = \frac{(F_m - F_0)}{F_m}$$

For measurements, a cooling block was used and set to the dark incubation temperature of 5°C to avoid temperature stress in the Antarctic benthic diatom samples. On the cooling block, 25-mm glass fiber filters (GF/6, Whatman, Little Chalfont, UK) were wetted with the respective culture medium. In a dark working space, a uniformly dense diatom cell layer was dripped on the filter and immediately measured. For detecting F_0 of the dark-adapted samples, a weak measuring light (<0.5 µmol photonsm^{-2} s^{-1}) was applied, while for F_m, an oversaturating light pulse (>10 000 µmol photons m^{-2} s^{-1}) was used (Malapascua et al. 2014).

4.3.8 Photometric chlorophyll *a* measurement

Five milliliters of algal biomass at T0 and T3 were filtered onto a Whatman GF/6 glass fiber filter (Ø 25 mm; n = 3), and chlorophyll a was extracted using 96 % ethanol (v/v) and measured spectrophotometrically using the equation given by HELCOM (2019).

To obtain a reference value for the chlorophyll a concentration, 5mL of algal suspension from each culture (n = 3) was fixed with Lugol solution at T0 and T3, and the cell number was determined in 1 mL, using a sedimentation chamber at 100x or 200x magnification and an inverted microscope (Olympus IX70, Hamburg, Germany). Always 400 morphologically intact

cells were counted, and empty or half-empty valves were ignored. The final amount of cells per mL suspension was calculated as follows:

$$cells/_{ml} = \frac{counted\ cells\ \times D\ \times A \times 1mL}{a \times Sq}$$

[D = dilution factor; A = total area of the chamber (mm²); Sq = amount of counted squares; a = area of one square (according to used magnification) (mm²)].

Chlorophyll *a* measurements were then correlated with the cell counts (*n* = 3 replicates).

4.3.9 Photosynthesis–irradiance curves (P–I curve)

The photosynthetic oxygen production and respiratory oxygen consumption of each strain were determined at 10 different light levels (0–~1,500 µmol photons m^{-2} s^{-1}) generated by LEDs (LUXEON Rebel1 LXML-PWN1-0100, neutral-white, Phillips, Amsterdam, Netherlands) implemented into a self-constructed P–I box as described by Prelle et al. (2019). Always, 3 mL of algal suspension was measured in airtight chambers [DW1 oxygen electrode chambers each placed on a magnetic stirrer (Hansatech Instruments, King's Lynn, United Kingdom)] using oxygen dipping probe DP sensors (PreSens Precision Sensing GmbH, Regensburg, Germany) connected to an Oxy 4-mini meter (PreSens Precision Sensing GmbH, Regensburg, Germany) in combination with the PreSens software OXY4v2_30 for measuring and calibration (twopoint calibration, 0 and 100 % oxygen saturation). The chambers were tempered at 5°C, and 30 µL of sodium bicarbonate (NaHCO3, final concentration 2mM) was added to each sample to avoid carbon deficiency (for details, see Prelle et al., 2019). After each P–I curve, diatom suspension from each cuvette was filtered onto an individual Whatman GF/6 glass fiber filter (Ø 25 mm) for chlorophyll a determination as reference parameter (Method see above). The photosynthetic model of Walsby (1997) was used for fitting and calculating different P–I curve parameters.

Since all clonal cultures were not axenic, we estimated the potential influence of bacterial respiration on the diatom net photosynthesis determination. The bacterial volume and the respective diatom volume of T0 samples were determined using DAPI (4′6-diamidine-2-phenylindole) staining. A measure of 500 µL of each glutaraldehyde-fixed T0 sample was filtered on a blackened Polycarbonate Track-Etched Filter (Ø 25 mm, pore size 0.2 µm, Sartorius Lab Instruments GmbH & Co. KG, Goettingen) and stained for 5 min with DAPI (Kapuscinski 1995). Micrographs of different locations of the filter were taken using an epifluorescence microscope BX-51 (Olympus,Hamburg, Germany) with a 40x lens and CellSens Standard imaging software (Olympus, Hamburg, Germany). For each culture, five micrographs were analyzed using Fiji–ImageJ (version 2.3.0; open source), detecting the area

of the blue signal after deleting the shapes of diatoms and determining the area of diatoms in each picture. Additionally, the average diameter of the bacterial cells and the diatoms was measured and used to calculate the volume of both groups. The resulting volume data should, therefore, be regarded as a rough approximation to evaluate the bacterial influence on the oxygen values.

4.3.10 Cell biology

To investigate changes in cell integrity after 3 months of dark incubation, 1mL of algae suspension was taken (n = 3) from T0 and T3 without further fixation and was directly stained with 1 µL of SYTOX Green (Catalog no. S7020, Thermo Fisher Scientific, Waltham, Massachusetts, USA; diluted in culture medium from a 5mM solution in DMSO). After 5 min of dark incubation, stained and unstained cells were quantified with an epifluorescence microscope (BX-51, Olympus, Hamburg, Germany) under blue excitation (U-MWB, Olympus, Hamburg, Germany). At least 400 unstained cells and the corresponding number of compromised cells were counted in each replicate.

The effects of dark incubation on the volume of lipid droplets were determined using Nile red lipid staining according to Greenspan et al. (1985). Twenty-five cells of each culture at T0 and T3, preferably in the same orientation, were imaged using epifluorescence microscopy (BX-51) under blue excitation (UMWB) along with a digital camera UC30 and CellSens standard imaging software (all from Olympus, Hamburg, Germany). The width and length of each cell and the respective sizes of lipid droplets were measured with Fiji–ImageJ (version 2.3.0; open source). The cell volume and the volume of a lipid droplet were modulated by an ellipsoid shape. Height and width were assumed to be identical, except for the centric species *Melosira* sp. D323_018, which exhibited numerous lipid droplets. In this study, the number of lipid droplets was counted, and the average diameter of the spherical lipid droplets was determined to calculate the total lipid volume. The cell volume of this culture was idealized and calculated using two hemispheres and a cylinder.

To obtain a more detailed picture of the cell biological changes in darkness, T0 and T3 samples were prepared and fixed by standard chemical fixation for transmission electron microscopy (TEM) according to Holzinger et al. (2009), using 2.5 % glutaraldehyde (25 % glutaraldehyde diluted with 50mM cacodylic acid buffer, pH 6.8) and osmium tetroxide (OsO4 diluted in cacodylic acid buffer) fixatives. These samples were dehydrated by increasing the alcohol series, embedded in modified Spurr resin according to Holzinger et al. (2009) before being sectioned using an ultra-microtome. Ultrathin sections were stained with uranyl acetate and lead

citrate and were investigated with a Zeiss LIBRA 120 transmission electron microscope at 80 kV. Images were captured with a TRS 2k SSCCD camera and further processed using Adobe Photoshop software (Adobe Systems Inc., San José, CA, USA).

4.3.11 GC-MS analysis

For fatty acid analysis of diatom samples at T0 and T3, a gas chromatograph connected to a mass spectrometer (GC-MS) was used according to Schaub et al. (2017). Since this analytical approach is time-consuming, we used only one replicate with three individual injections to identify at least the most conspicuous changes in the main fatty acids. Diatom samples were filtered onto Whatman GF/6 glass fiber filter (Ø 25 mm), freeze-dried and extracted with dichloromethane:methanol (2:1, v/v), and evaporated under nitrogen in a heat block (30°C), and the residue was re-dissolved in dichloromethane:methanol (2:1, v/v) and stored at -20◦C until further analysis (Schaub et al. 2017).

For transesterification, 1mL of lipid extract was evaporated under nitrogen to dryness, dissolved in 250 µL of hexane and heated for 4 h at 80°C with 1 mL of a 3 % concentrated sulfuric acid in methanol. Subsequently, fatty acid methyl esters (FAMEs) were extracted three times with hexane, transferred to GC vials, and concentrated under nitrogen down to ∼80 µL. GC analysis was carried on a fused silica capillary column (WCOT; 60m × 0.25mm I.D.; film thickness 0.25 µm; liquid phase: DB-FFAP; J&W, Germany) with a HP 6890 gas-liquid chromatograph coupled with a 5,970 Series mass selective detector (MSD; Hewlett-Packard GmbH, Germany) and a temperature program according to Kattner and Fricke (1986). The samples were injected at 60°C in splitless mode, with helium as carrier gas. Identification and quantification of fatty acids were according the protocol in Schaub et al. (2017).

4.3.12 Statistics and calculations

All calculations were performed using Microsoft Office Excel (2016). To calculate the P–I curves according to the Walsby model, the solver function was used to minimize the normalized deviation squares. The statistical analysis was performed using SPSS Statistics (version 27). To calculate significance levels among all means, oneway ANOVA was used followed by a post-hoc Tukey test. If the data did not fulfill the assumptions of variance homogeneity or normal distribution for one-way ANOVA, the Mann-Whitney test was used in case of two independent groups—in case of three or more independent groups, the Kruskal-Wallis one-factor ANOVA was applied. The significance level was set to < 0.05 for all analyses.

4.4 Results

4.4.1 Species identification and the description of a new benthic diatom taxon

Five strains from the four sample locations were investigated in this study. The morphological and molecular analyses confirmed the assignment to four distinct species. The taxonomic identity of some strains was already published before (D288_003, D296_001, D300_015; Prelle et al. 2022; Schimani et al. 2023).

D288_003 was identified as *Navicula criophiliforma* Witkowski, Riaux-Gob. & Daniszewska-Kowalczyk. This taxon was first published by Witkowski et al. (2010) from the Kerguelen Islands coastal area, Southern Ocean, and more recently also reported from Livingston Island, north of the Antarctic Peninsula (Zidarova et al. 2022). LM and SEM pictures of this strain can be found in Prelle et al. (2022).

D296_001 was identified as *Chamaepinnularia gerlachei* Van de Vijver & Sterken. This species was first published by Van de Vijver et al. (2010) from dry soil samples from James Ross Island, near the northeastern extremity of the Antarctic Peninsula, and has been observed until now just from maritime Antarctica (Kopalová et al. 2012; Sterken et al. 2015; Zidarova et al. 2016). A thorough examination of this strain can be found in Schimani et al. (2023).

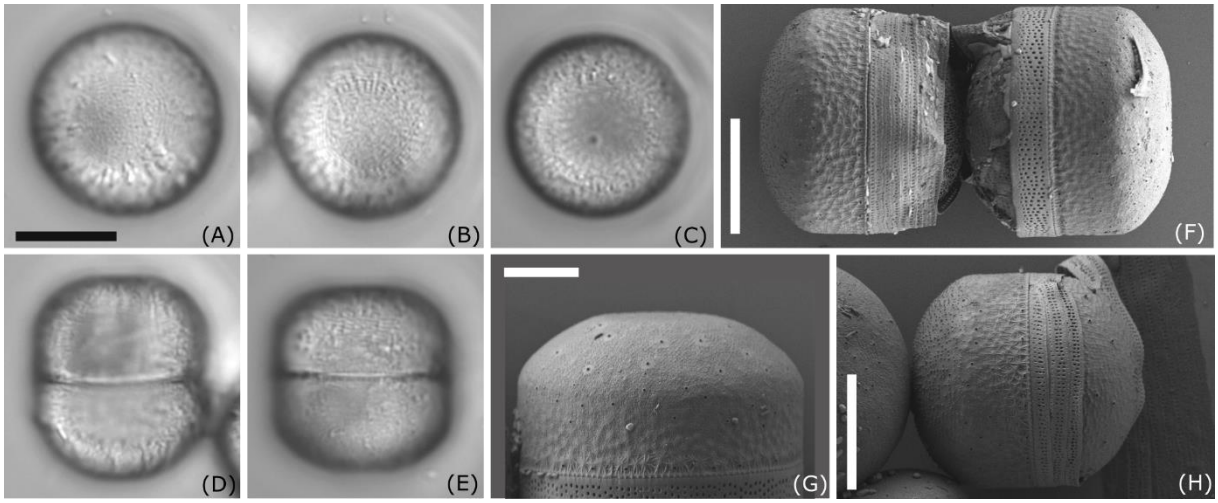

Figure 2 Morphology of *Melosira* sp. D332_018. **A–E** Light microscopy images **F–H** scanning electron microscopy images external view; Scale bar: A–E,H 10 µm, G 5 µm.

D323_018 (Figure 2) could only be identified at the genus level as *Melosira* sp. Cells are subcylindrical with a diameter ranging between 18.6 and 20.9 µm and a pervalvar axis ranging between 19.4 and 22.0 µm (Figures 2A–E). The hypovalve is more rounded than the epivalve (Figure 2H), which exhibits at the mantel a more cylindrical shape. Our strain resembles *Melosira moniliformis* C.Agardh in Crawford (1977), who examined the type and new material.

However, in *M. moniliformis*, ridges on the outer mantle surface fuse to form bigger spines, which are not visible in our strain. Therefore, unambiguous taxonomic assignment of this strain to a particular *Melosira* species is not possible at this stage.

D300_015 was only identified at the genus level as *Planothidium* sp. in Prelle et al. (2022). Morphological and molecular investigations showed that strain D300_025 is the same species. With the new data generated from those strains and two other strains obtained from the same location (D300_019, D300_020), this species is described as new.

***Planothidium wetzelii* Schimani, N.Abarca et R. Jahn sp. nov.**

Description:

Living material (Figures 3Q–AB, AP–BA): One plate of the C-shaped plastid lies appressed to the valve face. The concavity of the plastid is visible on the valve side lacking the cavum. Pyrenoids are not clearly visible, but Figures 3AR, AT suggest that there is one pyrenoid located in the vicinity of the cavum. In the girdle view, especially in the larger cells before cell division (Figure 3BA), two lobes of the chloroplast are visible appressed to the valves and connected in the center of the cell.

LM (Figures 3A–P, AC–AO, BB–BN): The outline ranged from elliptic with slightly protracted rostrate apices in smaller valves to elliptic or lanceolate with protracted, rostrate to capitate apices in larger valves. One valve side - especially strain D300_020 - appeared more convex than the other. The length of the valves varied between 10.9 and 18.8 μm and the width between 5.6 and 6.7 μm (n = 43). Sternum valve (SV): Axial area narrow, becoming wider toward the center of the valve. Central area asymmetrical with an oblong cavum with parallel sides, extending slightly over the axial area on one side and with shortened striae on the other side. The parallel margins of the cavum widen just shortly before the mantle, and its aperture is seen as a roundish line close to the mantle. Striae parallel or weakly radiating in the center, becoming more radiate near the apices (16–18 in 10 μm in smaller valves and 14–16 in 10 μm in larger valves). Raphe valve (RV): Axial area narrow. The central area widened due to three to four shortened striae on both sides. Raphe straight with enlarged proximal endings. Distal endings are not visible in light microscopy. Striae are parallel or weakly radiating in the center, becoming more radiating near the apices (16–18 in 10 μm in smaller valves and 14–15 in 10 μm in larger valves).

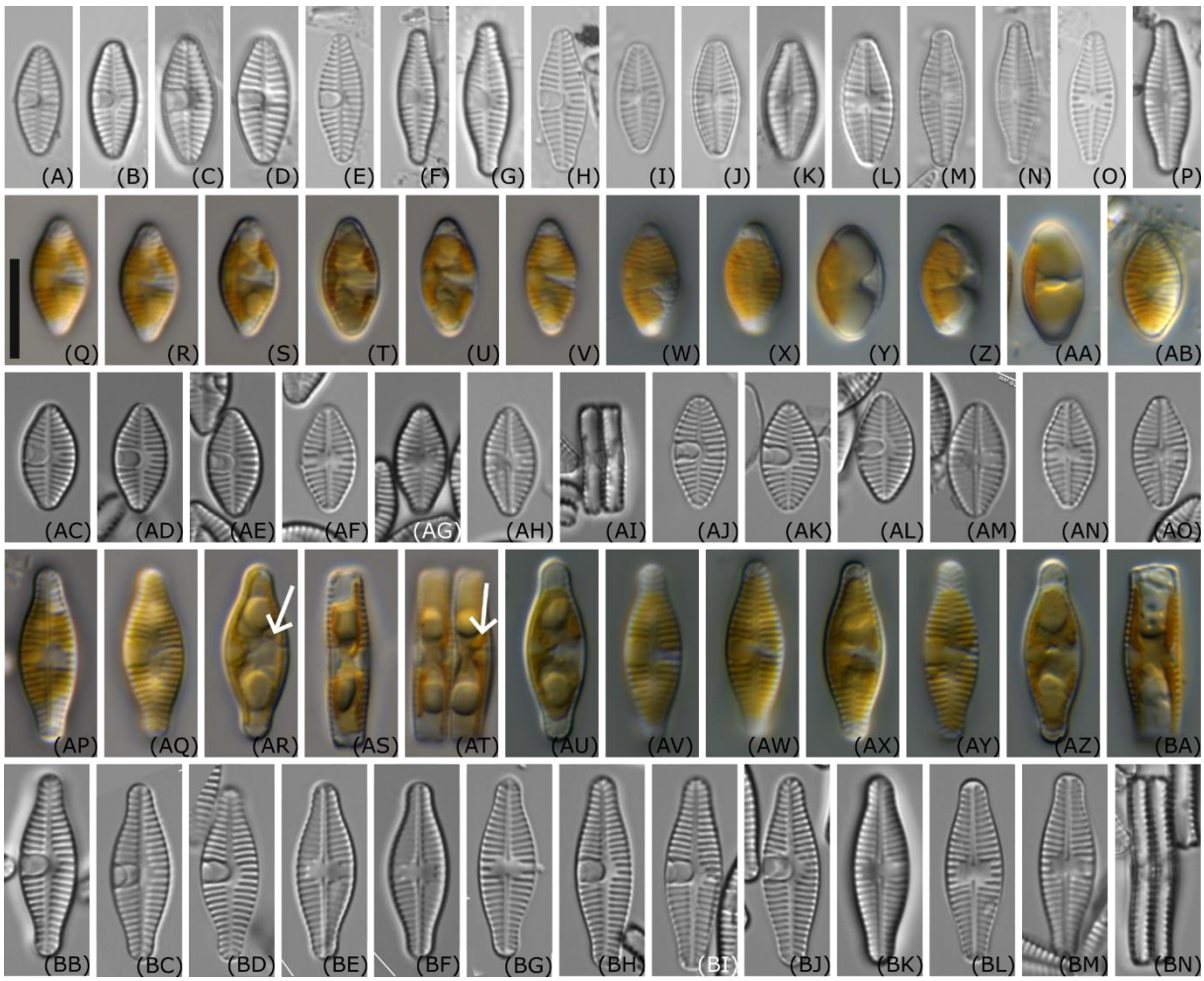

Figure 3 Light microscopy images of *Planothidium wetzelii* sp. nov. **A–P** valves of environmental samples **Q–V** live material of strain D300_015 **W–AB** live material of strain D300_019 **AC–AI** oxidized material of strain D300_015 **AJ–AO** oxidized material of strain D300_019 **AP–AT** live material of strain D300_020 **AR, AT** arrows indicate possible location of one pyrenoid in vicinity of the cavum **AU–BA** live material of strain D300_025 **BB–BG** oxidized material of D300_020 **BH–BN** oxidized material of strain D300_025; Scale bar: 10 µm.

SEM (Figures 4A–W) SV: The striae are composed of three to four rows of small rounded areolae exceeding the width of the virgae. Striae near the center of the valve become pointed with one or two areolae near the axial area. Externally, striae reach over the mantle with up to four rows of areolae. Irregularly rounded depressions are externally present along the axial area and concentrated in the central area. Internally, areolae are covered by hymenate occlusions. The broad cavum had a tight hood opening close to the mantle. Cingulum is composed of unperforated girdle bands. RV: The striae are composed of usually three to four

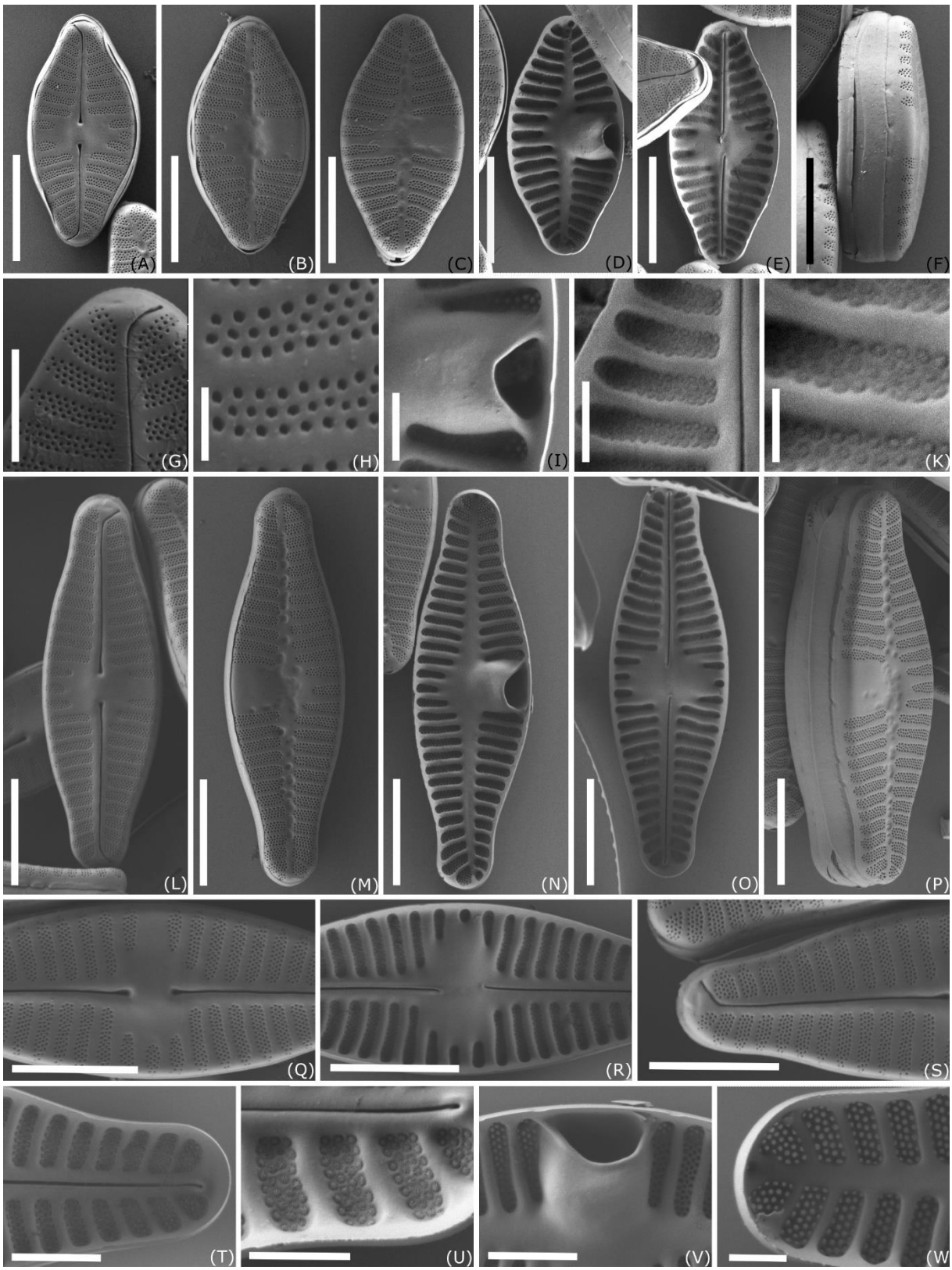

Figure 4 Scanning electron microscopy images of *Planothidium wetzelii* sp. nov. **A–K** strain D300_015 **L–W** strain D300_025 **A, E, G, H, J–L, O–T** raphe valve (RV) **B–D, F, I, M, N, P, V,W** sternum valve (SV) **A–C, F–H, L, M, P, Q, S** external view **J, K, U** internal view of RV, showing three to four rows of same sized hymenate areolae in one stria **I, V** internal view of central area in RLV showing cavum; Scale bar: A–F, L–P 5 µm; Q–S 4 µm; G, T,V 2 µm; I, J, U, W 1 µm; H, K 0.5 µm.

rows of rounded areolae exceeding the width of the virgae. Similar to the central striae on the SV, the shortened central striae on the RV gradually narrow toward the axial area. At each stria, one to three areolae reach over the edge of the valve face. Internally, areolae are covered with the same hymenate occlusions as in SV. Externally, the raphe straight with drop-like expanded proximal ends and distal raphe fissures unilaterally deflected, not or just shortly continuing onto the valve mantle. Internally, proximal raphe endings are slightly bent to opposite sides, and raphe endings terminate on a small helictoglossae not continuing on the valve mantle.

Holotype: Slide B 40 0045341a, Botanic Garden and Botanical Museum, Berlin, Figure 3BJ for SV and Figure 3BK for RV from the strain D300_025 illustrate the holotype. SEM-stub deposited as B 40 0045341b. For molecular material and data, see Methods.

Type locality: Drinking water reservoir of Carlini Station, Potter Cove, King George Island, South Shetland Islands, collected by J. Zimmermann on 01 February 2020, coordinates: S 62.237861, W 58.662250.

Registration: http://phycobank.org/103793. For INSDC Accession numbers see Table 1.

Habitat: Freshwater biofilm on stones.

Etymology: With this name, we would like to acknowledge the morphological and taxonomic work on the genus *Planothidium* done by Carlos Wetzel (Luxembourg Institute of Science and Technology, Luxembourg) in recent years, as well as his help in finding the identity of this species.

Differential diagnosis: *Planothidium wetzelii* shares similarities with several cavum-bearing species and species with external shallow rounded depressions on the rapheless valve (as defined by Wetzel et al., 2019): The smaller valves of *P. wetzelii* share similarities in shape with the small valves of *P. frequentissimum* (Lange-Bertalot), Lange-Bertalot as illustrated from type material in Wetzel et al. (2019). However, they can be distinguished by the form of the cavum, which is oblong with parallel sides and extending slightly over the axial area, vs. a round cavum in *P. frequentissimum*. The shape of the central area on the RV is much smaller in *P. wetzelii* compared to the type of *P. frequentissimum*. In SEM, the virgae in the SL and to some extent on the RV are wider in *P. wetzelii* compared to images of the type of *P. frequentissimum.* Additionally, the striae on the RV do not continue over the mantle in *P. frequentissimum* as they do in *P. wetzelii*. Larger valves of *P. frequentissimum* are lanceolate with less developed rostrate apices than those of *P. wetzelii*. Valves of *P. victorii* Novis, Braidwood & Kilroy (syn. *P. caputium*) are in contrast to *P. wetzelii* lanceolate to weakly

elliptic-lanceolate with protracted but never capitate apices (Jahn et al. 2017; Wetzel et al. 2019). The species can be differentiated by the form of the cavum too as it is rounder or has a V-shape in *P. victorii*. In addition, the tight hood opening in *P. wetzelii* (SEM), seen as a roundish line close to the mantle (LM), differs from the wider hood opening (SEM) in *P. victorii*, which is present as an almost straight line distant from the mantle (LM). The axial area is narrower in this species and the cavum has a wider aperture toward the mantle than *P. wetzelii*. Some of the medium sized valves could be confused with *P. naradoense* R.Jahn & J.Zimmermann but differ from *P. wetzelii* by the outline, as *P. naradoense* is lanceolate to elliptic lanceolate and somewhat asymmetric with slightly rostrate and rounded apices. The axial area is narrow on both valves (Jahn et al. 2017). Larger valves of *P. wetzelii* share similarities with *P. tujii* and *P. gallicum* C. E. Wetzel & Ector (Wetzel et al. 2019). However, the valves of *P. tujii* are shorter, while the width is almost in the same range. The central area in the RV of *P. tujii* is bowtie-shaped instead of the smaller rounded central area in *P. wetzelii*. The virgae are wider in *P. tujii* and have almost the same width as the striae; the helictoglossa is continuing onto the valve mantle. *P. gallicum* has clear broadly elliptic-lanceolate shaped valves with markedly rostrate apices. Furthermore, *P. gallicum* has a more prominent aperture of the cavum toward the mantle, and the striae located in the central area are not becoming narrower toward the axial areal as in *P. wetzelii*. *P. straubianum* C. E. Wetzel, Van de Vijver & Ector has elliptic-lanceolate valves with slightly parallel margins and round, obtuse ends with smaller dimensions than *P. wetzelii* (length 6.0–14.0 μm vs. 10.9–18.8 μm and width 4.0–5.5 μm vs. 5.6–6.7 μm; Wetzel et al. 2019). Striae are composed of four to five rows of areolae, in contrast to three to four in *P. wetzelii*. *P. biporomum* (M. H. Hohn & Hellerman) Lange-Bertalot can be differentiated from *P. wetzelii* in SEM by the striae on the rapheless valve (Wetzel et al. 2013). The striae start externally with one, rarely two, areolae at the axial area and end in two or three rows toward the valve face/mantle junction. Additionally, they are interrupted at the junction with the valve mantle. Furthermore, the cavum aperture is wide with its borders linked to the neighboring striae. *P. alekseevae* Gogorev & E. K. Lange has smaller dimensions (length 9.5–13.5 μm, width 4.5–5.0 μm) and wider apices in relation to the valve width. This feature is more apparent in smaller valves (Wetzel et al. 2019).

Molecular results: The four strains of *P. wetzelii* showed no intraspecific variability in the 18S V4 and the *rbc*L sequences (Supplementary Tables 1, 2). Compared to the available sequences of other *Planothidium* species, genetic distances are apparent in both marker genes. It is placed within the F2 subclade (Jahn et al. 2017, p. 84, Figure 1): strains of *P. victorii* (e.g., type strain from New Zealand), *P. straubianum* (strain B86_3 from Lake Baikal, renamed by Wetzel et al.

2019), and *P. tujii* show the smallest genetic divergence: in 18S V4 0.5-1.1, 0.7–0.9, and 0.9-1.1 %, respectively, which corresponds to 3–5 bp differences, and in *rbc*L 0.5-0.8, 0.5, and 0.5 % (3-7 bp). Higher genetic differences are evident for *P. naradoense* and *P. frequentissimum*: in 18S V4 2.5 % and 2.5-3.2 % (11 bp) and in *rbc*L 2.2 and 1.8-2.3 %, respectively (8-22 bp). Species with a sinus instead of a cavum [*P. lanceolatum* (Brébisson ex Kützing) Lange-Bertalot, *P. cf. subantarcticum*, *P. taeansa* R. Jahn & N. Abarca, *P. cryptolanceolatum* R. Jahn & N. Abarca, and *P. suncheonmanense* R. Jahn & J. Zimmermann] exhibit the highest divergence with a p-distance of 4.3-7.8 % (19-38 bp) in 18S V4 and 3.0-6.2 % (30-61 bp) in *rbc*L.

4.4.2 Photosynthesis and respiration

The values for $Y(II)_{max}$ at T0 and T3 are shown in Table 2 (mean values ± SD, n=3). All results were between 0.53 (*P. wetzelii* (D300_025) at T3) and 0.63 (*N. criophiliforma* and *C. gerlachei* at T0) and therefore within a range reflecting "good" physiological activity of all diatom cells during the dark incubation. Small, but significant differences in $Y(II)_{max}$ between T0 and T3 were found only in both cultures of the limnic species *P. wetzelii* (Table 2).

The results of the chlorophyll a measurements, which were referenced to cell counts, showed species-specific responses (Table 2). In both strains of *P. wetzelii*, the chlorophyll a content per cell did not significantly change during 3 months of dark treatment. In contrast, *N. criophiliforma* and *C. gerlachei* exhibited a pronounced chlorophyll a decline up to 74 % after dark incubation compared to the control, while the *Melosira* sp. decreased chlorophyll a by ~46 % (Table 2).

All measured P–I curves exhibited a typical shape without photoinhibition, as already reported for some of the species in detail in Prelle et al. (2022). The key parameters NPP_{max} and respiration were selected for all species before and after dark incubation (Table 2), and species-specific responses could be outlined. At T0, the highest value for NPP_{max} was determined in the marine species *N. criophiliforma* (80.0 ± 20.2 μmol O_2 mg^{-1} Chl a h^{-1}), while *P. wetzelii* (D200_015) showed the lowest NPP_{max} (16.7 ± 4.0 μmol O_2 mg^{-1} Chl a h^{-1}). While some species (*N. criophiliforma*, both *P. wetzelii* isolates) did not exhibit any significant NPP_{max} decline ($p < 0.05$) during dark treatment at T3, *C. gerlachei* and *Melosira* sp. showed a strong and significant decrease ($p < 0.05$) in NPP_{max} by 39.9 and 44.6 %, respectively (Table 2).

Although respiration rates were also species-specifically different and variable, we could not detect any significant difference in respiration between T0 and T3 among all benthic diatom species (Table 2). While the highest respiration values occurred in the marine species *N.*

criophiliforma (−72.2 ± 70.3 O_2 mg^{-1} Chl a h^{-1}), the lowest respiration rates were measured in the limnic culture *P. wetzelii* (D300_015, -7.8 ± 6.2 O_2 mg^{-1} Chl a h^{-1}).

Table 2 Results of different photosynthesis-related measurements before dark incubation (T0) and after 3 months of dark incubation (T3) of five Antarctic benthic diatom species. Maximum quantum yield (F_v/ F_m) of PS II measured by pulse amplitude modulation (PAM) fluorimetry. Data are shown as mean ± standard deviation (*n* = 3). Chlorophyll a content is given as ng Chl a per cell (n = 3). NPP_{max} represents the maximum net primary production rate derived from P–I curves in the PI box at 5°C (*n* = 4, D300_025 *n* = 3). Different lower-case letters (*a*, *b*) represent significance levels among all means as calculated by one-way ANOVA (Tukey's test, $p < 0.05$). Significance concerning NPP_{max}, respiration, and NPP_{max}: Respiration was analyzed by Kruskal–Wallis analysis ($p < 0.05$) due to non-normally distributed data points.

Culture		**F_v/F_m**	**Chl a per cell** [ng Chl per cell]	**NPP_{max}** [µmol O_2 mg^{-1} Chl a h^{-1}]	**Respiration** [µmol O_2 mg^{-1} Chl a h^{-1}]	**NPP_{max}: Respiration**
Navicula criophiliforma	T0	0.63± 0.01 *a*	8.18 ± 8.86 *a*	80.0 ±20.2 *a*	-72.2 ± 70.3 *a*	2.1 ±1.5 *a*
	T3	0.6 ± 0.02 *a*	2.21 ± 1.67 *a*	76.9 ± 8.4 *a*	-35.8 ± 14.5 *a*	2.3 ± 0.6 *a*
Chamaepinnularia gerlachei	T0	0.63 ± 0.01 *a*	0.43 ± 0.51 *a*	33.9 ± 2.2 *a*	-30.9 ± 10.0 *a*	1.2 ± 0.4 *a*
	T3	0.57± 0.02 *a*	0.13 ± 0.02 *a*	20.4 ± 2.9 *b*	-26.3 ± 1.8 *a*	0.8 ± 0.1 *a*
Melosira sp.	T0	0.57 ± 0.01 *a*	4.16 ± 2.69 *a*	76.1 ± 9.4 *a*	-16 ± 8.4 *a*	6.6 ± 5.0 *a*
	T3	0.55 ± 0 *a*	2.22 ± 1.57 *a*	42.2 ± 7.2 *b*	-9.4 ± 2.9 *a*	5.0 ± 2.2 *a*
Planothidium wetzelii (D300_015)	T0	0.61 ± 0 *a*	0.93 ± 0.08 *a*	16.7 ± 4.0 *a*	-7.8 ± 6.2 *a*	9.0 ± 14.0 *a*
	T3	0.57 ± 0.01 *b*	0.95 ±0.4 *a*	13.4 ± 4.7 *a*	-15.4 ± 2.4 *a*	0.9 ± 0.4 *a*
Planothidium wetzelii (D300_025)	T0	0.57 ± 0.03 *a*	1.53± 1.37 *a*	39.6 ± 9.8 *a*	-31.0 ± 4.3 *a*	1.3 ± 0.5 *a*
	T3	0.53 ± 0 *b*	1.34± 0.56 *a*	25.3 ± 11.2 *a*	-30.5 ± 19 *a*	1.2 ± 0.8 *a*

The NPP_{max}: Respiration ratios were relatively low for all isolates between 0.8 ± 0.1 and 2.9 ± 4.0 at T0 and T3, except for *Melosira* sp. which exhibited higher ratios of 6.6 ± 5.0 and 5.0 ± 2.2, respectively, due to proportionally lower respiration rates (Table 2). All diatom cultures were not axenic, and the bacterial abundance ranged from a very low 1.7 % bacteria volume when compared with the diatom volume in *Melosira* sp. to 23.7 % in *P. wetzelii* (D300_25; Table 2). All other species showed bacterial contamination between these extreme percentages.

4.4.3 Membrane integrity and ultrastructure

SYTOX Green staining was applied as a cell biological approach to evaluate membrane integrity during dark incubation. The percentage of damaged cells increased significantly in four out of the five tested benthic diatom species (Figure 5). In *N. criophiliforma*, *C. gerlachei*, and *Melosira* sp. at T0 only <5 % of the cells were damaged pointing to highly viable cell populations. After 3 months, dark incubation membrane integrity decreased in all three species, i.e., cells with compromised membranes accounted for between 16.4 and 39.0 % (Figure 5). Both *P. wetzelii* strains were already at T0 and less viable as reflected in approximately one third of the damaged cells. While isolate D300_025 exhibited 71.5 % compromised membranes, *P. wetzelii* (D300_015) maintained membrane integrity over 3 months of dark incubation (Figure 5).

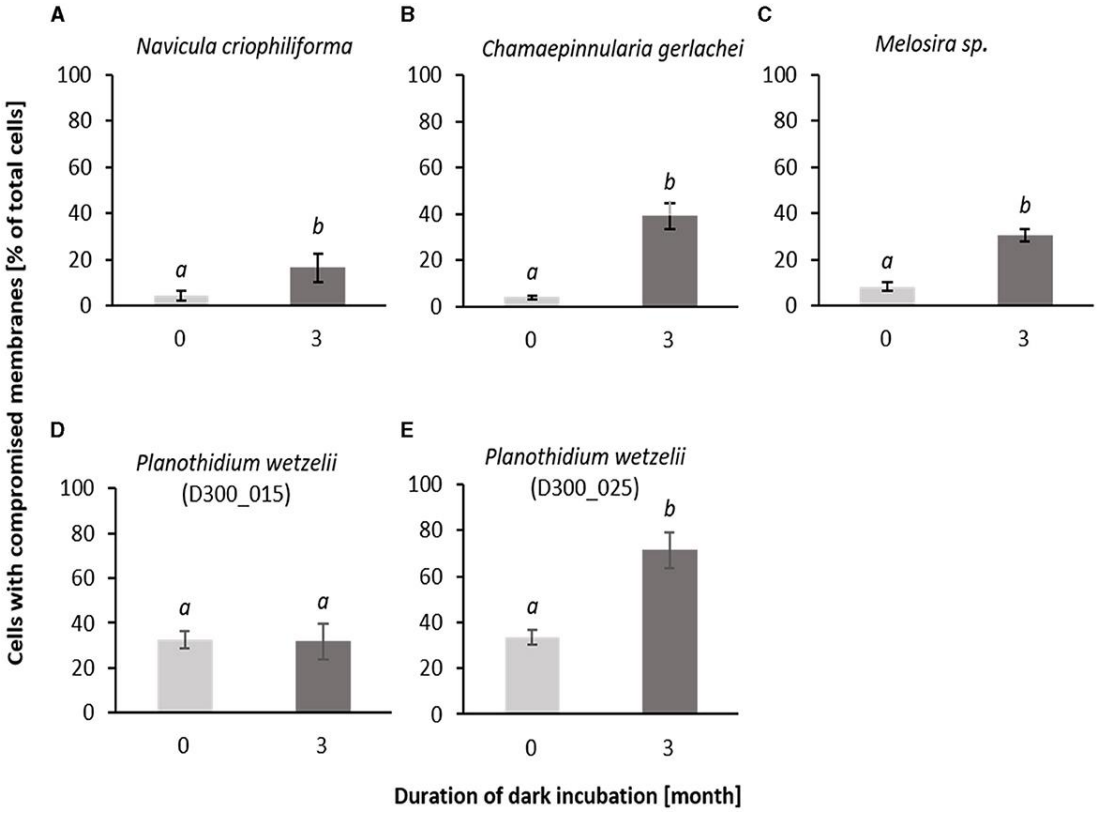

Figure 5 Stained cells of all investigated Antarctic benthic diatoms. **A–E** with SYTOX Green as the percentage of total counted cells (stained and not stained) before and after 3 months of dark incubation. 400–700 cells were counted for each treatment and taxon. Data are shown as mean ± standard deviation (n = 3). Different lower-case letters (*a* and *b*) represent significance differences calculated by one-way ANOVA (Tukey's test, $p < 0.05$).

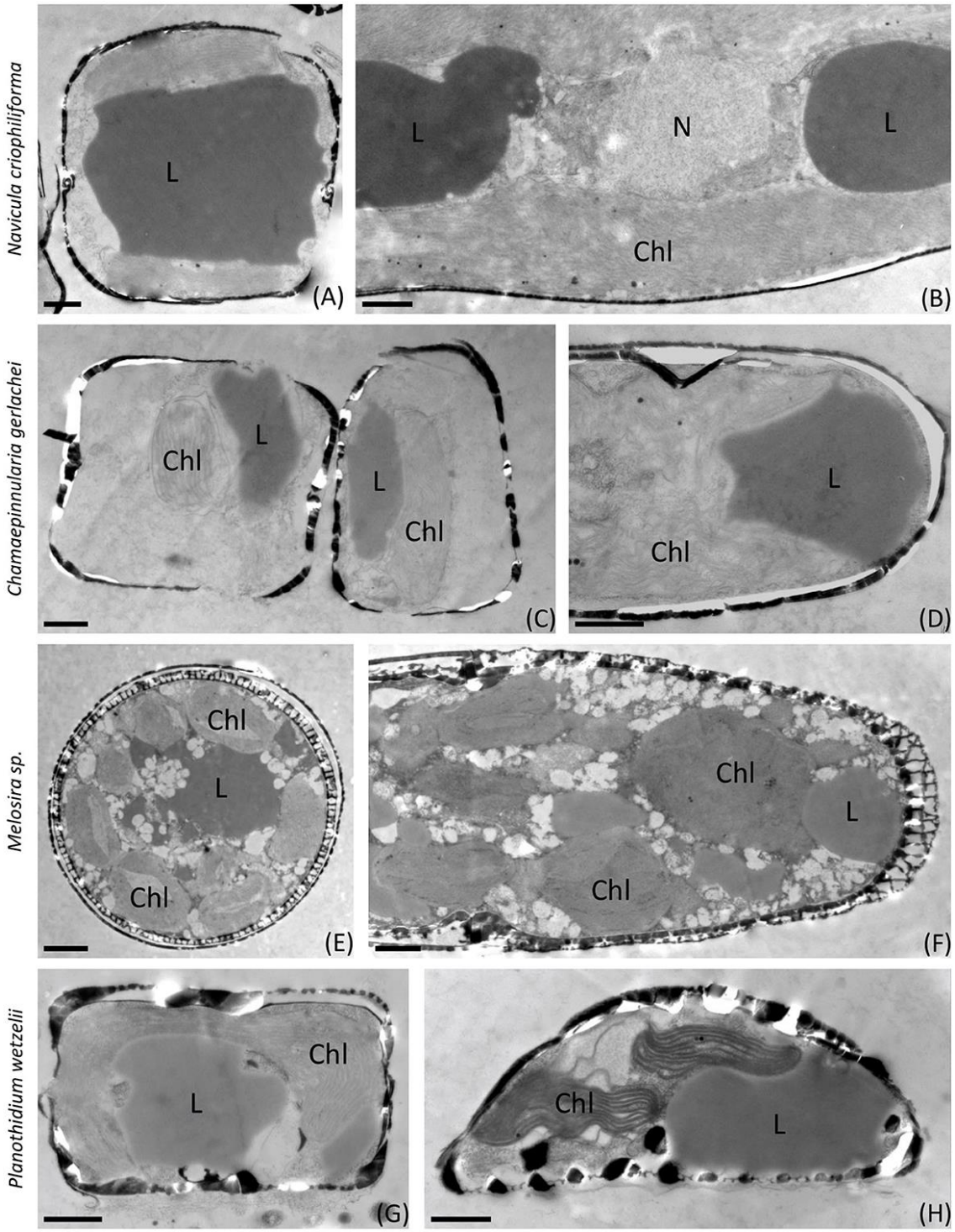

Figure 6 Transmission electron micrographs of control samples (T0). **A, B** *Navicula criophiliforma*, massive lipid droplets on both sides of the nucleus, intact chloroplast with thylakoid membranes **C, D** *Chamaepinnularia gerlachei*, lipid droplets and intact chloroplasts **E, F** *Melosira* sp., several small chloroplasts visible, lipid droplets and small electron translucent particles in the cell lumen, characteristic cell wall pattern **G, H** *Planothidium wetzelii* (D300_015). Chl, chloroplast; L, lipid droplet; N, nucleus. Scale bars: 1 μm.

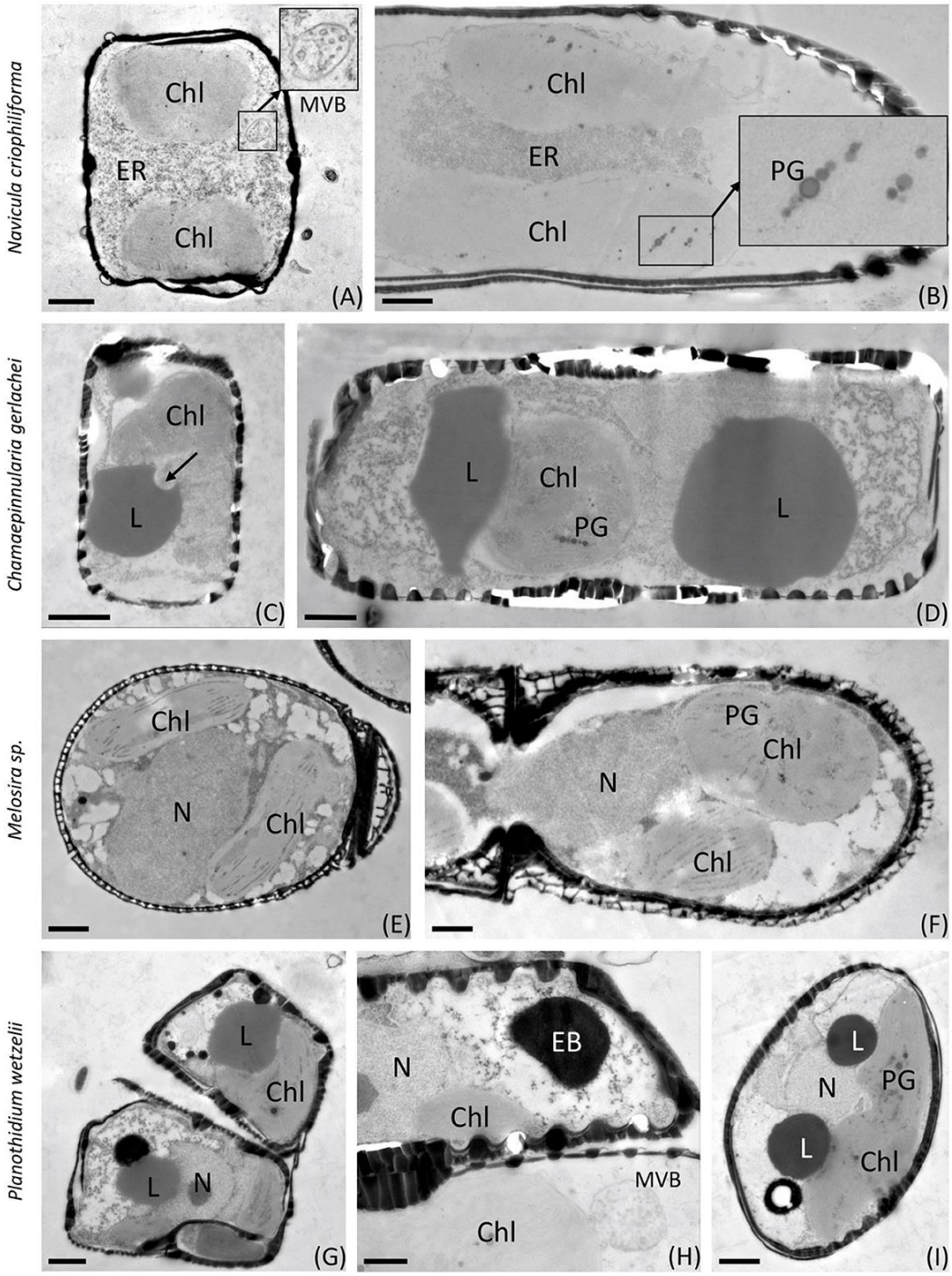

Figure 7 Transmission electron micrographs of 3 months of dark-treated samples (T3). **A, B** *Navicula criophiliforma*, chloroplasts are virtually lacking thylakoids, rows of plastoglobules are visible, massive accumulations of ER in the cell center, no lipid droplets are visible **C, D** *Chamaepinnularia gerlachei*, lipid droplets are visible, and signs of lipid degradation are marked with an arrow; (E, F) Melosira sp., chloroplasts with reduced thylakoid membranes, containing plastoglobules **G–I** *Planothidium wetzelii* (D300_015), chloroplasts reduced, lipid droplets visible, sometimes in close contact with electron-dense bodies. Chl, chloroplast; EB, electron-dense body; ER, endoplasmic reticulum; L, lipid droplet; MVB, multivesicular body; N, nucleus; PG, plastoglobules. Scale bars: 1 μm; (insets) 250 nm.

Figures 6, 7 show the first transmission electron micrographs (TEMs) of benthic diatom species from Antarctica under control (T0, Figure 6) conditions and after 3 months of dark incubation (T3, Figure 7). The three pennate (*N. criophiliforma*, *C. gerlachei*, and *P. wetzelii*) and one-centric diatom species (*Melosira* sp.) exhibited the typical cellular ultrastructure of a diatom cell. All cells contained a central nucleus, several chloroplasts, and, most conspicuously, one or more large lipid droplets that occupied large parts of the cell volume (Figure 6).

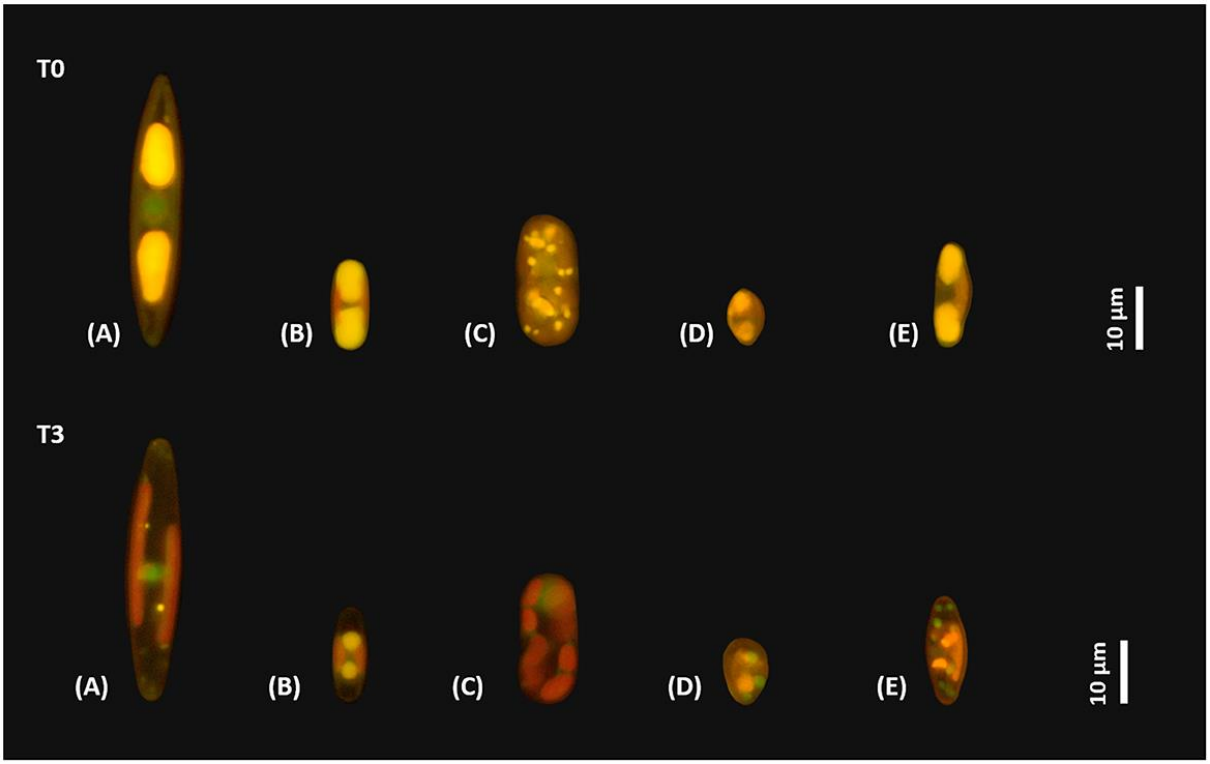

Figure 8 Micrographs of five Antarctic benthic diatom strains stained with Nile red. Upper row shows lipid droplets of the control, and lower row shows lipid droplets after 3 months of dark incubation. **A** *Navicula criophiliforma* **B** *Chamaepinnularia gerlachei* **C** *Melosira* sp. **D** *Planothidium wetzelii* (D300_015) **E** *Planothidium wetzelii* (D300_025).

After the dark treatment, ultrastructural changes could be detected (Figure 7). The most conspicuous observations were degraded chloroplasts with plastoglobules (PGs) in all species and partially more endoplasmic reticulum (ER). In addition, the volume or number of lipid droplets drastically decreased (Figure 7). In *N. criophiliforma*, lipid droplets were virtually absent (Figures 7A, B) and only observed in a few cases. Similarly, in *Melosira* sp., no or only very small lipid droplets occurred at T3. In contrast, in *C. gerlachei* and *P. wetzelii* (D300_015), well-developed lipid droplets could be identified. However, in Figure 7C of *C. gerlachei* beginning, the degradation of a lipid droplet was observed (marked by an arrow). In addition, *N. criophiliforma* and *P. wetzelii* (D300_015) exhibited multivesicular bodies (MVBs) after 3

months of darkness (Figures 7A,H), a typical sign of apoptosis. Additionally, in *P. wetzelii*, several larger electron-dense bodies were observed (Figures 7G,H). While the origin of these bodies remains unknown, they might resemble the degradation products of the chloroplasts.

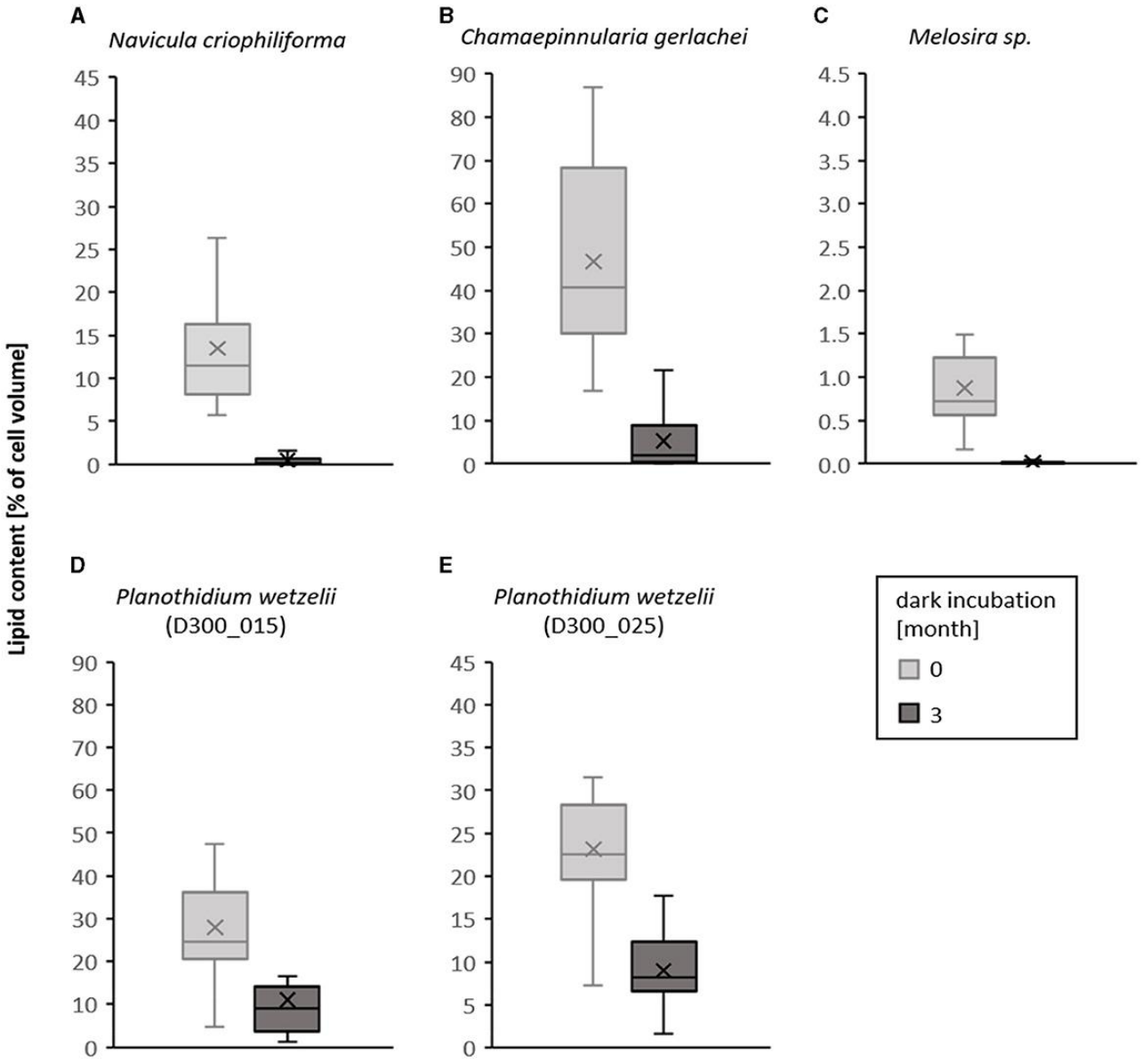

Figure 9 Boxplots of lipid content per cell calculated as percentage cell volume before dark incubation (light gray) and after 3 months of dark incubation (dark gray) in five Antarctic benthic diatom strains. **A–E** For each culture and time, 25 cells were measured. Scaling of the Y-axis is proportional but different as the lipid content differs. Different lower-case letters represent significance differences calculated by Mann–Whitney U-test ($p < 0.05$).

The chemical GC-MS analysis of the total lipid content supports the results shown in Figures 8, 9, i.e., the marine isolates *N. criophiliforma*, *C. gerlachei*, and *Melosira* sp. exhibited concentration declines between 90.0 and 94.5 % (Table 3). In both limnic *P. wetzelii* strains, the lipid content decreased by 20.6 and 35.2 % after 3 months of darkness (Table 3). Saturated

fatty acids (SFAs), monounsaturated fatty acids (MUFAs), and polyunsaturated fatty acids (PUFAs) before and after 3 months of dark incubation were also evaluated, but a clear trend is not visible, since all species showed different response patterns. The quantitatively most abundant fatty acids in all benthic diatoms were the saturated 16:0 and the monosaturated 16:1n7 (Table 3). While the percentage proportion of 16:0 in relation to all measured fatty acids increased in *N. criophiliforma* (from 43.6 to 58.4 %) and *C. gerlachei* (from 38.3 to 48.1 %) after 3 months of darkness, it strongly decreased in the remaining species (e.g., in *Melosira* sp. from 36.2 to 16.9 %). Reversely, the percentage proportion of 16:1n7 in relation to all fatty acids strongly declined in *N. criophiliforma*, *C. gerlachei*, and *Melosira* sp., while both *P. wetzelii* strains exhibited a slight increase (Table 3).

Table 3 Lipid analysis using gas chromatography connected to a mass spectrometer (GC-MS). Total fatty acid content was normalized to cell number and is shown before dark incubation (T0) and after 3 months of dark incubation (T3) in five Antarctic benthic diatom species. Standard deviation was calculated according to Gaussian error propagation (n = 3). The percentage decrease in the total fatty acid content during this time was calculated. Saturated fatty acids (SFAs), monounsaturated (MUFA), and polyunsaturated (PUFA) fatty acids at T0 and T3 are given as the percentage of the total lipid content, as well as the ratio (SFA+MUFA)/(PUFA). In addition, the most abundant fatty acids detected in all strains, 16:0 and 16:1n7 are shown in the percentage proportion of all measured fatty acids.

Dark incubation [months]	***Navicula criophiliforma***		***Chamaepinnularia gerlachei***		***Melosira* sp.**		***Planothidium wetzelii* (D300_015)**		***Planothidium wetzelii* (D300_025)**	
	T0	**T3**	**T0**	**T3**	**T0**	**T3**	**T0**	**T3**	**T0**	**T3**
Total lipid content [pg/cell]	43.6 ± 59.5	2.4 ± 1.2	9.6 ± 6.1	1.2 ± 0.3	27.8 ± 17.3	2.8 ± 2.2	6.5 ± 2.5	4.2 ± 1.7	21.9 ± 6.6	17.4 ± 4.8
Decrease in total lipid content [%]	-94.5		-87.6		-90		-35.2		-20.6	
Saturated fatty acids (SFAs) [%]	52.8	73.8	43.9	58.3	55.6	34.7	47.9	36.4	79.0	43.8
Monounsaturated fatty acids (MUFAs) [%]	29.0	11.7	46.4	24.8	32.9	31.7	37.1	43.6	10.7	18.8
Polyunsaturated fatty acids (PUFAs) [%]	18.2	14.5	9.7	16.9	11.5	33.7	15.0	20.0	10.3	37.4
(SFA+MUFA) (PUFA)$^{-1}$	4.5	5.9	9.3	4.9	7.7	2.0	5.7	4.0	8.7	1.7
16:0 [%]	43.6	58.4	38.3	48.1	36.2	16.9	41.0	31.9	53.3	25.0
16:1n7	23.5	1.3	40.3	13.0	24.0	8.7	33.3	36.5	8.8	11.5

4.5 Discussion

Since Antarctic benthic diatoms are regularly confronted with the polar night, we isolated five strains at Potter Cove, established clonal cultures, and investigated their physiological,

biochemical, and cell biological traits after 3 months of darkness to better understand the underlying tolerance mechanisms.

4.5.1 Importance of taxonomy as baseline for ecophysiological investigations

However, the first step, prior to ecophysiological experiments, is always to carefully address the taxonomic position of freshly collected field material. Two of the investigated diatom species were morphologically and molecular-genetically identified as species only known from maritime Antarctica (*Chamaepinnularia gerlachei*) or the Southern Indian Ocean (*Navicula criophiliforma*). Two additional cultures belong to the newly described freshwater species *Planothidium wetzelii*, which is so far unknown in any other region of the world. Finally, one centric species was investigated in this study, which does not fit morphologically and genetically to any described *Melosira* species, and most probably represents a new taxon, which was not further investigated in the present study.

Due to a thorough identification of the investigated cultures, a restricted geographical distribution in the southern hemisphere could be verified for all of them, and some might even be endemic to the Antarctic region. Morphological variability of the newly described species *Planothidium wetzelii* shows that valves from environmental samples need to be complemented with molecular and morphological information gained by cultures. This case highlights once again the importance of integrative taxonomy for the investigation of diatom biodiversity. In addition to an integrated taxonomy, the establishment of clonal cultures is the prerequisite for a combined taxonomical and physiological investigation of benthic diatoms. The two *P. wetzelii* strains D300_015 and D300_025 exhibit some variability in valve morphology. They might be considered two separate species when just examined by light microscopy, based on their differences in shape and size. However, diatoms can exhibit phenotypic plasticity due to environmental changes (Andrejic et al. 2018) or when observed over long time in culture (Mohamad et al. 2022). Both strains represent the same species based on molecular markers and micromorphology, and the results from this study show very similar response patterns during dark incubation.

As a result of the inaccessibility of Antarctica, the diversity of benthic diatoms is still poorly known. Considerable taxonomic work needs to be done in polar regions, which can then be used as a baseline for physiological, biochemical, and cell biological studies, allowing important conclusions, such as, for example, if geographic boundaries and environmental conditions led to many endemic taxa.

4.5.2 Variable light conditions and photosynthesis

Phototrophic organisms in the polar regions such as benthic diatoms cope with strong diurnally and seasonally fluctuating light conditions. The review of Pavlov et al. (2019) comprehensively summarized the underwater light climate and all main controlling factors in the Arctic Kongsfjorden, one of the best studied polar field sites, which is discussed here as a representative high latitude coastal habitat since adequate data for Antarctica are missing. In addition to the seasonal changes from midnight sun to polar night, clouds, sea ice conditions, and the optical seawater properties further strongly influence dose and spectral composition of solar radiation penetrating into the water column, thus defining the underwater light conditions. In addition, input of local run-off and glacial meltwater introducing inorganic and organic matter into the system, and phytoplankton blooms at diverse times and locations. Together, these factors result in a complex underwater light climate with high variability in time and space (Pavlov et al. 2019). Although not comprehensively investigated, similar processes and physico-chemical properties can be assumed for Potter Cove (Hoffmann et al. 2019) and other bays around the Antarctic Peninsula. Polar benthic diatoms are additionally affected by huge amounts of particles released into the water column due to coastal glacier retreat and melt under global change conditions, resulting in increased turbidity and hence less available light (Hoffmann et al. 2019).

Photosynthesis is the essential mechanism for the energy metabolism and, thus, not only responsible for viability and survival of benthic diatoms, but also primarily dependent on light availability. All benthic diatom species examined in this study showed $Y(II)_{max}$ of 0.57–0.63 before dark incubation as physiological marker for photosynthetic activity. Other studies on Antarctic benthic diatoms reported similar maximum $Y(II)_{max}$ values between 0.6 and 0.7, indicating that the strains were in good physiological conditions prior to dark incubation (Longhi et al. 2003; Wulff et al. 2008a).

Prelle et al. (2022) used for their P–I curves various Antarctic benthic diatoms, including the species also investigated in the present study: *Navicula criophiliforma*, *Chamaepinnularia gerlachei*, and *P. wetzelii* strain D300_015, and demonstrated generally low light requirements, as light-saturated photosynthesis was reached at <70 µmol photons m^{-2} s^{-1}. A similarly low light demand was observed for *Melosira* sp. and *P. wetzelii* strain D300_025 (data not shown). Other polar benthic diatoms are also known for their shade acclimation with low light compensation (I_c) and light saturation points (I_k) as well as steep initial slopes (a value) in their P–I curves (Wulff et al. 2008a). At the same time, they are also described as phototrophic

microorganisms with a pronounced photophysiological plasticity, allowing them to cope with high solar radiation (Prelle et al. 2022).

Remarkable are the relatively high respiration rates, which were about as high as the net photosynthetic rates in some of the studied benthic diatom species, resulting in low ratios of NPP_{max}: respiration, and which can be explained by co-occurring bacteria in the cultures. Overall, we cannot rule out that diatom-associated bacteria could affect the results of the P–I curves through their respiration, particularly when present in high cell numbers. However, bacteria and diatoms are known to have complex biotic interactions that affect each other's viability, and diatoms can even control their own phycosphere (microbiome; Amin et al. 2012). Therefore, the often-applied antibiotic treatment prior to experiments could potentially not only reduce essential bacteria but also affect diatom viability with unforeseen consequences for dark survival.

4.5.3 Physiological traits during darkness

Three months of darkness did not negatively affect $Y(II)_{max}$ values in the studied benthic diatom species, which provides at least a crude measure for still-existing photosynthetic viability, which is confirmed by the oxygen data. Previous studies on the dark survival of polar diatoms showed a decrease in various photosynthetic parameters during dark incubation (Wulff et al. 2008a; Reeves et al. 2011; Karsten et al. 2012; Lacour et al. 2019). The only study on Antarctic benthic diatoms was performed by Wulff et al. (2008b) on semi-natural cultures with a dark period of 64 days. Their results revealed significant decreases in the parameters F_v/F_m, rETR (relative electron transport rate), and α (light-using efficiency).

All species revealed oxygen production after the dark period but to different degrees. While *C. gerlachei* and *Melosira* sp. showed a moderate decline in NPP_{max} (39.9 and 44.6 %, respectively), the remaining species (*N. criophiliforma*, both *P. wetzelii* isolates) exhibited unaffected NPP_{max} values. Furthermore, the chlorophyll a data pointed to species-specific responses. While chlorophyll a decreased in *N. criophiliforma*, *C. gerlachei*, and *Melosira* sp. after 3 months of dark incubation, it remained more or less stable in both *P. wetzelii* strains. This observation is further supported by the TEM observations, which showed that some of the thylakoid membranes remained intact in this species. In contrast, in *N. criophiliforma*, much more degradation of the thylakoid system was observed with an increased number of plastoglobules. The lower NPP_{max} values can be related to the decline in chlorophyll a content as discussed by Wulff et al. (2008a) and Reeves et al. (2011), who explained the decrease in photosynthetic potential in Antarctic diatoms with a progressive degradation of the antenna

complex and the reaction center. The decline in chlorophyll a concentration in some of the benthic diatom species can also be explained by chloroplast degradation after 3 months of darkness, but remarkably, this did not seem to have an effect neither on the physiological performance nor on the viability. Apparently, parts of the thylakoid membranes are degraded in darkness, but a functional part seems to remain intact and thus contributes to a basal level of photosynthetic activity. Kennedy et al. (2019) found similar results in Antarctic sea ice diatoms during 4 months of dark incubation and reported a rapid reduction of light-harvesting complexes and photosystems while maintaining photosynthetic capacity. Applying SYTOX Green to the Arctic benthic diatoms *Surirella* cf. *minuta* and *Navicula directa* during 5 months of darkness indicated that an increasing number of cells exhibited damaged membranes over time in the first species (Karsten et al. 2019a), while the latter one was almost unaffected (Karsten et al. 2019b). In the present study, SYTOX Green staining was applied for the first time to Antarctic benthic diatoms, and the results are comparable to those on both Arctic species. While the percentage of damaged cells increased significantly in *N. criophiliforma*, *C. gerlachei*, *Melosira* sp., and *P. wetzelii* (D300_025) after 3 months of dark incubation, *P. wetzelii* (D300_015) maintained membrane integrity over this period of darkness. Although some diatom cells could not cope with longer darkness, others maintained viability and hence guaranteed the survival of the population after re-irradiation.

4.5.4 Cell biological traits during darkness

These are the first transmission electron micrographs of Antarctic benthic diatoms after dark treatment. They showed degraded chloroplasts in all benthic diatom species after 3 months of dark incubation with a markedly increased amount of plastoglobules (PGs) in the stroma of the plastids. PG appearance is a common response of plant cells to high light stress (Meier and Lichtenthaler, 1981) or any other stress, leading to a reduction of thylakoid membranes, as PGs contain the building blocks for thylakoids, including the enzymatic setting. The increase in PG in the Antarctic benthic diatoms can thus also be interpreted as a stress response; in this case, however, it is a response to long-term darkness. Schwarz et al. (2017) reported in the green microalga *Micrasterias* sp. how lipid droplets are released from the chloroplast into the cytoplasm during starvation, where they are degraded by autophagy. In addition, multivesicular bodies (MVBs) were also found in the cytoplasm after 7 weeks of starvation in darkness in *Micrasterias* sp., confirming autophagy (Schwarz et al. 2017). In the literature, it has been discussed that apoptosis and autophagy are both distinct processes but strongly interlinked (Mariño et al. 2014). In our study, the observable TEM structures are MVBs, which were present in *N. criophiliforma* and *P. wetzelii* (D300_015). Along with the numerous PGs and the

degradation of the chloroplasts, this could indicate a mobilization of energy reserves by the autophagy of chloroplast components to survive the polar night. Furthermore, the chlorophyll a content per cell after 3 months of darkness strongly decreased in *N. criophiliforma*, *C. gerlachei*, and *Melosira* sp., supporting the ultrastructural results.

The cell biological data on Antarctic benthic diatoms confirm the few results on their Arctic pendants, which also reported, for example, a 30–50 % decrease in chloroplast length (Karsten et al. 2012, 2019b). In addition, Wulff et al. (2008a) demonstrated condensed chloroplasts after dark treatment, which recovered within hours after re-exposure to light. Thus, no long-term damage appears to have been caused by the partial decomposition of chloroplasts during the prolonged darkness. According to Karsten et al. (2019b), the degradation of chloroplast compounds seems to be a key mechanism in Arctic benthic diatoms to survive the polar night and generate energy for their maintenance metabolism. The results of this study confirm that this is also a survival strategy for the examined Antarctic benthic diatoms.

4.5.5 Lipid content after 3 months of dark incubation

Both the light microscopic and the TEM images indicated significant differences in the lipid content of all species between control and after 3 months of dark incubation, which was additionally supported by the GC-MS analysis. *N. criophiliforma* and *Melosira* sp. consumed most of their lipid reserves in darkness, *C. gerlachei* depleted ~85 % of their lipids, and both *P. wetzelii* strains still exhibited lipid droplets even after 3 months of darkness, which could suggest that this species might survive additional months in darkness. Enhanced lipid content, as well as the consumption of storage substances during darkness to maintain the cellular metabolism, have been described before for Arctic diatoms (Zhang et al. 1998; McMinn and Martin 2013; Karsten et al. 2019b). Only a few studies on Arctic benthic diatoms quantified the decrease of lipid storage compounds during darkness (Schaub et al. 2017; Karsten et al. 2019a). Investigations on Antarctic benthic diatoms in this regard are entirely lacking so far.

Diatoms carry two pathways of b-oxidation for the breakdown of lipid compounds, the plant-like and the animal-like metabolic capabilities (Armbrust et al. 2004; Schaub et al. 2017). In the darkness, the mechanism of animal-like b-oxidation, located in the mitochondria, is upregulated and thus can provide energy from lipid storages during the polar night (Chauton et al. 2013), which probably allows diatoms to survive long periods of darkness, thereby maintaining their metabolism and the fundamental functions of their organelles (Armbrust et al., 2004). Thus, the results of the present study confirm the described metabolic pathway in Armbrust et al. (2004) and Chauton et al. (2013). In addition, in the more recent review of

Leyland et al. (2020), the authors describe the storage of lipids in droplets and characterize these structures as organelles composed of a core of neutral lipids, mostly triacylglycerol (TAG), surrounded by a polar lipid monolayer. Most interestingly, lipid droplets can store not only reserves of energy but also membrane components, carbon skeletons, carotenoids, and even proteins (Leyland et al. 2020, and references therein).

While the membrane lipids of polar diatoms are mainly composed of polyunsaturated fatty acids in order to maintain membrane fluidity at low temperatures (Murata and Los, 1997), the storage lipids are mainly formed by triacylglycerol (TAG), which has three fatty acids that are mainly saturated or monounsaturated (Schaub et al. 2017). The latter authors carefully investigated qualitatively and quantitatively the lipid classes of the Arctic benthic diatom *Navicula perminuta* during 2 months of dark incubation. Schaub et al. (2017) demonstrated by the ratio of SFA and MUFA to PUFA that, indeed, lipid reserves were depleted, while membrane lipids remained unchanged, including thylakoid membranes. In the Antarctic *C. gerlachei*, *Melosira* sp., and both *P. wetzelii* strains, a decline in the ratio of fatty acids groups was observed, indicating enhanced degradation of storage lipids. In contrast, *N. criophiliforma* showed a slight increase in the ratio of fatty acids after 12 weeks, which points to a stronger increase in membrane degradation compared to lipid consumption. Apparently, both the consumption of storage lipids and the partial degradation of chloroplasts took place in the investigated Antarctic benthic diatoms during prolonged darkness in order to obtain energy for the maintenance metabolism.

4.6 Conclusion

In conclusion, all Antarctic benthic diatom species exhibited similar response patterns after 3 months of darkness. The combination of ecophysiological, biochemical, and cell biological data led to a better understanding of the underlying mechanisms. All benthic diatoms degrade parts of their chloroplasts and utilize their lipid energy reserves but at the same time maintained a functional photosynthetic apparatus that guarantees rapid recovery after re-irradiation. The combination of both mechanisms, presumably using storage lipids and degrading chloroplasts, is a key strategy for dark survival and hence for coping with the polar night.

4.7 Funding

This study was funded within the framework of the SPP 1158 Antarktisforschung by the DFG under grant numbers ZI 1628/2-1 and KA899/38-1. This study was further supported by the Austrian Science Fund Grant P34181-B to AH.

4.8 Acknowledgments

The authors would like to thank the team of the Argentinian Antarctic Research Station: Carlini of the Instituto Antártico Argentino (IAA) for their support and logistics, especially Gabriela L. Campana and María Liliana Quartino. The authors acknowledge the contribution of Regine Jahn to the description of the new species and thank Wolf-Henning Kusber for his support of the nomenclature act. Furthermore, the authors would like to thank Akihiro Tuji from the National Museum of Nature and Science, Japan, for sharing the sequence data of *P. tujii*. The authors are grateful to Jana Bansemer for work in the molecular laboratory and to Juliane Bettig for support at the SEM at the BGBM Berlin. The authors thank Matthias Woll, AWI Bremerhaven, for undertaking the GC-MS analysis. Moreover, the authors thank Sabrina Obwegeser, University of Innsbruck, for expert technical assistance in transmission electron microscopy.

4.9 References

Abarca N, Jahn R, Zimmermann J, Enke N (2014) Does the cosmopolitan diatom *Gomphonema parvulum* (Kützing) Kützing have a biogeography? PLoS ONE 9: e86885. https://doi.org/10.1371/journal.pone.0086885

Al-Handal AY, Torstensson A, Wulff A (2022) Revisiting Potter Cove, King George Island, Antarctica, 12 years later: new observations of marine benthic diatoms. Botanica Marina. 65: 81–103. https://doi.org/10.1515/bot-2021-0066

Amin SA, Parker MS, Armbrust EV (2012) Interactions between diatoms and bacteria. Microbiology and Molecular Biology Reviews 76: 667–684. https://doi.org/10.1128/MMBR.00007-12

Andrejic JZ, Spaulding SA, Manoylov KM, Edlund MB (2018) Phenotypic plasticity in diatoms: Janus cells in four *Gomphonema* taxa. Diatom Research 33: 453–470. https://doi.org/10.1080/0269249X.2019.1572652

Antia NJ (1976) Effects of temperature on the darkness survival of marine microplanktonic algae. Microbial Ecology 3: 41–54. https://doi.org/10.1007/BF02011452

Armbrust EV (2009) The life of diatoms in the world's oceans. Nature 459: 185–192. https://doi.org/10.1038/nature08057

Armbrust EV, Berges JA, Bowler C, Green BR, Martinez D, Putnam NH, et al. (2004) The genome of the diatom *Thalassiosira pseudonana*: ecology, evolution, and metabolism. Science 306: 79–86. https://doi.org/.1126/science.1101156

Chauton MS, Winge P, Brembu T, Vadstein O, Bones AM (2013) Gene regulation of carbon fixation, storage, and utilization in the diatom *Phaeodactylum tricornutum* acclimated to light; dark cycles. Plant Physiology 161: 1034–1048. https://doi.org/10.1104/pp.112.206177

Cottier F, Potter M (2020) The marine physical environment during the polar night. In: Johnsen G, Leu E, Gradinger R (eds) Polar Night Marine Ecology, Life and Light in the Dead of Night, Cham: Springer, 17–36. https://doi.org/10.1007/978-3-030-33208-2_2

Crawford RM (1977) The taxonomy and classification of the diatom genus *Melosira* C. Ag. II. *M. moniliformis* (Müll.) C. Ag. Phycologia 16: 277–285. https://doi.org/10.2216/i0031-8884-16-3-277.1

Droege G, Barker K, Seberg O, Coddington J, Benson E, Berendsohn WG, et al. (2016) The Global Genome Biodiversity Network (GGBN) data standard specification. Database 2016: baw125. https://doi.org/10.1093/database/baw125

Durbin EG (1978) Aspects of the biology of resting spores of *Thalassiosira nordenskioeldii* and *Detonula confervacea*. Marine Biology 45, 31–37. https://doi.org/10.1007/BF00388975

Fahl K, Kattner G (1993) Lipid content and fatty acid composition of algal communities in sea-ice and water from the Weddell Sea (Antarctica). Polar Biology 13: 405–409. https://doi.org/10.1007/BF01681982

Field CB, Behrenfeld MJ, Randerson JT, Falkowski P (1998) Primary production of the biosphere: integrating terrestrial and oceanic components. Science 281: 237–240. https://doi.org/10.1126/science.281.5374.237

Fryxell GA (1989) Marine phytoplankton at the Weddell Sea ice edge: seasonal changes at the specific level. Polar Biology 10: 1–18. https://doi.org/10.1007/BF00238285

Gemeinholzer B, Droege G, Zetzsche H, Haszprunar G, Klenk HP, Güntsch A, et al. (2011) The DNA Bank Network: the start from a German initiative. Biopreservation Biobanking 9: 51–55. https://doi.org/10.1089/bio.2010.0029

Glud RN, Kühl M, Wenzhöfer F, Rysgaard S (2002) Benthic diatoms of a high Arctic fjord (Young Sound, NE Greenland): importance for ecosystem primary production. Marine Ecology Progress Series 238: 15–29. https://doi.org/10.3354/meps238015

Glud RN, Woelfel J, Karsten U, Kühl M, Rysgaard S (2009) Benthic microalgal production in the Arctic: applied methods and status of the current database. Bot. Mar. 52, 559–571. https://doi.org/10.1515/BOT.2009.074

Gómez I, Wulff A, Roleda MY, Huovinen P, Karsten U, Quartino ML, et al. (2009) Light and temperature demands of marine benthic microalgae and seaweeds in polar regions. Botanica Marina 52: 593–608. https://doi.org/10.1515/BOT.2009.073

Greenspan P, Mayer EP, Fowler SD (1985) Nile red: a selective fluorescent stain for intracellular lipid droplets. Journal of Cell Biology 100: 965–973. https://doi.org/10.1083/jcb.100.3.965

Guillard RRL, Ryther JH (1962) Studies of marine planktonic diatoms: I. *Cyclotella nana* Hustedt, and *Detonula confervacea* (Cleve) Gran. Can. Journal of Microbiology 8: 229–239. https://doi.org/10.1139/m62-029

HELCOM (2019) Guidelines-for-Measuring-Chlorophyll-a. Baltic Marine Environment Protection Commission. Available online at: https://helcom.fi/post_type_publ/guidelines-for-measuring-chlorophyll-a/ (accessed October 15, 2022).

Hellebust JA, Lewin J (1977) Heterotrophic nutrition. In: Werner D (ed) The Biology of Diatoms. University of California Press. Berkeley, 169–197.

Hernández EA, Lopez JL, Piquet AMT, Mac Cormack WP, Buma AGJ (2019) Changes in salinity and temperature drive marine bacterial communities' structure at Potter Cove, Antarctica. Polar Biology 42: 2177–2191. https://doi.org/10.1007/s00300-019-02590-5

Hoffmann R, Al-Handal AY, Wulff A, Deregibus D, Zacher K, Quartino ML, et al. (2019) Implications of glacial melt-related processes on the potential primary production of a microphytobenthic community in Potter Cove (Antarctica). Frontiers in Marine Science 6: 655. d https://doi.org/10.3389/fmars.2019.00655

Holzinger A, Roleda MY, Lütz C (2009) The vegetative arctic freshwater green alga *Zygnema* is insensitive to experimental UV exposure. Micron 40: 831–838. https://doi.org/10.1016/j.micron.2009.06.008

Hu Q, Sommerfeld M, Jarvis E, Ghirardi M, Posewitz M, Seibert M, et al. (2008) Microalgal triacylglycerols as feedstocks for biofuel production: perspectives and advances. Plant Journal 54: 621–639. https://doi.org/10.1111/j.1365-313X.2008.03492.x

Jahn R, Abarca N, Gemeinholzer B, Mora D, Skibbe O, Kulikovskiy M, et al. (2017) *Planothidium lanceolatum* and *Planothidium frequentissimum* reinvestigated with molecular methods and morphology: four new species and the taxonomic importance of the sinus and cavum. Diatom Research 32: 75–107. https://doi.org/10.1080/0269249X.2017.1312548

Kapuscinski J (1995) DAPI: a DNA-specific fluorescent probe. Biotechnic Histochemestry 70: 220–233. https://doi.org/10.3109/10520299509108199

Karsten U, Schaub I, Woelfel J, Sevilgen, DS, Schlie C, Becker B, et al. (2019a) Living on cold substrata: new insights and approaches in the study of microphytobenthos ecophysiology and ecology in Kongsfjorden. In: Hop H, Wiencke C (eds) The Ecosystem of Kongsfjorden, Svalbard. Cham: Springer International Publishing, 303–330. https://doi.org/10.1007/978-3-319-46425-1_8

Karsten U, Schlie C, Woelfel J, Becker B (2012) Benthic diatoms in arctic seas-Ecological functions and adaptations. Polarforschung 81: 77–84. https://doi.org/10.2312/polarforschung.81.2.77

Karsten U, Schumann R, Holzinger A (2019b) Ecophysiology, cell biology and ultrastructure of a benthic diatom isolated in the arctic. In: Seckbach J, Gordon R (eds) Diatoms. Fundamentals and Applications. Wiley, Scrivener. Hoboken, NJ; Salem, MA, 273–287. https://doi.org/10.1002/9781119370741.ch12

Kattner G, Fricke HSG (1986) Simple gas–liquid chromatographic method for the simultaneous determination of fatty acids and alcohols in wax esters of marine organisms. Journal of Chromatography 361: 263–268. https://doi.org/10.1016/S0021-9673(01)86914-4

Kennedy F, Martin A, Bowman JP, Wilson R, McMinn A (2019) Dark metabolism: a molecular insight into how the Antarctic sea-ice diatom *Fragilariopsis cylindrus* survives long-term darkness. New Phytologist 223: 675–691. https://doi.org/10.1111/nph.15843

Kopalová K, Veselá J, Elster J, Nedbalová L, Komárek J, Van de Vijver B (2012) Benthic diatoms (Bacillariophyta) from seepages and streams on James Ross Island (NW Weddell Sea, Antarctica). Plant Ecology and Evolution 145: 190–208. https://doi.org/10.5091/plecevo.2012.639

Lacour T, Morin P, Sciandra T, Donaher N, Campbell DA, Ferland J, et al. (2019) Decoupling light harvesting, electron transport and carbon fixation during prolonged darkness supports rapid recovery upon re-illumination in the Arctic diatom *Chaetoceros neogracilis*. Polar Biology 42: 1787–1799. https://doi.org/10.1007/s00300-019-02507-2

Leyland B, Boussiba S, Khozin-Goldberg I (2020) A review of diatom lipid droplets. Biology 9, 38. https://doi.org/10.3390/biology9020038

Longhi ML, Schloss IR, Wiencke C (2003) Effect of irradiance and temperature on photosynthesis and growth of two antarctic benthic diatoms, *Gyrosigma subsalinum* and *Odontella litigiosa*. Botanica Marina 46: 276–284. https://doi.org/10.1515/BOT.2003.025

Malapascua JRF, Jerez CG, Sergejevová M, Figueroa FL, Masojídek J (2014) Photosynthesis monitoring to optimize growth of microalgal mass cultures: application of chlorophyll fluorescence techniques. Aquatic Biology 22: 123–140. https://doi.org/10.3354/ab00597

Mariño G, Niso-Santano M, Baehrecke E, Kroemer G (2014) Selfconsumption: the interplay of autophagy and apoptosis. Nature Reviews Molecular Cell Biology 15: 81–94. https://doi.org/10.1038/nrm3735

McMinn A, Ashworth C, Bhagooli R, Martin A, Salleh S, Ralph P, et al. (2012) Antarctic coastal microalgal primary production and photosynthesis. Marine Biology 159: 2827–2837. https://doi.org/10.1007/s00227-012-2044-0

McMinn A, Martin A (2013) Dark survival in a warming world. Proceedings: Biological Sciences 280: 20122909. https://doi.org/10.1098/rspb.2012.2909

McQuoid MR, Hobson LA (1996) Diatom resting stages. Journal of Phycology 32: 889–902. https://doi.org/10.1111/j.0022-3646.1996.00889.x

Meier D, Lichtenthaler HK (1981) Ultrastructural development of chloroplasts in radish seedlings grown at high- and low-light conditions and in the presence of the herbicide bentazon. Protoplasma 107, 195–207. https://doi.org/10.1007/BF01275618

Mohamad H, Mora D, Skibbe O, Abarca N, Deutschmeyer V, Enke N, et al. (2022) Morphological variability and genetic marker stability of 16 monoclonal pennate diatom strains under medium-term culture. Diatom Research 37: 307–328. https://doi.org/10.1080/0269249X.2022.2141346

Morales M, Aflalo C, Bernard O (2021) Microalgal lipids: a review of lipids potential and quantification for 95 phytoplankton species. Biomass Bioenergy 150: 106108. https://doi.org/10.1016/j.biombioe.2021.106108

Müller J, Müller K, Neinhuis C, Quandt D (2010) PhyDE® -Phylogenetic Data Editor. Available online at: http://www.phyde.de/

Murata N, Los DA (1997) Membrane fluidity and temperature perception. Plant Physiol. 115, 875–879. https://doi.org/10.1104/pp.115.3.875

Nelson DM, Tréguer P, Brzezinski MA, Leynaert A, Quéguiner B (1995) Production and dissolution of biogenic silica in the ocean: revised global estimates, comparison with regional data and relationship to biogenic sedimentation. Global Biogeochemical Cycles 9: 359–372. https://doi.org/10.1029/95GB01070

Palmisano AC, Sullivan CW (1982) Physiology of sea ice diatoms. I. Response of three polar diatoms to a simulated summer-winter transition. Journal of Phycology 18: 489–498. https://doi.org/10.1111/j.1529-8817.1982.tb03215.x

Palmisano AC, Sullivan CW (1983) Physiology of sea ice diatoms. II. Dark survival of three polar diatoms. Canadian Journal of Microbiology 29: 157–160. https://doi.org/10.1139/m83-026

Pavlov A, Leu E, Hanelt D, Bartsch I, Karsten U, Hudson SR, et al. (2019) Underwater light regime in Kongsfjorden and its ecological implications. In: Hop H, Wiencke C (eds) The Ecosystem of Kongsfjorden, Svalbard, Advances in Polar Ecology 2. Cham: Springer, 137–170.

Prelle LR, Graiff A, Gründling-Pfaff S, Sommer V, Kuriyama K, Karsten U (2019) Photosynthesis and respiration of Baltic Sea benthic diatoms to changing environmental conditions and growth responses of selected species as affected by an adjacent peatland (Hütelmoor). Frontiers in Microbiology 10: 1500. https://doi.org/10.3389/fmicb.2019.01500

Prelle LR, Schmidt I, Schimani K, Zimmermann J, Abarca N, Skibbe O, et al. (2022) Photosynthetic, respirational, and growth responses of six benthic diatoms from the Antarctic peninsula as functions of salinity and temperature variations. Genes 13: 71264. https://doi.org/10.3390/genes13071264

Reeves S, McMinn A, Martin A (2011) The effect of prolonged darkness on the growth, recovery and survival of Antarctic sea ice diatoms. Polar Biology 34: 1019–1032. https://doi.org/10.1007/s00300-011-0961-x

Schaub I, Wagner H, Graeve M, Karsten U (2017) Effects of prolonged darkness and temperature on the lipid metabolism in the benthic diatom *Navicula perminuta* from the Arctic Adventfjorden, Svalbard. Polar Biology 40: 1425–1439. https://doi.org/10.1007/s00300-016-2067-y

Schimani K, Abarca N, Zimmermann J, Skibbe O, Jahn R, Kusber W-H, et al. (2023) Molecular phylogenetics coupled with morphological analyses of Arctic and Antarctic strains place *Chamaepinnularia* (Bacillariophyta) within the Sellaphoraceae. Fottea 24: 1–22. https://doi.org/10.5507/fot.2023.002

Schlie C, Karsten U (2017) Microphytobenthic diatoms isolated from sediments of the Adventfjorden (Svalbard): growth as function of temperature. Polar Biology 40: 1043–1051. https://doi.org/10.1007/s00300-016-2030-y

Schwarz V, Andosch A, Geretschläger A, Affenzeller M, Lütz-Meindl U (2017) Carbon starvation induces lipid degradation via autophagy in the model alga Micrasterias. Journal of Plant Physiology 208: 115–127. https://doi.org/10.1016/j.jplph.2016.11.008

Sterken M, Verleyen E, Jones V, Hodgson D, Vyverman W, Sabbe K, et al. (2015) An illustrated and annotated checklist of freshwater diatoms (Bacillariophyta) from Livingston, Signy and Beak Island (Maritime Antarctic Region). Plant Ecology and Evolution 148: 431–455. https://doi.org/10.5091/plecevo.2015.1103

Tamura K, Stecher G, Kumar S (2021) MEGA11: molecular evolutionary genetics analysis version 11. Molecular Biology and Evolution 38: 3022–3027. https://doi.org/10.1093/molbev/msab120

Tuchman NC, Schollett MA, Rier ST, Geddes P (2006) Differential heterotrophic utilization of organic compounds by diatoms and bacteria under light and dark conditions. Hydrobiologia 561: 167–177. https://doi.org/10.1007/s10750-005-1612-4

Van de Vijver B, Sterken M, Vyverman W, Mataloni G, Nedbalová L, Kopalová K, et al. (2010) Four new non-marine diatom taxa from the Subantarctic and Antarctic regions. Diatom Research 25: 431–443. https://doi.org/10.1080/0269249X.2010.9705861

Verleyen E, Van de Vijver B, Tytgat B, Pinseel E, Hodgson DA, Kopalová K, et al. (2021) Diatoms define a novel freshwater biogeography of the Antarctic. Ecography 44: 548–560. https://doi.org/10.1111/ecog.05374

Walne PR (1970) Studies on the food value of nineteen genera of algae to juvenile bivalves of the genera Ostrea, Crassostrea, Mercenaria and Mytilus. Fishery Investigations Series 2: 1–62.

Walsby AE (1997) Numerical integration of phytoplankton photosynthesis through time and depth in a water column. New Phytologist 136: 189–209. https://doi.org/10.1046/j.1469-8137.1997.00736.x

Wetzel CE, Van de Vijver B, Blanco S, Ector L (2019) On some common and new cavum-bearing Planothidium (Bacillariophyta) species from freshwater. Fottea 19: 50–89. https://doi.org/10.5507/fot.2018.016

Wetzel CE, Van de Vijver B, Hoffmann L, Ector L (2013) *Planothidium incuriatum* sp. nov. a widely distributed diatom species (Bacillariophyta) and type analysis *of Planothidium biporomum*. Phytotaxa 138: 43–57. https://doi.org/10.11646/phytotaxa.138.1.6

Witkowski A, Riaux-Gobin C, Daniszewska-Kowalczyk G (2010) New marine diatom (Bacillariophyta) species described from Kerguelen Islands coastal area and pertaining to *Navicula* S.S. with some remarks on morphological variation of the genus. Vie et Milieu 60: 265–281.

Woelfel J, Schumann R, Peine F, Flohr A, Kruss A, Tegowski J, et al. (2010) Microphytobenthos of Arctic Kongsfjorden (Svalbard, Norway): biomass and potential primary production along the shore line. Polar Biology 33: 1239–1253. https://doi.org/10.1007/s00300-010-0813-0

Wulff A, Roleda MY, Zacher K, Wiencke C (2008a) Exposure to sudden light burst after prolonged darkness - a case study on benthic diatoms in Antarctica. Diatom Research 23: 519–532. https://doi.org/10.1080/0269249X.2008.9705774

Wulff A, Roleda MY, Zacher K, Wiencke C (2008b) UV radiation effects on pigments, photosynthetic efficiency and DNA of an Antarctic marine benthic diatom community. Aquatic Biology 3: 167–177. https://doi.org/10.3354/ab00076

Zacher K, Rautenberger R, Hanelt D, Wulff A, Wiencke C (2009) The abiotic environment of polar marine benthic algae. Botanica Marina 52: 483–490. https://doi.org/10.1515/BOT.2009.082

Zhang Q, Gradinger R, Spindler M (1998) Dark survival of marine microalgae in the high arctic (greenland sea). Polarforschung 65: 111–116.

Zidarova R, Ivanov P, Hineva E, Dzhembekova N (2022) Diversity and habitat preferences of benthic diatoms from South Bay (Livingston Island, Antarctica). Plant Ecology and Evolution 155: 70–106. https://doi.org/10.5091/plecevo.84534

Zidarova R, Kopalová K, Van de Vijver B (2016) Ten new Bacillariophyta species from James Ross Island and the South Shetland Islands (Maritime Antarctic Region). Phytotaxa 272: 37. https://doi.org/10.11646/phytotaxa.272.1.2

Zimmermann J, Jahn R, Gemeinholzer B (2011) Barcoding diatoms: evaluation of the V4 subregion on the 18S rRNA gene, including new primers and protocols. Organisms Diversity and Evolution 11: 173. https://doi.org/10.1007/s13127-011-0050-6

5 Photosynthetic, respirational, and growth responses of six benthic diatoms from the Antarctic Peninsula as functions of salinity and temperature variations

Lara R. Prelle[1], Ina Schmidt[1], Katherina Schimani[2], Jonas Zimmermann[2], Nelida Abarca[2], Oliver Skibbe[2], Desiree Juchem[1] and Ulf Karsten[1]

[1] Applied Ecology and Phycology, Institute of Biological Sciences, Albert-Einstein-Strasse 3, University of Rostock, 18057 Rostock, Germany

[2] Botanic Garden and Botanical Museum Berlin-Dahlem, Freie Universität Berlin, 14163 Berlin, Germany

Genes 13:1264, https://doi.org/10.3390/genes13071264

5.1 Abstract

Temperature and salinity are some of the most influential abiotic parameters shaping biota in aquatic ecosystems. In recent decades, climate change has had a crucial impact on both factors - especially around the Antarctic Peninsula - with increasing air and water temperature leading to glacial melting and the accompanying freshwater increase in coastal areas. Antarctic soft and hard bottoms are typically inhabited by microphytobenthic communities, which are often dominated by benthic diatoms. Their physiology and primary production are assumed to be negatively affected by increased temperatures and lower salinity. In this study, six representative benthic diatom strains were isolated from different aquatic habitats at King George Island, Antarctic Peninsula, and comprehensively identified based on molecular markers and morphological traits. Photosynthesis, respiration, and growth response patterns were investigated as functions of varying light availability, temperature, and salinity. Photosynthesis–irradiance curve measurements pointed to low light requirements, as light-saturated photosynthesis was reached at <70 µmol photons m^{-2} s^{-1}. The marine isolates exhibited the highest effective quantum yield between 25 and 45 S_A (absolute salinity), but also tolerance to lower and higher salinities at 1 S_A and 55 S_A, respectively, and in a few cases even <100 SA. In contrast, the limnic isolates showed the highest effective quantum yield at salinities ranging from 1 S_A to 20 S_A. Almost all isolates exhibited high effective quantum yields between 1.5 and 25 °C, pointing to a broad temperature tolerance, which was supported by measurements of the short-term temperature-dependent photosynthesis. All studied Antarctic

benthic diatoms showed activity patterns over a broader environmental range than they usually experience in situ. Therefore, it is likely that their high ecophysiological plasticity represents an important trait to cope with climate change in the Antarctic Peninsula.

Keywords: growth rate; climate change; tolerance; ecophysiology; 18 S; *rbc*L

5.2 Introduction

Global warming is unequivocal, as is now evident from observations of increases in average global air and ocean temperatures, leading to the widespread melting of snow and ice in the polar regions, and rising average global sea levels (IPCC 2014). However, the effects are quite different in Antarctica and the Arctic. While global warming is already strongly affecting the whole Arctic region (Overland et al 2014), in Antarctica, thus far, mainly the Antarctic Peninsula has gotten warmer, where the air temperature and near-surface sea temperature have risen by 3 °C and 1 °C, respectively, in the past 50 years. This has resulted in a significant retreat of ice shelves, increased coastal erosion, less snow, and more meltwater and rain, with strong consequences for Antarctic organisms and ecosystems (IPCC 2014; Winterfeld et al 2018).

A particularly ecologically important group of eukaryotic microorganisms in Antarctic and Arctic shallow-water coastal zones are benthic diatoms (living on top of or associated with sediments or rocks), which are poorly studied in terms of biodiversity, biogeography, and ecology. Knowledge on these phototrophs, which form a key assemblage known as microphytobenthos, stems mainly from temperate to tropical marine soft-bottom regions worldwide—for example, tidal flats. Here, they exert multiple important functions as high primary producers providing a major food source for benthic suspension- or depositfeeders (Cahoon 1999), as control barriers for oxygen/nutrient fluxes at the sediment–water interface (Risgaard-Petersen et al 1994), and as stabilizers of sediment surfaces against hydrodynamic erosion by the excretion of sticky extracellular polymeric substances (Beninger et al 2018). Microphytobenthic communities, together with planktonic diatoms, contribute about 45 % of total marine carbon fixation (Mann 1999).

A pioneer study of the Young Sound, Greenland, indicated that benthic diatoms contributed to 40 % of the total marine primary production (60 % originated from kelps, Glud et al 2002). These data were later confirmed for the Arctic Kongsfjorden (Svalbard, Norway), in which microphytobenthic production was as high as in temperate regions (Woelfel et al 2010; Woelfel et al 2014; Sevilgen et al. 2014). Consequently, benthic diatoms are regarded as playing an exceptionally important role in Arctic coastal food webs (Glud et al. 2009), while similar studies

for Antarctica are lacking. To this day, remarkably little is known about marine benthic diatom biodiversity and ecophysiology in Antarctica. In contrast, the various microalgae of the Antarctic phytoplankton, as well as those associated with sea ice, with snow fields, or inhabiting terrestrial sites, are much better studied (Morgan-Kiss et al. 2008; Zhang et al. 2020; Gilbertson et al. 2022; Hüner et al. 2022, and references therein). In addition, more recent publications have applied next-generation sequencing (NGS) technologies, greatly expanding current knowledge by providing fundamental information on the underlying molecular mechanisms of physiological and biochemical adaptations to polar environmental conditions.

The Antarctic microphytobenthos - especially along the Antarctic Peninsula - experiences strong seasonal variability in abiotic parameters on the edge of extremes such as temperature, salinity, and light availability (e.g., polar day versus polar night). Sea ice coverage has a strong effect on photosynthesis, as light penetration decreases with ice thickness and snow coverage (Maykut and Grenfell 1975; Lazzara et al. 2007). However, coastal regions of the Antarctic Peninsula face strong deglaciation due to warming and, hence, are less and less covered with ice, allowing benthic communities to occupy and develop on such pristine sediments (Post et al. 2014). The temperature variations in this region can lead to freezing in winter and melting of snow and ice during the warm season. Especially shallow coastal sites are strongly influenced by melting and freezing processes, along with temperature, creating strong seasonal salinity changes. Increasing melting enhances terrestrial freshwater runoff, thereby decreasing salinity, and vice versa - freezing in winter decreases freshwater runoff, increasing salinity in the remaining aquatic environment. In addition, the Antarctic Peninsula receives 450 mm of precipitation per year; however, due to global warming, this is now mainly received as rain (Kanz et al. 2020 thereby also decreasing the sea surface salinity.

The few data available indicate that Antarctic benthic diatoms generally live most of the time under low-light conditions. Nevertheless, these phototrophic microorganisms have been reported to adjust their photosynthetic activity very efficiently to changing irradiance (Wulff et al. 2008; Wulff et al. 2009). The benthic diatom *Trachyneis aspera* was found to grow at ambient photon fluence rates of <1 µmol photons m^{-2} s^{-1}, with saturated photosynthetic rates (I_k values) already between 7 and 16 µmol photons m^{-2} s^{-1} (Palmisano et al. 1985). Hence, benthic diatoms, in virtue of their low light requirements for photosynthesis, are capable to colonize deeper soft bottoms (Cahoon 1999). The ability of Antarctic benthic diatoms to acclimate not only to such extreme low-radiation environments, but also to high-radiation environments, has been documented in some studies (Wulff et al. 2008; Wulff et al. 2009). Two underlying processes for the regulation of the rapid switch from a light-harvesting to a photoprotective

state have been reported: One is non-photochemical fluorescence quenching - a mechanism involving the quenching of singlet excited-state chlorophylls via enhanced internal conversion back to the ground state of these pigments. As a consequence, excessively absorbed radiation energy is harmlessly dissipated as heat through molecular vibrations (Wilhelm et al. 2006). The second process is the cycling of electrons around photosystem II and/or photosystem I (Wilhelm et al. 2006). Both mechanisms support the safe dissipation of excessively absorbed radiation energy during a sudden increase in the incident light conditions, and contribute to a rather unusual photosynthetic flexibility in diatoms, providing optimal photoprotection and rapid photoacclimation under the fluctuating and highly variable Antarctic light climate. In addition, many but not all benthic diatoms also exhibit a behavioral trait in response to changes in the light field by vertical migration into or out of the sediment to avoid photoinhibition (Harper 1969).

While Arctic benthic diatoms can be characterized as eurythermal and psychrotolerant microalgae with growth optima at around 15 °C (Schlie and Karsten 2017; Karsten et al. 2019), this seems to be in sharp contrast to their Antarctic counterparts, which show stenothermal and psychrophilic traits (Longhi et al. 2003). Psychrophilic and psychrotolerant species can be physiologically distinguished, as the former can survive at freezing temperatures but will die at more moderate temperatures (Morita 1975). Typical examples include the psychrotolerant green microalga *Coccomyxa subellipsoidea* C-169, which was isolated from a terrestrial site in Antarctica (Blanc et al. 2012), and the psychrophilic unicellular green alga *Chlamydomonas* sp. ICE-L that thrives in floating Antarctic sea ice (Zhang et al. 2020). Psychrophilic traits are exemplarily documented in the Antarctic benthic diatoms *Odontella litigiosa* and *Gyrosigma subsalinum* var. *antarctica*, both collected at Potter Cove, King George Island, which exhibit optimal growth at 0°C and full inhibition of cell division at <7–9 °C (Longhi et al. 2003). Whether other Antarctic benthic diatoms follow the low temperature demand for growth is unknown, but already Wiencke and Tom Dieck (1990) have reported extremely low temperature requirements for growth and survival in various seaweed species endemic to Antarctica, compared to the Arctic and more temperate regions. Although the number of such ecophysiological studies is small, it can be assumed that the conspicuous differences in the temperature requirements for growth in Arctic and Antarctic benthic diatoms are related to the much longer isolation and cold-water history of the Southern polar region (at least 23 million years, Sabbe et al. 2003) compared to the Northern high latitudes (approximately 2 million years). These striking differences in both cold-water systems have supported the development

of many endemic marine organisms in Antarctica, most of which are extremely sensitive to warming (Gómez et al. 2009).

In contrast to the fragmentary data on marine benthic diatoms, Antarctic freshwater diatoms are much better studied in terms of biodiversity, ecology, and biogeography (Verleyen et al. 2021). These authors studied biogeographic patterns of freshwater diatom communities of >400 lakes spread across the Antarctic realm, and identified highly distinct diatom florae, in terms of both composition and richness. More importantly, 44 % of all determined species were convincingly reported to be endemic to Antarctica (Verleyen et al. 2021).

In contrast to light and temperature conditions, salinity is typically a local environmental factor, which may strongly vary in Antarctic near-shore waters, where meltwater - particularly during summer - mixes with marine water bodies. Here, horizontal and vertical gradients between freshwater and fully marine conditions can be measured. In addition, tidal flows, hydrological conditions, wind, precipitation, and evaporation strongly influence the salt concentration of the water body in question. The effect of salinity on benthic diatoms and other algae from polar waters is generally little studied, in strong contrast to temperate regions (Kirst and Wiencke 1995; Glaser and Karsten 2020).

In this study we investigated the ecophysiological response patterns of six Antarctic benthic diatom strains under a temperature, light, and salinity gradient. The diatoms were isolated from two marine shallow-water stations and one freshwater reservoir at Potter Cove, Antarctic Peninsula, and subsequently identified using morphological and molecular markers. Based on the study of Longhi et al. (2003), we expected stenothermal and low-light acclimated response patterns in terms of photosynthesis and growth. In addition, we expected euryhaline and stenohaline responses for the marine and freshwater isolates, respectively.

5.3 Materials and methods

5.3.1 Study site

Sediment surface samples taken in January/February 2020 from four study sites (Figure 1, Table 1) near the Argentinian research station Carlini Base (S 62°14′17.45″, W 58°40′2.19″) on King George Island were used for benthic diatom isolation. All isolates were established from samples collected in Potter Cove, which is separated into an inner part with a maximum depth of 50 m, and an outer part connected to the open ocean, with maximum depths of 100–200 m (Klöser et al. 1994).

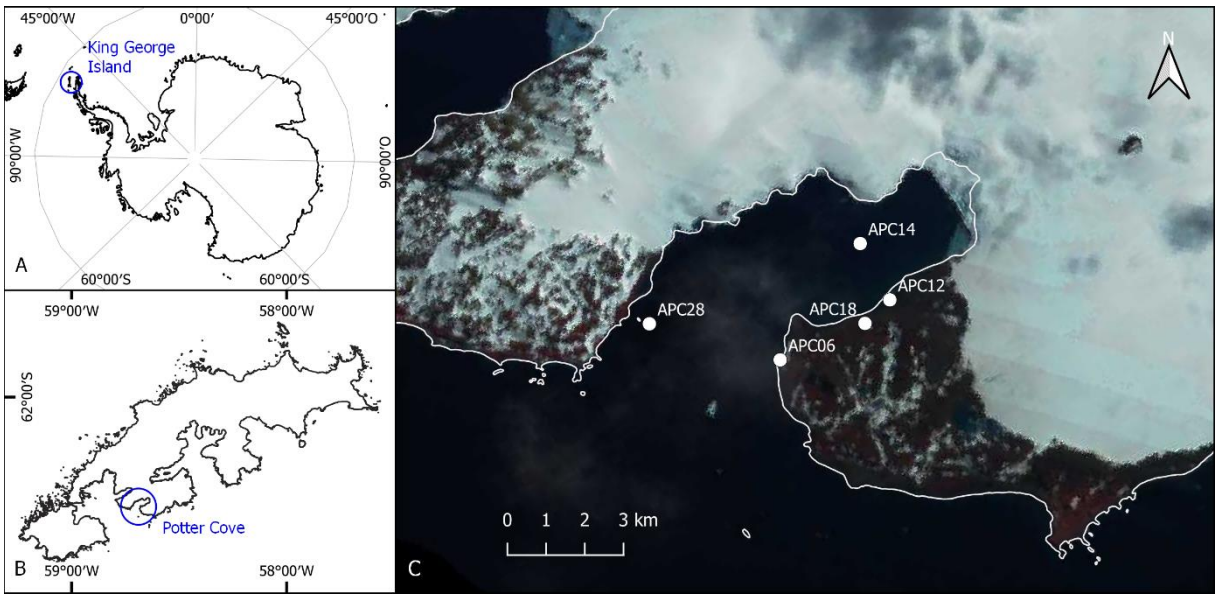

Figure 1 Sampling points. **A** Map of the Antarctic **B** Map of King George Island **C** sample points in the Potter Cove: limnic location APC18, brackish water location APC12, and marine locations APC06, APC14, and APC28. Basemap: Landsat image mosaic of Antarctica (LIMA).

Table 1 List of sample locations at Carlini Station, King George Island, Potter Cove, in austral summer 2020 (January/February), with information on sample site, altitude or water depth, sample date, collector georeferenced, and sampled substrate; a.s.l.: above sea level.

Sample Location	Site	Sample Origin	Altitude / Water Depth	Date of Sampling	Collector	Georeference
APC06	Potter Cove, coast at Penon 0	Marine	0 m	29 January 2020	J. Zimmermann	S 62°14′30.55”, W 58°40′54.96”
APC12	Potter Cove, coast east of Carlini Station	Brackish	0 m	30 January 2020	J. Zimmermann	S 62°14‘07.78”, W 58°39′27.91”
APC14	Potter Cove, Island A4	Marine	15 m depth	31 January 2020	J. Zimmermann, G.L. Campana, Diver Team	S 62°13′43.61”, W 58°39′49.36”
APC18	Potter Cove, drinking water reservoir	Freshwater	51 m a.s.l.	01 February 2020	J. Zimmermann	S 62°14′16.30”, W 58°39′44.10”
APC28	Potter Cove, coast at Penon de Pesca	Marine	5 m depth	07 February 2020	J. Zimmermann, G.L. Campana, Diver Team	S 62°14′16.5’’, W 58°42′44.2”

5.3.2 Culture establishment and maintenance conditions

Six unialgal benthic diatom strains were established: *Navicula criophiliforma* A.Witkowski, C. Riaux-Gobin, & G. Daniszewska-Kowalczyk (Naviculaceae, strain APC06 D288_003), *Chamaepinnularia gerlachei* Van de Vijver and Sterken (Naviculaceae, strain APC14 D296_001), *Navicula concordia* C. Riaux-Gobin & A.Witkowski (Naviculaceae, strain APC28

D310_004), *Nitzschia annewillemsiana* Hamsher, Kopalová, Kociolek, Zidarova, & Van de Vijver (Bacillariaceae, strain APC18 D300_012), *Planothidium* sp. (Achnanthidiaceae, strain APC18 D300_015), and *Psammothidium papilio* (D.E. Kellogg, Stuiver, T.B. Kellogg, & G.H. Denton) K. Kopalová & Van de Vijver (Achnanthaceae, strain APC18 D399_023).

The marine culture *N. criophiliforma* originated from sample location APC06 (S 6214030.5500, W58 40054.9600), which was an intertidal rock pool. Due to its location in the intertidal zone, abiotic parameters such as temperature and salinity strongly varied. *C. gerlachei* was isolated from a sample at the inner part of Potter Cove (APC14, S 62°13′43.61″, W 58°39′49.36″), at 15 m depth, from a biofilm on top of a sediment. Unfortunately, oxidized material from the strain *N. criophiliforma* had low quality, and species identification on this isolate alone was not possible. A genetically identical species was isolated from brackish water at sample location APC12, and material of this strain was used for identification. *Navicula concordia* from a sample location at the outer cove (S 62°14′16.50″, W 58°42′44.20″), at 5 m depth, originated from a biofilm on top of stones. According to Hernández et al. (2019), the minimum water temperature was measured at -1.69 °C in the inner part of Potter Cove and -1.4°C at the outer part, while the maximum temperature was 2.89 C and 1.98 C, respectively. Furthermore, the salinity of the outer cove is stable at ca. 33.5 S_A, while the salinity in the inner cove can drop down to 29.6 S_A.

The limnic isolates (*N. annewillemsiana*, *Planothidium* sp., and *P. papilio*) were established from biofilms on top of stones in a freshwater drinking reservoir (S 62°14′16.30″, W 58°39′44.10″). During sampling, no measurements of pH, temperature, or conductivity were taken, due to malfunctioning instruments.

The diatom cells were isolated from aliquots of environmental samples to establish clonal cultures. Under an inverse light microscope (100–400x magnification, Olympus, Japan), single cells were transferred using a microcapillary glass pipette onto microwell plates containing culture medium (Guillard's f/2 medium, Guillars and Ryther 1962, Guillard 1975 or Walne's medium Walne 1970; 34 S_A for marine samples and 1 S_A for freshwater samples). All samples and isolated diatom cells from Antarctica were maintained at 5–7 °C. Irradiation was provided by white-light LEDs at 5000 K under a 16:8 h light:dark cycle, with several dark phases during the day to prevent photo-oxidative stress. After successful establishment of clonal cultures, they were separated into subsamples for DNA extraction, morphological analysis, and ecophysiological experiments. For the latter, diatom cultures were cultivated in sterile filtered Baltic Sea water, enriched with Guillard's f/2 medium, Guillars and Ryther 1962, Guillard 1975

and sodium metasilicate (Na_2SiO_3 5 H_2O; 10 g 100 mL^{-1}) to a final concentration of 0.6 mM (further referred to as cultivation medium). Salinity of 33 S_A for the marine cultures was adjusted by using artificial sea salt (hw-Marinemix® professional, Wiegandt GmbH, Germany), while 1 S_A for the limnic cultures was achieved by dilution with deionized water.

All stock cultures for the ecophysiological experiments were kept at 8–9 °C at 15–20 µmol photons m^{-2} s^{-1} under a 16:8 h light:dark cycle (Osram Daylight Lumilux Cool White lamps L36W/840, Osram, Munich, Germany).

5.3.3 Acquisition and identification of morphometric data

In order to obtain clean diatom frustules, material harvested from the unialgal cultures was treated with 35 % hydrogen peroxide at room temperature to oxidize the organic material, and then washed with distilled water. To prepare permanent slides for light microscopy (LM) analyses, the cleaned material (frustules and valves) was dispersed on glass coverslips, dried at room temperature, and embedded with the high-refraction-index mounting medium Naphrax® (Morphisto GmbH, Offenbach, Germany).

Observations were conducted with a Zeiss Axioplan Microscope equipped with differential interference contrast (DIC), using a Zeiss 100 x Plan Apochromat objective, and microphotographs were taken with an AXIOAM MRc camera. Aliquots of cleaned sample material for scanning electron microscopy (SEM) observations were mounted on stubs and observed under a Hitachi FE 8010 scanning electron microscope operated at 1.0 kV.

5.3.4 DNA extraction, amplification, and sequencing

Culture material was transferred to 1.5 mL tubes. DNA was isolated using the NucleoSpin® Plant II Mini Kit (Macherey and Nagel, Düren, Germany), following the manufacturer's instructions. DNA fragment size and concentrations were evaluated via gel electrophoresis (1.5 % agarose gel) and NanoDrop® (PeqLab Biotechnology LLC; Erlangen, Germany), respectively. DNA samples were stored at -20 °C until further use, and finally deposited in the Berlin collection of the DNA Bank Network (Gemeinholzer et al. 2011).

Amplification was conducted by polymerase chain reaction (PCR) as described by Zimmermann et al. (2011) for the V4 region of 18 S. For the strain *C. gerlachei*, the whole 18 S gene was amplified as described by Jahn et al. (2017). The protein-coding plastid gene *rbc*L was amplified as described by Abarca et al. (2014). PCR products were visualized in a 1.5 % agarose gel and cleaned with MSB Spin PCRapace® (Invitek Molecular GmbH; Berlin, Germany), following the manufacturer's instructions. The samples were normalized to a total DNA content > 100 ng/µL using NanoDrop (PeqLab Biotechnology) for further sequencing.

Sanger sequencing of the PCR products was conducted bidirectionally by Starseq® (GENterprise LLC; Mainz, Germany).

5.3.5 Data curation

Vouchers and DNA of all strains were deposited in the collections at Botanischer Garten und Botanisches Museum Berlin, Freie Universität Berlin (B). DNA samples were stored in the Berlin DNA bank, and are available via the Genome Biodiversity Network (GGBN, Droege et al. 1016). All sequences were submitted to the European Nucleotide Archive (ENA, http://www.ebi.ac.uk/ena/) using the software tool annonex2embl (accessed on 11 July 2022, Gruenstaeudl 2019) and can be retrieved from ENA under the study number PRJEB54671. All cultures are available from the authors at the culture collection of the Department of Applied Ecology and Phycology, University of Rostock.

5.3.6 Photosynthetic efficiency

The photosynthetic potential of the six Antarctic benthic diatom strains as a function of salinity and temperature was measured using the pulse amplitude modulation (PAM) approach (PAM-2500, HeinzWalz GmbH, Effeltrich, Germany). The effective photochemical quantum yield of photosystem II in light-adapted cells, Y(II), was calculated (Equation (1)) by measurement of Fm0 (maximum chlorophyll fluorescence yield) and F (base fluorescence):

$$Y(II) = \frac{(F_m{}' - F)}{F_m{}'} \quad (1)$$

Equation (1): Calculation of the effective photochemical quantum yield of photosystem II (Y(II))

Intensity of the measured light and gain were adjusted to reach F_t (continuous base fluorescence) values between 0.15 and 0.2. Measurements were excluded from calculation when biomass did not surpass the F_t value of 0.15 at the highest measured light intensity and gain.

All cultures were kept under culture conditions before transfer into the respective test media, with three replicates of. Two drops of thin diatom culture suspension were applied on a 25 mm glass-fiber filter (GF/6, Whatman, Little Chalfont, UK) and incubated in 2 mL of the respective treatment medium. To avoid nutrient deficiency, 1 mL of the medium was replaced with fresh medium every day. A radiator block was used during the measurements to avoid excessive temperature stress in the laboratory.

Different salinity treatments were performed using sterile, filtered deionized water and artificial sea salt, with the addition of cultivation media. For the salinity treatments, marine isolates were incubated for three days under cultivation conditions at 1, 5, 10, 15, 25, 35, 45, 55, 65, 75, 85, and 100 S_A. Limnic isolates were exposed to salinities of 1, 5, 10, 20, 30, 35, 40, 45, 55, and 65 S_A. The isolates were incubated for three days prior to PAM measurements.

For the temperature treatments, experimental media were based on sterile, filtered deionized water and artificial sea salt (1 S_A for limnic cultures and 35 S_A for marine cultures), with the addition of cultivation media. All isolates were incubated for five days (t_5) at average temperatures of 1.5, 5, 7, 10, 15, 20, and 25°C. Temperatures were achieved using a temperature organ. For 1.5°C, an ice bath was used, with an exchange of ice every 12 h. The isolates were incubated for three days prior to PAM measurements.

PAM measurements were performed every 24 h, starting at day 0 (t_0), immediately after the transfer of the diatom cells onto the filter, until t_3 and t_5.

5.3.7 Light irradiance curves (P–I curves)

Photosynthetic activity as a function of light availability was measured as described by Prelle et al. (2919) in a self-constructed P–I (photosynthesis–irradiance) box. Three (n = 3) airtight oxygen electrode chambers (DW1, Hansatech Instruments, King's Lynn, UK), tempered at 8°C, were filled with 3 mL of thin algal-log-phase suspension, with the addition of 30 µL of sodium bicarbonate ($NaHCO_3$, final concentration 2 mM) to avoid carbon deficit during the measurements. Oxygen concentration measurements along 10 increasing photon flux density levels, ranging from 3.6 to ~1670 µmol photons m^{-2} s^{-1} of photosynthetically active radiation (PAR), were undertaken using oxygen dipping probe DP sensors (PreSens Precision Sensing GmbH, Regensburg, Germany) linked to fiber-optic oxygen transmitters via optical fibers (Oxy 4 mini meter, PreSens Precision Sensing GmbH, Regensburg, Germany). Measurements started with a 30-min respirational phase, followed by a series of 10-min photosynthetic phases for each increasing light level.

Chlorophyll a concentration per chamber was measured after each final measurement by the extraction of 3 mL of the algal suspension using 96 % ethanol (v/v). Chlorophyll a was measured spectrophotometrically at 665 nm and 750 nm (Shimadzu UV-2401 PC, Kyoto, Japan; HELCOM 2015, and calculated according to Equation (2):

$$\mu g\ Chl\ a = \frac{(E665 - E750) * v * 10^6}{83 * V * d} \quad (2)$$

Equation (2): Chlorophyll a calculation, where v is the extraction volume (mL), d is the cell length (cm), and V is the volume of filtered suspension (mL).

Due to photoinhibition in some of the diatom strains, the mathematical photosynthesis model of Walsby (1997) was used for fitting and calculation of the maximum rates of net primary production (NPPmax), respiration (R), light utilization coefficient (α), photoinhibition coefficient (β), light saturation point (I_k), and light compensation point (I_c).

5.3.8 Temperature-dependent photosynthesis and respiration

Photosynthetic and respirational rates of the six Antarctic diatom strains in response to temperatures between 5°C and 40°C were measured using the same P–I box as for the P–I curves, following the approach of Karsten et al. (2010). In contrast to the P–I curves, light was switched off during the respirational phase and set to photosynthesis-saturated 342.2 ± 40 µmol photons m^{-2} s^{-1} PAR during the photosynthetic phase. Starting at 5°C, a 20-min dark incubation phase was followed by a 10-min respirational phase and a 10-min photosynthetic phase. Afterwards, the temperature was increased by 5°C, and the process was repeated until reaching 40°C. Oxygen concentration measurements were also normalized to the total Chlorophyll a concentration (HELCOM 2015).

5.3.9 Growth rates

Growth rates of the marine diatom strain *C. gerlachei* and the limnic diatom strain *P. papilio* in response to salinity and temperature were determined as described by Karsten et al. (1996), Gustavs et al. (2009), and Prelle et al. (2021). Measurement of the in vivo fluorescence of chlorophyll a was used as a proxy for biomass. Using an MFMS fluorimeter (Hansatech Instruments, King's Lynn, UK), Chlorophyll a was excited by blue light emission and detected as relative units by an amplified photodiode that was separated from scattered excitation light. This method is particularly suitable for benthic diatoms, as chlorophyll a fluorescence units correlate well with chlorophyll a and cell carbon concentrations, as well as cell numbers, in diatoms (Karsten et al. 1996; Karsten et al. 2010). Both diatom cultures were cultivated in disposable Petri dishes (n = 3) with cover lids, in a volume of 15 mL of the respective treatment medium, and measured every 24 h for 8 days. To avoid the measurement of potential initial shock reactions of the isolates, 1 mL of log-phase algae suspension was incubated in 14.5 mL of the respective trial medium for four days under experimental conditions.

Growth as a function of salinity was tested by exposure to salinities of 1, 5, 25, 35, 45, 65, 85, and 100 S_A for the marine species *C. gerlachei*, and 1, 5, 10, 20, and 30 S_A for the limnic species *P. papilio*. Salinities were adjusted using artificial sea salt (hw-Marinemix® professional)

dissolved in deionized water. All cultures were enriched with f/2 and metasilicate, and kept at 8–9°C under standard cultivation conditions.

Furthermore, growth in response to five temperatures (5, 8, 15, 20, and 30 °C) at salinities of 1 S_A (*C. gerlachei*) and 35 SA (*P. papilio*), with added f/2 and metasilicate, was investigated. Treatments at 5°C were kept in a wine storage refrigerator with added LEDs; treatments at 8, 15, and 20°C were kept in climate chambers; and treatments at 30°C were carried out in a tempered water bath, with all reflecting light settings similar to cultivation conditions. After measurements, the growth rates of the logarithmic phase were calculated using the following equation: $N = N_0 \times e^{(\mu \times dt)}$, where N is the fluorescence on the measuring day, dt is the difference in time (days) between the measuring day and the starting day, and μ is the growth rate, Gustavs et al. 2009).

5.3.10 Statistical analysis

Our statistical analysis was similar to that of Prelle et al. 2021), as Microsoft Office Excel (2016) was used for the calculation—partially by application of the solver function, by minimizing the sum of normalized squared deviations for the fitting of the model of Walsby (1997) - and creation of figures. R (Version: 4.0.2) was used for the calculation of significance levels using one-way ANOVA followed by a post hoc Tukey's honestly significant differences test (critical p-value < 0.05), as well as for the fitting of the model of Yan and Hunt (1999) for the temperature-dependent photosynthesis. Confidence intervals were calculated using the library nlstools in R.

5.4 Results

5.4.1 Species identification

Five of the Antarctic isolates were identified to the species level, and one to the genus level. Table 2 lists the taxa, with information on the morphology and respective accession numbers of the marker genes *rbc*L and 18 SV4/18 S, while Figures 2–4 depict the LM and SEM images.

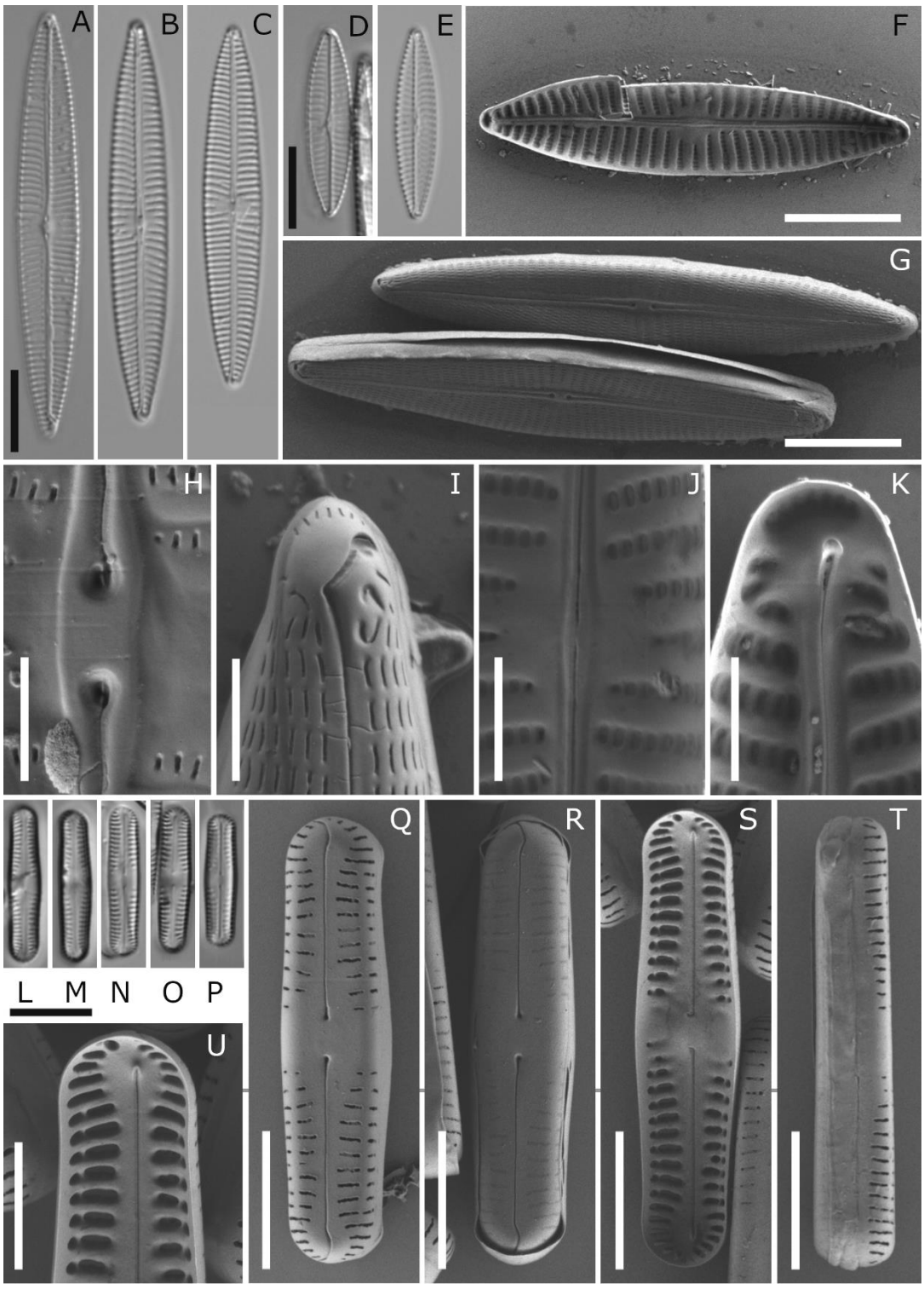

Figure 2 LM and SEM Image Set 1 **A–U: A–K** *Navicula criophiliforma* **A–E** LM pictures; development of auxospores led to size differences in the valves in the culture **F–K** SEM pictures **F** whole-valve internal view **G** whole-valve external view **H** external central raphe endings **I** valve apex external view **J** internal proximal raphe endings **K** valve apex internal view **L–T** *Chamaepinnularia gerlachei*, APC12 D294_006, and *Chamaepinnularia gerlachei*: **L,M** LM pictures of the strain *Chamaepinnularia gerlachei* **N–P** LM pictures of the strain APC12 D294_006 **Q–U** SEM pictures of APC12 D294_006 **Q,R** whole-valve external view, hymenate occlusion of areolae partly corroded **S** whole-valve internal view **T** valve in girdle view **U** valve apex internal view. Scale bars: A–G and L–P 10 µm, H–K and U 2 µm, and Q–T 5 µm.

APC14 D296_001 was identified as *Chamaepinnularia gerlachei* Van de Vijver & Sterken (Figure 2L–T; valves of strain D294_006 are depicted as well, since this strain was used as a supplement for identification). This species was first published in the work of Van de Vijver et al. (2010), from dry soil samples collected at James Ross Island, near the northeastern extremity of the Antarctic Peninsula, and has been observed only in maritime Antarctica thus far (Sterken et al. 2015; Zidarova et al. 2016; Kopalová et al. 2019).

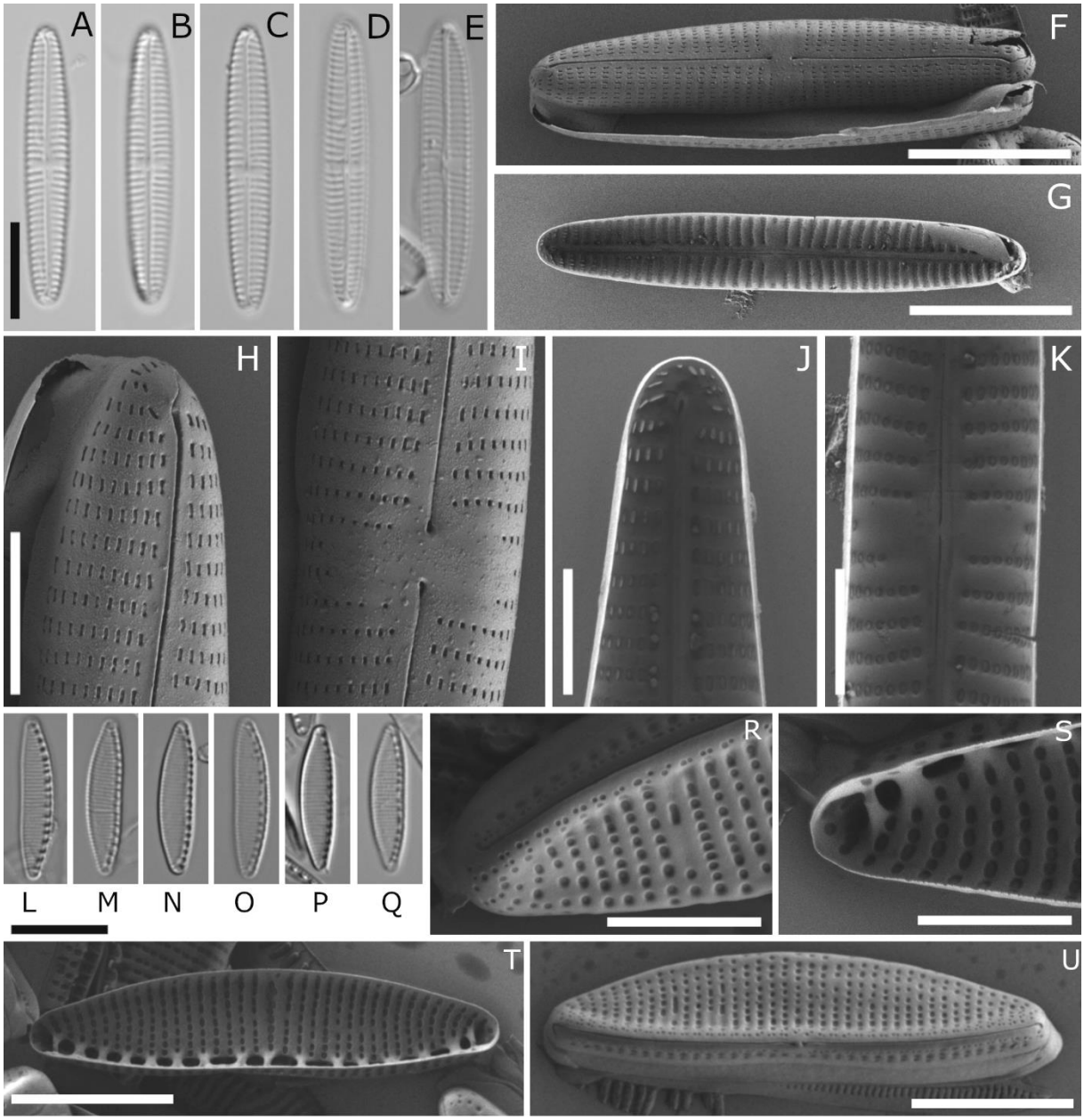

Figure 3 LM and SEM Image Set 2 **A–U: A–K** *Navicula concordia* **A–E** LM pictures **F–K** SEM pictures **F** whole-valve external view **G** whole-valve internal view **H** valve apex external view **I** external proximal raphe endings **J** valve apex internal view **K** internal proximal raphe endings **L–U** *Nitzschia annewillemsiana* **L–Q** LM pictures **R–U** SEM pictures **R** valve apex external view **S** valve apex internal view **T** whole-valve internal view **U** whole-valve ex-ternal view. Scale bars: A–G and L–Q 10 µm, H–K and R,S 3 µm, and T,U 5 µm.

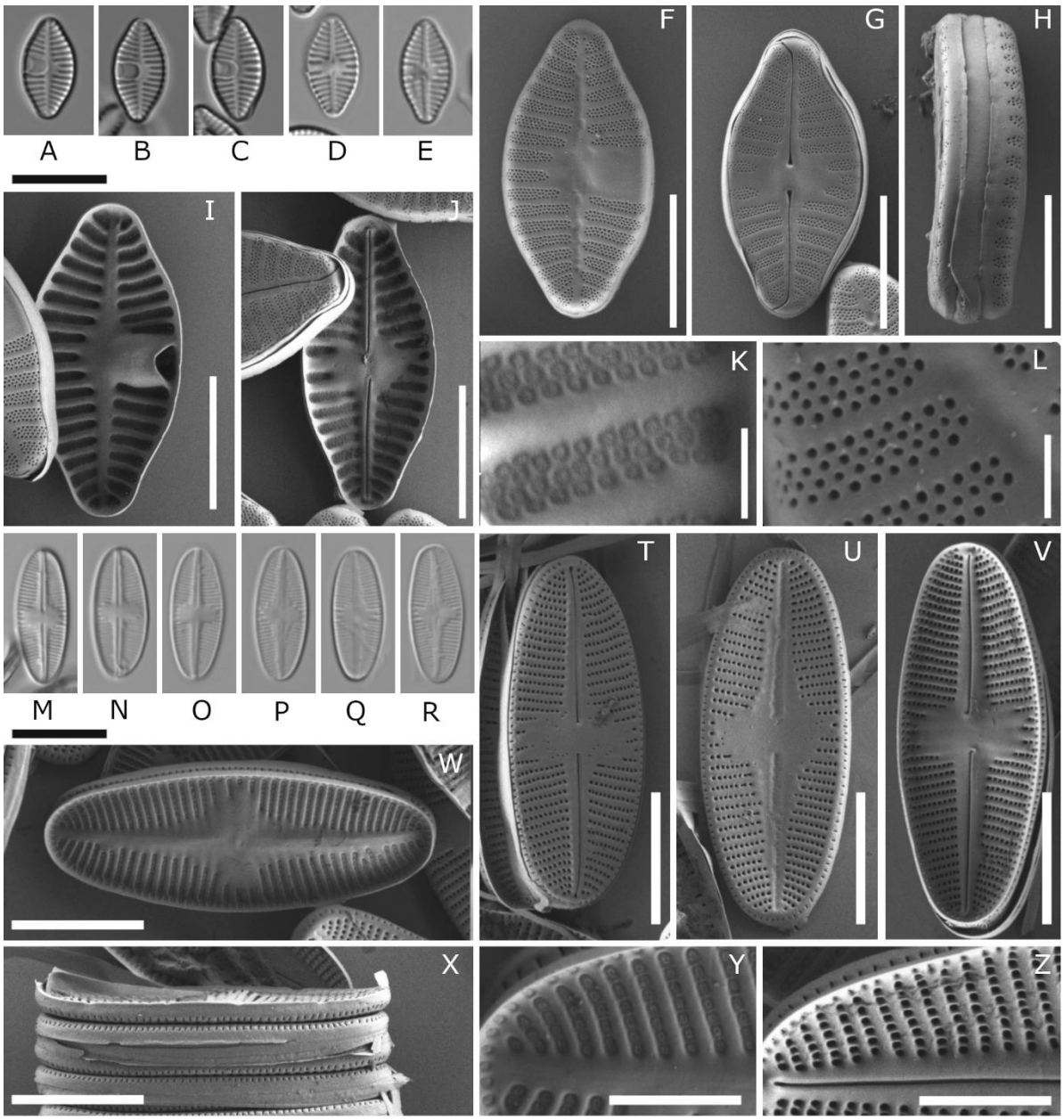

Figure 4 LM and SEM Image Set 3. **A–Z: A–L** *Planothidium* sp. **A–E** LM pictures **F–L** SEM pictures **F** whole-sternum-valve external view **G** whole-raphe-valve external view **H** valve in girdle view **I** whole-sternum-valve internal view **J** whole-raphe-valve internal view **K** internal valve view of one stria with rows of areolae with hymenate occlusions **L** internal valve view of one stria with rows of areolae **M–Z** *Psammothidium papilio* **M–R** LM pictures **T–Z** SEM pictures **T** whole-raphe-valve external view **U** whole-sternum-valve external view **V** whole-raphe-valve-internal view **W** whole-sternum-valve internal view **X** valves in girdle view **Y** internal sternum valve view of areolae with hymenate occlusions **Z** internal raphe valve view of areolae. Scale bars: A–E, F–J and T–X 5 µm, K,L 1 µm, and Y,Z 2 µm.

Navicula concordia (Figure 3A–K) was identified as *N. concordia* C. Riaux-Gobin & A. Witkowski, and APC06 D288_003 as *Navicula criophiliforma* A. Witkowski, C. Riaux-Gobin, & G. Daniszewska-Kowalczyk (Figure 2A–K). Both were first published in the work of Witkowski et al. (2019), from the Kerguelen Islands coastal area, in the Southern Ocean.

Recently, *N. criophiliforma* was reported from Livingston Island, north of the Antarctic Peninsula (Zidarova et al. 2022). This species formed auxospores during cultivation, leading to high variance in the dimensions of the valves.

APC18 D300_012 (Figure 3L–U) was identified as *Nitzschia annewillemsiana* Hamsher, Kopalová, Kociolek, Zidarova, & Van de Vijver. It was first published in the work of Hamsher et al. (2916), from freshwater and wet soil samples from James Ross Island and the South Shetland Islands, and has been only reported from this area to date Zidarova et al. 2016).

APC18 D300_023 was identified as Psammothidium papilio (D.E. Kellogg, Stuiver, T.B. Kellogg, & G.H. Denton) K. Kopalová and B. Van de Vijver (Figure 4M–Z). It was first described as Navicula papilio by Kellogg et al. (1980), but this species has been reported several times from maritime Antarctica under different synonyms Sabbe et al. 2003; Kopalová et al. 2012; Zidarova et al. 2016; Silva et al. 2019).

Table 2 List of strains established from Antarctic marine and freshwater samples collected at Carlini Station, King George Island, Potter Cove, in austral summer 2020 (January/February), with scientific name, information on dimensions of the valves, striae density, sequenced marker genes, and accession numbers. RV: raphe valve, SV: sternum valve.

Strain	Scientific Name	Marine/ Freshwater	Length [µm]	Width [µm]	Striae in 10 µm	Marker Genes
APC14 D296_001	*Chamaepinnularia gerlachei*	Marine	17.1–20.6	4.1–5.4	18–20	whole 18 S, *rbc*L
APC06 D288_003	*Navicula criophiliforma*	Marine	24.2–52.4	5.8–8.5	11–12	18 SV4, *rbc*L
APC28 D310_004	*Navicula concordia*	Marine	29.5–30.5	4.7–5.3	13–14	18 SV4, *rbc*L
APC18 D300_012	*Nitzschia annewillemsiana*	Freshwater	15.2–17.1	3.6–4.1	25–26	18 SV4, *rbc*L
APC18 D300_015	*Planothidium* sp.	Freshwater	10.9–11.3	5.6–6.1	16–18 (RV) 17–18 (SV)	18 SV4, *rbc*L
APC18 D300_023	*Psammothidium papilio*	Freshwater	13.8–14.7	5.4–5.9	28–30 (RV) 26–30 (SV)	18 SV4, *rbc*L

APC18 D300_015 was identified to the genus level as *Planothidium* sp. (Figure 4A–L). There was a high morphological resemblance to *P. frequentissimum* (Lange-Bertalot) Lange-Bertalot. However, molecular data showed differences in both marker genes compared to *P. frequentissimum* strains from GenBank. There were 4 base-pair differences in 18 SV4 and 20 in the *rbc*L gene compared to the *P. frequentissimum* strain PF1 (Accession numbers: KJ658409 and KJ658392). In comparison to the strain D06_139 (Accession numbers: KY650786 and KX650815), 11 bp differences were found in 18 SV4, and 19 in *rbc*L.

5.4.2 Photosynthetic potential

The photosynthetic potential of all six diatom strains exhibited wide tolerance ranges between the tested salinities from 1 S_A to 100 S_A after three days of incubation (Figure 5, Table S1).

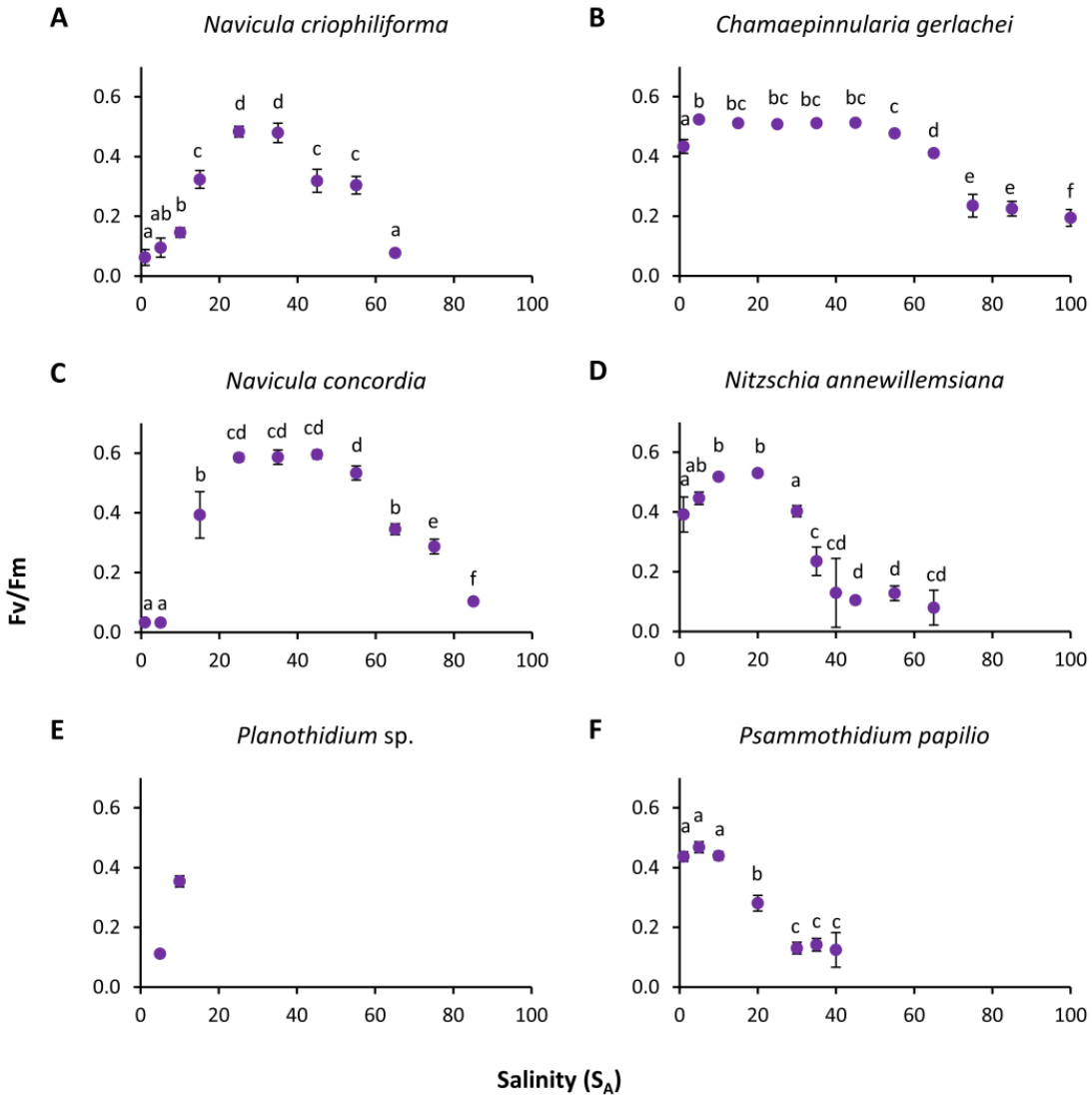

Figure 5 Effective quantum yield of photosystem II (F_v/F_m) as a function of salinity of six benthic diatom strains from Antarctica after 3 days of incubation **A–F**. Data represent mean values ± SD (n = 6). Different lowercase letters indicate significant means (p < 0.05; one-way ANOVA with post hoc Tukey's test) **A** *Navicula criophiliforma* **B** *Chamaepinnularia gerlachei* **C** *Navicula concordia* **D** *Nitzschia annewillemsiana* **E** *Planothidium* sp. and **F** *Psammothidium papilio*.

The overall highest and lowest optimal quantum yields were measured for *N. concordia*, with 0.595 at 45 S_A and 0.033 at 5 S_A, respectively. The three marine species *N. criophiliforma*, *C. gerlachei*, and *N. concordia* exhibited typical tolerance curve patterns, with significant optima at 25–35 S_A, 25–45 S_A and 5–45 S_A, respectively (p < 0.05, Figure 5). The tolerance range of *N. criophiliforma* was narrower compared to both other marine species after calculation of the

range of the highest effective quantum yield at the 80th percentile and above, between the 20th and 80th percentiles, and below the 20th percentile (Figure 6A). This taxon exhibited high effective quantum yields (upper 80th percentile) at only two experimental salinities, while the other isolates covered 4–6 salinities (Figure 6A). Nevertheless, all marine species exhibited a moderate effective quantum yield (between the 20th and 80th percentiles), ranging from 10 to 55/75 SA and up to 100 S_A.

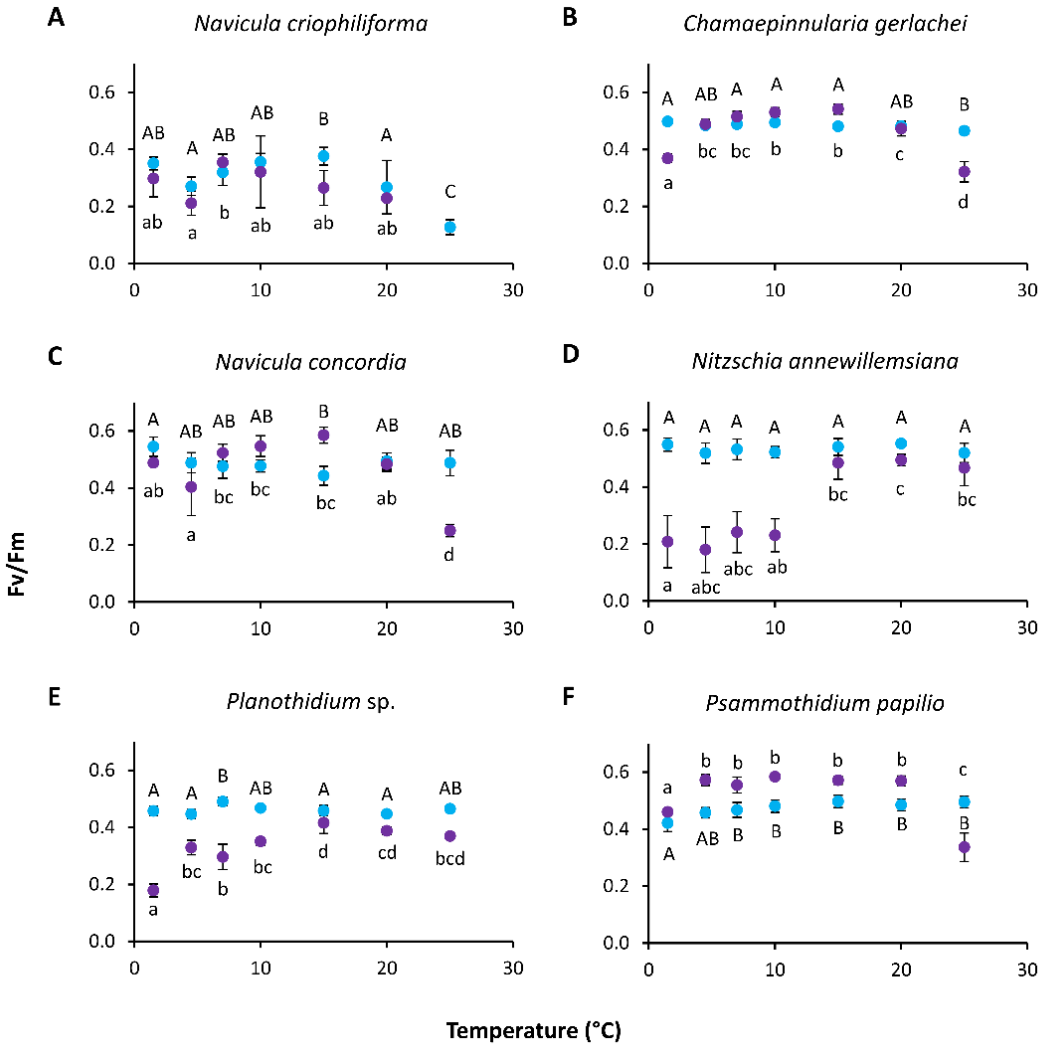

Figure 6 Effective quantum yield of photosystem II (F_v/F_m) as a function of temperature of six benthic diatom strains from Antarctica after 0 days (blue) and 5 days (purple) of incubation **A–F** Data represent mean values ± SD (n = 6). Different capital (t_0) and lowercase (t_5) letters indicate significant means ($p < 0.05$; one-way ANOVA with post hoc Tukey's test) **A** *Navicula criophiliforma* **B** *Chamaepinnularia gerlachei* **C** *Navicula concordia* **D** *Nitzschia annewillemsiana* **E** *Planothidium* sp. and **F** *Psammothidium papilio*.

In contrast, the two limnic species *Planothidium* sp. and *P. papilio* showed the highest significant optima at 10–20 S_A and 1–10 S_A, respectively ($p < 0.05$, Figure 5). Salinities higher than 10/20 S_A resulted in a decreasing effective quantum yield up to 40/55 S_A. Due to low

biomass, *Planothidium* sp. was only tested in two salinities, of which the highest effective quantum yield was measured at 10 S_A.

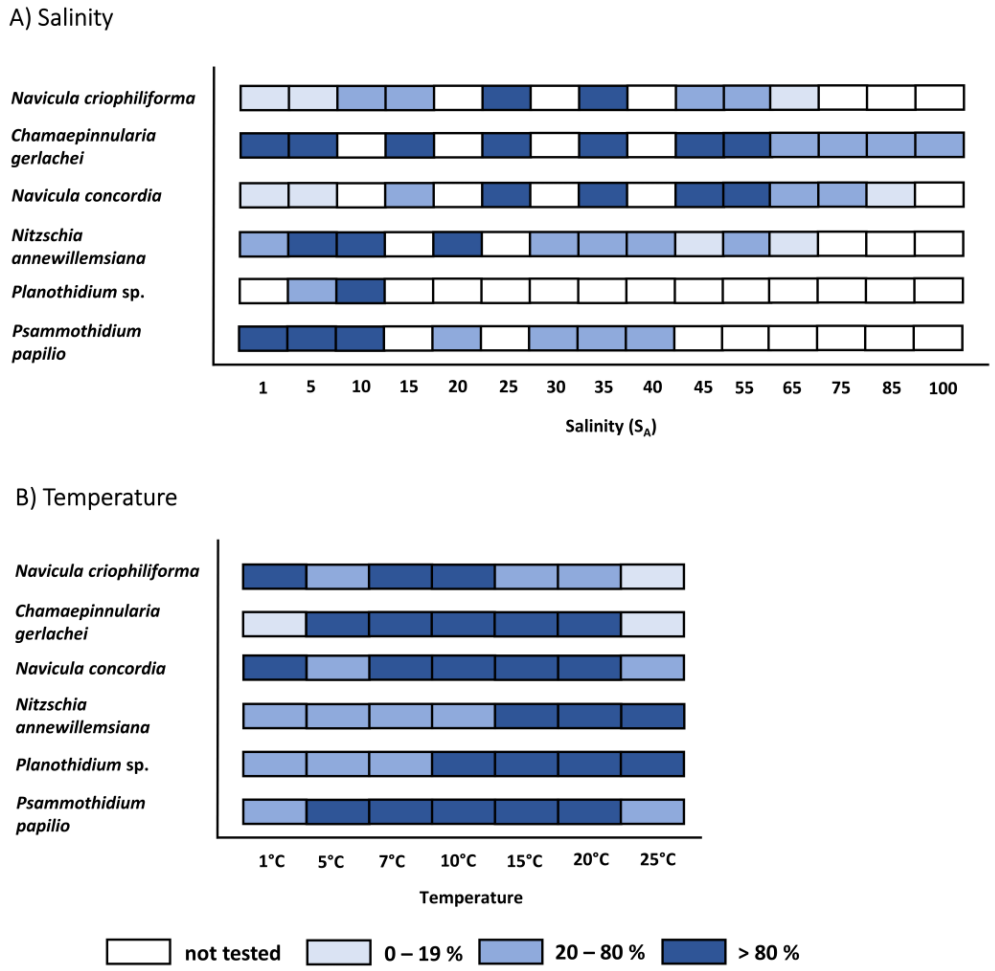

Figure 7 Effects of **A** salinity and **B** temperature on the effective quantum yield of photosystem II (F_v/F_m) of six benthic diatom strains from Antarctica. Dark blue symbols represent the range of the highest effective quantum yield at the 80th percentile and above, medium blue symbols are between the 20th and 80th percentiles, light blue symbols represent the 20th percentile and below, and white symbols were not tested. Data represent mean values (n = 6).

The photosynthetic potential of the six diatom strains after five days of incubation also exhibited broad tolerances for the investigated temperature range of 1.5 to 25°C (Figure 7, Table S1). The highest overall effective quantum yield was found for *N. concordia*, with 0.585 at 15°C, while the lowest was for *Planothidium* sp., with 0.123 at 25°C. Between 1.5 and 25°C, only small significant deviations of the effective quantum yield were found for all three marine taxa, as well as for *P. papilio*, while for *N. annewillemsiana* and *Planothidium* sp. The highest effective quantum yield was at 15 to 25°C ($p < 0.05$, Figure 7). With the exception of *N. criophiliforma* at 25°C and *C. gerlachei* at 1°C and 25°C, all species exhibited moderate photosynthetic

potential between 1.5°C and 25°C. In comparison to t_5, significance levels of t_0 between each temperature treatment of the marine species were not as distinct as for the limnic species (Figure 7).

5.4.3 Light-dependent photosynthesis

The photosynthetic and respirational rates of all six diatom strains exhibited species-specific responses towards increasing photon fluence rates, resulting in different P–parameters (Figure 8, Table 3).

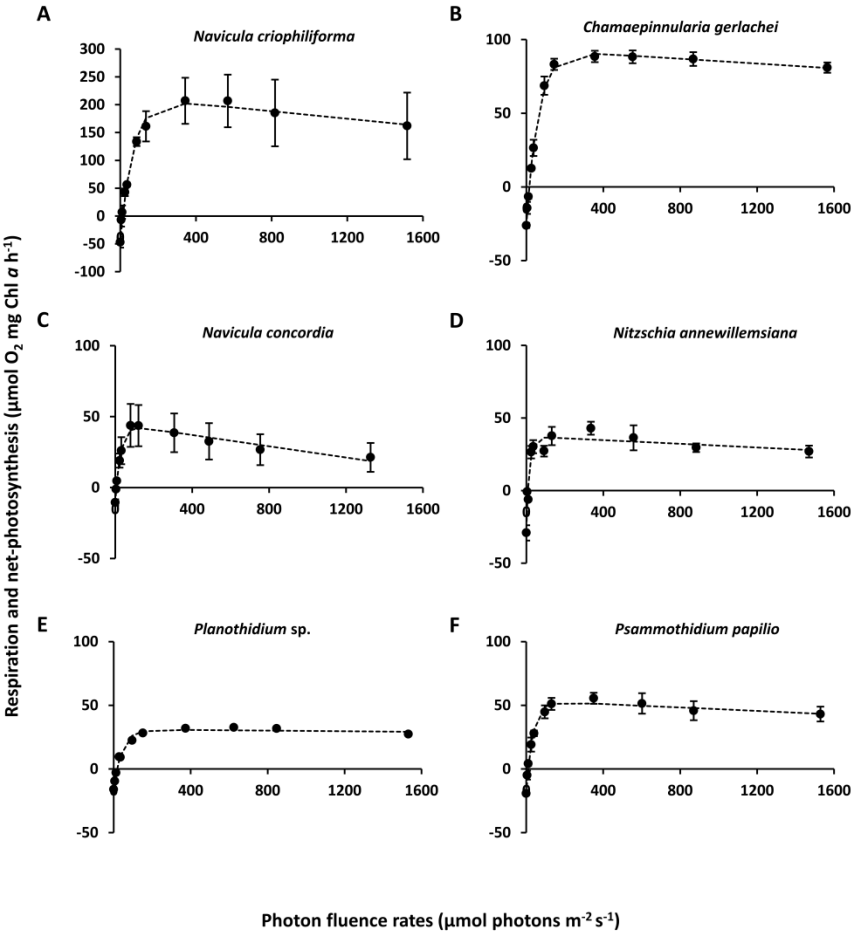

Figure 8 Photosynthesis and respiration rates (µmol O_2 mg^{-1} Chl a h^{-1}) as a function of increasing photon flux density (µmol photons m^{-2} s^{-1}) of six benthic diatom strains from Antarctica kept at 8 °C in f/2 medium: 33 S_A **A–C** and 1 S_A **D–F** Data represent mean values ± SD (n = 3). Data points were fitted using the model of Walsby (1997) **A** *Navicula criophiliforma* **B** *Chamaepinnularia gerlachei* **C** *Navicula concordia* **D** *Nitzschia annewillemsiana* **E** *Planothidium* sp. and **F** *Psammothidium papilio*.

The overall highest NPP_{max} was for the marine species *N. criophiliforma*, with 202.3 ± 45.4 µmol O_2 mg^{-1} Chl a h^{-1}, which was at least twice as high as that of the remaining isolates. Respiration rates varied among the isolates, between −47 8.9 µmol O_2 mg^{-1} Chl a h^{-1} (*N. criophiliforma*) and −10.5 ± 3.1 µmol O_2 mg−1 Chl a h^{-1} (*N. concordia*) (Figure 8, Table 3).

All isolates had low light compensation points (I_c), varying significantly between 5.8 ± 1 µmol photons m^{-2} s^{-1} (*N. concordia*) and 17.5 ± 3 µmol photons m^{-2} s^{-1} (*Planothidium* sp.) ($p < 0.05$, Table 3). The light saturation points (I_k) for all six isolates ranged between 64 ± 11.5 µmol photons m^{-2} s^{-1} (*N. criophiliforma*) and 16.3 ± 3.9 µmol photons m^{-2} s^{-1} (*N. annewillemsiana*). Photoinhibition was detected in almost all isolates except for *Planothidium* sp. and *P. papilio*. The highest photoinhibition was found in *N. criophiliforma*, with −0.03 ± 0.02, which was, however, not significant between *C. gerlachei*, *N. concordia*, and *N. annewillemsiana* ($p < 0.05$, Table 3).

Table 3 Parameters of respective P–I curves (Figure 8) of six benthic diatom species ($n = 3$) kept at 8 °C. Different lowercase letters represent significance levels among all means as calculated by one-way ANOVA (Tukey's test, $p < 0.05$). NPP_{max} represents the maximal oxygen production rate, α is the initial slope of production in the light-limited range, β is the terminal slope of production in extensive light range (photoinhibition), I_k is the light saturation point, and I_c is the light compensation point.

Species	NPP_{max} [µmol O_2 mg^{-1} Chl *a* h^{-1}]	Respiration [µmol O_2 mg^{-1} Chl *a* h^{-1}]	α [µmol O_2 mg^{-1}Chl *a* h^{-1}][µmol Photons m^{-2} $s^{-1}]^{-1}$	β [µmol O_2 mg^{-1} Chl *a* h^{-1}] [µmol Photons m^{-2} $s^{-1}]^{-1}$	I_k [µmol Photons m^{-2} s^{-1}]	I_c [µmol Photons m^{-2} s^{-1}]	NPP_{max}: Respiration
N. criophiliforma	202.3 ± 45.4 a	−47 ± 8.9 a	3.9 ± 0.4 a	−0.03 ± 0.02 a	64 ± 11.5 a	13.4 ± 1.4 ab	4.3 ± 0.9 a
C. gerlachei	90.3 ± 4.1 b	−26.2 ± 0.8 b	2 ± 0.1 b	−0.01 ± 0.00 bc	59.8 ± 1.7 a	15.3 ± 0.2 a	3.5 ± 0.1 ab
N. concordia	42 ± 14.5 bc	−10.5 ± 3.1 c	2 ± 0.6 b	−0.02 ± 0.01 ac	25.9 ± 2.7 bc	5.8 ± 1 c	4 ± 0.4 a
N. annewillemsiana	36.6 ± 5.4 bc	−25.9 ± 3.7 b	3.8 ± 0.69 a	−0.01 ± 0.00 bc	16.3 ± 3.9 b	8.7 ± 0.3 cd	1.4 ± 0 c
Planothidium sp.	30.7 ± 0.5 c	−16.0 ± 6.2 bc	1.1 ± 0.3 b	0.0 ± 0.0 b	23.6 ± 8.7 bc	17.5 ± 3 a	1.9 ± 0.4 c
P. papilio	52.2 ± 5 bc	−19.2 ± 1.7 bc	2.1 ± 0.2 b	−0.00 ± 0.00 bc	33.7 ± 1.8 c	10.6 ± 0.2 bd	2.7 ± 0.1 b

5.4.4 Temperature-dependent photosynthesis and respiration

Photosynthetic and respirational responses under increasing temperatures from 5 to 40°C resulted in individual response patterns (Figure 9). Photosynthesis and respiration rates typically rose with increasing temperature and decreased after reaching the optimal temperature. The overall highest photosynthesis and respiration rates were measured for *N. criophiliforma* at 15°C and 30°C, respectively (Figure 9). In general, positive net photosynthetic rates ranged between 5°C and 25/30°C, with varying optima for each strain (from 5°C to 20°C).

At temperatures > 25/30°C, photosynthesis was inhibited, and only respirational oxygen consumption could be measured (Figure 9). Respirational rates could be detected over the entire temperature range from 5 to 40°C, with optima between 20 and 35°C (Figure 9). Fitting of the measured data using the model of Yan and Hunt (1999) revealed maximum photosynthetic rates of the marine isolates between 11.1 and 15.7°C, and a positive net photosynthesis up to 32.5 and 35.6°C, respectively (Table 4). The optimal temperature for the limnic species was slightly lower - between 3.0 and 12.5°C, with positive net photosynthesis up to 26.0 and 33.5 °C. Fitting of the respirational data resulted in much higher optimal temperatures, ranging between 26.6°C (*N. annewillemsiana*) and 30.6°C (*C. gerlachei*), with maximal values up to 44.4°C (*N. concordia*).

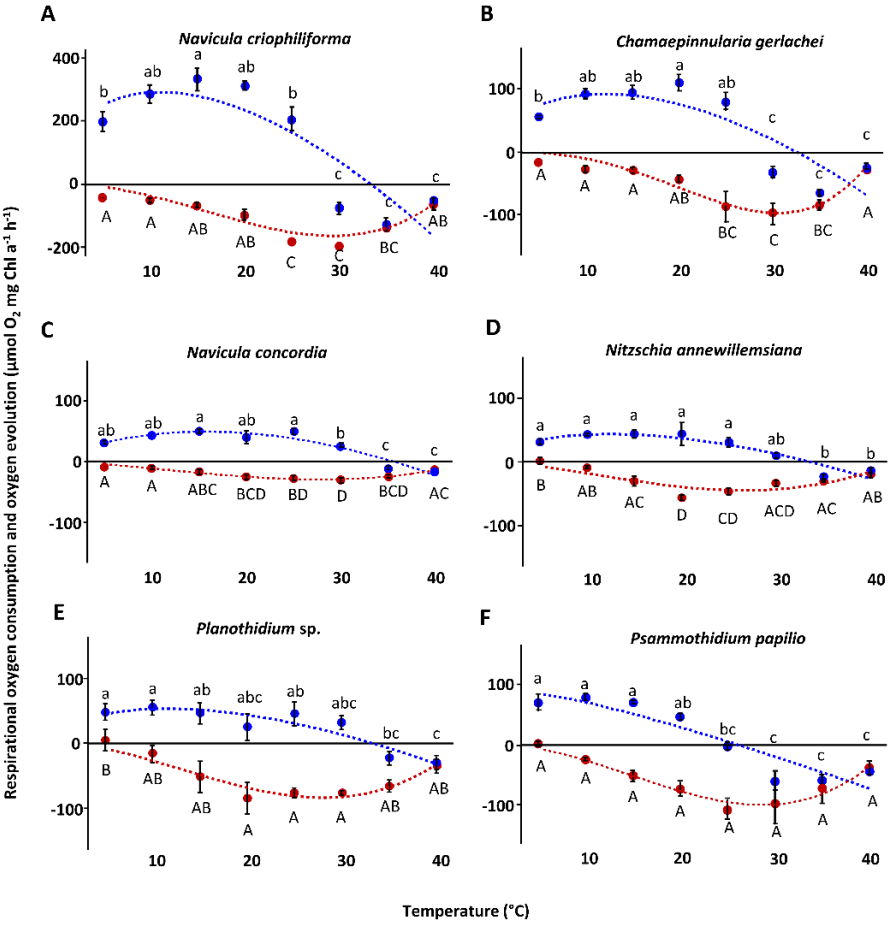

Figure 9 Photosynthetic (blue) oxygen production at 342 ± 40 µmol photons m^{-2} s^{-1} and respiratory (red) oxygen consumption in darkness of six benthic diatom strains from Antarctica, as a function of increasing temperature **A–F** The measured data were fitted using the model of Yan and Hunt (1999) (photosynthesis: blue dashed line; respiration: red dashed line). All cultures were kept in f/2 Baltic Sea media: 33 S_A **A–C** and 1 S_A **D–F** Data represent mean values ± SD (n = 3). Different lowercase (photosynthesis) and capital letters (respiration) indicate significant means ($p < 0.05$; one-way ANOVA with post hoc Tukey's test)

Table 4 Results of model calculation for temperature-dependent growth rate, photosynthetic rate, respirational rate, and salinity-dependent growth rate, following the model of Yan and Hunt (1999).

			Navicula criophiliforma	***Chamaepinnularia gerlachei***	***Navicula concordia***	***Nitzschia annewillemsiana***	***Planothidium* sp.**	***Psammothidium papilio***
Growth (salinity)	Maximal growth rate		-	0.58	-	-	-	0.42
	Optimal salinity		-	6.53	-	-	-	5.28
	Maximal salinity		-	93.69	-	-	-	29.26
	Residual sum of squares		-	0.0884	-	-	-	0.03172
	Salinity range for	Optimal growth (80 % growth rate)	-	0.13–31.79	-	-	-	0.90–13.71
		Growth (20 % growth rate)	-	0.00–79.23	-	-	-	0.00–25
Growth (temperature)	Maximal growth rate		-	0.44	-	-	-	0.30
	Optimal temperature		-	12.96	-	-	-	6.48
	Maximal temperature		-	28.85	-	-	-	6.53
	Residual sum of squares		-	0.9345	-	-	-	5.28
	Temperature range for	Optimal growth (80 % growth rate)	-	6.48–19.89	-	-	-	1.56–14.47
		Growth (20 % growth rate)	-	0.90–27.11	-	-	-	0.00–25.10
Photosynthesis	Maximal photosynthetic rate		292.59	91.37	48.93	43.46	53.49	85.82
	Optimal temperature		11.12	12.08	15.66	12.48	11.52	2.99
	Maximal temperature		33.35	32.47	35.63	33.49	30.30	26.03
	Residual sum of squares		199,464	31,639	2012	4575	13,940	10,575
	Temperature range for	Optimal photosynthesis (80 % photosynthetic rate)	4.11–20.14	5.01–20.56	7.67–24.32	5.19–21.23	4.44–20.43	0.2–10.05
		Photosynthesis (20 % photosynthetic rate)	0.2–30.68	0.37–30.1	0.99–33.34	0.38–31.04	0.25–30.71	0–22.48
Respiration	Maximal respirational rate		−185.99	−97.77	−28.98	−45.46	−84.06	−100.19
	Optimal temperature		29.67	30.59	27.65	26.61	28.04	28.66
	Maximal temperature		41.9	41.17	44.44	42.88	42.97	42.49
	Residual sum of squares		24,352	8086	343.9	2815	13,143	8103
	Temperature range for	Optimal respiration (80 % respirational rate)	22.26–35.62	23.91–35.79	18.57–35.57	17.83–34.28	19.62–35.16	20.64–35.31
		Respiration (20 % respirational rate)	10.34–40.77	12.4–40.21	6.33–42.8	6.03–41.3	7.51–41.54	8.55–41.18

5.4.5 Growth rates

One marine and one limnic culture were exemplarily investigated for growth as a function of salinity and temperature (Figure 10). *C. gerlachei* exhibited a strong optimum at 15°C, with growth rates of 0.84 µ d^{-1}, while the optimal growth temperature for *P. papilio* ranged between 5 and 15°C, with similar growth rates around 0.4 µ d^{-1} (Figure 10). Both diatom strains were unable to grow at temperatures > 20°C. Using the model of Yan and Hunt (1999), the optimal growth temperature of >80 % of the maximal growth ranged from 6.5 to 19.9°C for *C. gerlachei*, and from 1.6 to 14.5°C for *P. papilio* (Table 4). The overall maximal growth rate for *C. gerlachei* was at 13.0°C (0.44 µ d^{-1}), and for *P. papilio* it was at 6.5°C (0.30 µ d^{-1}). Growth rates as a function of salinity for the marine species *C. gerlachei* were determined over a range from 1 to 65 S_A. This species exhibited a broad salinity tolerance, as reflected in growth rates be-tween 0 and 79.2 S_A (0.2 to 0.4 µ d^{-1}), with a distinct optimum at 6.5 S_A (0.58 µ d^{-1}) (Table 4). In contrast, the limnic species *P. papilio* grew only over a range of 1 to 20 S_A, with optima between 1 and 10 SA. The model calculation for salinity exhibited highest growth rate of 0.42 µ d^{-1} at 5.28 S_A (Table 4). The optimal growth range >80 % growth rate for this isolate ranged between 0.9 and 13.7 S_A.

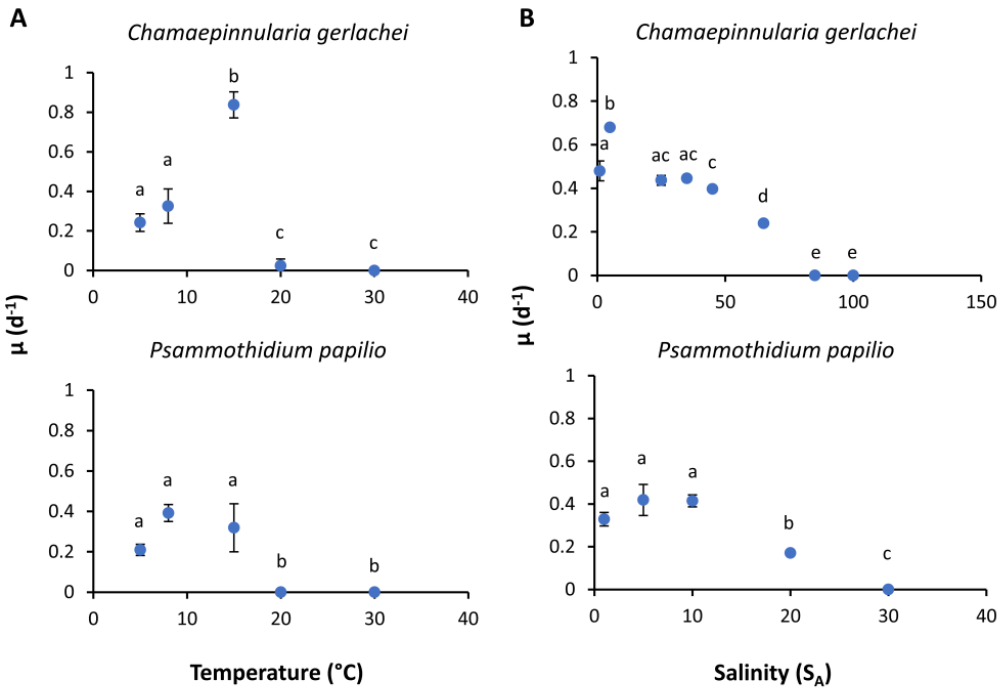

Figure 10 Growth rates (µ d^{-1}) in relation to **A** temperature and **B** salinity of the respective di-atom strains *Chamaepinnularia gerlachei* and *Psammothidium papilio*. Data represent mean values ± SD (*n* = 3). Different

lowercase letters represent significance levels among all means, as calculated per temperature or salinity by one-way ANOVA (Tukey's test, $p < 0.05$). Please note the different salinity ranges for both species.

5.5 Discussion

All six marine and limnic benthic diatom species from the maritime Antarctic Peninsula exhibited broad tolerances towards light availability as well as euryhaline and eurythermal traits, far surpassing the environmental conditions of their respective habitats. In general, Antarctic organisms are expected to be rather stenohaline and stenotherm due to the long cold-water history of the Southern Ocean. However, maritime Antarctica is characterized by stronger seasonal and diurnal fluctuations in the abiotic parameters compared to continental Antarctica; hence, broader ecophysiological tolerances of the inhabiting biota might be assumed. Nevertheless, an important aspect that should be considered is related to the fact that all six benthic diatom species were grown as clonal cultures for >1 year under controlled lab conditions before the experiments were undertaken. It might be possible that the measured ecophysiological response patterns do not always reflect the in-situ responses. Although logistically challenging in Antarctica, more field experiments are urgently needed to better understand the real world.

5.5.1 Light

Photosynthesis the driving force for the energy metabolism and, hence, essential for the viability and survival of benthic diatoms—is primarily dependent on light availability. All six diatom species exhibited taxon-specific response patterns over a wide range of photon fluence rates, with only slight photoinhibition. Overall, the marine isolates exhibited higher NPP_{max} compared to the limnic ones. The highest photo-synthetic rates were reached at low photon fluence rates, as reflected by low light compensation and light saturation points. All data clearly point to low light requirements for photosynthesis. In general, Antarctic diatoms are known for their fast growth in low-light conditions (Smetacek 1999), because their photosynthesis seems to be especially shade-adapted (Jones 1996). The few data available on benthic diatoms from polar regions confirm a high photophysiological plasticity to acclimate to the prevailing, often very low light conditions (Palmisano et al. 1985; Karsten et al. 2006; Woelfel et al. 2014; Sevilgen et al. 2014; Wulff et al. 2008; Wulff et al. 2009). In addition, this wide photophysiological plasticity seems to be a rather general trait of many diatom species [24], as documented in species from Arctic Kongsfjorden (Karsten et al. 2019), but also in numerous species from the shallow waters of the temperate Baltic Sea (Prelle et al. 2019; Prelle et al. 2021).

Particularly for benthic diatoms, low light adaptation is crucial, since Antarctic microphytobenthic communities experience a strong seasonally changing light climate, often with low average photon fluence rates. During winter periods, with ice cover and short daylight periods, little or no light reaches the benthic diatoms - especially if the ice is covered by snow (Drew and Hastings 1992). During summer, incident light penetration can be also reduced due to increased turbidity, which is driven by suspended particulate matter from glacial meltwater and riverine discharge (Hoffmann et al. 2019). In addition, wind- and organism-induced resuspension of the sediment can lead to a decline in the light availability through burial of the diatom cells. However, due to their motility, raphid diatoms are able to escape unfavorable low-light conditions in the sediment (Blommaert et al. 2018). Vertical migration of benthic diatoms has been identified as an important behavioral trait to control the short-term variability of photosynthesis—at least in temperate regions. Although published studies on the vertical migration of benthic diatoms in Antarctica and the Arctic under polar day and night conditions are lacking, a few reports also indicate motility in polar species (Karsten et al. 2019). After the sea ice breakup in spring, solar radiation penetrates the coastal water column, with strong attenuation of the short wavelengths due to the prevailing optical properties, which are influenced by particle load from glaciers and yellow substances originating from meltwater and terrestrial runoff (Hoffmann et al. 2019; Pavlov et al. 2019). At 10 m depth in the inner Potter Cove, PAR was measured between 10 and 200 µmol pho-tons m^{-2} s^{-1} in the winter and summer, respectively (Longhi et al. 2003). *Chamaepinnularia gerlachei* was sampled at 15 m depth in the inner Potter Cove, and showed a light compensation point of 15.3 µmol photons m^{-2} s^{-1} and a light saturation point of 59.8 µmol photons m^{-2} s^{-1}, which fit well to the prevailing in situ light conditions.

An interesting aspect was the overall twofold-higher NPP_{max} exclusively in *Navicula criophiliforma* (about 200 µmol O_2 mg^{-1} Chl a h^{-1}) compared to all other studied Antarctic benthic diatom species. At present, we can only speculate to explain these data, but the largest cell size of *N. criophiliforma* (<52 × 8.5 µm, Table 2, Figure 2) among all species leads to the highest cell volume and, hence, to more chloroplasts and pigments. Recent data on the green microalga *Dunaliella teriolecta* experimentally prove that the established package effect theory, which predicts that larger phytoplankton cells should show poorer photosynthetic performance because of reduced intracellular self-shading, is challenged (Malerba et al. 2018). The latter authors reported that larger cells of *D. teriolecta* showed substantially higher rates of oxygen production along with higher chlorophyll values compared to smaller cells.

All six species could not only cope well with low-light conditions, but also showed high photosynthetic rates up to 1600 µmol photons m^{-2} s^{-1}, with a minor-to-moderate degree of photoinhibition - especially in the marine strains. During the process of photoinhibition, diatoms are still able to perform photosynthesis without being completely inhibited. Excessive light is absorbed by the photosystems and harmlessly emit-ted via heat as a protective mechanism (non-photochemical quenching) for the photosynthetic apparatus (Serodio et al. 2008). Further exposure to excessive light, however, can lead to damage of the D1 protein, leading to a decrease in electron transfer (Han 2000). All benthic diatom species exhibited low light requirements for photosynthesis combined with a pronounced photophysiological plasticity that also allowed broad tolerance to high-incident-light conditions.

5.5.2 Temperature

Photosynthesis, respiration, and growth, along with their underlying enzymatic mechanisms, are strongly controlled by temperature. Therefore, reductions in photo-synthetic and respirational activity, as well as in growth under saturated light conditions, are a consequence of inhibition of the most temperature-sensitive enzymes. Low temperatures slow down electron transport, thereby decreasing the ability to use photons for photochemically produced energy. High temperatures can influence the photorespiration activity of RuBisCO (ribulose-1,5-bisphosphat-carboxylase/-oxygenase) by removing its specificity towards CO2 binding rather than that of O_2, thereby in-creasing energy demand (Young et al. 2014). Similar to other studies using the same methodological approach on Baltic Sea benthic diatoms (Prelle et al. 2019; Prelle et al. 2021), the photosynthetic and respirational rates of Antarctic diatom strains seemed to also be decoupled from one another, with respiration always showing optima at higher temperatures compared to photosynthesis. For temperate diatoms, but also for terrestrial green algae, temperature requirements for respiration and photosynthesis differ, as explained by the higher dependency of photosynthesis on light, while temperature-dependent enzymatic activities mainly control respiration (Atkin and Tjoelker 2003; Karsten et al. 2016). A more recent study partially confirmed that light-dependent photosynthetic reactions are indeed unaffected by temperature, while the carbon fixation reactions are driven by temperature (Gleich et al. 2020). Furthermore, respiratory and photosynthetic activities in diatoms are strongly coupled, which is mechanistically explained by tight physical interactions between mitochondria and chloroplasts (Bailleul et al. 2015). Consequently, light stimulates respiration, resulting in an optimal ATP/NADPH ratio for subsequent carbon dioxide fixation by RuBisCO.

Another important aspect is the observation that the optimal temperature for photosynthesis (Figure 9, c. 20°C) was higher compared to that for growth (Figure 10, <15°C). These differences in both physiological processes can be explained by the exposure time to the stressor temperature. The time scale of stress is relevant, as algae may cope temporarily with strong temperature stress if acting only for hours to days, and may subsequently recover from damage under optimal conditions (Eggert et al. 2003). However, on a longer time scale (weeks), the algae experience progressively more impaired cellular processes until the upper temperature for survival is reached. Consequently, temperature optima for photosynthesis are often higher than those for growth, because both physiological processes are not directly coupled and, hence, photosynthesis does not necessarily match the temperature–growth pattern. In addition, growth is a more general physiological process that integrates all positive and negative influences of temperature on the whole metabolism (Graiff et al. 2015). The data shown clearly indicate broad temperature tolerance of photosynthesis and respiration in the Antarctic benthic diatom isolates, far exceeding in situ temperatures in their respective habitats. While the temperature tolerance of Antarctic phytoplankton - which usually do not survive temperatures > 8–9°C, and which is consistent with the maximum in situ temperature—is recognized as stenotherm (Fiala and Oriol 1989; Gilstad and Sakhaug 1990), benthic diatoms in shallow waters or in tidal pools during the polar day can be exposed to temperatures that are several times higher compared to the water column. For Potter Cove, where the investigated strains were sampled, the tides are semi-diurnal, and the temperature in some tidal pools may change from 2 to 14°C within only 8 h (Klöser et al. 19994).

As already mentioned in the introduction, all benthic diatoms from the Arctic that have so far been experimentally studied under controlled conditions typically exhibit eurythermal and psychrotolerant traits, while those from Antarctica show stenothermal and psychrophilic features (Longhi et al. 2003; Karsten et al. 2019). These fundamental differences in the response patterns can be explained by the geologically 10-fold longer cold-water history of Antarctica compared to the Arctic, fostering adaptive and evolutionary processes in the inhabiting organisms, which finally led to many endemic marine organisms in Antarctica (Sabbe et al. 2003). However, in sharp contrast to the data of Longhi et al. (2003), all six benthic diatom species in the present study exhibited very similar ecophysiological response patterns, comparable not only to those from their Arctic counterparts, but also to those from temperate regions such as the Baltic Sea [48,54], hence pointing to eurythermal and psychrotolerant traits. The unexpectedly broad temperature tolerances are not easy to explain, but Potter Cove is one

of the few places in Antarctica where long-term ecological observational data exist. Based on >20-year time series of sea surface temperature, data prove a temperature increase of 0.7 to 0.8°C in the last two decades, accelerating biological activities and physicochemical processes in the shallow coastal waters of Potter Cove (Abele et al. 2017). As a consequence, summer meltwater runoff from coastal ice sheets and from thawing of coastal permafrost areas causes freshening of the shallow water, along with increasing turbidity due to mobilization of lithogenic particles, so that benthic biota are strongly affected by such highly dynamic and new climate-sensitive environmental conditions (Abele et al. 2017). Therefore, it is reasonable to assume that during the ca. 20-year time span between the study of Longhi et al. (2003) and the data presented here, changes within the benthic diatom community took place, i.e., from more stenoecious (endemic) to euryoecious (non-endemic) taxa. It might also be possible that non-endemic benthic diatoms invaded the Antarctic Peninsula from sub-Antarctic islands and from South America—for example, as hull biofouling organisms - as shown for other benthic organisms, such as invertebrates (Holland et al. 2021). However, comprehensive information on the biodiversity and biogeography of marine benthic diatoms in Antarctica is still lacking, while freshwater species are very well studied (Verleyen et al. 2021).

5.5.3 Salinity

In general, the photosynthetic potential of the six benthic diatom species exhibited broad tolerances, with habitat-typical salinity optima of 25 to 35 S_A for the marine strains and 1 to 10 S_A for the freshwater strains. Due to the topographic division within Potter Cove and the freshwater runoff, salinity in the inner part of the bay exhibits lower salinities > 29.6 S_A, compared to the outer part, which has fully marine salinities (Hernández et al. 2019). Salinity stress is related to the toxic effects of Na+ and Cl-, and often results in a decline in photosynthetic activity or a change in PS II efficiency (Palmisano et al. 1987; Ryan et al. 2004; Ralph et al. 2007; Petrou et al. 2011). This can lead to oxidative stress, consequently damaging lipid membranes, proteins, or nucleic acids (Ludwiczak et al. 2021), while also interfering with the photosynthetic and respiratory electron transport. The accompanying effect of changing cell volumes can also lead to the deactivation of the photosynthetic apparatus (Ralph et al. 2007).

In the marine rock pools, benthic diatoms are typically exposed to strong tidal-induced salinity changes, as they are cut off from the main body of marine water. In the rock pools, salinity can increase as a result of strong evaporation due to insolation and wind, or decrease because of precipitation or glacial freshwater inflow (Karsten et al. 1991). The marine strain *N. criophiliforma*, sampled from a rock pool in Potter Cove, exhibited a wide euryhaline tolerance,

with >20 % photosynthetic potential between 10 and 55 S_A, thereby able to cope well with this abiotic factor. The remaining two marine species were also euryhaline in terms of photosynthesis. Such broad tolerance ranges are typically found in diatoms living under and within the sea ice, and which can cope with salinities of up to 60–100 S_A (Ryan et al. 2004). However, apart from sea-ice diatoms, there exist only fragmentary data on salinity responses in polar benthic diatoms. For the Arctic *Nitzschia* cf. *aurariae*, growth between 15 and 45 S_A, with an optimum at 20 to 40 S_A, was reported, and it was thus characterized as moderately euryhaline (Karsten et al. 2012). In contrast to polar benthic diatoms, their temperate counterparts are well studied in terms of a commonly wide salinity tolerance. Numerous benthic diatoms from the North Sea exhibited high growth rates between 2 and 45 S_A (Admiraal 1977), and between 10 and 40 S_A (Scholz and Liebezeit 2012), while a study from the Baltic Sea reported growth between 1 and 50 S_A (Woelfel et al. 2014)

The underlying mechanisms of osmotic acclimation have not yet been studied in Antarctic benthic diatoms. In contrast, ice-associated diatoms trapped in the brine channels can experience salinities three times that of seawater. These algae typically synthesize and accumulate high concentrations of organic osmolytes and compatible solutes in response to hypersaline stress, such as proline, mannitol, glycine betaine, and/or dimethylsulfoniopropionate (DMSP, Thomas and Dieckmann 2002).

5.6 Conclusions

In conclusion, all six benthic diatom species isolated from the Antarctic Peninsula exhibited strong euryhaline and eurythermal traits far surpassing the environmental conditions of their respective habitats. Pronounced low light requirements and species-specific photophysiological plasticity with minor photoinhibition were present. With regard to the ongoing climate change - particularly in maritime Antarctica - the increasing water temperatures of Potter Cove, and the accompanying fluctuations in salinity and the light field, all of the isolates seemed to be well acclimated, as reflected in their eurythermal and euryhaline response patterns.

5.7 Funding

This study was conducted within the framework of the Research Training Group Baltic TRANS-COAST funded by the DFG (Deutsche Forschungsgemeinschaft) under grant number GRK 2000/1 (Subproject B2: Microphytobenthos). This is Baltic TRANSCOAST publication no. GRK2000/00XX.). Furthermore, this project was funded within the framework of the SPP 1158 Antarktisforschung by the DFG under the grant numbers KA899/38-1 and ZI 1628/2-1.

5.8 Acknowledgments

We would like to thank the team of the Argentinian Antarctic Research Station “Carlini” of the Instituto Antárctico Argentino (IAA), as well as Hans-Peter Grossart and Thomas Wichard, for their support and logistical assistance. The authors are grateful to Jana Bansemer for work in the molecular lab, and to Juliane Bettig for support with the SEM at the BGBM Berlin.

5.9 References

Abarca N, Jahn R, Zimmermann J, Enke N (2014) Does the cosmopolitan diatom *Gomphonema parvulum* (Kützing) Kützing have a biogeography? PloS ONE 9: e86885. https://doi.org/10.1371/journal.pone.0086885

Abele D, Vazquez S, Buma AG, Hernandez E, et al. (2017) Pelagic and benthic communities of the Antarctic ecosystem of Potter Cove: Genomics and ecological implications. Marine Genomics 33: 1-11.

Atkin OK, Tjoelker MG (2003) Thermal acclimation and the dynamic response of plant respiration to temperature. Trends in Plant Science 8: 343–351. https://doi.org/10.1016/s1360-1385(03)00136-5

Bailleul B, Berne N, Murik O, Petroutsos D, Prihoda J, Tanaka A, et al. (2015) Energetic coupling between plastids and mitochondria drives CO_2 assimilation in diatoms. Nature 524: 366–369. https://doi.org/10.1038/nature14599

Beninger PG, Cuadrado D, van de Koppel J. (2018) Sedimentary and biological patterns on mudflats. Mudflat Ecology 7, ed. P. Beninger (Cham: Springer).

Blommaert L, Lavaud J, Vyverman W, Sabbe K (2018) Behavioural versus physiological photoprotection in epipelic and epipsammic benthic diatoms. European Journal of Phycology 53: 146–155. https://doi.org/10.1080/09670262.2017.1397197

Cahoon LB (1999) The role of benthic microalgae in neritic ecosystems. Oceanography and Marine Biology: An Annual Review 37: 47–86.

Drew EA, Hastings RM (1992) A year-round ecophysiological study of *Himantothallus grandifolius* (Desmarestiales, Phaeophyta) at Signy Island, Antarctica. Phycologia 31: 262-277.

Droege G, Barker K, Seberg O, Coddington J, Benson E, Berendsohn WG, Bunk B, Butler C, Cawsey EM, Deck J, Döring M, Flemons P, Gemeinholzer B, Güntsch A, Hollowell T, Kelbert P, Kostadinov I, Kottmann R, Lawlor RT, Zhou X (2016) The Global Genome Biodiversity Network (GGBN) Data Standard specification. Database. https://doi.org/10.1093/database/baw125

Fiala M, Oriol L (1989) Light-temperature interactions on the growth of Antarctic diatoms. Polar Biology 10: 629–636.

Gilstad M, Sakshaug E (1990) Growth rates of ten diatom species from the Barents Sea at different irradiances and day lengths. Marine Ecology Progress Series 64: 169-173.

Glaser K, Karsten U (2020) Salinity tolerance in biogeographically different strains of the marine benthic diatom *Cylindrotheca closterium* (Bacillariophyceae). Journal of Applied Phycology 32: 3809–3816. https://doi.org/10.1007/s10811-020-02238-6

Gleich SJ, Plough LV, Gilbert, PM (2020) Photosynthetic efficiency and nutrient physiology of the diatom *Thalassiosira pseudonana* at three growth temperatures. Marine Biology 167:124. https://doi.org/10.1007/s00227-020-03741-7

Glud RN, Kühl M, Wenzhöfer F, Rysgaard S (2002) Benthic diatoms of a high Arctic fjord (Young Sound, NE Greenland): importance for ecosystem primary production. Marine Ecology Progress Series 238: 15–29. https://doi.org/10.3354/meps238015

Glud RN, Woelfel J, Karsten U, Kühl M, Rysgaard S (2009) Benthic microalgal production in the Arctic: applied methods and status of the current database. Biology of Polar Benthic Algae (Wiencke, C. Ed.), Walter de Gruyter, Berlin, 141-162.

Gómez I, Wulff A, Roleda MY, Huovinen P, Karsten U, Quartino ML, Dunton K, Wiencke C (2009) Light and temperature demands of marine benthic microalgae and seaweeds in polar regions. Biology of Polar Benthic Algae (Wiencke, C. Ed.), Walter de Gruyter, Berlin, 195-220.

Gruenstaeudl M (2019) Annonex2embl: Automatic preparation of annotated DNA sequences for bulk submissions to ENA. Bioinformatics 36: 3841–3848, https://doi.org/10.1093/bioinformatics/btaa209.

Guillard RRL, Ryther JH (1962) Studies or marine planktonic diatoms. I. *Cyclotella nana* Hustedt and *Detonula confervacea* Cleve. Canandian Journal of Microbiology 8: 229–239. https://doi.org/10.1139/m62-029

Guillard RRL (1975) Culture of phytoplankton for feeding marine invertebrates, in Culture of Marine Invertebrate Animals, eds W. L. Smith and M. H. Chanley (New York, NY: Plenum Press), 26–60.

Gustavs L, Schumann R, Eggert A, Karsten U (2009) In vivo growth fluorometry: accuracy and limits of microalgal growth rate measurements in ecophysiological investigations. Aquatic Microbial Ecology 55: 95–104. https://doi.org/10.3354/ame01291

Gemeinholzer B, Droege G, Zetzsche H, Haszprunar G, Klenk H-P, Güntsch A, Berendsohn W, Wägele JW (2011) The DNA Bank Network: The start from a German initiative. Biopreservation and Biobanking 9: 51-55. https://doi.org/10.1089/bio.2010.0029

Hamsher S, Kopalova K, Kociolek P, Zidarova R, Van de Vijver B (2016) The genus *Nitzschia* on the South Shetland Islands and James Ross Island. Journal of the Czech Phycological Society 16: 79-102. https://doi.org/10.5507/fot.2015.023

Han B-P (2000).Effect of photoinhibition on algal photosynthesis: a dynamic model. Journal of Plankton Research 22: 865–885. https://doi.org/10.1093/plankt/22.5.865

Harper MA (1969) Movement and migration of diatoms on sand grains. British Phycological Journal 4: 97-103.

Hoffmann R, Al-Handal AY, Wulff A, Deregibus D, Zacher K, Quartino ML, Wenzhöfer F and Braeckman U (2019) Implications of Glacial Melt-Related Processes on the Potential Primary Production of a Microphytobenthic Community in Potter Cove (Antarctica). Frontiers in Marine Science 6: 655. https://doi.org/10.3389/fmars.2019.00655

HELCOM (2015) Annex C-4. Phytoplankton chlorophyll a, in HELCOM Combine, (Helsinki: HELCOM), 257–263. Available online at: https://helcom.fi/media/publications/Manual-for-Marine-Monitoring-in-the-COMBINE-Programme-of-HELCOM.pdf

Hernández EA, Lopez JL, Piquet AM-T, Mac Cormack WP, Buma AGJ (2019) Changes in salinity and temperature drive marine bacterial communities' structure at Potter Cove, Antarctica. Polar Biology 42: 2177–2191. https://doi.org/10.1007/s00300-019-02590-5

IPCC 2014 Summary for policymaker.: Climate Change 2014: Impacts, Adaptation, and Vulnerability. Part A: Global and Sectoral Aspects. Contribution of Working Group II to the Fifth Assessment Report of the Intergovernmental Panel on Climate Change ed C B Field et al (Cambridge) (Cambridge University Press) (Cambridge, United Kingdom and New York, NY, USA), 1–32.

Jahn R, Abarca N, Gemeinholzer B, Mora D, Skibbe O, Kulikovskiy M, Gusev E, Kusber W-H, Zimmermann J (2017) *Planothidium lanceolatum* and *Planothidium frequentissimum* reinvestigated with molecular methods and morphology: four new species and the taxonomic importance of the sinus and cavum. Diatom Research 32: 75-107, https://doi.org/10.1080/0269249X.2017.1312548

Jones J (1996) The diversity, distribution and ecology of diatoms from Antarctic inland waters. Biodiversity and Conservation 5 (11), 1433–1449. https://doi.org/10.1007/BF00051986

Kanz B, Büdel B, Jung P, Karsten U, Printzen C (2020) Leben zwischen Eis und Felsen. Biologie in unserer Zeit 50: 122–133. https://doi.org/https://doi.org/10.1002/biuz.202010702

Karsten U, Wiencke C, Kirst GO (1991) The Effect of Salinity Changes upon the Physiology of Eulittoral Green Macroalgae from Antarctica and South-ern Chile. I. Cell Viability, Growth, Photosynthesis and Dark Respiration. Journal of Plant Physiology 138: 667–673. https://doi.org/10.1016/S0176-1617(11)81313-1

Karsten U, Klimant I, Holst G (1996) A new in vivo fluorimetric technique to measure growth of adhering phototrophic microorganisms. Applied and Environmental Microbiology 62: 237–243. https://doi.org/10.1128/aem.62.1.237-243.1996

Karsten U, Schumann R, Rothe S, Jung I Medlin L (2006) Temperature and light requirements for growth of two diatom species (Bacillariophyceae) isolated from an Arctic macroalga. Polar Biology 29: 476-486.

Karsten U, Lütz C, Holzinger A (2010) Ecophysiological performance of the aeroterrestrial green alga *Klebsormidium crenulatum* (Charophyceae, Streptophyta) isolated from an alpine soil crust with an emphasis on desiccation stress. Phycologia 46: 1187–1197. https://doi.org/10.1111/j.1529-8817.2010.00921.x

Karsten U, Schlie C, Woelfel J, Becker B (2012) Benthic diatoms in Arctic Seas-ecological functions and adaptions. Polarforschung 81: 77-84.

Karsten U, Herburger K, Holzinger A (2016) Photosynthetic plasticity in the green algal species *Klebsormidium flaccidum* (Streptophyta) from a terrestrial and a freshwater habitat. Phycologia 56: 213-220. https://doi.org/10.2216/16-85.1

Karsten U, Schaub I, Woelfel J, Sevilgen D, Schlie C, Becker B, Wulff A, Graeve M, Wagner H (2019) Living on cold substrata – new insights and approaches to study microphytobenthos ecophysiology and ecology in Kongsfjorden. Hop H, Wiencke C (eds) The ecosystem of Kongsfjorden, Svalbard. Advances in Polar Ecology 2; Springer, 303-330. https://doi.org/10.1007/978-3-319-46425-1_8

Kellogg DE, Stuiver M, Kellogg TB, Denton GH (1980) Non-marine diatoms from late Wisconsin perched deltas in Taylor Valley, Antarctica. Palaeogeography, Palaeoclimatology, Palaeoecology 30: 157-189. https://doi.org/10.1016/0031-0182(80)90055-3

Kirst GO, Wiencke C (1995) Ecophysiology of polar algae. Oceanographic Literature Review 12: 1094.

Klöser H, Ferreyra GA, Schloss IR, Mercuri G, Laturnus F, Curtosi A (1994) Hydrography of Potter Cove, a Small Fjord-like Inlet on King George Island (South Shetlands). Estuarine, Coastal and Shelf Science 38: 523-537. https://doi.org/10.1006/ecss.1994.1036

Kopalová K, Veselá J, Elster J, Nedbalová L, Komárek J, Van de Vijver B (2012) Benthic diatoms (Bacillariophyta) from seepages and streams on James Ross Island (NW Weddell Sea, Antarctica). Plant Ecology and Evolution, 145: 190-208.

Lazzara L, Nardello I, Ermanni C, Mangoni O, Saggiomo V (2007) Light environment and seasonal dynamics of microalgae in the annual sea ice at Terra Nova Bay, Ross Sea, Antarctica. Antarctic Science 19: 83–92. https://doi.org/10.1017/S0954102007000119

Longhi ML, Schloss IR, Wiencke C (2003) Effect of Irradiance and Temperature on Photosynthesis and Growth of Two Antarctic Benthic Diatoms, *Gyrosigma subsalinum* and *Odontella litigiosa*. Botanica Marina 46: 276–284. https://doi.org/10.1515/BOT.2003.025

Ludwiczak A, Osiak M, Cárdenas-Pérez S, Lubińska-Mielińska S, Piernik A (2021) Osmotic Stress or Ionic Composition: Which Affects the Early Growth of Crop Species More? Agronomy 11: 435. https://doi.org/10.3390/agronomy11030435

Mann DG (1999) The species concept in diatoms. Phycologia 38: 437–495. https://doi.org/10.2216/i0031-8884-38-6-437.1

Maykut GA, Grenfell TC (1975) The spectral distribution of light beneath first-year sea ice in the Arctic Ocean. Limnology and Oceanography 20: 554-563. https://doi.org/https://doi.org/10.4319/lo.1975.20.4.0554

Overland JE, Wang M, Walsh JE, Stroeve JC (2014) Future Arctic climate changes: Adaptation and mitigation time scales. Earth's Future 2: 68-74.

Palmisano AC, SooHoo JB, White DC, Smith GA, Stanton GR, Burckle LH (1985) Shade adapted benthic diatoms beneath Antarctic Sea Ice. Journal of Phycology 21: 664-667.

Palmisano AC, SooHoo JB, Moe RL, Sullivan CW (1987) Sea ice microbial communities. VII. Changes in under-ice spectral irradiance during the development of Antarctic sea ice microalgal communities. Marine Ecology Progress Series 35: 165–173.

Pavlov AK, Leu E, Hanelt D, et al. (2019) The underwater light climate in Kongsfjorden and its ecological implications. Hop H, Wiencke C (eds) The ecosystem of Kongsfjorden, Svalbard. Advances in Polar Ecology 2: 137-170.

Petrou K, Doblin MA, Ralph PJ (2011) Heterogeneity in the photoprotective capacity of three Antarctic diatoms during short-term changes in salinity and temperature. Marine Biology 158: 1029–1041. https://doi.org/10.1007/s00227-011-1628-4

Post AL, Meijers AJS, Fraser AD, Meiners KM, Ayers J, Bindoff NL. et al. (2014) Chapter 4 Environmental Setting. Scientific Committee on Antarctic Research, C. de Broyer, P.

Koubbi, H. J. Griffith, B. Raymond, C. Ude-kem d'Acoz, et al. (Eds.): Biogeographic Atlas of the Southern Ocean. Cambridge, 46–64.

Prelle LR, Graiff A, Gründling-Pfaff S, Sommer V, Kuriyama K, Karsten U (2019) Photosynthesis and respiration of Baltic Sea benthic diatoms to changing environmental conditions and growth responses of selected species as affected by an adjacent peatland (Hütelmoor). Frontiers in Microbiology 10: 1500. https://doi.org/10.3389/fmicb.2019.01500

Prelle LR, Albrecht M, Karsten U, Damer P, Giese T, Jähns J, Müller S, Schulz L, Viertel L, Glaser K (2021) Ecophysiological and Cell Biological Traits of Benthic Diatoms From Coastal Wetlands of the Southern Baltic Sea. Frontiers in Microbiology 12: 796. https://doi.org/10.3389/fmicb.2021.642811

Ralph PJ, Ryan KG, Martin A, Fenton G (2007) Melting out of sea ice causes greater photosynthetic stress in algae than freezing in 1. Journal of Phycology 43: 948–956. https://doi.org/10.1111/j.1529-8817.2007.00382.x

Risgaard-Petersen N, Rysgaard S, Nielsen LP, Revsbech NP (1994) Diurnal variation of denitrification and nitrification in sediments colonized by benthic microphytes. Limnology and Oceanography 39: 573–579

Ryan KG, Ralph P, McMinn A (2004) Acclimation of Antarctic bottom-ice algal communities to lowered salinities during melting. Polar Biology 27: 679–686. https://doi.org/10.1007/s00300-004-0636-y

Sabbe K, Verleyen E, Hodgson DA, Vanhoutte K, Vyverman W (2003) Benthic diatom flora of freshwater and saline lakes in the Larsemann Hills and Rauer Islands, East Antarctica. Antarctic Science 15: 227-248.

Schlie C, Karsten U (2017) Microphytobenthic diatoms isolated from sediments of the Adventfjorden (Svalbard): growth as function of temperature. Polar Biology 40: 1043–1051. https://doi.org/10.1007/s00300-016-2030-y

Serôdio J, Vieira S, Cruz S (2008) Photosynthetic activity, photoprotection and photoinhibition in intertidal microphytobenthos as studied in situ using variable chlorophyll fluorescence. Continental Shelf Research 28: 1363–1375. https://doi.org/10.1016/j.csr.2008.03.019

Sevilgen DS, de Beer D, Al-Handal AY, Brey T, Polerecky L (2014) Oxygen budgets in subtidal arctic (Kongsfjorden, Svalbard) and temperate (Helgoland, North Sea) microphytobenthic communities. Marine Ecology Progress Series 504: 27-42.

Silva JF, Oliveira MA, Alves RP, Cassol APV, Anunciação RR, Silva EP, Schünemann AL, Pereira AB (2019) Geographic distribution of epilithic diatoms (Bacillariophyceae) in Antarctic lakes, South Shetland Islands, Maritime Antarctica Region. Check List 15: 797-809. https://doi.org/10.15560/15.5.797

Smetacek V (1999) Diatoms and the Ocean Carbon Cycle. Protist 150: 25–32. https://doi.org/10.1016/S1434-4610(99)70006-4

Sterken M, Verleyen E, Jones VJ, Hodgson DA, Vyverman W, Sabbe K, Van de Vijver B (2015) An illustrated and annotated checklist of freshwater diatoms (Bacillariophyta) from Livingston, Signy and Beak Island (Maritime Antarctic Region). Plant Ecology and Evolution 148: 431-455. https://doi.org/10.5091/plecevo.2015.1103

Thomas DN, Dieckmann GS (2002) Antarctic Sea ice-a habitat for extremophiles. Science 295: 641–644. https://doi.org/10.1126/science.1063391

Van de Vijver B, Sterken M, Vyverman W, Mataloni G, Nedbalová L, Kopalová K, Elster J, Verleyen E, Sabbe K (2010) Four new non-marine diatom taxa from the Subantarctic and Antarctic regions. Diatom Research 25: 431-443. https://doi.org/10.1080/0269249X.2010.9705861

Verleyen E, Van de Vijver B, Tytgat B, et al. (2021) Diatoms define a novel freshwater biogeography of the Antarctic. Ecography 44: 548-560.

Walne PR (1970) Studies on the food value of nineteen genera of algae to juvenile bivalves of the genera Ostrea, Crassostrea, Mercenaria and Mytilus. Fishery investigations, series 2:26

Walsby AE (1997) Numerical integration of phytoplankton photosynthesis through time and depth in a water column. New Phytologist 136, 189–209. https://doi.org/10.1046/j.1469-8137.1997.00736.x

Wiencke C, Dieck IT (1989) Temperature requirements for growth and temperature tolerance of macroalgae endemic to the Antarctic region. Marine Ecology Progress Series 54: 189-197.

Wiencke C, Dieck IT (1990) Temperature requirements for growth and survival of macroalgae from Antarctica and southern Chile. Marine Ecology Progress Series 59: 157-170.

Wilhelm C, Büchel C, Fisahn J, et al. (2006) The regulation of carbon and nutrient assimilation in diatoms is significantly different from green algae. Protist 157: 91–124. https://doi.org/10.1016/j.protis.2006.02.003

Winterfeld M, Mollenhauer G, Dummann W, et al. (2018) Deglacial mobilization of pre-aged terrestrial carbon from degrading permafrost. Nature Communications 9: 1-12. https://doi.org/10.1038/s41467-018-06080-w

Witkowski A, Riaux-Gobin C, Daniszewska-Kowalczyk G (2010) New marine diatom (Bacillariophyta) Species described from Kerguelen Islands coastal area and pertaining to *Navicula* S.S. with some remarks on morphological variation of the genus. Vie et Milieu 60.

Woelfel J, Schumann R, Peine F, Flohr A, Kruss A, Tegwoski J, Blondel P, Wiencke C, Karsten U (2010) Microphytobenthos of Arctic Kongsfjorden (Svalbard, Norway) – Biomass and potential primary production along the shoreline. Polar Biology 33: 1239-1253.

Woelfel J, Eggert A, Karsten U (2014) Global warming could stimulate Arctic microphytobenthos primary production in Kongsfjorden (Svalbard, Norway) - in situ measurements and modelled changes. Marine Ecology Progress Series 501: 25–40.

Wulff A, Roleda MY, Zacher K, Wiencke C (2008) Exposure to sudden light burst after prolonged darkness – a case study on benthic diatoms in Antarctica. Diatom Research 23: 519–532.

Wulff A, Iken K, Quartino ML, Al-Handal A, Wiencke C, Clayton MN (2009) Biodiversity, biogeography and zonation of benthic micro- and macroalgae in the Arctic and Antarctic. Botanica Marina 52: 491–507.

Yan W, Hunt LA (1999) An equation for modelling the temperature response of plants using only the cardinal temperatures. Annals of Botany 84: 607–614. https://doi.org/10.1006/anbo.1999.0955

Young JN, Goldman JA, Kranz SA, Torell PD, Morel FM (2014) Slow carboxylation of Rubisco constrains the maximum rate of carbon fixation during Antarctic phytoplankton blooms. New Phytologist 205: 172–181. https://doi.org/10.1111/nph.13021

Zidarova R, Kopalova K, Van de Vijver B (2016) Diatoms from the Antarctic Region. I: Maritime Antarctica (Vol. 24). Koeltz Botanical Books.

Zidarova R, Ivanov P, Hineva E, Dzhembekova N (2022) Diversity and habitat preferences of benthic diatoms from South Bay (Livingston Island, Antarctica). Plant Ecology and Evolution 155: 70-106. https://doi.org/10.5091/plecevo.84534

Zimmermann J, Jahn R, Gemeinholzer B (2011) Barcoding diatoms: evaluation of the V4 subregion on the 18S rRNA gene, including new primers and protocols. Organisms Diversity & Evolution 11: 173. https://doi.org/10.1007/s13127-011-0050-6

6 General conclusion and outlook

6.1 Insights into biodiversity and biogeography of benthic diatoms in the West Antarctic

Biodiversity research has increased across Antarctica driven by the realization that any fundamental quest to understand life's diversity and plasticity requires exploration of the polar regions (Griffiths 2010, Chown et al. 2015, Danis et al. 2020). Furthermore, climate change and economic activity are rapidly transforming polar ecosystems and their biodiversity. Increased research is required in the light of desynchrony between the pace of change in polar regions and information demands to face engendered challenges (Danis et al. 2020).

This thesis constitutes the first study to add knowledge to benthic diatom biodiversity via identification by means of morphology, culturing and DNA metabarcoding in this region. An astonishingly high benthic diatom diversity with 238 infrageneric taxa was revealed for coastal zones of the West Antarctic Peninsula. A combination of morphological and metabarcoding approaches together with culturing increases the detection and identification of diatoms as the methods provide complementary information on biodiversity of benthic diatoms. However, many species still have no record in reference databases, which highlights the demand for continuing culturing efforts. Only 43 % of the marine and 81 % of the freshwater taxa could be identified to species level. Further, the metabarcoding dataset suggests a high cryptic diversity with many taxa not even fitting to a current genus concept. Inferring from this, a large proportion of the biodiversity remains unknown.

The low identification rate by metabarcoding and morphology suggests a high number of undescribed species, which are probably only occurring in the Southern Ocean or Antarctica. Already 56 % of here identified marine taxa exhibit a restricted dispersal to coastal Antarctica or the sub-Antarctic islands, thereby exceeding the estimated rate of endemicity of freshwater taxa (Verleyen et al. 2021). However, further taxonomic investigation in this region is irrefutably needed.

All voucher material as well as the data generated by this thesis are deposited at the Herbarium Berolinense and could be used as a baseline for further investigations to resolve questions concerning biodiversity and biogeography or as a reference for metabarcoding monitoring routines to screen community changes and to predict for instance the potential impact of climate change on the coastal ecosystems of this region.

6.2 Considerations about taxonomy, phylogeny and genomics

The micro-morphological characters seen by SEM, the morphometric data measured by LM together with molecular data from marker genes set the standard for an improved and in-depth taxonomy in benthic diatoms as fundamental base for investigating their biodiversity and biogeography. Especially the many valves from the cultured strains show the variability of diatom frustules. In some cases, morphological features, which have been determined as differentiating characters in the identification of diatom taxa, occur together in one culture proving this character as obsolete (Abarca et al. 2014). In addition, the size range of diatom strains undergoing auxospore formation span an astonishingly broad range.

The micro-morphological characters need to be underpinned by molecular data, which often demonstrate an even higher genetic diversity than based on morphological identification only. This was the case in both newly described taxa of this thesis: *Planothidium wetzelii* and *Chamaepinnularia australis*. Only the synopsis of the morphological and molecular data revealed their taxonomic separation and therefore provides a much better understanding of speciation and diversity in benthic diatoms. Further, a molecular phylogeny in combination with the investigation of morphological traits uncovered the placement of the genus *Chamaepinnularia* to the family Sellaphoraceae. This showed once more that molecular data is valuable in revealing the phylogenetic position of diatom taxa.

The generated dataset of this thesis showed a high number of Antarctic diatom species that are probably new to science and await taxonomic investigation. The obtained data allows the morphological and molecular analysis of those taxa in subsequent projects. Due to the enormous number of undescribed species, taxonomic investigation of all of them was not possible within the framework of this thesis.

Phylogenetic studies based on only a few marker loci have their limitations, as deeper relationships are essentially unresolved or sensitive to locus selection, alignment strategy, and outgroup choice (Parks et al. 2018, Mann et al. 2021). Access to genome-scale data opens now an amazing range of new application perspectives for phylogenetic evaluation (Scornavacca et al. 2020) as well as diatom genomes and transcriptomes can be used to infer perennially difficult species relationships (Parks et al. 2018). Further, investigation of whole genomes allows evaluation of fine-scale genetic differentiation over large geographic areas, ecotypic differentiation and speciation as well as contributes to the discovery of the extent of cryptic species and the invasions of species (Postel et al. 2020, Rastogi et al. 2020, Wenne 2023).

6.3 Environmental adaptations of benthic diatoms

As environmental conditions in the polar regions are rapidly changing, the ecophysiological response patterns of benthic diatom species are urgently needed to understand their adaptive traits and plasticity. It has been shown that the utilization of storage lipids is one of the key mechanisms in Antarctic benthic diatoms. All benthic diatoms from the Arctic that have so far been experimentally studied under controlled conditions typically exhibit eurythermal and psychrotolerant traits, while those from Antarctica show stenothermal and psychrophilic features (Longhi et al. 2003, Karsten et al. 2019). These fundamental differences in the response patterns can be explained by the geologically 10-fold longer cold-water history of Antarctica compared to the Arctic, fostering adaptive and evolutionary processes in the inhabiting organisms. However, the six strains studied in the framework of this project indicated comparable ecophysiological response patterns to those from their Arctic counterparts. Then again, only a few species were investigated and transport as well as cultivation might have selected for the most tolerant species while sensitive taxa were outcompeted.

In general, the exploitation of multi-omics data is required for the comprehensive evaluation to reveal how life evolved and adapted to permanently cold environments with extreme seasonality (Clark et al. 2023). The enormous dataset and the already available numerous established clonal cultures of benthic diatoms from this thesis can be used to investigate not only the biodiversity of Antarctic benthic diatoms, but also their evolution and adaptive divergence by the use of multi-omics approaches. A combination of morphometric, genetic, ecophysiological and transcriptomic comparisons can be applied for a detailed characterization of patterns of genetic diversity of this ecologically important group of protists and how the genetic structure influence the species potential to adapt to its environment in Antarctica.

6.4 Climate change and the effects on diatoms

Climate change is heavily affecting Antarctica and especially the West Antarctic Peninsula. Threats to Antarctic biodiversity are accelerating at an unparalleled rate. It is estimated that 65 % of Antarctic terrestrial biodiversity are likely to decline by 2100 under current trajectories (Lee et al. 2022). In the marine environment, changing sea ice has large impacts on ecosystem processes, while ocean acidification and the increased influx of freshwater are expected to have major impacts (Convey and Peck 2019). Further, warmer temperatures together with increasing ship activities and declining of sea ice rises the probability of the introduction of non-native species (McCarthy et al. 2019).

Diatoms are highly sensitive organisms quickly responding to altered environments. First studies reveal a substantial decrease in diatom biomass due to poleward warming (Costa et al. 2021, Ducklow et al. 2013). Model results suggest that climate change leads to more nutrient-depleted conditions in the surface ocean that favors small phytoplankton at the expense of diatoms (Bopp et al. 2005). Additional, decreasing seawater pH decelerates the chemical dissolution of silica causing diatoms frustules to sink into deeper water layers before they chemically dissolve. Ocean acidification thereby reduces the availability of silicic acid in the surface ocean triggering an estimated global decline of diatoms by 13–26 % by the year 2200 (Taucher et al. 2022). As one of the key primary producers, diatoms play an essential role in aquatic food webs and changes in their abundance and species composition are probably resulting in cascading effects across all higher trophic levels (Ducklow et al. 2013, Duncan et al. 2022, Montes-Hugo et al. 2009). There is an urgent need to investigate further how these organisms will be affected by the changes in the Southern Ocean. Continuous monitoring is required to evaluate alterations in diatom abundance in Antarctica and whether the endemic diversity in this region will be preserved or whether non-native species are being introduced.

References

Abarca N, Jahn R, Zimmermann J, Enke N (2014) Does the cosmopolitan diatom *Gomphonema parvulum* (Kützing) Kützing have a biogeography? PloS ONE 9: e86885. https://doi.org/10.1371/journal.pone.0086885

Adl SM, Simpson AGB, Farmer MA, Andersen RA, Anderson OR, Barta JR, Bowser SS, Brugerolle G, Fensome RA, Fredericq S, James TY, Karpov S, Kugrens P, Krug J, Lane CE, Lewis LA, Lodge J, Lynn DH, Mann DG, McCourt RM, Mendoza L, Moestrup Ø, Mozley-Standridge SE, Nerad TA, Shearer CA, Smirnov AV, Spiegel FW, Taylor MFJR (2005) The new higher level classification of eukaryotes with emphasis on the taxonomy of protists. Journal of Eukaryotic Microbiology 52: 399-451. https://doi.org/10.1111/j.1550-7408.2005.00053.x

Al-Handal AY, Riaux-Gobin C, Romero OE, Wulff A (2008) Two new marine species of the diatom genus *Cocconeis* Ehrenberg: *C. melchioroides* sp. nov. and *C. dallmannii* sp. nov., from King George Island, Antarctica. Diatom Research 23: 269-281. https://doi.org/10.1080/0269249X.2008.9705758

Al-Handal AY, Riaux-Gobin C, Wulff A (2010) *Cocconeis pottercovei* sp. nov. and *Cocconeis pinnata* var. *matsii* var. nov., two new marine diatom taxa from King George Island, Antarctica. Diatom Research 25: 1-11. https://doi.org/10.1080/0269249X.2010.9705825

Al-Handal AY, Thomas EW, Torstensson A, Jahn R, Wulff A (2018) *Gomphonemopsis ligowskii*, a new diatom (Bacillariophyceae) from the marine Antarctic and a comparison to other *Gomphonemopsis*. Diatom Research 33: 97-103. https://doi.org/10.1080/0269249X.2018.1428916

Al-Handal AY, Torstensson A, Wulff A (2022) Revisiting Potter Cove, King George Island, Antarctica, 12 years later: new observations of marine benthic diatoms. Botanica Marina 65: 81-103. https://doi.org/10.1515/bot-2021-0066

Al-Handal AY, Wulff A (2008a) Marine benthic diatoms from Potter Cove, King George Island, Antarctica. Botanica Marina 51: 51-68. https://doi.org/10.1515/BOT.2008.007

Al-Handal AY, Wulff A (2008b) Marine epiphytic diatoms from the shallow sublittoral zone in Potter Cove, King George Island, Antarctica. Botanica Marina 51: 411-435. https://doi.org/10.1515/BOT.2008.053

Almandoz GO, Ferrario ME, Sullivan MJ, Ector L, Schloss IR (2014) A new *Pteroncola* species (Bacillariophyceae) from the South Shetland Islands, Antarctica. Phycologia 53: 188-194. https://doi.org/10.2216/13-210.1

Alverson AJ (2008) Molecular systematics and the diatom species. Protist 159: 339-53. https://doi.org/10.1016/j.protis.2008.04.001

Alverson AJ, Theriot EC (2003) Taxon sampling and inferences about diatom phylogeny. Journal of Phycology 39: 1-1. https://doi.org/10.1111/j.0022-3646.2003.03906001_1.x

Armbrust EV, Berges JA, Bowler C, Green BR, Martinez D, Putnam NH, Zhou S, Allen AE, Apt KE, Bechner M (2004) The genome of the diatom *Thalassiosira pseudonana*: ecology, evolution, and metabolism. Science 306: 79-86. http://doi.org/10.1126/science.1101156

Armbrust VE (2009) The life of diatoms in the world's oceans. Nature 459: 185-192. https://doi.org/10.1038/nature08057

Ask J, Rowe O, Brugel S, Strömgren M, Byström P, Andersson A (2016) Importance of coastal primary production in the northern Baltic Sea. Ambio 45: 635-648. https://doi.org/10.1007/s13280-016-0778-5

Bailet B, Apothéloz-Perret-Gentil L, Baričević A, Chonova T, Franc A, Frigerio J-M, Kelly M, Mora D, Pfannkuchen M, Proft S, Ramon M, Vasselon V, Zimmermann J, Kahlert M (2020) Diatom DNA metabarcoding for ecological assessment: Comparison among bioinformatics pipelines used in six European countries reveals the need for standardization. Science of the Total Environment 745: 140948. https://doi.org/10.1016/j.scitotenv.2020.140948

Bailet B, Bouchez A, Franc A, Frigerio J-M, Keck F, Karjalainen S-M, Rimet F, Schneider S, Kahlert M (2019) Molecular versus morphological data for benthic diatoms biomonitoring in Northern Europe freshwater and consequences for ecological status. Metabarcoding and Metagenomics 3: e34002. https://doi.org/10.3897/mbmg.3.34002

Bar-On YM, Phillips R, Milo R (2018) The biomass distribution on Earth. Proceedings of the National Academy of Sciences 115: 6506-6511. https://doi.org/10.1073/pnas.1711842115

Barberán A, Casamayor EO, Fierer N (2014) The microbial contribution to macroecology. Frontiers in Microbiology 5. https://doi.org/10.3389/fmicb.2014.00203

Barczewski S (2023) The Heroic Age of Antarctic Exploration, 1890 to the Present. In: The Cambridge History of the Polar Regions, edited by A. Howkins and P. Roberts, 1811. Cambridge University Press

Bavestrello G, Arillo A, Calcinai B, Cattaneo-Vietti R, Cerrano C, Gaino E, Penna A, Sarà M (2000) Parasitic diatoms inside Antarctic sponges. Biology Bulletin 198: 29-33. https://doi.org/10.2307/1542801

Bedoshvili YD, Popkova T, Likhoshway YV (2009) Chloroplast structure of diatoms of different classes. Cell and Tissue Biology 3: 297-310. https://doi.org/10.1134/S1990519X09030122

Bell RE, Seroussi H (2020) History, mass loss, structure, and dynamic behavior of the Antarctic Ice Sheet. Science 367: 1321-1325. https://doi.org/10.1126/science.aaz5489

Berkaloff C, Caron L, Rousseau B (1990) Subunit organization of PSI particles from brown algae and diatoms: polypeptide and pigment analysis. Photosynthesis Research 23: 181-193. https://doi.org/10.1007/BF00035009

Bondoc KG, Lembke C, Vyverman W, Pohnert G (2016) Searching for a mate: Pheromone-directed movement of the benthic diatom *Seminavis robusta*. Microbial Ecology 72: 287-94. https://doi.org/10.1007/s00248-016-0796-7

Bopp L, Aumont O, Cadule P, Alvain S, Gehlen M (2005) Response of diatoms distribution to global warming and potential implications: A global model study. Geophysical Research Letters 32: L19606, https://doi.org/10.1029/2005GL023653

Borowski D, Olbers D, Völker C, Wölff J-O (2004) The dynamical balance, transport and circulation of the Antarctic Circumpolar Current. Antarctic Science 16: 439-470. https://doi.org/10.1017/S0954102004002251

Bowler C, Allen AE, Badger JH, Grimwood J, Jabbari K, Kuo A, Maheswari U, Martens C, Maumus F, Otillar RP, Rayko E, Salamov A, Vandepoele K, Beszteri B, Gruber A, Heijde M, Katinka M, Mock T, Valentin K, Verret F, Berges JA, Brownlee C, Cadoret J-P, Chiovitti A, Choi CJ, Coesel S, De Martino A, Detter JC, Durkin C, Falciatore A, Fournet J, Haruta M, Huysman MJJ, Jenkins BD, Jiroutova K, Jorgensen RE, Joubert Y, Kaplan A, Kröger N, Kroth PG, La Roche J, Lindquist E, Lommer M, Martin–Jézéquel V, Lopez PJ, Lucas S, Mangogna M, McGinnis K, Medlin LK, Montsant A, Secq M-POL, Napoli C, Obornik M, Parker MS, Petit J-L, Porcel BM, Poulsen N, Robison M, Rychlewski L, Rynearson TA, Schmutz J, Shapiro H, Siaut M, Stanley M, Sussman MR, Taylor AR, Vardi A, von Dassow P, Vyverman W, Willis A, Wyrwicz LS, Rokhsar DS, Weissenbach J, Armbrust EV, Green BR, Van de Peer Y, Grigoriev IV (2008) The *Phaeodactylum* genome reveals the evolutionary history of diatom genomes. Nature 456: 239-244. https://doi.org/10.1038/nature07410

Bruder K, Medlin L (2007) Molecular assessment of phylogenetic relationships in selected species/genera in the naviculoid diatoms (Bacillariophyta). I. The genus *Placoneis.* Nova Hedwigia 85: 331 - 352. https://doi.org/10.1127/0029-5035/2007/0085-0331

Bryłka K, Alverson AJ, Pickering RA, Richoz S, Conley DJ (2023) Uncertainties surrounding the oldest fossil record of diatoms. Scientific Reports 13: 8047. https://doi.org/10.1038/s41598-023-35078-8

Büchel C, Goss R, Bailleul B, Campbell DA, Lavaud J, Lepetit B (2022) Photosynthetic light reactions in diatoms. I. The lipids and light-harvesting complexes of the thylakoid membrane. In: The Molecular Life of Diatoms, edited by A. Falciatore and T. Mock, 397-422. Springer.

Cahoon LB (1999) The role of benthic microalgae in neritic ecosystems. In: Oceanography and Marine Biology. An annual review, edited by Alan Ansell, R.N. Gibson and Margaret Barnes, 47-86. London: CRC Press, Taylor & Francis.

Cahoon LB, Cooke JE (1992) Benthic microalgal production in Onslow Bay, North Carolina, USA. Marine Ecology Progress Series. 84: 185-196.

Campana GL (2018) Benthic micro– and macroalgae in a coastal Antarctic system (Potter Cove, South Shetland Islands): Efects of ultraviolet radiation and grazing on their colonization and succession, National Unversity of La Plata, Buenos Aires, Argentina.

Castracane AF (1886) Report on the Diatomaceae collected by HMS Challenger during the years 1873-76. The voyage of H.M.S. Challanger.

Cavalier-Smith T (1999) Principles of protein and lipid targeting in secondary symbiogenesis: Euglenoid, Dinoflagellate, and Sporozoan plastid origins and the eukaryote family tree. Journal of Eukaryotic Microbiology 46: 347-366. https://doi.org/10.1111/j.1550-7408.1999.tb04614.x

Chan CX, Bhattacharya D, Reyes-Prieto A (2012) Endosymbiotic and horizontal gene transfer in microbial eukaryotes: Impacts on cell evolution and the tree of life. Mobile Genetic Elements 2: 101-105. https://doi.org/10.4161/mge.20110

Chepurnov VA, Mann DG, Sabbe K, Vyverman W (2004) Experimental studies on sexual reproduction in diatoms. In: International Review of Cytology, 91-154. Academic Press.

Chonova T, Rimet F, Bouchez A, Kahlert M, Schneider SC, Bailet B, Eulin-Garrigue A, Gassiole G, Monnier O, Ouattara A, Rey S, Rhoné M, Keck F (2023) Revisiting global diversity and biogeography of freshwater diatoms: New insights from molecular data. Environmental DNA. https://doi.org/10.1002/edn3.475

Chown SL, Clarke A, Fraser CI, Cary SC, Moon KL, McGeoch MA (2015) The changing form of Antarctic biodiversity. Nature 522: 431-438. https://doi.org/10.1038/nature14505

Cirri E, De Decker S, Bilcke G, Werner M, Osuna-Cruz CM, De Veylder L, Vandepoele K, Werz O, Vyverman W, Pohnert G (2019) Associated bacteria affect sexual reproduction by altering gene expression and metabolic processes in a biofilm inhabiting diatom. Frontiers in Microbiology 10: 1790. https://doi.org/10.3389/fmicb.2019.01790

Clark MS, Hoffman JI, Peck LS, Bargelloni L, Gande D, Havermans C, Meyer B, Patarnello T, Phillips T, Stoof-Leichsenring KR, Vendrami DLJ, Beck A, Collins G, Friedrich MW, Halanych KM, Masello JF, Nagel R, Norén K, Printzen C, Ruiz MB, Wohlrab S, Becker B, Dumack K, Ghaderiardakani F, Glaser K, Heesch S, Held C, John U, Karsten U, Kempf S, Lucassen M, Paijmans A, Schimani K, Wallberg A, Wunder LC, Mock T (2023) Multi-omics for studying and understanding polar life. Nature Communications 14: 7451. https://doi.org/10.1038/s41467-023-43209-y

Cocquyt C (2000) Biogeography and species diversity of diatoms in the Northern basin of Lake Tanganyika. In: Advances in Ecological Research 125-150. Academic Press.

Colijn F, de Jonge VN (1984) Primary production of microphytobenthos in the Ems-Dollard Estuary. Marine Ecology Progress Series 14: 185-196.

Convey P, Chown SL, Clarke A, Barnes DKA, Bokhorst S, Cummings V, Ducklow HW, Frati F, Green TGA, Gordon S, Griffiths HJ, Howard-Williams C, Huiskes AHL, Laybourn-Parry J, Lyons WB, McMinn A, Morley SA, Peck LS, Quesada A, Robinson SA, Schiaparelli S, Wall DH (2014) The spatial structure of Antarctic biodiversity. Ecological Monographs 84: 203-244. https://doi.org/10.1890/12-2216.1

Convey P, Peck LS (2019) Antarctic environmental change and biological responses. Science Advvances 27:eaaz0888. https://doi:10.1126/sciadv.aaz0888.

Cooper R, Fox AJ, Paul A (1994) Measured properties of the Antarctic ice sheet derived from the SCAR Antarctic digital database. Polar Record 30: 201-206. https://doi.org/10.1017/S0032247400024268

Costa RR., Mendes CRB, Ferreira A, Tavano VM, Dotto TS, Secchi ER (2021) Large diatom bloom off the Antarctic Peninsula during cool conditions associated with the 2015/2016 El Niño. Commun Earth Environ 2: 252. https://doi.org/10.1038/s43247-021-00322-4

Cox E, Williams D (2006) Systematics of naviculoid diatoms (Bacillariophyta): A preliminary analysis of protoplast and frustule characters for family and order level classification. Systematics and Biodiversity 4: 385-399. https://doi.org/10.1017/S1477200006001940

Cox EJ (2014) Diatom identification in the face of changing species concepts and evidence of phenotypic plasticity. Journal of Micropalaeontology 33: 111-120. https://doi.org/10.1144/jmpaleo2014-014

Crawford RM, Hinz F, Honeywill C (1998) Three species of the diatom genus *Corethron* Castracane: structure, distribution and taxonomy. Diatom Research 13: 1-28. https://doi.org/10.1080/0269249X.1998.9705432

Danis B, Van de Putte A, Convey P, Griffiths H, Linse K, Murray AE (2020) Editorial: Antarctic Biology: Scale Matters. Frontiers in Ecology and Evolution 8: 91. https://doi.org/10.3389/fevo.2020.00091

Davidovich NA, Kaczmarska I, Ehrman MJ (2010) Heterothallic and homothallic sexual reproduction in *Tabularia fasciculata* (Bacillariophyta). Fottea 10: 251-266. https://doi.org/10.5507/fot.2010.016

Davidovich NA, Davidovich OI, Witkowski A, Li C, Dabek P, Mann DG, Zgłobicka I, Kurzydłowski KJ, Gusev E, Górecka E, Krzywda M (2017) Sexual reproduction in *Schizostauron* (Bacillariophyta) and a preliminary phylogeny of the genus. Phycologia 56: 77-93. https://doi.org/10.2216/16-29.1

Davies BJ, Hambrey MJ, Smellie JL, Carrivick JL, Glasser NF (2012) Antarctic Peninsula Ice Sheet evolution during the Cenozoic Era. Quaternary Science Reviews 31: 30-66. https://doi.org/10.1016/j.quascirev.2011.10.012

Day TA, Ruhland CT, Xiong FS (2008) Warming increases aboveground plant biomass and C stocks in vascular-plant-dominated Antarctic tundra. Global Change Biology 14: 1827-1843. https://doi.org/10.1111/j.1365-2486.2008.01623.x

Dayrat B (2005) Towards integrative taxonomy. Biological Journal of the Linnean Society 85: 407-417. https://doiorg/10.1111/j.1095-8312.2005.00503.x

de Brouwer JFC, Wolfstein K, Ruddy GK, Jones TER, Stal LJ (2005) Biogenic stabilization of intertidal sediments: the importance of extracellular polymeric substances produced by benthic diatoms. Microbial Ecology 49: 501-512. https://doi.org/10.1007/s00248-004-0020-z

De Broyer C, Clarke A, Koubbi P, Pakhomov E, Scott F, Vanden Berghe E, Danis B (2024) Register of Antarctic Marine Species.

De Luca D, Kooistra WH, Sarno D, Gaonkar CC, Piredda R (2019) Global distribution and diversity of *Chaetoceros* (Bacillariophyta, Mediophyceae): integration of classical and novel strategies. PeerJ 7: e7410. https://doi.org/10.7717/peerj.7410

de Queiroz K, Gauthier J (1990) Phylogeny as a central principle in taxonomy: Phylogenetic definitions of taxon names. Systematic Zoology 39: 307-322. https://doi.org/10.2307/2992353

Dickey JR, Swenie RA, Turner SC, Winfrey CC, Yaffar D, Padukone A, Beals KK, Sheldon KS, Kivlin SN (2021) The utility of macroecological rules for microbial biogeography. Frontiers in Ecology and Evolution 9. https://doi.org/10.3389/fevo.2021.633155

Ducklow HW, Clarke A, Dickhut R, Doney S, Geisz H, Huang K, Martinson D, Meredith M, Moeller H, Montes M, Schofield O, Stammerjohn S, Steinberg D, Fraser W (2012) The marine ecosystem of the West Antarctic Peninsula. In Antarctic Ecosystems: An Extreme Environment in a Changing World, edited by A. D. Rogers, N. M. Johnston, E. J. Murphy and A. Clarke, 121-59.

Ducklow HW, Fraser WR, Meredith MP, Stammerjohn SE, Doney SC, Martinson DG, Sailley SF, Schofield OM, Steinberg DK, Venables HJ, Amsler CD (2013) West Antarctic Peninsula: An ice-dependent coastal marine ecosystem in transition. Oceanography 26:190–203. https://doi.org/10.5670/oceanog.2013.62

Duncan RJ, Nielsen DA, Sheehan CE, Deppeler S, Hancock AM, Schulz KG, Davidson AT, Petrou K (2022) Ocean acidification alters the nutritional value of Antarctic diatoms. New Phytologist 233: 1813-1827. https://doi.org/10.1111/nph.17868

Edgar SM, Theriot EC (2004) Phylogeny of *Aulacoseira* (Bacillariophyta) based on molecules and morphology 1. Journal of Phycology 40: 772-788. https://doi.org/10.1111/j.1529-8817.2004.03126.x

Ehrenberg CG (1844) Einige vorläufige Resultate seiner Untersuchungen der ihm von der Südpolreise des Capitain Ross, so wie von den Herren Schayer und Darwin zugekommenen Materialien über das Verhalten des kleinsten Lebens in den Oceanen und den grössten bisher zugänglichen Tiefen des Weltmeeres, Bericht über die zurBekanntmachung Geeigneten Verhandlungen der KöniglichPreußische Akademie der Wissenschaften zu Berlin 1844:182–207.

Escalas A, Hale L, Voordeckers JW, Yang Y, Firestone MK, Alvarez-Cohen L, Zhou J (2019) Microbial functional diversity: From concepts to applications. Ecology and Evolution 9: 12000-12016. https://doi.org/10.1002/ece3.5670

Evans KM, Wortley AH, Mann DG (2007) An assessment of potential diatom "barcode" genes (cox1, rbcL, 18S and ITS rDNA) and their effectiveness in determining relationships in *Sellaphora* (Bacillariophyta). Protist 158: 349-364. https://doi.org/10.1016/j.protis.2007.04.001

Falciatore A, Jaubert M, Bouly J-P, Bailleul B, Mock T (2019) Diatom molecular research comes of age: Model species for studying phytoplankton biology and diversity. The Plant Cell 32: 547-572. https//doi.org/10.1105/tpc.19.00158

Fenchel T, Finlay BJ (2004) The ubiquity of small species: Patterns of local and global diversity. BioScience 54: 777-784. https://doi.org/10.1641/0006-3568(2004)054[0777:TUOSSP]2.0.CO;2

Field CB, Behrenfeld MJ, Randerson JT, Falkowski P (1998) Primary production of the biosphere: integrating terrestrial and oceanic components. Science 281: 237-40. https://doi.org/10.1126/science.281.5374.237

Finlay B (2002) Global dispersal of free-living microbial eukaryote species. Science 296: 1061-1063. https://doi.org/10.1126/science.1070710

Flori S, Jouneau P-H, Bailleul B, Gallet B, Estrozi LF, Moriscot C, Bastien O, Eicke S, Schober A, Bártulos CR, Maréchal E, Kroth PG, Petroutsos D, Zeeman S, Breyton C, Schoehn G, Falconet D, Finazzi G (2017) Plastid thylakoid architecture optimizes photosynthesis in diatoms. Nature Communications 8: 15885. https://doi.org/10.1038/ncomms15885

Foets J, Wetzel CE, Teuling AJ, Pfister L (2020) Temporal and spatial variability of terrestrial diatoms at the catchment scale: controls on productivity and comparison with other soil algae. PeerJ 8: e9198. https://doi.org/10.7717/peerj.9198

Furey P, Manoylov K, Lowe R (2020) New and interesting aerial diatom assemblages from southwestern Iceland. Phytotaxa 428: 173-208. https://doi.org/10.11646/phytotaxa.428.3.2

Geitler L (1973) Auxosporenbildung und Systematik bei pennaten Diatomeen und die Cytologie von *Cocconeis*-Sippen. Österreichische Botanische Zeitschrift 122: 299-321.

Gilbert NS (1991) Primary production by benthic microalgae in nearshore marine sediments of Signy Island, Antarctica. Polar Biology 11: 339-346. https://doi.org/10.1007/BF00239026

Glud RN, Kühl M, Wenzhoefer F, Rysgaard S (2002) Benthic diatoms of a high Arctic fjord (Young Sound, NE Greenland): Importance for ecosystem primary production. Marine Ecology Progress Series 238. https://doi.org/10.3354/meps238015

Glud RN, Woelfel J, Karsten U, Kühl M, Rysgaard S (2009) Benthic microalgal production in the Arctic: Applied methods and status of the current database. Botanica Marina 52: 559-571. https://doi.org/10.1515/BOT.2009.074

González-Herrero S, Barriopedro D, Trigo RM, López-Bustins JA, Oliva M (2022) Climate warming amplified the 2020 record-breaking heatwave in the Antarctic Peninsula. Communications Earth & Environment 3: 122. https://doi.org/10.1038/s43247-022-00450-5

Griffiths HJ (2010) Antarctic marine biodiversity – What do we know about the distribution of life in the Southern Ocean? PLoS ONE 5: e11683. https://doi.org/10.1371/journal.pone.0011683

Griffiths HJ, Barnes DKA, Linse K (2009) Towards a generalized biogeography of the Southern Ocean benthos. Journal of Biogeography 36: 162-177. https://doi.org/10.1111/j.1365-2699.2008.01979.x

Gu L, Grodzinski B, Han J, Marie T, Zhang YJ, Song YC, Sun Y (2022) Granal thylakoid structure and function: explaining an enduring mystery of higher plants. New Phytologist 236: 319-329. https://doi.org/10.1111/nph.18371

Guerrero JM, Riaux-Gobin C, Debandi JI, Zacher K, Quartino ML, Campana GL (2021) Morphology of *Australoneis* gen. nov. and *A. frenguelliae* comb. nov. (Achnanthales, Bacillariophyta) from the Antarctic Peninsula. Phytotaxa 513: 81-98. https://doi.org/10.11646/phytotaxa.513.2.1

Guiry MD, Guiry GM. 2024. Algaebase. World-wide electronic publication. National University of Ireland, Galway.

Guo L, Sui Z, Zhang S, Ren Y, Liu Y (2015) Comparison of potential diatom 'barcode' genes (the 18S rRNA gene and ITS, COI, rbcL) and their effectiveness in discriminating and determining species taxonomy in the Bacillariophyta. International Journal of Systematic and Evolutionary Microbiology 65: 1369-1380. https://doi.org/10.1099/ijs.0.000076

Hamsher SE, Evans KM, Mann DG, Poulíčková A, Saunders GW (2011) Barcoding diatoms: exploring alternatives to COI-5P. Protist 162: 405-22. https://doi.org/10.1016/j.protis.2010.09.005

Hanson CA, Fuhrman JA, Horner-Devine MC, Martiny JB (2012) Beyond biogeographic patterns: processes shaping the microbial landscape. Nature Reviews Microbiology 10: 497-506. https://doi.org/10.1038/nrmicro2795

Hargrave BT, Prouse NJ, Phillips GA, Neame PA (1983) Primary production and respiration in pelagic and benthic communities at two intertidal sites in the Upper Bay of Fundy. Canadian Journal of Fisheries and Aquatic Sciences 40: s229-s243. https://doi.org/10.1139/f83-286

Hebert PDN, Cywinska A, Ball SL, deWaard JR (2003) Biological identification through DNA barcodes. Proceedings of th Royal Society B 270: 313-321. https://doi.org/10.1098/rspb.2002.2218

Heiden H, Kolbe RW (1928) Die marinen Diatomeen der Deutschen Südpolar-Expedition 1901-1903. Vol. 8: W. de Gruyter & Company.

Henley SF, Schofield OM, Hendry KR, Schloss IR, Steinberg DK, Moffat C, Peck LS, Costa DP, Bakker DCE, Hughes C, Rozema PD, Ducklow HW, Abele D, Stefels J, Van Leeuwe MA, Brussaard CPD, Buma AGJ, Kohut J, Sahade R, Friedlaender AS, Stammerjohn SE, Venables HJ, Meredith MP (2019) Variability and change in the west Antarctic Peninsula marine system: Research priorities and opportunities. Progress in Oceanography 173: 208-237. https://doi.org/10.1016/j.pocean.2019.03.003

Hennig W (1966) Phylogenetic Systematics: University of Illinois Press.

Hildebrand M, Lerch SJ, Shrestha RP (2018) Understanding diatom cell wall silicification—moving forward. Frontiers in Marine Science 5: 125. https://doi.org/10.3389/fmars.2018.00125

Hoegh-Guldberg O, Jacob D, Bindi M, Brown S, Camilloni I, Diedhiou A, Djalante R, Ebi K, Engelbrecht F, Guiot J (2018) Impacts of 1.5 C global warming on natural and human systems. In: Global warming of 1.5° C. An IPCC Special Report on the Impacts of Global Warming of 1.5°C Above Pre-industrial Levels and Related Global Greenhouse Gas Emission Pathways, in the Context of Strengthening the Global Response to the Threat of Climate Change, Sustainable Development, and Efforts to Eradicate Poverty, edited by V. Masson-Delmotte, P. Zhai, H.-O. Pörtner, D. Roberts, J. Skea, P. R. Shukla, A. Pirani, W. Moufouma-Okia, C. Péan, R. Pidcock, S. Connors, J.B.R. Matthews, Y. Chen, X. Zhou, M.I. Gomis, E. Lonnoy, T. Maycock, M. Tignor and T. Waterfield.

Huang W, Haferkamp I, Lepetit B, Molchanova M, Hou S, Jeblick W, Río Bártulos C, Kroth PG (2018) Reduced vacuolar β-1, 3-glucan synthesis affects carbohydrate metabolism as well as plastid homeostasis and structure in Phaeodactylum tricornutum. Proceedings of the National Academy of Sciences 115: 4791-4796. https://doi.org/10.1073/pnas.1719274115

Hughes KA, Ashton GV (2017) Breaking the ice: the introduction of biofouling organisms to Antarctica on vessel hulls. Aquatic Conservation: Marine and Freshwater Ecosystems 27: 158-164. https://doi.org/10.1002/aqc.2625

Hustedt F (1958) Diatomeen aus der Antarktis und dem Südatlantik. Deutsche Antarktische Expedition 1938/1939. Hamburg: Geographisch-Kartographische Anstalt Mundus.

Jahn R, Abarca N, Gemeinholzer B, Mora D, Skibbe O, Kulikovskiy M, Gusev E, Kusber W-H, Zimmermann J (2017) *Planothidium lanceolatum* and *Planothidium frequentissimum* reinvestigated with molecular methods and morphology: four new species and the taxonomic importance of the sinus and cavum. Diatom Research 32: 75-107. https://doi.org/10.1080/0269249X.2017.1312548

Kaczmarska I, Mather L, Luddington IA, Muise F, Ehrman JM (2014) Cryptic diversity in a cosmopolitan diatom known as *Asterionellopsis glacialis* (Fragilariaceae): Implications for ecology, biogeography, and taxonomy. American Journal of Botany 101: 267-286. https://doi.org/10.3732/ajb.1300306

Kapli P, Yang Z, Telford MJ (2020) Phylogenetic tree building in the genomic age. Nature Reviews Genetics. 21: 428-444. https://doi.org/10.1038/s41576-020-0233-0

Karsten G (1906) Das Phytoplankton des antarktischen Meeres nach dem Material der deutschen Tiefsee-Expedition, 1898-1899. Vol. 2: G. Fischer.

Karsten U, Schaub I, Woelfel J, Sevilgen DS, Schlie C, Becker B, Wulff A, Graeve M, Wagner H (2019) Living on cold substrata: new insights and approaches in the study of microphytobenthos ecophysiology and ecology in Kongsfjorden. In: The Ecosystem of Kongsfjorden, Svalbard, edited by Haakon Hop and Christian Wiencke, 303-330. Basle, Switzerland: Springer Nature Switzerland AG:.

Karsten U, Schlie C, Woelfel J, Becker B (2012) Benthic diatoms in Arctic Seas-ecological functions and adaptations. Polarforschung 81: 77-84.

Karsten U, Wulff A, Roleda MY, Müller R, Steinhoff FS, Fredersdorf J, Wiencke C (2009) Physiological responses of polar benthic algae to ultraviolet radiation. Botanica Marina 52: 639-654. https://doi.org/10.1515/BOT.2009.077

Kellogg TB, Kellogg DE (2002) Non-marine and littoral diatoms from Antarctic and Subantarctic Regions. Edited by Andrzej Witkowski, Diatom Monographs: A.R.G. Gantner Verlag K.G.

Kelly M, Juggins S, Mann DG, Sato S, Glover R, Boonham N, Sapp M, Lewis E, Hany U, Kille P (2020) Development of a novel metric for evaluating diatom assemblages in rivers using DNA metabarcoding. Ecological Indicators 118: 106725. https://doi.org/10.1016/j.ecolind.2020.106725

Kermarrec L, Franc A, Rimet F, Chaumeil P, Humbert JF, Bouchez A (2013) Next-generation sequencing to inventory taxonomic diversity in eukaryotic communities: a test for freshwater diatoms. Molecular Ecology Resources 13: 607-19. https://doi.org/10.1111/1755-0998.12105

Kim JH, Ajani P, Murray SA, Kim J-H, Lim HC, Teng ST, Lim PT, Han M-S, Park BS (2020) Sexual reproduction and genetic polymorphism within the cosmopolitan marine diatom *Pseudo-nitzschia pungens*. Scientific Reports 10: 10653. https://doi.org/10.1038/s41598-020-67547-9

Kivlin SN, Fei S, Kalisz S, Averill C (2020) Microbial ecology meets macroecology. Bulletin of the Ecological Society of America. 101: 1-4. https://doi.org/10.1002/bes2.1645

Knowlton N (1993) Sibling Species in the Sea. Annual Review of Ecology and Systematics. 24: 189-216.

Kociolek JP, Spaulding SA (2002) Morphological variation, species concepts, and classification of an unusual fossil centric diatom (Bacillariophyta) from western North America. Journal of Phycology 38: 821-833. https://doi.org/10.1046/j.1529-8817.2002.02009.x

Kociolek JP, Stepanek JG, Lowe RL, Johansen JR, Sherwood AR (2013) Molecular data show the enigmatic cave-dwelling diatom *Diprora* (Bacillariophyceae) to be a raphid diatom. European Journal of Phycology 48: 474-484. https://doi.org/10.1080/09670262.2013.860239

Kohler TJ, Howkins A, Sokol ER, Kopalová K, Cox A, Darling JP, Gooseff MN, McKnight DM (2021) From the Heroic Age to today: What diatoms from Shackleton's Nimrod

expedition can tell us about the ecological trajectory of Antarctic ponds. Limnology and Oceanography Letters 6: 379-387. https://doi.org/10.1002/lol2.10200

Kooistra WH, Sarno D, Balzano S, Gu H, Andersen RA, Zingone A (2008) Global diversity and biogeography of *Skeletonema* species (Bacillariophyta). Protist 159: 177-93. https://doi.org/10.1016/j.protis.2007.09.004

Kooistra WHCF, Gersonde R, Medlin LK, Mann DG (2007) The origin and evolution of the diatoms: Their adaptation to a planktonic existence. In: Evolution of primary producers in the sea, edited by Paul G. Falkowski and Andrew H. Knoll, 207-249. Burlington: Academic Press.

Kooistra WHCF, Kusber W-H, Hernández-Becerril DU, Montresor M, Sarno D (2022) The type species of the diatom genus *Chaetoceros*. Diatom Research 37: 81-88. https://doi.org/10.1080/0269249X.2022.2066182

Kopalová K, Kociolek JP, Lowe RL, Zidarova R, Van de Vijver B (2015) Five new species of the genus *Humidophila* (Bacillariophyta) from the Maritime Antarctic Region. Diatom Research 30: 117-131. https://doi.org/10.1080/0269249X.2014.998714

Kulaš A, Udovič MG, Tapolczai K, Žutinić P, Orlić S, Levkov Z (2022) Diatom eDNA metabarcoding and morphological methods for bioassessment of karstic river. Science of The Total Environment 829: 154536. https://doi.org/10.1016/j.scitotenv.2022.154536

Kulikovskiy M, Andreeva S, Gusev E, Kuznetsova I, Annenkova N (2016) Molecular phylogeny of monoraphid diatoms and raphe significance in evolution and taxonomy. Biology Bulletin 43: 398-407. https://doi.org/10.1134/S1062359016050046

Kuriyama K, Gründling-Pfaff S, Diehl N, Woelfel J, Karsten U (2021) Microphytobenthic primary production on exposed coastal sandy sediments of the Southern Baltic Sea using ex situ sediment cores and oxygen optodes. Oceanologia 63: 247-260. https://doi.org/10.1016/j.oceano.2021.02.002

Lange-Bertalot H, Hofmann G, Werum M, Cantonati M, Kelly M (2017) Freshwater benthic diatoms of Central Europe: over 800 common species used in ecological assessment. Vol. 942: Koeltz Botanical Books Schmitten-Oberreifenberg.

Lazzara L, Nardello I, Ermanni C, Mangoni O, Saggiomo V (2007) Light environment and seasonal dynamics of microalgae in the annual sea ice at Terra Nova Bay (Ross Sea, Antarctica). Antarctic Science 19: 83-92. https://doi.org/10.1017/S0954102007000119

Lee JR, Terauds A, Carwardine J, Shaw JD, Fuller RA, Possingham HP, Chown SL, Convey P, Gilbert N, Hughes KA, McIvor E, Robinson SA, Ropert-Coudert Y, Bergstrom DM, Biersma EM, Christian C, Cowan DA, Frenot Y, Jenouvrier S, Kelley L, Lee MJ, Lynch HJ, Njåstad B, Quesada A, Roura RM, Shaw EA, Stanwell-Smith D, Tsujimoto M, Wall DH, Wilmotte A, Chadès I (2022) Threat management priorities for conserving Antarctic biodiversity. PLOS Biology 20(12): e3001921, https://doi.org/10.1371/journal.pbio.3001921

Leyland B, Boussiba S, Khozin-Goldberg I (2020) A review of diatom lipid droplets. Biology (Basel). 9. https://doi.org/10.3390/biology9020038

Lim HC, Tan SN, Teng ST, Lundholm N, Orive E, David H, Quijano-Scheggia S, Leong SCY, Wolf M, Bates SS, Lim PT, Leaw CP (2018) Phylogeny and species delineation in the

marine diatom *Pseudo-nitzschia* (Bacillariophyta) using cox1, LSU, and ITS2 rRNA genes: A perspective in character evolution. Journal of Phycology 54: 234-248. https://doi.org/10.1111/jpy.12620

Longhi M, Schloss I, Wiencke C (2003) Effect of irradiance and temperature on photosynthesis and growth of two Antarctic benthic diatoms, *Gyrosigma subsalinum* and *Odontella litigiosa*. Botanica Marina 46: 276-284. https://doi.org/10.1515/BOT.2003.025

Lüning K. (1990) Seaweeds: their environment, biogeography and ecophysiology. New York: Wiley.

MacIntyre HL, Geider RJ, Miller DC (1996) Microphytobenthos: The ecological role of the "secret garden" of unvegetated, shallow-water marine habitats. I. Distribution, abundance and primary production. Estuaries 19: 186-201. https://doi.org/10.2307/1352224

Majewska R, Gambi MC, Totti CM, De Stefano M (2013) Epiphytic diatom communities of Terra Nova Bay, Ross Sea, Antarctica: structural analysis and relations to algal host. Antarctic Science 25: 501-513. https://doi.org/10.1017/S0954102012001101

Maltsev Y, Maltseva S, Kociolek JP, Jahn R, Kulikovskiy M (2021) Biogeography of the cosmopolitan terrestrial diatom *Hantzschia amphioxys* sensu lato based on molecular and morphological data. Scientific Reports 11: 4266. https.//doi.org/10.1038/s41598-021-82092-9

Malviya S, Scalco E, Audic S, Vincent F, Veluchamy A, Poulain J, Wincker P, Iudicone D, de Vargas C, Bittner L, Zingone A, Bowler C (2016) Insights into global diatom distribution and diversity in the world's ocean. Proceedings of the National Academy of Sciences 113: E1516. https://doi.org/10.1073/pnas.1509523113

Mann A (1937) Report of the diatoms collected by the Australian Anarctic Expedition 1911-1914. Scientific Reports - Series C-Zoology and Botany 1: 5-82.

Mann DG (1999) The species concept in diatoms. Phycologia 38: 437-495. https://doi.org/10.2216/i0031-8884-38-6-437.1

Mann DG, Droop SJM (1996) Biodiversity, biogeography and conservation of diatoms. Hydrobiologia 336: 19-32. https://doi.org/10.1007/BF00010816

Mann DG, McDonald SM, Bayer MM, Droop SJ, Chepurnov VA, Loke RE, Ciobanu A, Du Buf JH (2004) The *Sellaphora pupula* species complex (Bacillariophyceae): morphometric analysis, ultrastructure and mating data provide evidence for five new species. Phycologia 43: 459-482.

Mann DG, Trobajo R, Sato S, Li C, Witkowski A, Rimet F, Ashworth MP, Hollands RM, Theriot EC (2021) Ripe for reassessment: A synthesis of available molecular data for the speciose diatom family Bacillariaceae. Molecular Phylogenetics and Evolution 158: 106985. https://doi.org/10.1016/j.ympev.2020.106985

Mann DG, Vanormelingen P (2013) An inordinate fondness? The number, distributions, and origins of diatom species. The Journal of Eukaryotic Microbiology 60: 414-20. https://doi.org/10.1111/jeu.12047

Martin W, Stoebe B, Goremykin V, Hansmann S, Hasegawa M, Kowallik KV (1998) Gene transfer to the nucleus and the evolution of chloroplasts. Nature 393: 162-165. https://doi.org/10.1038/30234

Martiny JBH, Bohannan BJ, Brown JH, Colwell RK, Fuhrman JA, Green JL, Horner-Devine MC, Kane M, Krumins JA, Kuske CR (2006) Microbial biogeography: putting microorganisms on the map. Nature Reviews Microbiology 4: 102-112. https://doi.org/10.1038/nrmicro1341

McCarthy AH, Peck LS, Aldridge DC (2022) Ship traffic connects Antarctica's fragile coasts to worldwide ecosystems. Proceedings of the National Academy of Sciences 119: e2110303118. https://doi.org/10.1073/pnas.211030311

McCarthy AH, Peck LS, Hughes KA, Aldridge DC (2019) Antarctica: The final frontier for marine biological invasions. Global Change Biology 25: 2221-2241. https://doi.org/10.1111/gcb.14600

McMinn A, Ashworth C, Bhagooli R, Martin A, Salleh S, Ralph P, Ryan K (2012) Antarctic coastal microalgal primary production and photosynthesis. Marine Biology 159. https://doi.org/10.1007/s00227-012-2044-0

Medlin LK (2016) Evolution of the diatoms: major steps in their evolution and a review of the supporting molecular and morphological evidence. Phycologia 55: 79-103. 10.2216/15-105.1

Medlin LK, Kaczmarska I (2004) Evolution of the diatoms: V. Morphological and cytological support for the major clades and a taxonomic revision. Phycologia 43: 245-270. https://doi.org/10.2216/i0031-8884-43-3-245.1

Moeys S, Frenkel J, Lembke C, Gillard JTF, Devos V, Van den Berge K, Bouillon B, Huysman MJJ, De Decker S, Scharf J, Bones A, Brembu T, Winge P, Sabbe K, Vuylsteke M, Clement L, De Veylder L, Pohnert G, Vyverman W (2016) A sex-inducing pheromone triggers cell cycle arrest and mate attraction in the diatom *Seminavis robusta*. Scientific Reports 6: 19252. https://doi.org/10.1038/srep19252

Mohamad H, Mora D, Skibbe O, Abarca N, Deutschmeyer V, Enke N, Kusber W-H, Zimmermann J, Jahn R (2022) Morphological variability and genetic marker stability of 16 monoclonal pennate diatom strains under medium-term culture. Diatom Research 37: 307-328. https://doi.org/10.1080/0269249X.2022.2141346

Moniz MB, Kaczmarska I (2009) Barcoding diatoms: Is there a good marker? Molecular Ecology Resources 9: 65-74. https://doi.org/10.1111/j.1755-0998.2009.02633.x

Montes-Hugo M, Doney SC, Ducklow HW, Fraser W, Martinson D, Stammerjohn SE, Schofield O (2009) Recent changes in phytoplankton communities associated with rapid regional climate change along the Western Antarctic Peninsula. Science 323: 1470-1473. https://doi.org/10.1126/science.1164533

Montresor M, Vitale L, D'Alelio D, Ferrante M (2016) Sex in marine planktonic diatoms: insights and challenges. Perspectives in Phycology Vol. 3: 61-75. https://doi.org/10.1127/pip/2016/0045

Mora C, Tittendor DP, Adl S, Simpson AGB, Worm B (2011) How many species are there on Earth and in the ocean? PLOS Biology 9: e1001127. https://doi.org/10.1371/journal.pbio.1001127

Mora D, Abarca N, Proft S, Grau JH, Enke N, Carmona J, Skibbe O, Jahn R, Zimmermann J (2019) Morphology and metabarcoding: a test with stream diatoms from Mexico

highlights the complementarity of identification methods. Freshwater Science 38: 448-464. https://doi.org/10.1086/704827

Morales E, A., Siver PA, Trainor FR (2001) Identification of diatoms (Bacillariophyceae) during ecological assessments: Comparison between Light Microscopy and Scanning Electron Microscopy techniques. Proceedings of the Academy of Natural Sciences of Philadelphia 151: 95-103.

Moritz C, Cicero C (2004) DNA barcoding: promise and pitfalls. PLoS biology 2: e354. https://doi.org/10.1371/journal.pbio.0020354

Morozov AA, Galachyants YP (2019) Diatom genes originating from red and green algae: Implications for the secondary endosymbiosis models. Marine Genomics 45: 72-78. https://doi.org/10.1016/j.margen.2019.02.003

Mortágua A, Vasselon V, Oliveira R, Elias C, Chardon C, Bouchez A, Rimet F, João Feio M, F.P. Almeida S (2019) Applicability of DNA metabarcoding approach in the bioassessment of Portuguese rivers using diatoms. Ecological Indicators 106: 105470. https://doi.org/10.1016/j.ecolind.2019.105470

Moser G, Lange-Bertalot H, Metzeltin D (1998) Island of endemics New Caledonia–a geobotanical phenomenon. Bibliotheca Diatomologica 38.

Moustafa A, Beszteri B, Maier UG, Bowler C, Valentin K, Bhattacharya D (2009) Genomic footprints of a cryptic plastid endosymbiosis in diatoms. Science 324: 1724-6. https://doi.org/10.1126/science.1172983

Murray C (2005) Mapping Terra Incognita. Polar Record 41: 103-112. https://doi.org/10.1017/S0032247405004249

Myklestad S (1974) Production of carbohydrates by marine planktonic diatoms. I. Comparison of nine different species in culture. Journal of Experimental Marine Biology and Ecology 15: 261-274. https://doi.org/10.1016/0022-0981(74)90049-5

Nadler SA (1995) Advantages and disadvantages of molecular phylogenetics: a case study of ascaridoid nematodes. The Journal of Nematology 27: 423-32.

Nakov T, Beaulieu JM, Alverson AJ (2018a) Accelerated diversification is related to life history and locomotion in a hyperdiverse lineage of microbial eukaryotes (Diatoms, Bacillariophyta). New Phytologist 219: 462-473. https://doi.org/10.1111/nph.15137

Nakov T, Beaulieu JM, Alverson AJ (2018b) Insights into global planktonic diatom diversity: The importance of comparisons between phylogenetically equivalent units that account for time. ISME Journal 12: 2807-2810. https://doi.org/10.1038/s41396-018-0221-y

Nisbet RER, Kilian O, McFadden GI (2004) Diatom genomics: Genetic acquisitions and mergers. Current Biology 14: R1048-R1050. https://doi.org/10.1016/j.cub.2004.11.043

Nissen C, Lovenduski NS, Brooks CM, Hoppema M, Timmermann R, Hauck J (2024) Severe 21st-century ocean acidification in Antarctic Marine Protected Areas. Nature Communications 15: 259. https://doi.org/10.1038/s41467-023-44438-x

Palmisano AC, SooHoo JB, White DC, Smith GA, Stanton GR, Burckle LH (1985) Shade adapted benthic diatoms beneath Antarctic sea ice. Journal of Phycology 21: 664-667. https://doi.org/10.1111/j.0022-3646.1985.00664.x

Pan XL, Li BF, Watanabe YW (2022) Intense ocean freshening from melting glacier around the Antarctica during early twenty-first century. Scientific Reports 12: 383. https://doi.org/10.1038/s41598-021-04231-6

Parks MB, Wickett NJ, Alverson AJ (2018) Signal, uncertainty, and conflict in phylogenomic data for a diverse lineage of microbial eukaryotes (Diatoms, Bacillariophyta). Molecular Biology and Evolution 35: 80-93. https://10.1093/molbev/msx268

Pavlov A, Leu E, Dieter H, Bartsch I, Karsten U, Hudson S, Gallet J-C, Cottier F, Cohen J, Berge J, Johnsen G, Maturilli M, Kowalczuk P, Sagan S, Meler J, Granskog M (2019) The underwater light climate in Kongsfjorden and its ecological implications. In The Ecosystem of Kongsfjorden, Svalbard, edited by Haakon Hop and Christian Wiencke, 137-170. Springer, Cham.

Peck L (2018) Antarctic marine biodiversity: Adaptations, environments and responses to change. In Oceanography and Marine Biology, edited by S. J. Hawkins, A. J. Evans, A.C. Dale, L. B. Firth and I. P. Smith, 105-236.

Peragallo M (1921) Botanique: Diatomées d'eau douce et Diatomées d'eau salée. Paper read at Expédition Antarctique Française 1908-1910.

Pérez-Burillo J, Trobajo R, Vasselon V, Rimet F, Bouchez A, Mann DG (2020) Evaluation and sensitivity analysis of diatom DNA metabarcoding for WFD bioassessment of Mediterranean rivers. Science of The Total Environment 727: 138445. https://doi.org/10.1016/j.scitotenv.2020.138445

Pérez-Burillo J, Valoti G, Witkowski A, Prado P, Mann DG, Trobajo R (2022) Assessment of marine benthic diatom communities: insights from a combined morphological–metabarcoding approach in Mediterranean shallow coastal waters. Marine Pollution Bulletin 174: 113183. https://doi.org/10.1016/j.marpolbul.2021.113183

Pinckney JL (2018) A mini-review of the contribution of benthic microalgae to the ecology of the continental shelf in the South Atlantic Bight. Estuaries and Coasts 41: 2070-2078. https://doi.org/10.1007/s12237-018-0401-z

Pinseel E, Janssens SB, Verleyen E, Vanormelingen P, Kohler TJ, Biersma EM, Sabbe K, Van de Vijver B, Vyverman W (2020) Global radiation in a rare biosphere soil diatom. Nature Communications 11: 2382. https://doi.org/10.1038/s41467-020-16181-0

Pinseel E, Kulichová J, Scharfen V, Urbánková P, Van de Vijver B, Vyverman W (2019) Extensive cryptic diversity in the terrestrial diatom *Pinnularia borealis* (Bacillariophyceae). Protist 170: 121-140. https://doi.org/10.1016/j.protis.2018.10.001

Piredda R, Claverie J-M, Decelle J, de Vargas C, Dunthorn M, Edvardsen B, Eikrem W, Forster D, Kooistra WHCF, Logares R, Massana R, Montresor M, Not F, Ogata H, Pawlowski J, Romac S, Sarno D, Stoeck T, Zingone A (2018) Diatom diversity through HTS-metabarcoding in coastal European seas. Scientific Reports 8: 18059. 10.1038/s41598-018-36345-9

Postel U, Glemser B, Salazar Alekseyeva K, Eggers SL, Groth M, Glöckner G, John U, Mock T, Klemm K, Valentin K, Beszteri B (2020) Adaptive divergence across Southern Ocean gradients in the pelagic diatom *Fragilariopsis kerguelensis*. Molecular Ecology 29: 4913-4924. https://doi.org/10.1111/mec.15554

Poulíčková A, Mann DG (2019) Diatom sexual reproduction and life cycles. In: Diatoms: Fundamentals and Applications, 245-272.

Poulsen NC, Spector I, Spurck TP, Schultz TF, Wetherbee R (1999) Diatom gliding is the result of an actin-myosin motility system. Cell Motility 44: 23-33. https://doi.org/10.1002/(SICI)1097-0169(199909)44:1<23::AID-CM2>3.0.CO;2-D

Preston TM, King CA, Hyams JS (1990) The cytoskeleton and cell motility: Springer.

Prihoda J, Tanaka A, de Paula WB, Allen JF, Tirichine L, Bowler C (2012) Chloroplast-mitochondria cross-talk in diatoms. Journal of Experimental Botany 63: 1543-57. https://doi.org/10.1093/jxb/err441

Prosser JI, Bohannan BJ, Curtis TP, Ellis RJ, Firestone MK, Freckleton RP, Green JL, Green LE, Killham K, Lennon JJ, Osborn AM, Solan M, van der Gast CJ, Young JP (2007) The role of ecological theory in microbial ecology. Nature Reviews Microbiology 5: 384-92. https://doi.org/10.1038/nrmicro1643

Rastogi A, Vieira FRJ, Deton-Cabanillas AF, Veluchamy A, Cantrel C, Wang G, Vanormelingen P, Bowler C, Piganeau G, Hu H, Tirichine L (2020) A genomics approach reveals the global genetic polymorphism, structure, and functional diversity of ten accessions of the marine model diatom *Phaeodactylum tricornutum*. Isme j 14: 347-363. https://doi.org/10.1038/s41396-019-0528-3

Ricklefs RE (1987) Community diversity: relative roles of local and regional processes. Science 235: 167-171. https://doi.org/10.1126/science.235.4785.167

Rignot E, Mouginot J, Scheuchl B, Van Den Broeke M, Van Wessem MJ, Morlighem M (2019) Four decades of Antarctic Ice Sheet mass balance from 1979–2017. Proceedings of the National Academy of Sciences 116: 1095-1103. https://doi.org/10.1073/pnas.1812883116

Rimet F, Gusev E, Kahlert M, Kelly MG, Kulikovskiy M, Maltsev Y, Mann DG, Pfannkuchen M, Trobajo R, Vasselon V, Zimmermann J, Bouchez A (2019) Diat.barcode, an open-access curated barcode library for diatoms. Scientific Reports 9: 15116. 10.1038/s41598-019-51500-6

Rimet F, Pinseel E, Bouchez A, Japoshvili B, Mumladze L (2023) Diatom endemism and taxonomic turnover: Assessment in high-altitude alpine lakes covering a large geographical range. Science of The Total Environment 871: 161970. https://doi.org/10.1016/j.scitotenv.2023.161970

Rimet F, Vasselon V, A.-Keszte B, Bouchez A (2018) Do we similarly assess diversity with microscopy and high-throughput sequencing? Case of microalgae in lakes. Organisms Diversity & Evolution 18: 51-62. 10.1007/s13127-018-0359-5

Risgaard-Petersen N, Rysgaard S, Nielsen LP, Revsbech NP, oceanography (1994) Diurnal variation of denitrification and nitrification in sediments colonized by benthic microphytes. Limnology and Oceanography 39: 573-579. https://doi.org/10.4319/lo.1994.39.3.0573

Ross JC (1847) A voyage of discovery and research in the Southern and Antarctic Regions, during the years 1839-43: London J. Murray.

Round FE, Crawford RM, Mann DG (1990) The diatoms: biology and morphology of the genera: Cambridge University Press.

Ruck EC, Theriot EC (2011) Origin and evolution of the canal raphe system in diatoms. Protist 162: 723-737. https://doi.org/10.1016/j.protis.2011.02.003

Rynearson TA, Bishop IW, Collins S (2022) The population genetics and evolutionary potential of diatoms. In: The molecular life of diatoms, edited by A. Falciatore and T. Mock. Springer International Publishing. https://doi.org/10.1007/978-3-030-92499-7_2

Sandall EL, Maureaud AA, Guralnick R, McGeoch MA, Sica YV, Rogan MS, Booher DB, Edwards R, Franz N, Ingenloff K, Lucas M, Marsh CJ, McGowan J, Pinkert S, Ranipeta A, Uetz P, Wieczorek J, Jetz W (2023) A globally integrated structure of taxonomy to support biodiversity science and conservation. Trends in Ecology & Evolution 38: 1143-1153. https://doi.org/10.1016/j.tree.2023.08.004

Schaub I, Wagner H, Graeve M, Karsten U (2017) Effects of prolonged darkness and temperature on the lipid metabolism in the benthic diatom *Navicula perminuta* from the Arctic Adventfjorden, Svalbard. Polar Biology 40: 1425-1439. https://doi.org/10.1007/s00300-016-2067-y

Schlie C, Karsten U (2017) Microphytobenthic diatoms isolated from sediments of the Adventfjorden (Svalbard): growth as function of temperature. Polar Biology 40. https://doi.org/10.1007/s00300-016-2030-y

Schnell IB, Bohmann K, Gilbert MTP (2015) Tag jumps illuminated – reducing sequence-to-sample misidentifications in metabarcoding studies. Molecular Ecology Resources 15: 1289-1303. https://doi.org/10.1111/1755-0998.12402

Scornavacca C, Delsuc F, Galtier N (2020) Phylogenetics in the genomic era: No commercial publisher. Authors open access book, p.p. 1-568, 978-2-9575069-0-3. hal-02535070v3

Sevilgen DS, de Beer D, Al-Handal A, Brey T, Polerecky L (2014) Oxygen budgets in subtidal arctic (Kongsfjorden, Svalbard) and temperate (Helgoland, North Sea) microphytobenthic communities. Marine Ecology Progress Series 504: 27-42. https://doi.org/10.3354/meps10672

Shetye SS, Mohan R, Patil S, Kumar A (2021) Diatom distribution in the Enderby Basin, East Antarctica. Polar Science 30: 100748. https://doi.org/10.1016/j.polar.2021.100748

Shih PM, Matzke NJ (2013) Primary endosymbiosis events date to the later Proterozoic with cross-calibrated phylogenetic dating of duplicated ATPase proteins. Proceedings of the National Acadamy of Sciiences of the United States of America 110: 12355-60. https://doi.org/10.1073/pnas.1305813110

Siegert M, Atkinson A, Banwell A, Brandon M, Convey P, Davies B, Downie R, Edwards T, Hubbard B, Marshall G, Rogelj J, Rumble J, Stroeve J, Vaughan D (2019) The Antarctic Peninsula Under a 1.5°C Global Warming Scenario. Frontiers in Environmental Science 7. https://doi.org/10.3389/fenvs.2019.00102

Silva PC (2008) Historical review of attempts to decrease subjectivity in species identification, with particular regard to algae. Protist 159: 153-161. https://doi.org/10.1016/j.protis.2007.10.001

Simonsen R. (1992) The diatom types of Heinrich Heiden in Heiden & Kolbe 1928. Vol. 24, Bibliotheca Diatomologica: J. Cramer

Skibbe O, Abarca N, Forrest F, Werner P (2022) Exploring diatom diversity through cultures-a case study from the Bow River, Canada. Journal of Limnology 81. https://doi.org/10.4081/jlimnol.2022.2095

Smayda TJ (2011) Cryptic planktonic diatom challenges phytoplankton ecologists. Proceedings of the National Academy of Sciences 108: 4269-4270. https://doi.org/10.1073/pnas.1100997108

Snoeijs P (1996) The establishment of Lunella gen. nov. (Bacillariophyta). Diatom Research 11: 143-154. https://doi.org/10.1080/0269249X.1996.9705369

Sohail T, Gayen B, Klocker A (2023) Future decline of Antarctic Circumpolar Current due to polar ocean freshening.

Srivastava N, Gupta B, Gupta S, Danquah MK, Sarethy IP. (2019) Analyzing functional microbial diversity: An overview of techniques. In: Microbial diversity in the genomic era, edited by Surajit Das and Hirak Ranjan Dash, 79-102. Academic Press.

Stachura-Suchoples K, Enke N, Schlie C, Schaub I, Karsten U, Jahn R (2015) Contribution towards a morphological and molecular taxonomic reference library of benthic marine diatoms from two Arctic fjords on Svalbard (Norway). Polar Biology 39: 1933-1956. 10.1007/s00300-015-1683-2

Stiller JW, Schreiber J, Yue J, Guo H, Ding Q, Huang J (2014) The evolution of photosynthesis in chromist algae through serial endosymbioses. Nature Communications 5: 5764. https://doi.org/10.1038/ncomms6764

Stoof-Leichsenring KR, Epp LS, Trauth MH, Tiedemann R (2012) Hidden diversity in diatoms of Kenyan Lake Naivasha: a genetic approach detects temporal variation. Molecular Ecology 21: 1918-1930. https://doi.org/10.1111/j.1365-294X.2011.05412.x

Summerhayes C, Ainley D, Barrett P, Bindschadler R, Clarke A, Convey P, Fahrbach E, Gutt J, Hodgson D, Meredith M, Murray AS, Pörtner H-O, di Prisco G, Schiel K, Speer K, Turner J, Verde C, Willems A (2009) The Antarctic environment in the global system. In Antarctic climate change and the environment, edited by John Turner, R. Bindschader, P. Convey, G. di Prisco, E. Fahrbach, J. Gutt, D. Hodgson, P. Mayewski and C. Summerhayes, 1-32.

Taberlet P, Bonin A, Zinger L, Coissac É (2018) Environmental DNA: For Biodiversity Research and Monitoring: Oxford University Press.

Taberlet P, Coissac E, Pompanon F, Brochmann C, Willerslev E (2012) Towards next-generation biodiversity assessment using DNA metabarcoding. Molecular Ecology 21: 2045-2050. https://doi.org/10.1111/j.1365-294X.2012.05470.x

Taucher J, Bach LT, Prowe AEF, Boxhammer T, Kvale K, Riebesell U (2022) Enhanced silica export in a future ocean triggers global diatom decline. Nature 605: 696–700. https://doi.org/10.1038/s41586-022-04687-0

Terauds A, Chown SL, Morgan F, J. Peat H, Watts DJ, Keys H, Convey P, Bergstrom DM (2012) Conservation biogeography of the Antarctic. Diversity and Distributions 18: 726-741. https://doi.org/10.1111/j.1472-4642.2012.00925.x

Theriot EC, Cannone JJ, Gutell RR, Alverson AJ (2009) The limits of nuclear-encoded SSU rDNA for resolving the diatom phylogeny. European Journal of Phycology 44: 277-290. https://doi.org/10.1080/09670260902749159

Thomas EW, Stepanek JG, Kociolek JP (2016) Historical and current perspectives on the systematics of the 'enigmatic' diatom genus *Rhoicosphenia* (Bacillariophyta), with single and multi-molecular marker and morphological analyses and discussion on the monophyly of 'monoraphid' diatoms. PLoS One 11: e0152797. https://doi.org/10.1371/journal.pone.0152797

Torstensson A, Jiménez C, Nilsson AK, Wulff A (2019) Elevated temperature and decreased salinity both affect the biochemical composition of the Antarctic sea-ice diatom *Nitzschia lecointei*, but not increased pCO2. Polar Biology 42: 2149-2164. https://doi.org/10.1007/s00300-019-02589-y

Tréguer P, Bowler C, Moriceau B, Dutkiewicz S, Gehlen M, Aumont O, Bittner L, Dugdale R, Finkel Z, Iudicone D, Jahn O, Guidi L, Lasbleiz M, Leblanc K, Levy M, Pondaven P (2018) Influence of diatom diversity on the ocean biological carbon pump. Nature Geoscience 11: 27-37. https://doi.org/10.1038/s41561-017-0028-x

Trobajo R, Mann DG, Clavero E, Evans KM, Vanormelingen P, McGregor RC (2010) The use of partial cox 1, rbc L and LSU rDNA sequences for phylogenetics and species identification within the Nitzschia palea species complex (Bacillariophyceae). European Journal of Phycology 45: 413-425. https://doi.org/10.1080/09670262.2010.498586

Turner J, Anderson P, Lachlan-Cope T, Colwell S, Phillips T, Kirchgaessner A, Marshall GJ, King JC, Bracegirdle T, Vaughan DG, Lagun V, Orr A (2009) Record low surface air temperature at Vostok station, Antarctica. Journal of Geophysical Research: Atmospheres 114. https://doi.org/10.1029/2009JD012104

Underwood GJC, Kromkamp J. (1999) Primary production by phytoplankton and microphytobenthos in estuaries. In: Advances in Ecological Research, edited by D. B. Nedwell and D. G. Raffaelli, 93-153. Academic Press.

Van De Vijver B, Kopalová K, Zidarova R, Kociolek JP (2016) Two new *Gomphonema* species (Bacillariophyta) from the Maritime Antarctic Region. Phytotaxa 269: 209–220-209–220. https://doi.org/10.11646/phytotaxa.269.3.4

Van de Vijver B, Kopalová K, Zidarova R, Levkov Z (2014) Revision of the genus *Halamphora* (Bacillariophyta) in the Antarctic Region. Plant Ecology and Evolution 147: 374-391. https://doi.org/10.5091/plecevo.2014.979

Van de Vijver B, Ledeganck P, Beyens L (2002) Soil diatom communities from Ile de la Possession (Crozet, sub-Antarctica). Polar Biology 25: 721-729. https.//doi.org/10.1007/s00300-002-0392-9

Van Heurck H (1909) Voyage du SY Belgica 1897-1899. Botanique: Diatomées.

Vanormelingen P, Verleyen E, Vyverman W (2008) The diversity and distribution of diatoms: from cosmopolitanism to narrow endemism. Biodiversity and Conservation 17: 393-405. https://doi.org/10.1007/s10531-007-9257-4

Vasselon V, Rimet F, Tapolczai K, Bouchez A (2017) Assessing ecological status with diatoms DNA metabarcoding: Scaling-up on a WFD monitoring network (Mayotte island, France). Ecological Indicators. 82: 1-12. https://doi.org/10.1016/j.ecolind.2017.06.024

Verleyen E, Van de Vijver B, Tytgat B, Pinseel E, Hodgson DA, Kopalová K, Chown SL, Van Ranst E, Imura S, Kudoh S, Van Nieuwenhuyze W, Sabbe K, Vyverman W (2021)

Diatoms define a novel freshwater biogeography of the Antarctic. Ecography 44: 548-560. https://doi.org/10.1111/ecog.05374

Vyverman W, Verleyen E, Wilmotte A, Hodgson DA, Willems A, Peeters K, Van de Vijver B, De Wever A, Leliaert F, Sabbe K (2010) Evidence for widespread endemism among Antarctic micro-organisms. Polar Science 4: 103-113. https://doi.org/10.1016/j.polar.2010.03.006

Wagner H, Jakob T, Wilhelm C (2006) Balancing the energy flow from captured light to biomass under fluctuating light conditions. New Phytologist 169: 95-108. https://doi.org/10.1111/j.1469-8137.2005.01550.x

Wang Y, Liu S, Wang J, Yao Y, Chen Y, Xu Q, Zhao Z, Chen N (2022) Diatom biodiversity and speciation revealed by comparative analysis of mitochondrial genomes. Frontiers in Plant Science 13. https://doi.org/10.3389/fpls.2022.749982

Wenne R (2023) Single Nucleotide Polymorphism Markers with Applications in Conservation and Exploitation of Aquatic Natural Populations. Animals 13. https://doi.org/10.3390/ani13061089

Wetzel CE, Martínez-Carreras N, Hlúbiková D, Hoffmann L, Pfister L, Ector L (2013) New combinations and type analysis of *Chamaepinnularia* species (Bacillariophyceae) from aerial habitats. Cryptogamie, Algologie 34: 149-168. https://doi.org/10.7872/crya.v34.iss2.2013.149

Witkowski A, Ashworth M, Li C, Sagna I, Yatte D, Górecka E, Franco AOR, Kusber W-H, Klein G, Lange-Bertalot H, Dąbek P, Theriot EC, Manning SR (2020) Exploring diversity, taxonomy and phylogeny of diatoms (Bacillariophyta) from marine habitats. Novel taxa with internal costae. Protist 171: 125713. https://doi.org/10.1016/j.protis.2020.125713

Witkowski A, Lange-Bertalot H, Metzeltin D (2000) Diatom Flora of Marine Coasts I. Edited by Horst Lange-Bertalot. Vol. 7, Iconographia Diatomologica: Koeltz Scientific Books.

Woelfel J, Schumann R, Peine F, Flohr A, Kruss A, Tegowski J, Blondel P, Wiencke C, Karsten U (2010) Microphytobenthos of Arctic Kongsfjorden (Svalbard, Norway): biomass and potential primary production along the shore line. Polar Biology 33: 1239-1253. https://doi.org/10.1007/s00300-010-0813-0

Wulff A, Roleda M, Zacher K, Wiencke C (2008) Exposure to sudden light burst after prolonged darkness - A case study on benthic diatoms in Antarctica. Diatom Research 23: 519-532. https://doi.org/10.1080/0269249X.2008.9705774

Xu XJ, Chen ZY, Lundholm N, Li Y (2019) Diversity in the section Compressa of the genus *Chaetoceros* (Bacillariophyceae), with description of two new species from Chinese warm waters. Journal of Phycology 55: 104-117. https://doi.org/10.1111/jpy.12807

Zacher K, Hanelt D, Wiencke C, Wulff A (2007) Grazing and UV radiation effects on an Antarctic intertidal microalgal assemblage: a long-term field study. Polar Biology 30: 1203-1212. https://doi.org/10.1007/s00300-007-0278-y

Zacher K, Rautenberger R, Dieter H, Wulff A, Wiencke C (2009) The abiotic environment of polar marine benthic algae. Botanica Marina 52: 483-490. https://doi.org/10.1515/BOT.2009.082

Zidarova R, Ivanov P, Hineva E, Dzhembekova N (2022) Diversity and habitat preferences of benthic diatoms from South Bay (Livingston Island, Antarctica). Plant Ecology and Evolution 155: 70-106. https://doi.org/10.5091/plecevo.84534

Zidarova R, Kopalová K, Van de Vijver B (2016) Ten new Bacillariophyta species from James Ross Island and the South Shetland Islands (Maritime Antarctic Region). Phytotaxa 272: 37. https://doi.org/10.11646/phytotaxa.272.1.2

Zimmermann J, Abarca N, Enke N, Skibbe O, Kusber W-H, Jahn R (2014) Taxonomic reference libraries for environmental barcoding: a best practice example from diatom research. PloS ONE 9: e108793. 10.1371/journal.pone.0108793

Zimmermann J, Glöckner G, Jahn R, Enke N, Gemeinholzer B (2015) Metabarcoding vs. morphological identification to assess diatom diversity in environmental studies. Molecular Ecology Resources 15: 526-542. https://doi.org/10.1111/1755-0998.12336

Zimmermann J, Jahn R, Gemeinholzer B (2011) Barcoding diatoms: evaluation of the V4 subregion on the 18S rRNA gene, including new primers and protocols. Organisms diversity & evolution 11: 173-192. https://doi.org/10.1007/s13127-011-0050-6

Zinger L, Bonin A, Alsos IG, Bálint M, Bik H, Boyer F, Chariton AA, Creer S, Coissac E, Deagle BE, De Barba M, Dickie IA, Dumbrell AJ, Ficetola GF, Fierer N, Fumagalli L, Gilbert MTP, Jarman S, Jumpponen A, Kauserud H, Orlando L, Pansu J, Pawlowski J, Tedersoo L, Thomsen PF, Willerslev E, Taberlet P (2019) DNA metabarcoding - Need for robust experimental designs to draw sound ecological conclusions. Molecular Ecology 28: 1857-1862. https://doi.org/10.1111/mec.15060

List of publications with contributions

Chapter 2

Schimani K, Abarca N, Skibbe O, Mohamad H, Jahn R, Kusber W-H, Campana GL, Zimmermann J (2023) Exploring benthic diatom diversity in the West Antarctic Peninsula: insights from a morphological and molecular approach. Metabarcoding and Metagenomics 7:339-384. https://doi.org/10.3897/mbmg.7.110194

KS and JZ developed the concept of this study. JZ and GC sampled and OS isolated, purified and established clonal cultures. KS, HM and JZ performed the metabarcoding analysis. KS provided the light microscopic analysis and KS, NA and RJ did the taxonomic identification. NA and WHK are responsible for the curation and data curation. KS wrote the first version of the paper. All authors edited and approved the final version of this manuscript.

Chapter 3

Schimani K, Abarca N, Zimmermann J, Skibbe O, Jahn R, Kusber W-H, Leya T, Mora D (2023) Molecular phylogenetics coupled with morphological analyses of Arctic and Antarctic strains place *Chamaepinnularia* (Bacillariophyta) within the Sellaphoraceae. Fottea 24(1):1-22. https://doi.org/10.5507/fot.2023.002

DM, KS, RJ developed the idea and elaborated the concept. OS and TL provided the isolates and parts of the text. KS and NA provided taxonomical data. KS, DM and JZ performed molecular analysis. WHK, RJ, NA and KS performed the nomenclature act. KS and DM wrote the manuscript, which was commented, edited, and finally accepted by all authors.

Chapter 4

Juchem DP, **Schimani K**, Holzinger A, Permann C, Abarca N, Skibbe O, Zimmermann J, Graeve M, Karsten U (2023) Lipid degradation and photosynthetic traits after prolonged darkness in four Antarctic benthic diatoms, including the newly described species *Planothidium wetzelii* sp. nov. Frontiers in Microbiology 14:1241826.
https://doi.org/10.3389/fmicb.2023.1241826

DJ and KS contributed equally to this work and share first authorship.

UK and JZ developed the concept for this manuscript. JZ sampled and OS isolated, purified, and established clonal cultures. DJ conducted the ecophysiological and biochemical parts of the manuscript. KS provided the light microscopic and scanning electron microscopic analyses. CP and AH undertook the transmission electron microscopy, combined the transmission electron micrographs, and edited the manuscript. KS and NA performed the taxonomic treatment. MG provided the GC-MS data. DJ and KS wrote the first version of the manuscript and prepared most of the figures. UK edited the first draft. All authors interpreted the data and edited and approved the final version of this manuscript.

Chapter 5

Prelle LR, Schmidt I, **Schimani K**, Zimmermann J, Abarca N, Skibbe O, Juchem D, Karsten U (2022) Photosynthetic, Respirational, and Growth Responses of Six Benthic Diatoms from the Antarctic Peninsula as Functions of Salinity and Temperature Variations. Genes 13: 1264. https://doi.org/10.3390/genes13071264

LRP. and UK developed the idea and elaborated the concept. IS and DJ provided the experimental data. KS, NA and JZ provided the taxonomical data. OS isolated and established clonal cultures. LRP, KS, JZ, UK and IS wrote the manuscript, and LRP provided all statistical data. All authors have read and agreed to the published version of the manuscript.

Appendix

Supplementary files to Chapter 2

Supplementary Table 1 Taxa Richness and Shannon diversity index of the sample sites with the morphological and DNA metabarcoding inventories (*rbc*L and 18SV4).

	LM		***rbc*L**		**18SV4**	
	Taxa richness	**Shannon index**	**Taxa richness**	**Shannon index**	**Taxa richness**	**Shannon index**
D283	10	0.41	42	1.13	5	0.23
D284	12	1.23	42	2.52	60	2.72
D285	17	1.48	24	1.59	34	1.89
D286	13	1.70	37	1.97	55	2.11
D288	4	0.48	42	1.34	13	0.33
D289	44	2.91	70	2.90	132	2.99
D290	45	2.54	56	2.25	154	3.15
D292	40	2.46	78	2.27	171	2.78
D293	35	2.57	48	1.91	169	3.19
D294	15	1.65	31	2.05	68	1.70
D295	16	1.61	48	2.42	92	2.13
D296	48	2.94	65	1.31	178	1.82
D297	47	2.95	69	1.28	197	1.82
D299	15	1.62	84	2.60	88	2.24
D300	10	0.95	52	1.66	45	2.26
D301	29	2.13	135	3.17	79	2.69
D302	36	2.89	77	2.39	128	3.08
D303	8	0.58	37	1.72	84	2.45
D304	6	0.47	28	1.02	28	1.57
D305	47	2.90	127	1.78	248	2.22
D306	4	0.14	50	1.12	16	0.32
D307	7	0.49	58	2.24	34	1.58
D308	9	0.73	45	2.02	26	1.19
D309	14	1.53	61	1.66	104	1.57
D310	29	1.87	106	1.78	92	3.01
D311	7	0.54	60	1.92	39	1.16
D312	5	0.41	33	1.52	32	1.27
D313	8	1.04	41	2.25	52	2.12
D314	12	0.73	35	1.64	71	1.84
D315	4	0.38	51	2.07	15	1.51
D316	2	0.03	29	1.21	18	0.63
D317	6	0.85	61	2.76	45	2.03
D318	10	0.77	58	2.67	33	1.76
D319	11	1.29	37	0.84	56	0.85
D320	7	0.42	80	2.48	28	1.04
D321	8	0.87	49	2.23	14	0.18
D322	38	2.51	116	2.81	202	2.97
D324	42	2.71	44	1.28	94	1.50
D325	51	3.10	58	1.85	136	2.24

Supplementary Table 2 SIMPER results listing the four most contributing species or ASV's to the dissimilarities between samples taken from different water types (freshwater, brackish water and marine) and substratum types (epipsammic biofilm, biofilm on rocks) for the LM, the *rbc*L and the 18SV4 inventories, CC: Cumulative contribution to dissimilarity, AA: Average abundance across all samples.

LM			***rbc*L**			**18SV4**		
Most influential diatom species	**CC [%]**	**AA [%]**	**Most influential diatom species**	**CC [%]**	**AA [%]**	**Most influential diatom species**	**CC [%]**	**AA [%]**
Marine-freshwater								
Navicula cf. *perminuta*	26.0	38.6	*Mayamaea sweetloveana*	7.8	3.3	*Navicula* cf. *perminuta*	13.2	15.4
Nitzschia annewillemsiana	35.6	4.0	*Navicula* cf. *perminuta*	14.0	9.5	*Pinnularia australomicrostauron*	24.2	10.0
Nitzschia kleinteichiana	43.6	3.3	*Fragilaria* sp.	19.5	2.4	NA	32.7	18.8
Mayamaea sweetloveana	54.7	2.3	*Navicula* cf. *perminuta*	24.8	8.1	*Navicula* cf. *frustulum*	37.9	2.0
Marine-brackish water								
Navicula gregaria	26.2	2.8	*Navicula gregaria*	16.0	1.4	*Pinnularia australomicrostauron*	29.3	10.0
Navicula cf. *perminuta*	52.3	38.6	*Navicula* cf. *perminuta*	23.5	9.3	*Navicula gregaria*	42.0	1.3
Navicula australoshetlandica	59.0	0.7	*Navicula* cf. *perminuta*	30.0	8.1	*Navicula* sp.	52.2	15.4
Chamaepinnularia australis	62.5	0.5	*Navicula australoshetlandica*	35.7	0.5	NA	59.9	18.8
Freshwater-brackish water								
Navicula gregaria	26.8	2.8	*Navicula gregaria*	14.5	1.4	*Pinnularia australomicrostauron*	28.7	10.0
Nitzschia annewillemsiana	36.7	4.0	*Mayamaea sweetloveana*	23.	3.3	*Navicula gregaria*	43.4	1.3
Nitzschia kleinteichiana	44.9	3.3	*Fragilaria* sp.	29.4	2.4	*Nitzschia* cf. *frustulum*	48.4	2.0
Navicula australoshetlandica	51.8	0.7	*Nitzschia kleinteichiana*	34.6	2.0	*Navicula* cf. *veneta*	53.1	0.6
Epipsammic biofilm-biofilm on stones								
Navicula cf. *perminuta*	27.9	2.8	NA	12.0	7.9	NA	22.7	18.8
Navicula sp. 5	34.5	17.4	*Navicula* cf. *perminuta*	19.1	9.5	*Navicula* cf. *perminuta*	31.8	15.4
Navicula gregaria	39.1	2.8	NA	26.0	4.5	*Pinnularia australomicrostauron*	39.1	10.0
Minidiscus chilensis	43.6	5.2	*Navicula* cf. *perminuta*	32.5	8.1	NA	43.9	3.6

Supplementary files to Chapter 3

Supplementary file 1 Culture medium recipe can be downloaded at:

https://fottea.czechphycology.cz/attachments/000180.pdf

Supplementary table 2 List of taxa included in this study obtained from GenBank with strain name, taxon name, accession number 18S and *rbc*L as well as reference, where the sequence was published, strains with * were just added in the additional ML tree (supplementary material 4)

Strain	Taxon name	Accession number 18 S	Accession number *rbc*L	Reference
UTEX FD13	*Scoliopleura peisonis*	HQ912609	HQ912473	Theriot et al. 2010 - A preliminary multigene phylogeny of the diatoms (Bacillariophyta): challenges for future research
I57*	*Envekadea pseudocrassirostris*	KY026086	KY026087	Maltsev et al. 2017 - Molecular phylogeny of the diatom genus *Envekadea*
UTEX FD116	*Neidium productum*	HQ912582	HQ912446	Theriot et al. 2010
UTEX FD417	*Neidium bisulcatum*	HQ912591	HQ912455	Theriot et al. 2010
UTEX FD127	*Neidium affine*	HQ912583	HQ912447	Theriot et al. 2010
SH381	*Haslea nipkowii*	KY320351	KY320290	An et al. 2017 - Identification of benthic diatoms isolated from the eastern tidal flats of the Yellow Sea: Comparison between morphological and molecular approaches
SantaRosa cor. green "Trachy-1"	*Parlibellus hamulifer*	KU179137	KU179122	Witkowski et al. 2016 - Multigene Assessment of Biodiversity of Diatom (Bacillariophyceae) Assemblages from the Littoral Zone of the Bohai and Yellow Seas in Yantai Region of Northeast China with some Remarks on Ubiquitous Taxa
GU44AK-4Parlibellus	*Parlibellus hamulifer*	KJ577866	KJ577903	Nakov et al. 2015 - Comparative analysis of the interaction between habitat and growth form in diatoms
TA387	*Parlibellus delognei f. ellipticus*	KY320352	KY320291	An et al. 2017
ECT3896 Meuneira	*Meuniera membranacea*	KC309482	KC309554	Ashworth et al. 2013 - Revisiting Ross and Sims (1971): Towards a molecular phylogeny of the Biddulphiaceae and Eupodiscaceae (Bacillariophyceae)
UTKSA0019	*Pleurosigma* sp.	KX981840	KX981822	ASHWORTH et al. 2016 - Molecular and Morphological Investigations of the Stauros-bearing, Raphid Pennate Diatoms (Bacillariophyceae): *Craspedostauros* E.J. Cox, and *Staurotropis* T.B.B. Paddock, and their Relationship to the Rest of the Mastogloiales
TA34	*Pleurosigma* sp.	KY320349	KY320288	An et al. 2017
KSA2015-37 Donk-G6	*Donkinia* sp.	MH063463	MH064087	Sabir et al. 2018 - Phylogenetic analysis and a review of the history of the accidental phytoplankter, *Phaeodactylum tricornutum* Bohlin (Bacillariophyta)
ECT3743Clima cund	*Climaconeis undulata*	KC309478	KC309550	Ashworth et al. 2013
ECT3568Amphipl	*Amphipleura pellucida*	KC309477	KC309549	Ashworth et al. 2013
Coz1 peanut penn1	*Diploneis* sp.	KX981839	KX981819	Ashworth et al. 2013
Coz1 cren-cp penn1	*Diploneis* sp.	KX981838	KX981820	Ashworth et al. 2013

UTEX FD282	*Diploneis subovalis*	HQ912597	HQ912461	Theriot et al. 2010
BIOTAII 43	*Haslea silbo*	MG189639	MG189641	Soler et al. 2021 - *Haslea silbo*, A Novel Cosmopolitan Species of Blue Diatoms
TA280	*Haslea pseudostrearia*	KY320350	KY320289	An et al. 2017
UTEX FD109	*Navicula cryptocephala*	HQ912603	HQ912467	Theriot et al. 2010
TCC587	*Navicula cryptotenelloides*	KT072980	KT72927	Keck et al. 2016 - Phylogenetic signal in diatom ecology: perspectives for aquatic ecosystems biomonitoring
TCC604	*Navicula symmetrica*	KT072983	KT072930	Keck et al. 2016
TCC659	*Navicula cincta*	KT072988	KT072934	Keck et al. 2016
TCC580	*Navicula tripunctata*	KT072979	KT072925	Keck et al. 2016
SantaRosaCor. green Nav3	*Trachyneis* sp.	KX981845	KX981824	Ashworth et el. 2016
GU7X-7 Seminav-1	*Seminavis robusta*	MH040330	MH040279	Macatugal et al. 2019 Three new *Licmophora* species (Bacillariophyta: Fragilariophyceae) from Guam, two with an axial wave in the valve
UTEX FD317	*Gyrosigma acuminatum*	HQ912598	HQ912462	Theriot et al. 2010
UTEX FD51	*Stauroneis acuta*	HQ912579	HQ912443	Theriot et al. 2010
KEL-2015 clone JAR44 5ARun6	*Stauroneis* cf. *gracilis*	KM998976	KM999045	Hamilton et al. 2015 - Single cell PCR amplification of diatoms using fresh and preserved samples
UTEX FD35	*Craticula cuspidata*	HQ912581	HQ912445	Ruck and Theriot 2011 - Origin and evolution of the canal raphe system in diatoms
TCC107	*Craticula accomoda*	KF959652	KF959638	Larras et al. 2014 - Linking diatom sensitivity to herbicide to phylogeny: A step forward for biomonitoring?
TCC535	*Fistulifera saprophila*	KF959658	KF959644	Larras et al. 2014
ECT3602Brut	*Berkeleya rutilans*	KJ577848	KJ577883	Nakov et al. 2015
TA424	*Berkeleya fennica*	KY320346	KY320285	An et al. 2017
TCC366	*Mayamaea fossalis* var. *fossalis*	KF959655	KF959641	Larras et al. 2014
AT-115Gel07	*Mayamaea atomus* var. *atomus*	AM501968	AM710434	Bruder and Medlin 2007 - Molecular assessment of phylogenetic relationships in selected species/genera in the Naviculoid diatoms (Bacillariophyta). I. The genus *Placoneis*
TCC540	*Mayamaea permitis*	KC736630	KC736600	Kermarrec et al. 2013 - Next-generation sequencing to inventory taxonomic diversity in eukaryotic communities: a test for freshwater diatoms
AT-101Gel04	*Mayamaea atomus* var. *permitis*	AM501969	AM710435	Bruder and Medlin 2007
(Ecrins4)a	*Pinnularia* cf. *marchica*	JN418569	JN418639	Souffreau et al. 2011 - A time-calibrated multi-gene phylogeny of the diatom genus *Pinnularia*
(Tor12)d	*Pinnularia borealis*	JN418570	JN418640	Souffreau et al. 2011
UTEX FD274	*Pinnularia brebissonii*	HQ912604	HQ912468	Theriot et al. 2010
(Enc2)a	*Pinnularia viridiformis*	JN418574	JN418644	Souffreau et al. 2011
Pin 870 MG	*Pinnularia viridiformis*	JN418589	JN418659	Souffreau et al. 2011
(B2)c	*Pinnularia* cf. *microstauron*	JN418568	JN418638	Souffreau et al. 2011
Cal 878	*Pinnularia* cf. *isselana*	JN418594	JN418664	Souffreau et al. 2011
(Tor1)a	*Pinnularia neomajor*	JN418571	JN418641	Souffreau et al. 2011
UTEX FD484	*Pinnularia termitina*	HQ912601	HQ912465	Theriot et al. 2010

12	*Pinnularia* cf. *gibba*	EF151977	EF143304	Evans et al. 2008
TCC608	*Pinnularia subgibba*	KT072984	KT072931	Keck et al. 2016
Corsea 10	*Pinnularia subcommutata* var. *nonfasciata*	JN418584	JN418654	Souffreau et al. 2011
CH2*	*Rossia* sp.	AJ535144		Medlin & Kaczmarska 2003 - Evolution of the diatoms: V.Morphological and cytological support for the major clades and a taxonomic revision
TF-2014 clone 05DB9 20*	*Rossia* sp.	KF417669		Brinkmann et al. 2015 - Diversity of cyanobacterial and diatom communities along pCO2 and calcite saturation gradients in biofilms of karstic streams, Germany
E3333	*Rossia* sp.	EF151968	EF143281	Evans et al 2008
UTEX FD254	*Fallacia monoculata*	HQ912596	HQ912460	Theriot et al. 2010
GU52X-3 HK482	*Fallacia* sp.	MH063467	MH064092	Sabir et al 2018
UTEX FD294	*Fallacia pygmaea*	HQ912605	HQ912469	Theriot et al 2010
E3661*	*Fallacia* sp.		EF143274	Evans et al 2008
33*	*Fallacia* sp.	KJ961671		Medlin 2014 - Evolution of the Diatoms: VIII. Re-examination of the SSU-rRNA gene using multiple outgroups and a cladistic analysis of valve features
isolate F1	*Fallacia tateyamensis*	MW917199	MW924345	Li et al 2022 - Morphology, molecular phylogeny and systematics of the diatom genus *Fallacia* (Sellaphoraceae), with descriptions of three new species
isolate F4*	*Fallacia laevis*		MW924348	Li et al. 2022
isolate F2	*Fallacia bosoensis*	MW917200	MW924346	Li et al. 2022
Fallacia8	*Fallacia* cf. *forcipata*	EF151960	EF143289	Evans et al. 2008
isolate F3	*Fallacia litoricola*	MW917201	MW924347	Li et al. 2022
isolate F6	*Fallacia hodgeana*	MW917203	MW924350	Li et al. 2022
isolate F5	*Fallacia tenera*	MW917202	MW924349	Li et al. 2022
strain Cal 890 TM	*Caloneis silicula*	JN418593	JN418663	Souffreau et al. 2011
UTEX FD54	*Caloneis lewisii*	HQ912580	HQ912444	Theriot et al. 2010
AT-177.07	*Caloneis amphisbaena*	AM501954	AM710507	Bruder & Medlin 2007
8296 Dipr001	*Diprora haenaensis*	KC954571	KC954572	Kociolek et al. 2013 - Molecular data show the enigmatic cave-dwelling diatom *Diprora* (Bacillariophyceae) to be a raphid diatom
AT-70Gel18	*Eolimna minima*	AM501962	AM710427	Bruder & Medlin 2007
SNA15*	*Eolimna minima*	AJ243063		Beszteri et al. 2001 - Phylogeny of six naviculoid diatoms based on 18S rDNA sequences
TCC661	*Eolimna subminuscula*	KT072989	KT072935	Keck et al. 2016
TCC461	*Sellaphora seminulum*	KC736642	KC736613	Kermarrec et al. 2013
THR7	*Sellaphora pupula*	EF151976	EF143302	Evans et al. 2008
AUS4	*Sellaphora pupula*	EF151983	EF143317	Evans et al. 2008
(Bfp5x8)F1-3	*Sellaphora blackfordensis*	JN418599	JN418669	Souffreau et al. 2011
BLA6	*Sellaphora blackfordensis*	EF151969	EF143282	Evans et al. 2008
BLA13	*Sellaphora lanceolata*	EF151978	EF143305	Evans et al. 2008
THR4	*Sellaphora laevissima*	EF151981	EF143309	Evans et al. 2008
DUN1	*Sellaphora auldreekie*	EF151965	EF143276	Evans et al. 2008
RBG1	*Sellaphora pupula*	EF151962	EF143271	Evans et al. 2008

TCC487	*Nitzschia inconspicua*	KC736636	KC736607	Kermarrec et al. 2013
TA353	*Nitzschia liebethruthii*	KY320378	KY320317	An et al. 2017
EW234	*Bacillaria paxillifer*	KY320376	KY320315	An et al. 2017
TCC901-sq1	*Hantzschia amphioxys*	MN696729	MN66780	Gorzerino et al. - Direct submission
TRY947CAT	*Tryblionella apiculata*	MN750508	MN734090	Mann et al. 2021 - Ripe for reassessment: A synthesis of available molecular data for the speciose diatom family Bacillariaceae.

Supplementary files 3 and 4 18S and *rbc*L Alignments see https://fottea.czechphycology.cz/artkey/fot-202401-0001_molecular_phylogenetics_coupled_with_morphological_analyses_of_arctic_and_antarctic_strains_place_chamaepinnula.php

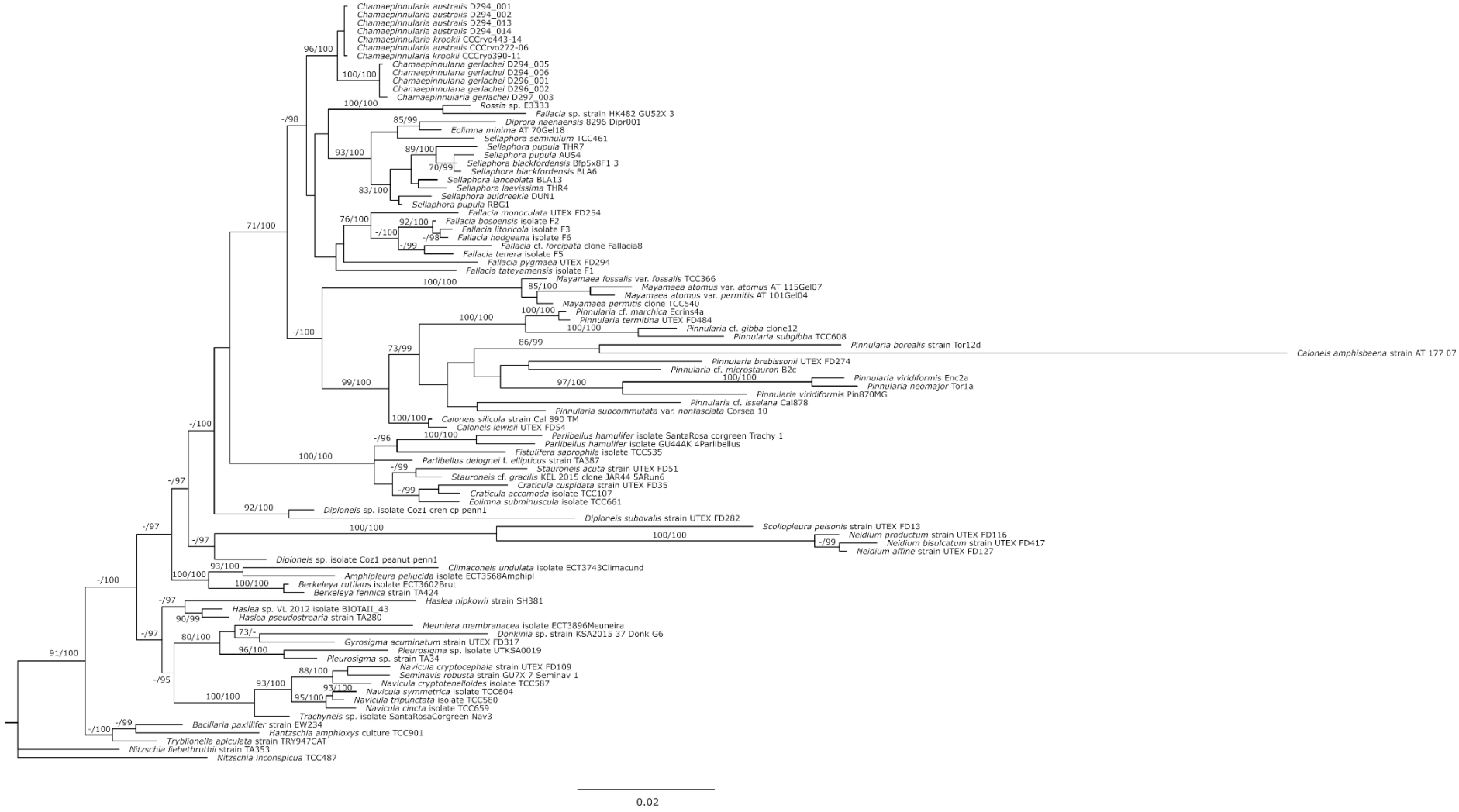

Supplementary figure 5 Maximum likelihood (ML) and Bayesian inference (BI) phylogenetic tree based on the 18S rRNA gene sequence. Nodal support for branches in the ML and BI trees is marked in order (ML/BI). Only bootstrap values over 70 % and posterior probability over 96 % are shown in the tree

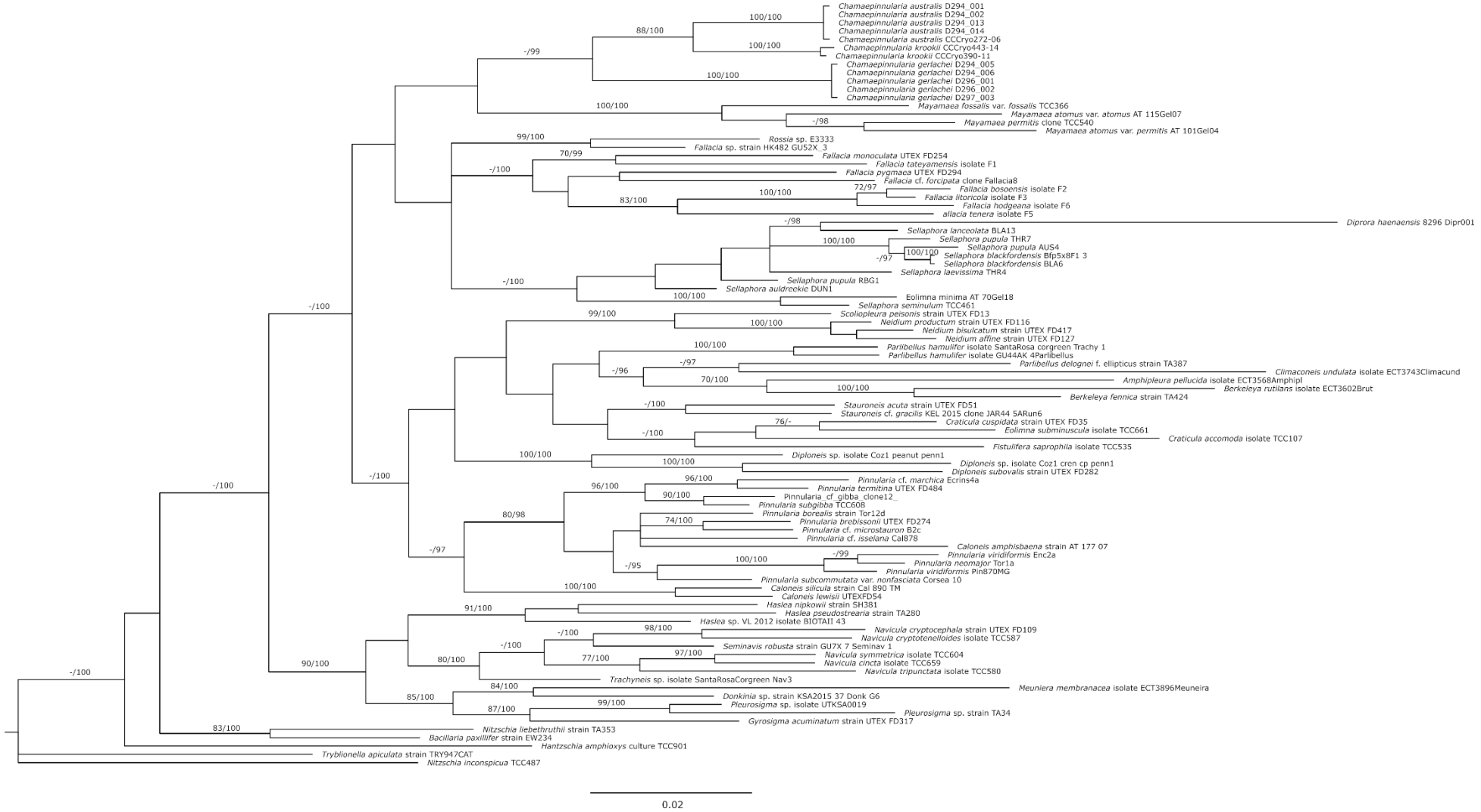

Supplementary figure 6 Maximum likelihood (ML) and Bayesian inference (BI) phylogenetic tree based on the *rbc*L gene sequence. Nodal support for branches in the ML and BI trees is marked in order (ML/BI). Only bootstrap values over 70 % and posterior probability over 96 % are shown in the tree

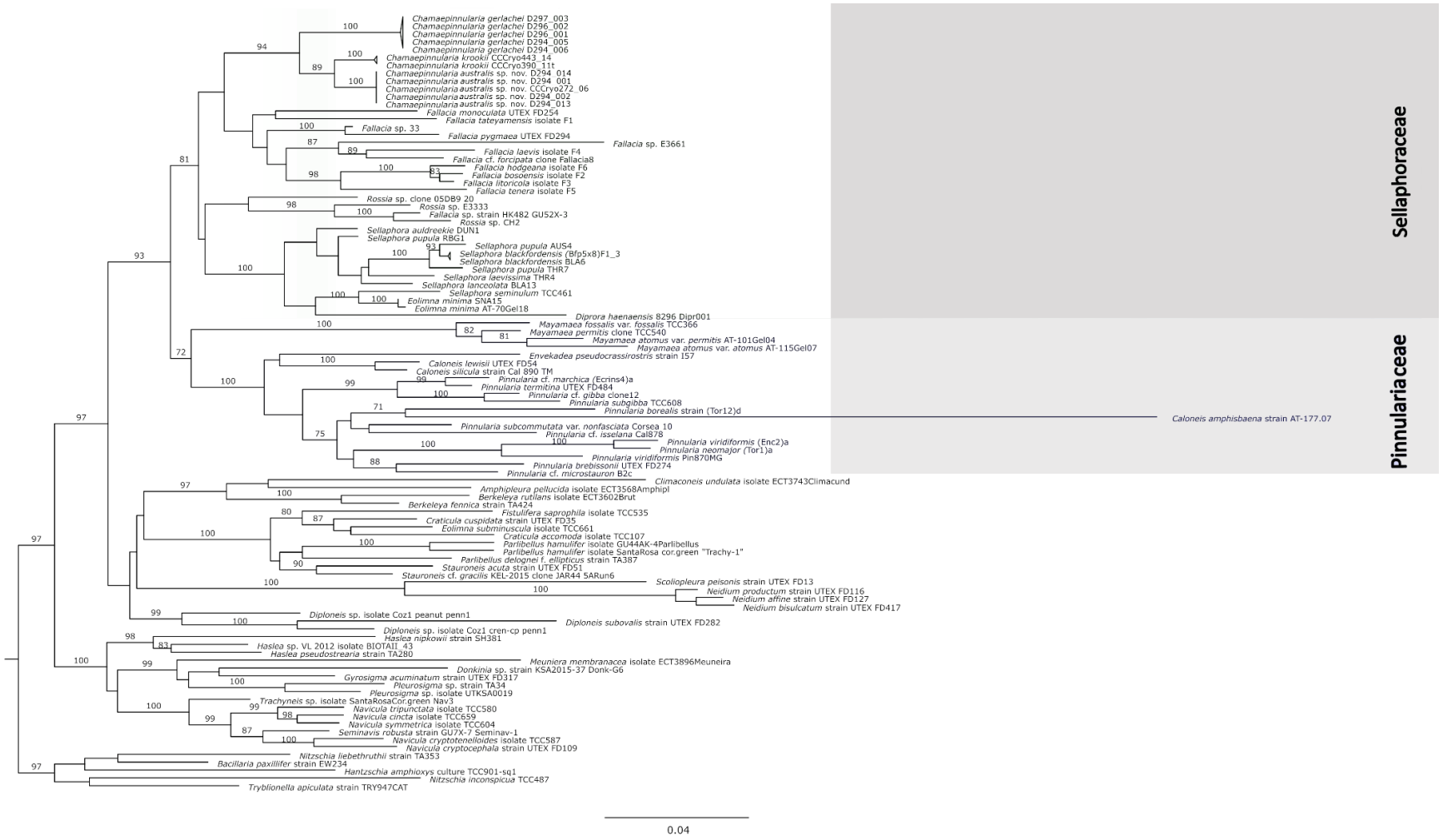

Supplementary figure 7 Maximum likelihood (ML) and Bayesian inference (BI) phylogenetic tree based on the 18S rRNA and *rbc*L gene sequences including seven additional, shorter sequences. Nodal support for branches in the ML and BI trees is marked in order (ML/BI). Only bootstrap values over 70 % and posterior probability over 96 % are shown in the tree

Supplement material 8 Percent dissimilarity (p–distance) matrices

Percent dissimilarity (p–distance) matrix of 12 *Chamaepinnularia* strains on basis of the 18S rRNA gene including the V4 subregion (1530 bp).

	1	2	3	4	5	6	7	8	9	10	11
1. D294_001 *Chamaepinnularia australis*											
2. D294_002 *Chamaepinnularia australis*	0.0										
3. D294_013 *Chamaepinnularia australis*	0.0	0.0									
4. D294_014 *Chamaepinnularia australis*	0.0	0.0	0.0								
5. CCCryo 272-06 *Chamaepinnularia australis*	0.0	0.0	0.0	0.0							
6. D294_005 *Chamaepinnularia gerlachei*	0.7	0.7	0.7	0.7	0.7						
7. D294_006 *Chamaepinnularia gerlachei*	0.7	0.7	0.7	0.7	0.7	0.0					
8. D296_001 *Chamaepinnularia gerlachei*	0.7	0.7	0.7	0.7	0.7	0.8	0.0				
9. D296_002 *Chamaepinnularia gerlachei*	0.7	0.7	0.7	0.7	0.7	0.0	0.0	0.0			
10. D297_003 *Chamaepinnularia gerlachei*	0.8	0.8	0.8	0.8	0.8	0.1	0.1	0.1	0.1		
11. CCCryo 443-14 *Chamaepinnularia krookii*	0.1	0.1	0.1	0.1	0.1	0.8	0.8	0.8	0.8	0.9	
12. CCCryo 390-11 *Chamaepinnularia krookii*	0.1	0.1	0.1	0.1	0.1	0.8	0.8	0.8	0.8	0.9	0.0

Percent dissimilarity (p–distance) matrix of 12 *Chamaepinnularia* strains on basis of the barcode of the V4 region of the 18S rRNA commonly used in diatom DNA metabarcoding (282 bp).

	1	2	3	4	5	6	7	8	9	10	11
1. D294_001 *Chamaepinnularia australis*											
2. D294_002 *Chamaepinnularia australis*	0.0										
3. D294_013 *Chamaepinnularia australis*	0.0	0.0									
4. D294_014 *Chamaepinnularia australis*	0.0	0.0	0.0								
5. CCCryo 272-06 *Chamaepinnularia australis*	0.0	0.0	0.0	0.0							
6. D294_005 *Chamaepinnularia gerlachei*	2.1	2.1	2.1	2.1	2.1						
7. D294_006 *Chamaepinnularia gerlachei*	2.1	2.1	2.1	2.1	2.1	0.0					
8. D296_001 *Chamaepinnularia gerlachei*	2.1	2.1	2.1	2.1	2.1	0.0	0.0				
9. D296_002 *Chamaepinnularia gerlachei*	2.1	2.1	2.1	2.1	2.1	0.0	0.0	0.0			
10. D297_003 *Chamaepinnularia gerlachei*	2.1	2.1	2.1	2.1	2.1	0.0	0.0	0.0	0.0		
11. CCCryo 443-14 *Chamaepinnularia krookii*	0.7	0.7	0.7	0.7	0.7	2.8	2.8	2.8	2.8	2.8	
12. CCCryo 390-11 *Chamaepinnularia krookii*	0.7	0.7	0.7	0.7	0.7	2.8	2.8	2.8	2.8	2.8	0.000

Percent dissimilarity (p–distance) matrix of 12 *Chamaepinnularia* strains on basis of the *rbc*L gene (990 bp).

	1	2	3	4	5	6	7	8	9	10	11
1. D294_001 *Chamaepinnularia australis*											
2. D294_002 *Chamaepinnularia australis*	0.0										
3. D294_013 *Chamaepinnularia australis*	0.0	0.0									
4. D294_014 *Chamaepinnularia australis*	0.0	0.0	0.0								
5. CCCryo 272-06 *Chamaepinnularia australis*	0.0	0.0	0.0	0.0							
6. D294_005 *Chamaepinnularia gerlachei*	5.1	5.1	5.1	5.1	5.1						
7. D294_006 *Chamaepinnularia gerlachei*	5.1	5.1	5.1	5.1	5.1	5.1					
8. D296_001 *Chamaepinnularia gerlachei*	5.1	5.1	5.1	5.1	5.1	0.0	0.0				
9. D296_002 *Chamaepinnularia gerlachei*	5.1	5.1	5.1	5.1	5.1	0.0	0.0	0.0			
10. D297_003 *Chamaepinnularia gerlachei*	5.1	5.1	5.1	5.1	5.1	0.0	0.0	0.0	0.0		
11. CCCryo 443-14 *Chamaepinnularia krookii*	2.9	2.9	2.9	2.9	2.9	5.3	5.3	5.3	5.3	5.3	
12. CCCryo 390-11 *Chamaepinnularia krookii*	2.9	2.9	2.9	2.9	2.9	5.3	5.3	5.3	5.3	5.3	0.0

Percent dissimilarity (p–distance) matrix of 12 *Chamaepinnularia* strains on basis of the barcode of the *rbc*L gene commonly used in diatom DNA metabarcoding (263 bp).

	1	2	3	4	5	6	7	8	9	10	11
1. D294_001 *Chamaepinnularia australis*											
2. D294_002 *Chamaepinnularia australis*	0.0										
3. D294_013 *Chamaepinnularia australis*	0.0	0.0									
4. D294_014 *Chamaepinnularia australis*	0.0	0.0	0.0								
5. CCCryo 272-06 *Chamaepinnularia australis*	0.0	0.0	0.0	0.0							
6. D294_005 *Chamaepinnularia gerlachei*	7.6	7.6	7.6	7.6	7.6						
7. D294_006 *Chamaepinnularia gerlachei*	7.6	7.6	7.6	7.6	7.6	0.0					
8. D296_001 *Chamaepinnularia gerlachei*	7.6	7.6	7.6	7.6	7.6	0.0	0.0				
9. D296_002 *Chamaepinnularia gerlachei*	7.6	7.6	7.6	7.6	7.6	0.0	0.0	0.0			
10. D297_003 *Chamaepinnularia gerlachei*	7.6	7.6	7.6	7.6	7.6	0.0	0.0	0.0	0.0		
11. CCCryo 443-14 *Chamaepinnularia krookii*	5.3	5.3	5.3	5.3	5.3	5.3	8.7	8.7	8.7	8.7	
12. CCCryo 390-11 *Chamaepinnularia krookii*	5.3	5.3	5.3	5.3	5.3	5.3	8.7	8.7	8.7	8.7	0.0

Supplementary files to Chapter 4

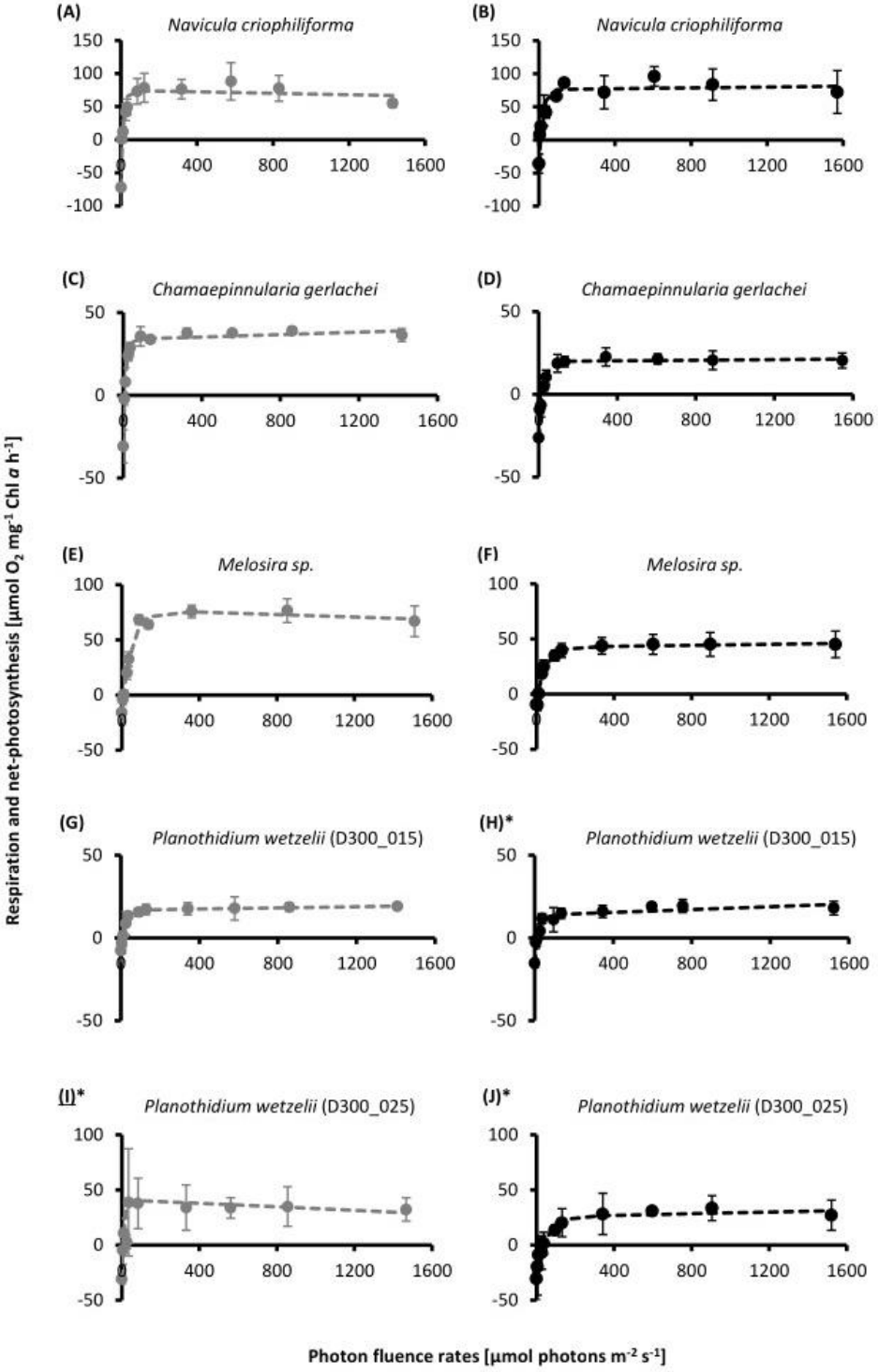

Supplementary figure 1 Photosynthesis-irradiance curves (PI-curves) of five benthic diatom strains form Antarctica. Each row shows a different strain, left column gives the control data of each culture (gray, T_0), the right column the measurements after 3 months of dark incubation (T_3) (black). **A, B** *Navicula criophiliforma* **C, D** *Chamaepinnularia gerlachei* **E, F** *Melosira* sp. **G, H** *Planothidium wetzelii* (D300_015) **I, J** *Planothidium wetzelii* (D300_025). The data points represent mean values ± SD (n = 4, if n = 3 marked *) and were fitted using the model of Walsby (1997).

Supplementary Table 1 Estimates of Evolutionary Divergence between Planothidium species (p-Distances) for the 18S V4 sequence.

	1	2	3	4	5	6	7	8	9	10	11	12	13	14	15	16	17	18	19	20	21	22	23	24	25
1. *P. wetzelii* D300_015																									
2. *P. wetzelii* D300_025	0.0																								
3. *P. wetzelii* D300_020	0.0	0.0																							
4. *P. wetzelii* D300_019	0.0	0.0	0.0																						
5. *P. tujii*	1.1	0.9	1.1	1.1																					
6. *P. victorii* D101_022	0.7	0.5	0.7	0.7	0.9																				
7. *P. victorii* B141	1.1	0.9	1.1	1.1	0.0	0.9																			
8. *P. victorii* B144	1.1	0.9	1.1	1.1	0.0	0.9	0.0																		
9. *P. victorii* D06_113	0.7	0.5	0.7	0.7	0.9	0.0	0.9	0.9																	
10. *P. victorii* D109_018	0.7	0.5	0.7	0.7	0.9	0.0	0.9	0.9	0.0																
11. *P. victorii* D06_014	0.9	0.7	0.9	0.9	0.2	0.7	0.2	0.2	0.7	0.7															
12. *P. victorii* type LCR-S-18-1-1	1.1	0.8	1.1	1.1	0.3	0.8	0.3	0.3	0.8	0.8	0.0														
13. *P. straubianum (= P.victorii)* B086_3	0.9	0.7	0.9	0.9	0.2	0.7	0.2	0.2	0.7	0.7	0.0	0.0													
14. *P. naradoense* D23_024	2.5	2.5	2.5	2.5	2.3	2.8	2.3	2.3	2.8	2.8	2.1	2.5	2.1												
15. *P. frequentissimum* D06_139	2.5	2.5	2.5	2.5	2.3	2.8	2.3	2.3	2.8	2.8	2.1	2.5	2.1	0.9											
16. *P. frequentissimum* D06_138	2.5	2.5	2.5	2.5	2.3	2.8	2.3	2.3	2.8	2.8	2.1	2.5	2.1	0.9	0.0										
17. *P. frequentissimum* TCC615	2.5	2.5	2.5	2.5	2.3	2.8	2.3	2.3	2.8	2.8	2.1	2.5	2.1	0.9	0.0	0.0									
18. *P. frequentissimum* LCR-S-2-1-1	3.2	3.2	3.2	3.2	2.9	3.5	2.9	2.9	3.5	3.5	2.6	2.9	2.6	1.2	0.0	0.0	0.0								
19. *P. lanceolatum* D06_047	4.6	4.6	4.6	4.6	4.8	5.3	4.8	4.8	5.3	5.3	4.8	5.9	4.8	4.1	3.9	3.9	3.9	4.9							
20. *P. lanceolatum* B146	5.3	5.3	5.3	5.3	5.5	5.9	5.5	5.5	5.9	5.9	5.5	6.2	5.5	4.8	4.6	4.6	4.6	5.2	0.7						
21. *P.* cf. *subantarcticum* D17_002	7.8	7.6	7.8	7.8	7.6	8.0	7.6	7.6	8.0	8.0	7.6	9.3	7.6	7.4	7.1	7.1	7.1	7.0	6.2	6.7					
22. *P. taeansa* D26_002	4.8	4.6	4.8	4.8	4.6	5.0	4.6	4.6	5.0	5.0	4.6	5.6	4.6	4.4	3.7	3.4	3.4	4.3	2.7	3.4	6.9				
23. *P. cryptolanceolatum* D26_017	4.3	4.1	4.3	4.3	4.3	4.6	4.3	4.3	4.6	4.6	4.3	5.3	4.3	4.6	4.1	4.1	4.1	5.2	2.7	3.4	6.2	2.7			
24. *P. cryptolanceolatum* D31_010	4.3	4.1	4.3	4.3	4.3	4.6	4.3	4.3	4.6	4.6	4.3	5.3	4.3	4.6	4.1	4.1	4.1	5.2	2.7	3.4	6.2	2.7	0.0		
25. *P. cryptolanceolatum* Ko8A0610-1	4.3	4.1	4.3	4.3	4.3	4.6	4.3	4.3	4.6	4.6	4.3	5.3	4.3	4.6	4.1	4.1	4.1	5.2	2.7	3.4	6.2	2.7	0.0	0.0	
26. *P. suncheonmanense* Ko0408	5.0	5.0	5.0	5.0	5.0	4.8	5.0	5.0	4.8	4.8	5.0	6.2	5.0	5.0	4.8	4.8	4.8	6.1	5.3	5.7	8.3	5.7	5.0	5.0	5.0

Supplementary Table 2 Estimates of Evolutionary Divergence between Planothidium species (p-Distances) for the *rbc*L sequence

	1	2	3	4	5	6	7	8	9	10	11	12	13	14	15	16	17	18	19	20	21	22	23	24	25
1. *P. wetzelii* D300_015																									
2. *P. wetzelii* D300_025	0.0																								
3. *P. wetzelii* D300_020	0.0	0.0																							
4. *P. wetzelii* D300_019	0.0	0.0	0.0																						
5. *P. tujii*	0.5	0.5	0.5	0.5																					
6. *P. victorii* D101_022	0.6	0.6	0.6	0.6	0.5																				
7. *P. victorii* B141	0.5	0.5	0.5	0.5	0.4	0.5																			
8. *P. victorii* B144	0.5	0.5	0.5	0.5	0.4	0.5	0.2																		
9. *P. victorii* D06_113	0.6	0.6	0.6	0.6	0.5	0.0	0.5	0.5																	
10. *P. victorii* D109_018	0.7	0.7	0.7	0.7	0.6	0.0	0.6	0.6	0.0																
11. *P. victorii* D06_014	0.6	0.6	0.6	0.6	0.5	0.0	0.5	0.5	0.0	0.0															
12. *P. victorii* type LCR-S-18-1-1	0.8	0.8	0.8	0.8	0.8	0.3	0.5	0.8	0.3	0.3	0.3														
13. *P. straubianum (= P.victorii)* B086_3	0.5	0.5	0.5	0.5	0.6	0.7	0.6	0.6	0.7	0.8	0.7	1.0													
14. *P. naradoense* D23_024	2.2	2.2	2.2	2.2	2.0	2.1	2.2	2.2	2.1	2.2	2.1	2.0	1.7												
15. *P. frequentissimum* D06_139	1.8	1.8	1.8	1.8	1.8	1.7	1.8	1.8	1.7	1.8	1.7	2.8	1.9	2.0											
16. *P. frequentissimum* D06_138	1.8	1.8	1.8	1.8	1.8	1.7	1.8	1.8	1.7	1.8	1.7	2.8	1.9	2.0	0.0										
17. *P. frequentissimum* TCC615	2.1	2.1	2.1	2.1	2.1	2.0	2.1	2.1	2.0	2.1	2.0	3.5	2.2	2.4	0.1	0.1									
18. *P. frequentissimum* LCR-S-2-1-1	2.3	2.3	2.3	2.3	2.6	2.1	2.3	2.6	2.1	2.1	2.1	2.3	2.6	2.1	0.5	0.5	0.4								
19. *P. lanceolatum* D06_047	3.8	3.8	3.8	3.8	3.7	3.9	3.8	3.8	3.9	4.0	3.9	4.6	3.6	3.7	3.9	3.9	4.1	4.7							
20. *P. lanceolatum* B146	3.7	3.7	3.7	3.7	3.6	3.9	3.7	3.7	3.9	3.9	3.9	4.6	3.5	3.5	3.8	3.9	4.1	4.7	0.1						
21. *P.* cf. *subantarcticum* D17_002	3.6	3.6	3.6	3.6	3.6	3.9	3.7	3.7	3.9	3.9	3.9	4.1	3.3	3.7	3.7	3.8	4.2	3.9	1.9	2.0					
22. *P. taeansa* D26_002	3.3	3.3	3.3	3.3	3.3	3.3	3.4	3.4	3.4	3.4	3.4	4.1	3.2	3.6	3.4	3.5	3.9	3.9	2.5	2.4	1.7				
23. *P. cryptolanceolatum* D26_017	3.0	3.0	3.0	3.0	3.0	3.0	3.1	3.1	3.1	3.1	3.1	4.1	2.9	3.5	3.3	3.4	3.9	3.9	2.6	2.5	1.8	0.5			
24. *P. cryptolanceolatum* D31_010	3.0	3.0	3.0	3.0	3.0	3.0	3.1	3.1	3.1	3.1	3.1	4.1	2.9	3.5	3.3	3.4	3.9	3.9	2.6	2.5	1.8	0.5	0.0		
25. *P. cryptolanceolatum* Ko8A0610-1	3.0	3.0	3.0	3.0	3.0	3.0	3.1	3.1	3.1	3.1	3.1	4.1	2.9	3.5	3.3	3.4	3.9	3.9	2.6	2.5	1.8	0.5	0.0	0.0	
26. *P. suncheonmanense* Ko0408	6.2	6.2	6.2	6.2	5.9	5.9	6.2	6.2	5.9	6.0	5.9	6.6	6.2	5.6	5.6	5.6	6.2	6.0	5.3	5.3	6.0	5.7	5.6	5.6	5.6

Supplementary files to Chapter 5

Supplementary table 1 Confidence intervals for salinity dependent growth rates and temperature-dependent growth rates, photosynthetic rates and respirational rates in the studied Antarctic benthic diatoms isolated from Carlini Station, King George Island Potter Cove in austral summer 2020 (January/February).

	Confidence intervals	
Species	**2.5 %**	**97.5 %**
Navicula criophiliforma		
maximal photosynthetic rate	231.663	353.517
optimum photosynthetic temperature	5.934	16.303
maximum photosynthetic temperature	30.825	35.868
maximum respirational rate	-212.388	-159.586
optimum respirational temperature	28.002	-81.961
maximum respirational temperature	40.141	43.668
Chamaepinnularia gerlachei		
maximum growth rate (salinity)	0.537	0.621
optimum growth salinity	2.593	10.457
maximum growth salinity	87.282	100.156
maximal growth rate	0.229	0.659
optimum growth temperature	4.620	21.302
maximum growth temperature	23.218	34.486
maximal photosynthetic rate	67.586	115.146
Navicula concordia		
maximal photosynthetic rate	43.144	54.717
optimum photosynthetic temperature	13.054	18.272
maximum photosynthetic temperature	34.235	37.026
maximum respirational rate	-31.895	-26.055
optimum respirational temperature	26.108	9.183
maximum respirational temperature	41.851	47.030
Nitzschia annewillemsiana		
maximal photosynthetic rate	34.524	52.401
optimum photosynthetic temperature	7.674	17.282
maximum photosynthetic temperature	31.121	35.854
maximum respirational rate	-53.619	-37.302
optimum respirational temperature	23.856	29.366
maximum respirational temperature	39.359	46.399
***Planothidium* sp.**		
maximal photosynthetic rate	37.561	69.429
optimum photosynthetic temperature	4.275	18.757
maximum photosynthetic temperature	29.766	36.829
maximum respirational rate	-102.387	-65.730
optimum respirational temperature	24.990	31.081
maximum respirational temperature	38.950	46.994
Psammothidium papilio		
maximum growth rate (salinity)	0.376	0.455
optimum growth salinity	3.400	7.167
maximum growth salinity	26.997	31.529
Maximal growth rate (temperature)	0.184	0.406
optimum growth temperature	-4.373	17.325
Maximum growth temperature	21.883	34.038
maximal photosynthetic rate	28.695	142.941
optimum photosynthetic temperature	-6.319	12.304

maximum photosynthetic temperature	21.837	30.219
maximum respirational rate	-123.938	-76.441
optimum respirational temperature	25.562	31.759
maximum respirational temperature	38.754	46.231